

Conformal Field Theory Between Supersymmetry and Indecomposable Structures

Dissertation

zur

Erlangung des Doktorgrades (Dr. rer. nat.)

der

Mathematisch-Naturwissenschaftlichen Fakultät

der

Rheinischen Friedrich-Wilhelms-Universität Bonn

vorgelegt von

Holger Eberle

aus

Neuss

Bonn 2006

Angefertigt mit Genehmigung der Mathematisch-Naturwissenschaftlichen Fakultät der Rheinischen Friedrich-Wilhelms-Universität Bonn

Diese Dissertation ist auf dem Hochschulschriftenserver der Universitäts- und Landesbibliothek Bonn http://hss.ulb.uni-bonn.de/diss_online elektronisch publiziert.

1. Referent: Prof. Dr. Werner Nahm
2. Referent: Prof. Dr. Hans-Peter Nilles

Tag der Promotion: 12. Juli 2006
Erscheinungsjahr: 2006

Abstract

This thesis considers conformal field theory in its supersymmetric extension as well as in its relaxation to logarithmic conformal field theory.

Compactification of superstring theory on four-dimensional complex manifolds obeying the Calabi-Yau conditions yields the moduli space of $N = (4, 4)$ superconformal field theories with central charge $c = 6$ which consists of two continuously connected subspaces. This thesis is concerned with the subspace of K3 compactifications which is not well known yet. In particular, we inspect the intersection point of the \mathbb{Z}_2 and \mathbb{Z}_4 orbifold subvarieties within the K3 moduli space, explicitly identify the two corresponding points on the subvarieties geometrically, and give an explicit isomorphism of the three conformal field theory models located at that point, a specific \mathbb{Z}_2 and a \mathbb{Z}_4 orbifold model as well as the Gepner model $(2)^4$. We also prove the orthogonality of the two subvarieties at the intersection point. This is the starting point for the programme to investigate generic points in K3 moduli space. We use the coordinate identification at the intersection point in order to relate the coordinates of both subvarieties and to explicitly calculate a geometric geodesic between the two subvarieties as well as its generator. A generic point in K3 moduli space can be reached by such a geodesic originating at a known model. We also present advances on the conformal field theoretic side of deformations along such a geodesic using conformal deformation theory. Since a consistent regularisation of the appearing deformation integrals has not been achieved yet, the completion of this programme is still an open problem.

Moreover, we regard a relaxation of conformal field theory to logarithmic conformal field theory. The latter allows the indecomposable action of the L_0 Virasoro mode within a representation of the conformal symmetry. In particular, we study general augmented $c_{p,q}$ minimal models which generalise the well-known (augmented) $c_{p,1}$ model series. We calculate logarithmic nullvectors in both types of models. But most importantly, we investigate the low lying Virasoro representation content and fusion algebra of two general augmented $c_{p,q}$ models, the augmented $c_{2,3} = 0$ model as well as the augmented Yang-Lee model at $c_{2,5} = -22/5$. These exhibit a much richer structure as the $c_{p,1}$ models with indecomposable representations up to rank 3. We elaborate several of these new rank 3 representations in great detail and uncover astonishing features. Furthermore, we argue that irreducible representations corresponding to the Kac table domain of the proper minimal models cannot be included into the theory. In particular, the true vacuum representation is rather given by a rank 1 indecomposable

but not irreducible subrepresentation of a rank 2 representation. We generalise these generic examples to give the representation content and the fusion algebra of general augmented $c_{p,q}$ models as a conjecture. Finally, we open a new connection between logarithmic conformal field theory and quantum spin chains by relating some representations of the augmented $c_{2,3} = 0$ model to the representation content of a $c = 0$ model which describes an XXZ quantum spin chain.

Contents

1	Introduction	7
2	Conformal field theory	15
2.1	General structures in conformal field theory	15
2.2	Logarithmic conformal field theory	24
2.3	Important models	26
2.3.1	The Kac determinant and minimal models	26
2.3.2	Torus sigma models	28
2.3.3	Orbifold sigma models	35
2.3.4	Supersymmetric minimal models and Gepner models	40
3	Observations on K3 moduli space	47
3.1	Introduction to the geometry of the K3 moduli space	48
3.2	Geometric intersection of the \mathbb{Z}_2 and \mathbb{Z}_4 subvarieties	50
3.2.1	Reference lattices and four-planes for \mathbb{Z}_2 and \mathbb{Z}_4 orbifold models	50
3.2.2	Identification of lattice vectors at the intersection point	55
3.3	Identification of CFTs at the $(\widehat{2})^4$ Gepner point	58
3.3.1	The symmetry algebra of $\mathcal{K}(\mathbb{Z}^4, 0)$	59
3.3.2	The symmetry algebra of $\mathbb{Z}_4(\frac{1}{\sqrt{2}}D_4, B^*)$	60
3.3.3	Non-twisted groundstate $(\frac{1}{4}, \frac{1}{4})$ fields	61
3.3.4	Twisted groundstate $(\frac{1}{4}, \frac{1}{4})$ fields in $\mathbb{Z}_4(\frac{1}{\sqrt{2}}D_4, B^*)$	62
3.3.5	Twisted groundstate $(\frac{1}{4}, \frac{1}{4})$ fields in $\mathcal{K}(\mathbb{Z}_4, 0)$	65
3.3.6	Fields of the Gepner model $(\widehat{2})^4$	66
3.3.7	Explicit identification of the three theories	68
3.4	A geometric geodesic in K3 moduli space	70
3.4.1	Finding the transition matrix	70
3.4.2	Calculating the generator of the geodesic	73
3.5	Deforming CFT along a geodesic	77
3.5.1	Conformal deformation theory	77
3.5.2	Conformal deformations in K3 moduli space	80
3.5.3	Calculation of the two-loop integral	82

4	Higher rank indecomposable structures	97
4.1	What are augmented minimal models?	98
4.2	Exploring logarithmic nullvectors	102
4.2.1	Jordan cells on lowest weight level	103
4.2.2	Logarithmic nullvectors for $c_{p,1}$	105
4.2.3	Possible logarithmic nullvectors for $c_{2,3} = 0$	108
4.3	How to calculate fusion products	112
4.3.1	The Nahm algorithm	113
4.3.2	Constraints for the fusion algebra	116
4.3.3	Implementation for the $c_{p,q}$ models	117
4.4	Fusion analysis of the augmented $c_{2,3} = 0$ model	118
4.4.1	Higher rank representations	118
4.4.2	Explicit calculation of the fusion products	135
4.4.3	Consistency of fusion products	135
4.4.4	An unexpected connection to quantum spin chains	137
4.5	Fusion analysis of the augmented Yang–Lee model	138
4.6	Representations and fusion for augmented $c_{p,q}$ models	142
4.6.1	The spectrum of representations	142
4.6.2	The fusion of irreducible representations	144
4.6.3	The fusion with higher rank representations	147
5	Conclusion	149
A	Explicit L_0 for rank 3 representations	155
A.1	$\mathcal{R}^{(3)}(0, 0, 1, 1)$	155
A.2	$\mathcal{R}^{(3)}(0, 0, 2, 2)$	156
A.3	$\mathcal{R}^{(3)}(0, 1, 2, 5)$	157
B	Fusion rules for two augmented models	159
B.1	Fusion rules for $c_{2,3} = 0$	159
B.2	Fusion rules for $c_{2,5} = -22/5$	171
C	Examples of logarithmic nullvectors	173
C.1	An explicit nullvector for $c_{3,1} = -7$	173
C.2	Explicit nullvectors on the border of $c_{2,3} = 0$	174
C.3	Explicit nullvectors in the bulk of $c_{2,3} = 0$	178
	Bibliography	181

Chapter 1

Introduction

Reality is a question of perspective; the further you get from the past, the more concrete and plausible it seems—but as you approach the present, it inevitably seems more and more incredible.
Salman Rushdie: *Midnight's Children*

Conformal field theory (CFT) has become a very important and vibrant area of research since its break-through on the mathematical physics' stage in the mid 80's. The mathematical elaboration of the Virasoro algebra [1], the algebra of local conformal transformations, and its representation theory [2, 3] inspired Belavin, Polyakov and Zamolodchikov to present the first concise study of two-dimensional quantum field theory which exhibits local conformal invariance and, at the same time, to construct an important series of examples, the so-called minimal models [4]. This was the final step of a long development in which conformal symmetry was slowly incorporated into a quantum field theoretic framework. Indeed, already in 1958, Thirring had constructed the first quantum CFT model in two dimensions, the famous Thirring model [5], not realising its local conformal properties at that time. This model is known today as one of the continuous CFT torus models at central charge $c = 1$. For a very enlightening review of this exciting historical development we refer to [6].

From that time on, conformal field theory quickly became a key ingredient in numerous branches of mathematical physics. It is important for the description of two-dimensional phase transitions in statistical physics (see e.g. [7, 8, 9]) as well as for the description of the quantised string theory worldsheet (see e.g. [10, 11]). And even in the modern string theoretic approach in the context of D-branes the so-called boundary conformal field theory provides the microscopical description [12, 13, 14, 15, 16]. Furthermore, implications of CFT can be found in Seiberg Witten theory [17], in solid state physics as e.g. the quantum Hall effect [18, 19, 20], and certainly in the whole field of integrable systems. And perhaps even most importantly, CFT has inspired quite a lot of modern mathematical work with such topics as vertex operator algebras [21, 22, 23] or mirror symmetry [24, 25, 26].

But the pure Virasoro algebra of local conformal transformations does not seem to be sufficient for current applications. The direction of research has, hence, diversified in several directions. Either the conditions of local conformal symmetry are restricted further by the inclusion of more symmetries; especially for theories with a lot of parameters, which e.g. describe higher dimensional string compactification spaces, a larger symmetry algebra often guarantees that the theory is well-behaved or, at least, that the number of representations stays comparatively small. Or one tries to generalise local conformal field theories by relaxing the conditions just in such a way that one keeps most of the astonishing properties of CFT and, at the same time, describes a much larger variety of theories.

In this thesis, we will present advances in both of these possible ways of extending CFT, the supersymmetric extension of the symmetry algebra as well as logarithmic conformal field theory which represents a generalised implementation of conformal symmetry in quantum field theory.

The supersymmetric extension of the conformal symmetry algebra is mainly motivated by string theory. String theory is a mathematically promising suggestion of how to bring together the two vital, but seemingly incompatible concepts in today's description of the physical world, general relativity and quantum theory. The conformal invariance of string theory's central physical entity, the Polyakov action, naturally incorporates CFT in the string theory framework. However, string theory cannot be developed into a consistent theory with any possible relation to the real world without the inclusion of supersymmetry, an extension of the usual Lie type symmetries by an odd symmetry between bosons and fermions. Indeed, without the inclusion of supersymmetry string theory would exhibit very unphysical states, so-called tachyons which exhibit a negative mass, and furthermore would suffer from a much more severe hierarchy problem in the mass scales.

String theory is a quantum field theory of one-dimensional objects whose spatial extension can be seen at length scales of order of the Planck scale $l_{\text{Planck}} = 4.13 \cdot 10^{-33}$ cm, the relevant scale for gravity phenomena. Actually, most efforts in describing string theory still resort to a string quantum mechanics; the advances in string field theory are still very scarce. In spacetime this one-dimensional string sweeps out a two-dimensional surface, the so-called worldsheet of the string. The above mentioned Polyakov action governs the embedding of this worldsheet into spacetime. Now, considerations of making the theory mathematically consistent force spacetime to be of dimension ten (for the supersymmetric string). This is a bitter pill to swallow for physicists, who think that they live in four spacetime dimensions, and it is a challenge to make sense of this. The most promising and very frequently used approach follows and generalises the ideas of Kaluza, who long before the advent of string theory described an electromagnetic theory in a higher dimensional space, and Klein, who got rid of their extra dimensions by simply curling them up to length scales which are not visible any more. This method of compactification can be performed on more general manifolds than the Kaluza Klein torus. These manifolds have to be compatible with supersymmetry as well as the conformal structure of the theory and, hence, have to obey the so-called Calabi

Yau conditions, i.e. they have to be complex Ricci flat manifolds of holonomy $SU(d/2)$. Other ideas of how to make sense of a higher dimensional string theory spacetime have arisen rather recently in connection with braneworld scenarios. These scenarios locate the standard model interactions on a four-dimensional subspace of spacetime, a so-called brane; only gravity is free to propagate in all of spacetime.

In this thesis we will be concerned with compactifications of superstring theory, actually of type II superstring theory. But instead of compactifying on six-dimensional Calabi-Yau manifolds, which would reduce the spacetime dimensionality to the desired four, we will rather regard compactifications on four-dimensional manifolds which respect the Calabi-Yau conditions. Due to the difficulties of a compactification on a general six-dimensional Calabi-Yau manifold, our proceeding proves to have several advantages. Besides the reduced dimensionality of space these four-dimensional compactification spaces induce an even higher amount of supersymmetry, $N = (4, 4)$ supersymmetry. Although pretty awkward from a phenomenological point of view this high amount of supersymmetry is very nice for structural studies as it avoids instanton corrections and induces the possibility to view problems from different perspectives due to the appearing further symmetry relations. On the other side, compactifying on four-dimensional manifolds we encounter as possibilities not only the well understood sixteen dimensional moduli space of torus compactifications, but also the eighty dimensional moduli space of quantum K3 surfaces. Hence, these four-dimensional compactifications provide us with interesting toy models in order to finally understand realistic six-dimensional compactifications and, as we will see, already this reduced problem proves to be very hard in the generic case.

Although the general mathematical properties of K3 surfaces are well known (see e.g. [27]), the precise physical properties of sigma models on these complex surfaces together with their quantum properties as the B-field and, hence, of the respective string vacua are only known for a nullset of theories in that moduli space, like Gepner or most of the orbifold models. A lot of pioneering work on the general structure of the K3 moduli space and the placement of the above mentioned special models within has been done in e.g. [28, 29, 30, 31, 32, 33]. In this thesis, we clarify some open points about the already known part of the moduli space and, furthermore, present advances towards an exploration of the generic points in K3 moduli space.

In [31, 32] it was shown that the subvarieties of \mathbb{Z}_2 and \mathbb{Z}_4 orbifold compactifications in the K3 moduli space intersect in one point. But their argument was given in a rather indirect way. First, it made use of the identification of the quantum surface with its conformal field theory and performed the identification on the level of the corresponding conformal field theories. The two corresponding \mathbb{Z}_2 and \mathbb{Z}_4 orbifold conformal field theories were proven to be equivalent to the Gepner like model $(\widehat{2})^4$, a \mathbb{Z}_2 orbifold of the Gepner model $(2)^4$. Secondly, it inferred the identification of two of these three conformal field theories from the identification of two other specific theories via the orbifold procedure.

In chapter 3 we first give an explicit identification of the two lattices and four-planes corresponding to the two different orbifold conformal field theories at the point

of intersection. This provides us with a geometric proof that the two quantum K3 surfaces are isomorphic. Secondly, we elaborate the explicit identification of the three conformal field theories at that point and prove the orthogonality of the two subvarieties of \mathbb{Z}_2 and \mathbb{Z}_4 orbifold compactifications at their point of intersection. This is a new feature of the intersection which has not been clear up to now. As a byproduct we see and confirm properties of twistfields in \mathbb{Z}_4 orbifold models.

This explicit identification of the \mathbb{Z}_2 and \mathbb{Z}_4 orbifold conformal field theories at the point of intersection enables us to relate the coordinates of the \mathbb{Z}_2 and \mathbb{Z}_4 orbifold subvarieties in moduli space. This is, indeed, not a trivial task as the algebraically geometric arguments [31] of how to embed the orbifold moduli spaces into the larger K3 moduli space lead to different ways of embedding for different orbifold groups. Using this coordinate transition we explicitly construct a geometric geodesic between these two subvarieties in moduli space and determine its generator. Although this last calculation can only be done by a numerical iteration process, we use the method of continued fractions in order to determine the exact transition element (of a desired form) and, in this way, the exact generator.

The main open problem in K3 moduli space is the study of the vast space of yet unknown sigma models besides the highly symmetric Gepner and orbifold models. Most promisingly this problem can be solved by studying the CFT models along geodesics in moduli space which originate and/or terminate at known points. Geometrically, it is possible to determine these geodesics as well as their generators as described above. On the conformal field theory side this problem is solved locally by the conformal deformation theory (see e.g. [34]). However, the integration of these conformal deformations along a geodesic prove to be intricate; we will describe and comment on advances in these studies.

The second part of this thesis deals with logarithmic conformal field theories (logarithmic CFTs) which have attracted quite a lot of attention in recent years. These theories are a generalisation of standard CFT which also allows for reducible but indecomposable action of the Virasoro modes. There are already quite a number of applications in such different fields as statistical physics (e.g. [35, 36, 20, 37]), string theory (e.g. [38, 39, 40]) and Seiberg Witten theory (e.g. [17]) which necessarily incorporate this generalisation of CFT. In particular, we will present a new connection of logarithmic CFTs to quantum spin chains [41], which have lately received great attention within the field of the AdS/CFT correspondence (see e.g. [42, 43]). Nevertheless, studying logarithmic CFTs has only just begun because we still know only few logarithmic models explicitly and the efforts to disentangle the general structure prove to be much more complicated and tedious as in ordinary CFT.

The most prominent examples of logarithmic CFTs up to now have emerged from studying a specific series of the so-called minimal models in CFT, the $c_{p,1}$ models. As standard minimal models these actually emerge to be trivial as they provide zero representation content. On the other hand, if one takes into account representations corresponding to an enlarged Kac table, one encounters non-trivial models which include representations with indecomposable structure. This is the reason why we like to

call these “augmented $c_{p,1}$ minimal models”. These models are fairly well-understood by now. The representation theory of their rank 2 indecomposable Virasoro representations has been analysed completely in [44, 45, 46, 47], and a thorough understanding of the representations of the modular group corresponding to the enlarged triplet \mathcal{W} -algebra [48] of these models has been reached in [49, 50, 51, 52]. Especially the $c_{2,1} = -2$ model has been understood very well as it is isomorphic to a free field construction of the symplectic fermions [53, 54].

But going beyond representation theory we find that the calculation of explicit correlation functions proves to be much more intricate and tedious than in the ordinary CFT case [55, 56]. The construction of nullvectors, the key tool in CFT for the calculation of correlation functions, has already been addressed in [57, 58, 59, 60] for the case of indecomposable representations. However, the type of logarithmic nullvectors calculated so far only describes a very special case. Already for the $c_{p,1}$ models the generic logarithmic nullvectors are beyond the scope of this procedure. In this thesis we will describe the more general situation which applies to all representations of the $c_{p,1}$ models and also to generalised models described below.

On the other hand, the $c_{p,1}$ models are only quite special representatives of the general class of augmented $c_{p,q}$ models [50]. Although these models have already been addressed in some papers (see e.g. [61]), not much is known yet, neither about higher rank representations nor about nullvectors nor about correlation functions. There are, however, good indications that exactly these models might describe important statistical systems, such as percolation. In particular, we will show that the augmented $c_{2,3} = 0$ model might describe the representations which were calculated numerically in [41].

In this thesis we want to uncover the Virasoro representation theory of the general augmented $c_{p,q}$ models. We will attack this problem from two sides. First, we will use the above mentioned refined version of logarithmic nullvector calculation in order to find constraints on the possible structure of higher rank representations in these models. As a main tool of exploration, however, we employ the calculation of the fusion product of representations. The concept of the fusion product lies at the heart of conformal representation theory and has been subject to many thorough mathematical studies (see e.g. [62, 63, 64, 65, 66]). It governs the representation theoretic aspects of the operator product expansion and, hence, puts severe constraints on all n -point-functions in CFT. It follows that the fusion product actually dictates which set of representations of the Virasoro algebra at a certain conformal weight can be combined into a consistent CFT model. Hence, starting with a set of representations known to be included in the theory the successive application of the fusion product will actually lead us to the whole consistent representation space of a model. Our calculation of the augmented $c_{p,q}$ models will pick as its starting point the augmentation of the minimal model Kac table domain by its border.

The algorithm which we use to compute these fusion products relies on the work of [67, 45]. In [67] W. Nahm showed that the main information characterising a representation can be found in a small quotient space of this representation, called the

special subspace, which is finite for the large class of so-called quasirational CFTs. He actually proved that the fusion of quasirational representations leads again to a finite number of quasirational representations. In [45] M. Gaberdiel and H. Kausch used the Nahm algorithm of the proof in [67] to propose a procedure how to efficiently calculate a fusion product of two quasirational representations. This procedure was successfully applied to the augmented $c_{p,1}$ models in [45].

For this thesis we have implemented the Nahm algorithm and the procedure of [45] to calculate the representation content and the fusion products of the lower lying Virasoro representations for the general augmented $c_{p,q}$ models. The explicit calculations comprise a wide range of examples for two specific models, the augmented $c_{2,3} = 0$ and the augmented Yang-Lee model at $c_{2,5} = -22/5$. Especially for the augmented $c_{2,3} = 0$ model we present a very thorough exploration of the full lower fusion algebra. These two special models are then used to deduce the general structure of the representation content and the fusion algebra in augmented $c_{p,q}$ models.

The resulting representation content appears to be much richer as in the special augmented $c_{p,1}$ models. We encounter several new types of rank 2 representations and, in particular, several examples of rank 3 representations. There have been studies of Jordan cells with rank higher than 2 on the level of correlation functions and Ward identities in the CFT literature before [68, 69, 70, 57, 55, 56, 71, 72]. However, the models and their representations discussed in this paper are the first ones where we can see explicitly how a higher rank structure appears while generating a representation as a Virasoro module from some groundstates. We discuss the three lowest rank 3 representations which are accessible for the augmented $c_{2,3} = 0$ model in great detail. To our surprise, they seem to be constructed out of rank 2 representations in much the same way as the rank 2 representations are constructed out of irreducible ones. As a further astonishing fact, we show that irreducible representations corresponding to weights in the Kac table domain of the proper minimal models cannot be included consistently into the model as soon as we augment it with irreducible representations corresponding to the Kac table border. In particular, the vacuum representation is not given by an irreducible representation, but appears to be a rank 1 indecomposable subrepresentation of a rank 2 representation.

This thesis is structured as follows. In chapter 2 we give an extensive introduction to conformal field theory. This presentation, though, does not claim completeness, but is mainly concerned with the topics of the vast field of CFT which are relevant for this thesis. In particular, it includes an introduction to the supersymmetric extension of CFT, to logarithmic CFT, as well as to the specific models which appear in this thesis. In the context of orbifold theories, we calculate the supersymmetric \mathbb{Z}_4 partition function very carefully and deduce special properties of twisted fields which are important to the next chapter.

Chapter 3 contains the first main part of this thesis. It deals with K3 compactifications of type II superstring theories. After a short introduction to the geometric aspects of K3 surfaces and the corresponding moduli space we analyse the point of intersection of the \mathbb{Z}_2 and \mathbb{Z}_4 subvarieties in moduli space in sections 3.2 – 3.3. Section 3.4 presents

the construction of a geometric geodesic as well as its generator, and, finally, section 3.5 discusses how to relate this geodesic to a deformation of conformal field theories and how to calculate such a deformation.

The second main part of this thesis is contained in chapter 4. It is concerned with the determination of higher rank representations in the framework of logarithmic CFT. After an introduction to the models of interest in this chapter we explain how to calculate nullvectors of representations with higher rank structure in section 4.2. Section 4.3, then, introduces the Nahm algorithm to calculate fusion products of representations. In section 4.4 - 4.5 this Nahm algorithm is exploited to determine the representation content and the fusion algebra of two special models, the augmented $c_{2,3} = 0$ and the augmented Yang-Lee model. In particular, it is shown how some representations of the augmented $c_{2,3} = 0$ model appear in the description of a XXZ quantum spin chain. Section 4.6 extrapolates these results and conjectures the representation content as well as the fusion rules for general augmented minimal models.

The appendices contain several explicit results of calculations of chapter 4. Appendix A presents the L_0 action on the lowest states of the three determined rank 3 representations, appendix B lists the fusion products as calculated using the Nahm algorithm on the computer, and appendix C comprises some examples of logarithmic nullvectors.

Some results of this work have already been published in

- H. Eberle, *On explicit results at the intersection of the \mathbb{Z}_2 and \mathbb{Z}_4 orbifold subvarieties in $K3$ moduli space*, *JHEP* **08** (2004) 015, [[hep-th/0407170](#)].
- H. Eberle and M. Flohr, *Notes on generalised nullvectors in logarithmic CFT*, *Nucl. Phys.* **B741** (2006) 441–466, [[hep-th/0512254](#)].
- H. Eberle and M. Flohr, *Virasoro representations and fusion for general augmented minimal models*, [[hep-th/0604097](#)].

Chapter 2

Conformal field theory

2.1 General structures in conformal field theory

In this section we want to give a brief introduction to the basics of conformal field theory (CFT). The importance of two-dimensional field theory which exhibits conformal symmetry has first been acknowledged in the seminal paper [4]. Since then, a vivid field of study has also lead to a plentitude of good reviews as e.g. [73, 74, 9]. A more axiomatic approach to the subject can be found in [75, 76, 32]. Our presentation collects the most important facts necessary for the subsequent chapters.

The following list contains the essential ingredients of a unitary conformal field theory:

- We start with a bigraded Hilbert space of states \mathcal{H} over \mathbb{C} , i.e.

$$\mathcal{H} = \bigoplus_{h, \tilde{h}} V(h; \tilde{h}) .$$

This space contains the unique vacuum $V(0; 0) = \mathbb{C} |0\rangle$. The subspaces of definite grading $V(h; \tilde{h})$ are finite dimensional and the grading is bounded from below as it represents the energy which is supposed to be bounded from below in a physical theory. The grading is called the holomorphic respectively antiholomorphic conformal weight.

- The Hilbert space \mathcal{H} is naturally endowed with a sesquilinear form, the so-called “Shapovalov form”

$$\langle \Phi_1 | \Phi_2 \rangle = C(\Phi_1, \Phi_2) \delta_{h_1, h_2} \delta_{\tilde{h}_1, \tilde{h}_2} \quad |\Phi_1\rangle \in V(h_1; \tilde{h}_1), |\Phi_2\rangle \in V(h_2; \tilde{h}_2)$$

where $C(\Phi_1, \Phi_2)$ signifies a constant depending on the two states. Furthermore, we demand that the vacuum is normalised to $\langle 0|0\rangle = 1$. Notice, that this sesquilinear form respects the bigrading of \mathcal{H} .

- The states in \mathcal{H} uniquely correspond to fields $\Phi(z, \bar{z})$ on a Riemann surface with local coordinates z . This “state-field correspondence” manifests itself in the application of a field to the vacuum which yields the corresponding state

$$\Phi(0, 0) |0\rangle = |\Phi\rangle .$$

- We also need maps F_n which map n states to the space $\mathcal{F}_n(z_1, \dots, z_n)$ of functions which are real analytic with the exception of countably many poles $(z_i - z_j)^{-m+r} (\bar{z}_k - \bar{z}_l)^{-n+r}$ ($i \neq j, k \neq l, r \in R \subset \mathbb{R}$ countable and $m, n \in \mathbb{N}$), i.e.

$$F_n : \mathcal{H}^{\otimes n} \rightarrow \mathcal{F}_n(z_1, \dots, z_n) .$$

- The fields are connected by a map called “operator product expansion” (OPE)

$$\mathcal{H} \times \mathcal{H} \longrightarrow \mathcal{H}\{z, \bar{z}\}$$

where $\mathcal{H}\{z, \bar{z}\}$ signifies the space of real analytic functions with the following pole structure at $z = 0$

$$f(z, \bar{z}) = \sum_{r \in R, n \in \mathbb{Z}} a_{rn} z^{r+n} \bar{z}^r \quad R \subset \mathbb{R} \text{ countable} .$$

To obtain a well-defined CFT we only allow for finitely many terms with $r < 0$ or $r + n < 0$ for which the coefficients $a_{rn} \neq 0$ in $f(z, \bar{z})$.

- We further need a special field $T(z)$ of conformal weight $(h, \tilde{h}) = (2, 0)$ as well as its antiholomorphic correspondence $\tilde{T}(\bar{z})$. The charge of a field wrt $T(z)$ is given by its grading. Hence, $T(z)$ represents the energy momentum tensor; sometimes it is also called “Virasoro field”.

Using the state field correspondence we can translate these n point functions or “correlators” to the better known appearance in terms of fields

$$|\Phi^{(1)}\rangle \otimes \dots \otimes |\Phi^{(n)}\rangle \xrightarrow{F_n} \langle 0 | \Phi^{(1)}(z_1, \bar{z}_1) \dots \Phi^{(n)}(z_n, \bar{z}_n) |0\rangle .$$

In this presentation we see that consistency requires the n point functions \mathcal{F}_n to be compatible with the Shapovalov form and the OPE as the OPE can be translated to an OPE of fields in a similar way

$$\Phi^{(1)}(z_1, \bar{z}_1) \Phi^{(2)}(z_2, \bar{z}_2) = \sum_{|\Phi^{(i)}\rangle \in \mathcal{H}} (z_1 - z_2)^{h_i - h_1 - h_2} (\bar{z}_1 - \bar{z}_2)^{\tilde{h}_i - \tilde{h}_1 - \tilde{h}_2} \Phi^{(i)}(z_i, \bar{z}_i) . \quad (2.1)$$

The special form of the exponents applies to fields corresponding to eigenstates of the zero-mode L_0 of the energy momentum tensor to be defined below; in particular, it applies to the important class of primary fields which will be introduced shortly.

The energy momentum tensor $T(z)$ is the generator of the conformal symmetry transformations on the fields of the theory and, hence, leads to conformal Ward identities. Its OPE with itself can be shown to be

$$T(z)T(w) \sim \frac{c/2}{(z-w)^4} + \frac{2T(w)}{(z-w)^2} + \frac{\partial T(w)}{(z-w)} + \text{non singular terms} . \quad (2.2)$$

The parameter c is called the “central charge” and is one of the main classifying parameters of a CFT model.

The Virasoro field is actually part of the most important subspace of \mathcal{H} , the space of holomorphic fields which is also called the holomorphic \mathcal{W} -algebra. These holomorphic fields generate the symmetry transformations of the theory. Certainly, there also is an antiholomorphic counterpart, the antiholomorphic \mathcal{W} -algebra.

In the following we want to restrict ourself to holomorphic fields on the Riemann sphere \mathbb{C}^* . All these fields can be expanded into Laurent series of modes

$$\Phi(z) = \sum_{n \in \mathbb{Z}} \Phi_n z^{-n-h}$$

where the modes Φ_n can be calculated as a contour integral

$$\Phi_n = \frac{1}{2\pi i} \oint_{|z|<\epsilon} dz z^{h+n-1} \Phi(z) .$$

The OPE of two fields can be translated into a commutator of the modes of these fields using the following contour prescription

$$\begin{aligned} [\Phi_m, \Psi_n] &= \oint_0 dz \oint_{0, |z|>|w|} dw z^{h_\Phi+m-1} w^{h_\Psi+n-1} \Phi(z) \Psi(w) \\ &\quad - \oint_0 dw \oint_{0, |w|>|z|} dz z^{h_\Phi+m-1} w^{h_\Psi+n-1} \Phi(z) \Psi(w) \\ &= \oint_0 dw \oint_w dz z^{h_\Phi+m-1} w^{h_\Psi+n-1} \Phi(z) \Psi(w) . \end{aligned} \quad (2.3)$$

Performing this with the above OPE of the Virasoro field (2.2) yields the celebrated “Virasoro algebra”

$$[L_m, L_n] = (m-n) L_{m+n} + \frac{c}{12} (m-1) m (m+1) \delta_{m+n,0} \quad m, n \in \mathbb{Z} .$$

In particular, the modes L_{-1} , L_0 and L_1 generate translations, scale transformations as well as the special conformal transformation, respectively. They are exactly the generators of the global conformal group $SL(2, \mathbb{C})$. These three generators close wrt the Virasoro algebra and, hence, form a subalgebra. The application of L_0 on a state $|\Phi_i\rangle \in V(h_i, \tilde{h}_i)$ yields its conformal weight h_i .

We will sometimes need the construction of a “normal ordered product” of two fields. In terms of the mode expansion this normal ordered product is given by an

ordering of the modes such that all modes which annihilate the vacuum are placed right to the creation modes. The normal ordered product can also be constructed directly from the OPE of two fields if the OPE exhibits only one singularity by

$$:\Phi_i\Phi_j:(z) = \lim_{w \rightarrow z} (\Phi_i(z)\Phi_j(w) - \langle \Phi_i(z)\Phi_j(w) \rangle) .$$

But often, the OPE of two fields exhibits more than one singularity which all have to be subtracted, e.g. for fields which are not free. Then, the subtraction scheme gets more involved and leads to a modified normal ordering prescription and a modified Wick theorem [9].

In unitary theories we can split \mathcal{H} completely into irreducible representations of the holomorphic and antiholomorphic Virasoro algebra. These are generated by “primary fields” $\psi_{h,\tilde{h}}$, i.e. fields with the following properties

$$\begin{aligned} L_0 \psi_{h,\tilde{h}} &= h \psi_{h,\tilde{h}} & L_n \psi_{h,\tilde{h}} &= 0 \quad \forall n > 0 \\ \tilde{L}_0 \psi_{h,\tilde{h}} &= \tilde{h} \psi_{h,\tilde{h}} & \tilde{L}_n \psi_{h,\tilde{h}} &= 0 \quad \forall n > 0 . \end{aligned}$$

The other fields in the representation are then constructed by application of L_n and \tilde{L}_n , $n < 0$. They are called “descendant fields”.

Let us have a closer look at these representations and let us, for simplicity, restrict to the holomorphic side of \mathcal{H} . Then the freely generated so-called “Verma module” on a highest weight state v_h to the highest weight h is given by

$$\mathcal{M}(h) = \{L_{-n_1} \dots L_{-n_k} v_h | n_1 \geq \dots \geq n_k > 0, k \in \mathbb{Z}^+\} .$$

In order to find the irreducible or at least indecomposable representation we need to identify the largest true subrepresentation of $\mathcal{M}(h)$ which decouples from the rest of the representation and need to construct the respective factor module.

A subrepresentation can be generated from any “singular vector” v in $\mathcal{M}(h)$, i.e. a vector which obeys $L_p v = 0 \forall p > 0$ and which is, hence, a highest weight state of its own; and certainly we can also have unions of such representations. On the other hand, a subrepresentation only decouples from the rest of the representation and can, thus, be factored out if it consists of “nullvectors”, i.e. vectors which are orthogonal to all other vectors in the Hilbert space of states \mathcal{H} wrt the Shapovalov form. As long as a representation is irreducible, singular vectors are at the same time nullvectors and generate subrepresentations which are null in \mathcal{H} . However, the interrelation between singular vectors and nullvectors becomes much more intricate as soon as we deal with indecomposable but not irreducible representations as in section 2.2 or in chapter 4.

The field content of a Verma module or any smaller irreducible representation \mathcal{R} of the Virasoro algebra which has been constructed from a Verma module by factoring out the maximal decoupling subrepresentation can be summarised in the so-called “character of the module”

$$\begin{aligned} \chi_{(c,h)}(\tau) &= \text{tr}_{\mathcal{R}} q^{L_0 - \frac{c}{24}} \quad q = e^{2\pi i \tau} \\ &= \sum_{n=0}^{\infty} \beta(h, c; n) q^{n+h-\frac{c}{24}} \end{aligned}$$

where the trace has to be taken over the whole representation \mathcal{R} and the integer constants $\beta(h, c; n)$ give the number of states in that representation at level n . The character of a generic Verma module is given by

$$\chi_{(c,h)}^{\text{Vir}}(\tau) = \frac{q^{h+\frac{1-c}{24}}}{\eta(q)};$$

$\eta(q)$ signifies the standard η function with

$$\frac{1}{\eta(q)} = q^{-\frac{1}{24}} \prod_{n=1}^{\infty} \frac{1}{1-q^n} = q^{-\frac{1}{24}} \sum_{i=0}^{\infty} p(i) q^i$$

where $p(i)$ denotes the number of partitions of the integer i .

The above properties of primary fields also induce their transformation properties under local conformal transformations $z \mapsto w(z)$

$$\Phi'(w, \bar{w}) = \left(\frac{dw}{dz} \right)^{-h} \left(\frac{d\bar{w}}{d\bar{z}} \right)^{-\bar{h}} \Phi(z, \bar{z}),$$

where the prime indicated the internal symmetry transformation of the field itself. An n point function of primary fields, hence, transforms according to

$$\begin{aligned} \langle \Phi_1(w_1, \bar{w}_1) \dots \Phi_n(w_n, \bar{w}_n) \rangle &= \\ &= \prod_{i=1}^n \left(\frac{dw_i}{dz_i} \right)^{-h_i} \left(\frac{d\bar{w}_i}{d\bar{z}_i} \right)^{-\bar{h}_i} \langle \Phi_1(z_1, \bar{z}_1) \dots \Phi_n(z_n, \bar{z}_n) \rangle. \end{aligned}$$

Now, the form of all 1, 2 and 3 point functions of primary fields is already restricted by their transformation properties, i.e. by the behaviour of primary fields under conformal transformations, to the form

$$\begin{aligned} \langle \Phi(z, \bar{z}) \rangle &= 0 \\ \langle \Phi_1(z, \bar{z}) \Phi_2(w, \bar{w}) \rangle &= \frac{C_{II} \delta_{h_1, h_2} \delta_{\bar{h}_1, \bar{h}_2}}{(z-w)^{h_1} (\bar{z}-\bar{w})^{\bar{h}_1}} \\ \langle \Phi_1(z_1, \bar{z}_1) \Phi_2(z_2, \bar{z}_2) \Phi_3(z_3, \bar{z}_3) \rangle &= C_{III} \prod_{i<j} \frac{1}{(z_i - z_j)^{h_{ij}}} \prod_{i<j} \frac{1}{(\bar{z}_i - \bar{z}_j)^{\bar{h}_{ij}}} \quad (2.4) \end{aligned}$$

where $h_{12} = h_1 + h_2 - h_3$ etc. and where C_{II} and C_{III} represent the structure constants of the 2 respectively 3 point function. The above form of the 3 point function finally justifies the special form of the OPE of two primary fields given in (2.1).

If we want to calculate the OPE of two fields $\Phi_1(z)$ and $\Phi_2(w)$ which belong to two representations of the Virasoro algebra the conformal representation theory restricts the possible representations of resulting fields quite severely. The result of such considerations is summarised in the so-called ‘‘fusion product’’ of two fields denoted

$$\Phi_1 \otimes_f \Phi_2 = \sum_{i \in \Delta} \Phi_i$$

where the set Δ is to be determined by representation theory. Except for the explicit structure constants the fusion product contains all vital information about the behaviour of the OPE in a CFT model; the analytic behaviour is already determined by conformal transformation properties as in the above 3 point function or in the OPE (2.1).

The CFT partition function

If we want to perform perturbation theory e.g. in string theory we have to take care that the CFT is well-defined on all Riemann surfaces. The most important restrictions to the field content can already be seen regarding the genus $g = 1$ surfaces.

The genus $g = 1$ zero point amplitude corresponds to the worldsheet of a torus, which we take to be defined by the two periods ω_0 and ω_1 . Making the fields propagate on this torus yields the so-called “partition function” of the theory of form

$$Z(\tau) = \text{tr}_{\mathcal{H}} \left(q^{L_0 - \frac{c}{24}} \bar{q}^{\tilde{L}_0 - \frac{c}{24}} \right) \quad q = \exp(2\pi i\tau)$$

with the “modular parameter” $\tau = \omega_0/\omega_1$. The trace in $Z(\tau)$, which has to be taken over the complete Hilbert space of states \mathcal{H} , originates in the additional periodicity in the time direction on the torus worldsheet. If we regard $Z(\tau)$ as a formal polynomial in q and \bar{q} it is easy to read off the field content which consistently propagates on this torus. Indeed, the coefficient of a monomial $q^{h - \frac{c}{24}} \bar{q}^{\tilde{h} - \frac{c}{24}}$ is an integer number and yields the number of fields with conformal weight (h, \tilde{h}) .

The reason for this very nice behaviour of the partition function can be found in the inherent symmetry of the torus worldsheet. The lattice periods of the torus are unique only up to transformations in the “modular group” $SL(2, \mathbb{Z})$. Hence, the partition function is also supposed to be invariant under this group action, i.e. modular invariant. A $SL(2, \mathbb{Z})$ transformation of the modular parameter τ can be written as

$$\tau \longmapsto \frac{a\tau + b}{c\tau + d} \quad a, b, c, d \in \mathbb{Z} \text{ and } ad - bc = 1.$$

The modular group is generated e.g. by the following two generators

$$\begin{aligned} T : \tau &\longmapsto \tau + 1 \\ S : \tau &\longmapsto \frac{-1}{\tau}. \end{aligned}$$

Thus, it is sufficient to show invariance under these two generators if one wants to show invariance under the whole modular group.

If one knows the characters of the complete set of representations in the CFT model one can also write down the partition function in terms of these characters

$$Z(\tau) = \sum_{h, \tilde{h}} N_{h, \tilde{h}} \chi_h(\tau) \chi_{\tilde{h}}(\bar{\tau})$$

where $N_{h,\tilde{h}}$ denotes the multiplicity of the occurrence of the respective (h, \tilde{h}) representation. Certainly, the possible $N_{h,\tilde{h}}$ are restricted to those which yield a modular invariant partition function $Z(\tau)$.

Modular invariance restricts the number of possible partition functions and, hence, the possible field content of CFT very severely. It can actually be shown to be sufficient to guarantee a well-defined CFT. Modular functions and modular forms, which are the building blocks of our modular invariant partition functions, are very well-studied objects of the mathematical literature with a plenitude of nice and astonishing properties. We will only need some special modular functions in this thesis and will quote them as well as some of their properties when needed.

Superconformal field theory

The holomorphic \mathcal{W} -algebra quite frequently contains more symmetry fields than just the Virasoro field. One very important case of such an extension is the superconformal field theory which incorporates supersymmetry in the CFT setting. Then, the \mathcal{W} -algebra additionally contains at least one supercurrent $G(z)$ with OPEs

$$\begin{aligned} T(z)G(w) &= \frac{3/2}{(z-w)^2} G(w) + \frac{\partial_w G(w)}{z-w} + \dots \\ G(z)G(w) &= \frac{2/3 c}{(z-w)^3} + \frac{2T(w)}{z-w} + \dots ; \end{aligned}$$

the fermionic $(h, \tilde{h}) = (3/2, 0)$ field $G(z)$ is the worldsheet superpartner of the Virasoro field $T(z)$. We will mainly deal with an extended form of supersymmetry, $N = 2$ supersymmetry. The extended supersymmetry introduces even three more fields to the \mathcal{W} -algebra besides the Virasoro field, two supercurrents $G^1(z)$ and $G^2(z)$ as well as a bosonic $U(1)$ current $J(z)$. We prefer to work in the following basis

$$G^\pm(z) = \frac{1}{\sqrt{2}} (G^1(z) \pm iG^2(z)) .$$

Then the complete $N = 2$ superconformal algebra is given by [77]

$$\begin{aligned} T(z)T(w) &= \frac{c/2}{(z-w)^4} + \frac{2T(w)}{(z-w)^2} + \frac{\partial T(w)}{z-w} + \dots \\ T(z)G^\pm(w) &= \frac{3/2}{(z-w)^2} G^\pm(w) + \frac{\partial_w G^\pm(w)}{z-w} + \dots \\ T(z)J(w) &= \frac{J(w)}{(z-w)^2} + \frac{\partial_w J(w)}{z-w} + \dots \\ G^+(z)G^-(w) &= \frac{2/3 c}{(z-w)^3} + \frac{J(w)}{(z-w)^2} + \frac{2T(w) + \partial_w J(w)}{z-w} + \dots \\ J(z)G^\pm(w) &= \pm \frac{G^\pm(w)}{z-w} + \dots \end{aligned}$$

$$J(z)J(w) = \frac{c/3}{(z-w)^2} + \dots \quad (2.5)$$

The supersymmetry which is mediated by the supercurrents associates a fermion to every boson and vice versa (due to the extended $N = 2$ supersymmetry bosons and fermions are collected in even larger $N = 2$ multiplets). Both bosons and fermions can fulfil two different types of boundary conditions; for both types of fields there are, hence, two different sectors in the theory: the ‘‘Ramond’’ (R) sector which obeys antiperiodic boundary conditions on the plane and the ‘‘Neveu-Schwarz’’ (NS) sector which obeys periodic boundary conditions on the plane. These two sectors lead to different mode expansions and, hence, to different expressions of the $N = 2$ mode algebra (with $a = 0$ for the R and $a = 1/2$ for the NS sector) [77]

$$\begin{aligned} [L_m, L_n] &= (n-m)L_{m+n} + \frac{c}{12}n(n^2-1)\delta_{m+n,0} \\ [J_m, J_n] &= -\frac{c}{3}m\delta_{m+n,0} \\ [L_m, J_n] &= mJ_{m+n} \\ [L_m, G_{n\pm a}^\pm] &= \left(n \pm a - \frac{m}{2}\right) G_{m+n\pm a}^\pm \\ [J_m, G_{n\pm a}^\pm] &= \pm G_{m+n\pm a}^\pm \\ \{G_{m+a}^+, G_{n-a}^-\} &= 2L_{m+n} + (n-m-2a)J_{n+m} + \frac{c}{3}\left((m+a)^2 - \frac{1}{4}\right)\delta_{m+n,0}. \end{aligned}$$

In a $N = 2$ superconformal field theory the conditions for a primary state extend to

$$L_n |\Phi\rangle = 0 \quad G_r^\pm |\Phi\rangle = 0 \quad J_m |\Phi\rangle = 0 \quad n, r, m > 0.$$

This leads to the following OPEs of a primary field with the symmetry currents

$$T(z)\Phi(w) = \frac{h}{(z-w)^2}\Phi(w) + \frac{1}{z-w}\partial_w\Phi(w) + \dots \quad (2.6)$$

$$J(z)\Phi(w) = \frac{q}{z-w}\Phi(w) + \dots \quad (2.7)$$

$$G^\pm(z)\Phi(w) = \frac{\tilde{\Phi}^\pm(w)}{z-w} + \dots \quad (2.8)$$

where q represents the $U(1)$ charge wrt $J(z)$ and $\tilde{\Phi}^\pm(z)$ the superpartners of $\Phi(z)$.

There is a special type of primary field which is of central importance for superconformal field theories, the so-called ‘‘chiral primary fields’’. These obey the additional condition

$$G_{-1/2}^+ |\Phi\rangle = 0 \quad \text{respectively} \quad G^+(z)\Phi(w) = \text{regular}.$$

It can be shown that

- a field is chiral exactly if $h = q/2$,
- the conformal weight of chiral primary fields has an upper bound of $c/6$,
- the OPE of two chiral primary fields does not contain a singular term and its constant term is a chiral primary again. Thus, the chiral primaries form a ring, the “chiral ring”.

Analogously, we define the “anti-chiral primary fields” by

$$G_{-1/2}^- |\Phi\rangle = 0 \quad \text{respectively} \quad G^-(z)\Phi(w) = \text{regular} .$$

They form the “anti-chiral ring” and obey $h = -q/2$. Coupling of the holomorphic and the antiholomorphic sector actually yields four rings, the (c, c) , (a, a) , (c, a) , and (a, c) ring.

The partition function of a superconformal field theory is defined to be that of the bosonic subtheory [32]. But, due to the different boundary conditions it naturally splits into four parts, the NS and R parts as well as the two twisted versions \widetilde{NS} and \widetilde{R}

$$Z(\tau) = \frac{1}{2} \left(Z_{NS} + Z_R + Z_{\widetilde{NS}} + Z_{\widetilde{R}} \right) .$$

The two twisted parts are constructed by inclusion of the fermion number operator $(-1)^F$ which commutes with bosons, anticommutes with fermions and is 1 on the $SL(2, \mathbb{C})$ invariant vacuum $|0\rangle$. The two NS parts are e.g. given by

$$\begin{aligned} Z_{NS}(\tau, z) &= \text{tr}_{NS} \left(q^{L_0 - \frac{c}{24}} \bar{q}^{\tilde{L}_0 - \frac{c}{24}} y^{J_0} \bar{y}^{\tilde{J}_0} \right) \\ Z_{\widetilde{NS}}(\tau, z) &= \text{tr}_{NS} \left((-1)^F q^{L_0 - \frac{c}{24}} \bar{q}^{\tilde{L}_0 - \frac{c}{24}} y^{J_0} \bar{y}^{\tilde{J}_0} \right) . \end{aligned}$$

with $y = \exp(2\pi iz)$. These supersymmetric partition functions, furthermore, include the $U(1)$ current $J(z)$ in order to keep track of the $U(1)$ charges of the fields. The coefficients of the different monoms in q , \bar{q} , y and \bar{y} yield the numbers of fields with the exponents as weights respectively charges.

Although the partition function only ranges over the bosonic space of states, this natural split makes it possible to access the full field content. Indeed, Z_{NS} and Z_R contain all bosonic and fermionic fields of the NS respectively R sectors.

Mapping the CFT from the plane to a cylinder, which we need to do in order to form a torus, actually inverts the boundary conditions; periodic (P) boundary conditions become antiperiodic (A) and vice versa. This leads to the following list of boundary conditions for the different sectors; they are presented as tuples denoting both the boundary condition in (imaginary) time as well as in space direction

$$\begin{aligned} (A, A) &\rightsquigarrow NS \\ (P, A) &\rightsquigarrow \widetilde{NS} \\ (A, P) &\rightsquigarrow R \\ (P, P) &\rightsquigarrow \widetilde{R} . \end{aligned} \tag{2.9}$$

On the other hand, $N = 2$ superconformal field theories can be shown to possess so-called “spectral flow operators” which transfer between the different sectors. This spectral flow allows to calculate all sectors of the partition function as soon as one part is fixed [77].

The explicit models of compactification on a complex two-dimensional torus or K3 examined in chapter 3 actually exhibit an even higher extension of supersymmetry, $N = 4$ supersymmetry in the holomorphic as well as in the antiholomorphic sector. The corresponding superconformal algebra is generated by four supercurrents, the Virasoro field and an $su(2)_1$ Kac-Moody algebra of three bosonic $U(1)$ currents [78, 79, 80, 81, 32]. But as for our purposes we will always choose a suitable $N = 2$ subalgebra of this, we will not explore $N = 4$ supersymmetry further.

2.2 Logarithmic conformal field theory

Logarithmic conformal field theory is a generalisation of ordinary CFT which allows for an indecomposable action of the L_0 Virasoro mode. These higher rank Jordan cells wrt the L_0 action actually lead to the appearance of logarithms in correlation functions and OPEs. It is this symptom which is responsible for the admittedly somewhat strange naming of “logarithmic CFT”. We will give a short introduction to this phenomenon as well as the terminology as needed in this thesis in the following. Logarithmic CFT models are non-unitary theories. Nevertheless, they mostly exhibit the same basic ingredients and conditions as the unitary CFTs introduced in section 2.1. An important exception applies to the $h = 0$ subspace of \mathcal{H} which might not contain only one unique state, the vacuum, but which also may exhibit a higher rank Jordan cell. Its Shapovalov form has to be adapted accordingly, and the vacuum may even not be normalisable as for ghost systems. The notation is intended to stay close to that of the review [82]. Other important introductions to this topic can be found in [83, 84, 85].

Let us regard such a representation with higher rank indecomposable L_0 action and let us first assume that we have a Jordan cell of lowest weight states with weight h of rank r . Without loss of generality this Jordan cell can be taken to be spanned by a basis of states

$$|h; n\rangle = \frac{1}{n!} \theta^n |h\rangle \quad \forall n = 0, \dots, r-1$$

on which the action of the Virasoro modes is given by

$$\begin{aligned} L_0 |h; n\rangle &= h |h; n\rangle + (1 - \delta_{n,0}) |h; n-1\rangle \\ &\equiv (h + \partial_\theta) |h; n\rangle, \\ L_p |h; n\rangle &= 0 \quad \forall p > 0; \end{aligned}$$

the basis can always be re-diagonalised in order to bring the matrix of the L_0 action into such a standard Jordan diagonal form. As already defined in [82], θ is a nilpotent variable with $\theta^r = 0$ and a handy tool to organise the Jordan cell states with the same

weight. Due to their almost primary behaviour with the only defect of an additional term in the indecomposable L_0 action we will call the $|h; n\rangle$ “logarithmic primary”. We also note that $|h; 0\rangle$ is indeed a true primary state. The variable $n = 0, \dots, r - 1$ denotes the position of the state in the Jordan cell; we will call this position the “Jordan level” of that state as well as its descendants in that respective Jordan cell. The states with Jordan level $n > 0$ are also frequently called the “logarithmic partners” of $|h; 0\rangle$, especially in the case of rank $r = 2$.

But, it is certainly not vital to assume that such a higher rank Jordan cell or the Jordan cell with the highest rank in the respective representation already appear at lowest weight level. We might e.g. encounter a rank 2 Jordan cell at level l , i.e. we have a groundstate $|h\rangle$ and a Jordan cell at level l

$$\begin{aligned} L_0 |h + l; 1\rangle &= (h + l) |h + l; 1\rangle + |h + 1; 0\rangle \\ L_0 |h + l; 0\rangle &= (h + l) |h + l; 0\rangle \end{aligned}$$

where $|h + l; 0\rangle$ is a descendant of $|h\rangle$. The logarithmic partner $|h + l; 1\rangle$, however, is a second generating state for this rank 2 representation. The important difference to the previous case is that the logarithmic partner state is now not logarithmic primary but can be and usually is mapped to lower level descendants of $|h\rangle$ by positive Virasoro modes. All other higher rank indecomposable representations can be treated in a similar manner.

It appears that all lowest states of a Jordan cell are always singular states. Up to now as well as in this thesis there is no indication that a higher rank representation could be constructed with another setup in a consistent way. In particular, the descendant $|h + l; 0\rangle$ which is a building block of the rank 2 Jordan cell in the above described rank 2 representation is a singular descendant of $|h\rangle$. But, different from the ordinary CFT case this singular vector is not automatically a nullvector of the theory. It certainly is a nullvector in the Virasoro module spanned on $|h\rangle$. However, the inclusion of the logarithmic partner state $|h + l; 1\rangle$ provides a state which has a non-vanishing Shapovalov form with this singular descendant.

The generalised L_0 action with higher rank behaviour also induces generalised logarithmic two-point-functions which yield the following Shapovalov form on a Jordan cell of states [55]

$$\langle h; k | h; l \rangle = \begin{cases} 0 & \forall l + k < r - 1 \\ 1 & \forall l + k = r - 1 \\ D_{l+k-r+1} & \forall l + k > r - 1 \end{cases} \quad (2.10)$$

for constant D_j , $j = 1, \dots, r - 1$.

Furthermore, we can exploit the introduced formalism to deduce that the action of any function of the Virasoro zero-mode and the central charge operator $f(L_0, C)$ on such a Jordan cell state is given by [82]

$$f(L_0, C) |h; n\rangle = \sum_{k=0}^n \frac{1}{k!} \left(\frac{\partial^k}{\partial h^k} f(h, c) \right) |h; n - k\rangle. \quad (2.11)$$

As in the ordinary CFT case we can associate a field $\Psi_{(h;n)}(w)$ to each state in Hilbert space $|h;n\rangle$. Going back to the case where the Jordan cell is spanned on the lowest weight level h , $\Phi_h(w) := \Psi_{(h;0)}(w)$ is a primary field and the $\Psi_{(h;n)}(w)$, $n > 0$, are its logarithmic primary partners. The action of the Virasoro modes onto these logarithmic fields is then given by

$$\begin{aligned} \mathcal{L}_{-k}(z) \Psi_{(h;n)}(w) \\ = \frac{(1-k)h}{(z-w)^k} \Psi_{(h;n)}(w) - \frac{1}{(z-w)^{k-1}} \frac{\partial}{\partial w} \Psi_{(h;n)}(w) + (1-\delta_{n,0}) \frac{1-k}{(z-w)^k} \Psi_{(h;n-1)}(w). \end{aligned}$$

However, due to the indecomposable structure \mathcal{L}_{-k} is not a diagonalisable operator any more. One can use these operators \mathcal{L}_{-k} to extend the conformal Ward identities to the logarithmic case. Then, these identify the logarithmic two- and three-point-functions uniquely up to structure constants.

These equations can easily be extended to the more complicated logarithmic representations taking into account the descendant behaviour of fields which are (singular) descendants of fields of lower conformal weight.

2.3 Important models

In the following we give an overview over the four types of conformal field theory models which are important in this thesis. These are the minimal models, the Gepner models as well as the torus sigma models and orbifolds thereof.

2.3.1 The Kac determinant and minimal models

The Kac determinant parameterises the relation between conformal charges c and spectra of conformal weights $h_{r,s}$ at which we encounter nullvectors. It is, hence, an ingenious tool to explore interesting conformal field theories with relatively few and small representations.

Let us start with the Gram matrix M of Shapovalov forms of all basis states of the Verma module $\mathcal{M}(h)$ with each other. This matrix is block diagonal as states of different descendant level l have vanishing Shapovalov form with each other. According to Kac, the determinant of the level l block M^l of M can be factorised according to (see e.g. [9])

$$\det M^{(l)} = \alpha_l \prod_{r,s \geq 1, rs \leq l} \left[h - h_{r,s}(c) \right]^{p(l-rs)}$$

where $p(l-rs)$ signifies the number of partitions of the integer $l-rs$ and α_l is a positive constant. The zeros of the Kac determinant are given by the central charge

$$c = c_{p,q} = 1 - 6 \frac{(p-q)^2}{pq} \quad 1 \leq p, q \in \mathbb{Z}$$

where p and q do not have a common divisor as well as the highest weight spectrum

$$h_{r,s} = \frac{(pr - qs)^2 - (p - q)^2}{4pq} \quad 1 \leq r \in \mathbb{Z}, 1 \leq s \in \mathbb{Z}.$$

Accordingly, theories with weights of the form $h_{r,s}$ at the corresponding central charge $c_{p,q}$ exhibit a rich nullvector structure to be described below. Furthermore, this Kac determinant shows that for central charge $c < 1$ we can only consistently construct unitary theories, i.e. theories which do not exhibit negative norm states, for the restricted series of $c_{m+1,m}$.

The so-called “minimal models” are a series of such conformal field theories which manage to extract the smallest possible representation theory from the Kac table of weights for some central charge $c_{p,q}$ by relating all weights to some standard cell $\{(r, s) | 1 \leq r < q, 1 \leq s < p\}$ subject to the relation [4, 9]

$$h_{r,s} = h_{q-r,p-s}. \quad (2.12)$$

All larger weights are related to this standard cell by the addition of integers according to the relations [4, 9]

$$\begin{aligned} h_{r,s} &= h_{r+q,s+p} \\ h_{r,s} + rs &= h_{q+r,p-s} = h_{q-r,p+s} \\ h_{r,s} + (q-r)(p-s) &= h_{r,2p-s} = h_{2q-r,s} \end{aligned} \quad (2.13)$$

as long as they are in the bulk and not on the border or corners of this standard cell Kac table, i.e. as long as their indices do not obey $r = iq$ or $s = jp$ for some $i, j \in \mathbb{Z}$.

These larger weights in the Kac table bulk are exactly the weights of the nullvector descendants of the highest weights in the above standard cell. To be precise we actually find that the maximal subrepresentation of $\mathcal{M}(h)$ for h in the bulk of the Kac table is generated by two singular vectors v_1, v_2 . The highest weight representations generated on v_1 and v_2 , however, each contain two subrepresentations which are again both generated from two singular vectors; but actually both subrepresentations of $\mathcal{M}(v_1)$ and $\mathcal{M}(v_2)$ coincide. We therefore arrive at an embedding structure or “embedding cascade” of nullvectors as depicted in figure 2.1b [3, 9] whose weights are exactly the integer shifted weights appearing in the Kac table.

The corresponding characters are given by the Rocha-Caridi character formula [86]

$$\chi_{(r,s)}(\hat{q}) = \frac{1}{\eta(\hat{q})} \sum_{n \in \mathbb{Z}} \left[\hat{q}^{(2pqn+pr-qs)^2/4pq} - \hat{q}^{(2pqn+pr+qs)^2/4pq} \right]$$

where we have changed the customary name for the modular parameter to $\hat{q} = e^{2\pi i\tau}$ just for this equation in order to prevent the reader from mixing this up with the parameter q of the minimal model.

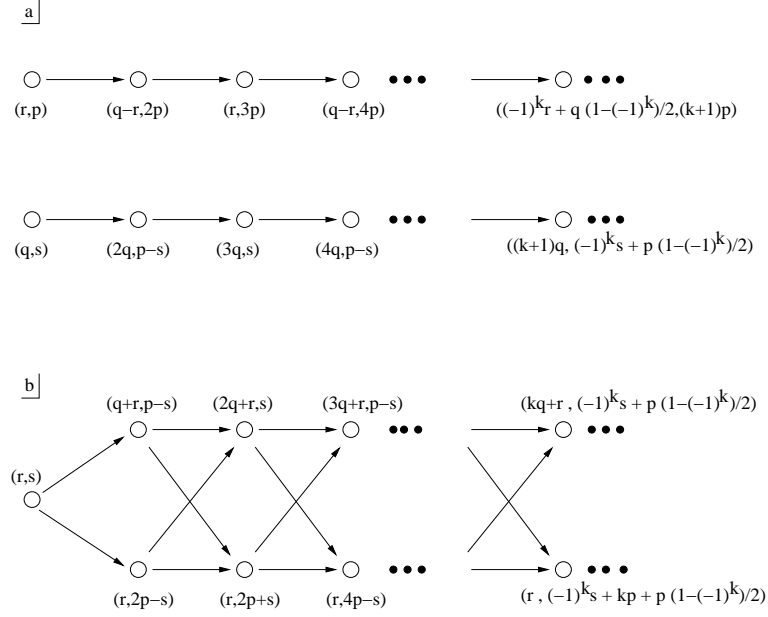


Figure 2.1: Nullvector embedding structure [9]

The irreducible representations $\mathcal{V}_{(r,s)}$ with weights $h_{r,s}$ in this standard cell and the described nullvector embedding structure have been shown to close under the following so-called BPZ fusion rules [4]

$$\mathcal{V}_{(r_1,s_1)} \otimes_f \mathcal{V}_{(r_2,s_2)} = \sum_{\substack{r_3=|r_1-r_2|+1 \\ \text{step } 2}}^{\min(r_1+r_2-1, 2q-r_1-r_2-1)} \sum_{\substack{s_3=|s_1-s_2|+1 \\ \text{step } 2}}^{\min(s_1+s_2-1, 2p-s_1-s_2-1)} \mathcal{V}_{(r_3,s_3)},$$

where \otimes_f denotes the fusion product. We notice that the above excluded weights for $r = iq$ or $s = jp$ with $i, j \in \mathbb{Z}$, do not pop up in these fusion rules; they are, hence, simply ignored in these minimal models.

2.3.2 Torus sigma models

Bosonic toroidal CFTs

Another important example of CFT models is represented by “toroidal conformal field theories”, which are mainly motivated by string theory. A bosonic toroidal CFT is given by a nonlinear sigma model of the Polyakov action

$$S_{\text{Pol}} = \int d^2z (G_{ij} + B_{ij}) \partial X_i \bar{\partial} X_j$$

whose coordinate fields X_i , $i = 1 \dots d$, are compactified on a torus; the dimensionality of this torus target space is denoted by d . The geometry of this sigma model is described

by the two background fields, the metric G_{ij} and the asymmetric background B-field B_{ij} , $B \in \text{Skew}(d \times d, \mathbb{R})/\text{Skew}(d \times d, \mathbb{Z})$.

The torus which this theory is compactified on is given by a lattice Λ ; it is isomorphic to the coset space \mathbb{R}^d/Λ . Let λ_i be the generators of this lattice Λ and let $\mu_i \in \Lambda^*$ be the dual vectors to these generators. We want to restrict to the examination of closed strings, i.e. we introduce the worldsheet periodicity in the spatial direction. But, due to the periodicity conditions in the coset target space this worldsheet periodicity condition on the coordinate fields has to be relaxed to

$$X_i(e^{2\pi i} z, e^{-2\pi i} \bar{z}) = X_i(z, \bar{z}) + 2\pi w_i \quad w \in \Lambda$$

(as the complex coordinate z has been chosen to be radial $z = e^{\sigma_0 + i\sigma_1}$). The vector w describes the winding of the string around the compact dimensions.

The field content of the torus CFT is described by quantum numbers wrt the d holomorphic $U(1)$ currents $j_i(z) = i\partial X_i$ with OPE

$$j_i(z) j_j(w) \sim \frac{\delta_{ij}}{(z-w)^2}$$

as well as their antiholomorphic counterparts $\tilde{j}_i(z)$. The Sugawara construction then yields an energy momentum tensor

$$T_{\text{bos}}(z) = \sum_i : j_i j_i : (z) .$$

The central charge can, thus, be calculated to be $c = d$.

The primary fields of this theory are given by vertexoperators $V_{(P_l, P_r)}(z, \bar{z})$ whose charges (P_l, P_r) wrt the above $U(1)$ currents $J = (j_1, \dots, j_d)^t$ span the charge lattice $\Gamma(\Lambda, B) \subset \mathbb{R}^{d,d}$. The conformal weight of a vertexoperator is then given by $(h, \tilde{h}) = \left(\frac{P_l^2}{2}, \frac{P_r^2}{2}\right)$. Each element of this charge lattice $\Gamma(\Lambda, B)$ can be parameterised by two vectors $\lambda \in \Lambda$ and $\mu \in \Lambda^*$ (with $B^* = \Lambda^T B \Lambda$, $\tilde{B} = \frac{1}{2}B^*$) [9, 32]

$$\begin{aligned} (P_l(\mu, \lambda), P_r(\mu, \lambda)) &= \frac{1}{\sqrt{2}} \left(\mu - B^* \lambda + \lambda, \mu - B^* \lambda - \lambda \right) \\ &= \left(p + \left(\frac{1}{2} - \tilde{B} \right) w, p - \left(\frac{1}{2} + \tilde{B} \right) w \right) ; \end{aligned}$$

$p = \frac{1}{\sqrt{2}}\mu$ signifies the momentum, and $w = \sqrt{2}\lambda$ the winding of the string on the respective torus. The scalar product is the standard scalar product on $\mathbb{R}^{d,d}$

$$\left\langle (P_l(\mu, \lambda), P_r(\mu, \lambda)), (P'_l(\mu', \lambda'), P'_r(\mu', \lambda')) \right\rangle = P_l(\mu, \lambda) P'_l(\mu', \lambda') - P_r(\mu, \lambda) P'_r(\mu', \lambda') .$$

Hence, we see that $\Gamma(\Lambda, B)$ is actually a selfdual even integer lattice with signature (d, d) , i.e.

- $\Lambda = \Lambda^*$
- $\langle e, e \rangle \in 2\mathbb{Z} \quad \forall e \in \Gamma(\Lambda, B)$.

The even integrality of this lattice is a direct consequence of the locality of conformal fields wrt each other and the integrality of the conformal spin $h - \tilde{h}$. The torus partition function whose form is dictated by modular invariance is then responsible for the selfduality of the lattice. Indeed, the partition function of a bosonic torus theory can be shown to be [9]

$$\mathcal{Z}_\Gamma^{\text{tor}}(\tau) = \frac{1}{|\eta(\tau)|^2} \sum_{(P_l, P_r) \in \Gamma(\Lambda, B)} q^{\frac{P_l^2}{2}} q^{\frac{P_r^2}{2}} \quad q = e^{2\pi i \tau}. \quad (2.14)$$

The OPE of such vertexoperators is given by

$$V_{P_1}(z_1, \bar{z}_1) V_{P_2}(z_2, \bar{z}_2) = c_{P_2}(-P_1) z_{12}^{P_{1r}^t P_{2r}} \bar{z}_{12}^{P_{1l}^t P_{2l}} V_{P_1+P_2}(z_2, \bar{z}_2) + \dots$$

$c_{P_2}(-P_1)$ is called a cocycle factor and depends on the charge vectors of both vertexoperators. These cocycle factors arise because in higher dimensional lattices the representation of affine algebras via the Kac-Frenkel-Siegel mechanism produces non-trivial structure constants and, hence, relative phases cannot be neglected any more, but have to be chosen such as to conform with the respective representation.

Rules for cocycle factors of a holomorphic vertexoperator algebra

The following presentation refers to [87]. The OPE of holomorphic vertexoperators can be written as

$$V_\alpha(z) V_\beta(w) = \epsilon(\alpha, \beta) (z - w)^{\alpha \cdot \beta} V_{\alpha + \beta},$$

with $\alpha, \beta \in \Xi$ the lattice of a Lie group. The relation to the above convention is given by $\lambda = \alpha/\sqrt{2}$, $\mu = (\alpha + B^* \alpha)/\sqrt{2}$. Besides the bare exponential $:\exp(i\alpha\phi(z)):$, these vertexoperators $V_\alpha(z)$ include a cocycle-operator $c(\alpha)$ which behaves according to

$$c(\alpha)c(\beta) = \epsilon(\alpha, \beta)c(\alpha + \beta).$$

Analysing this algebra, [87] find the following rules for the cocycle sign $\epsilon(\alpha, \beta)$ of the vertexoperator OPE

- $\epsilon(-\alpha, -\beta) = \epsilon(\alpha, \beta)$
- $\epsilon(\alpha, -\alpha) = 1$, the hermiticity condition
- $\epsilon(\alpha, 0) = \epsilon(0, \beta) = 1$
- $\epsilon(\alpha, \beta)\epsilon(\alpha + \beta, \gamma) = \epsilon(\alpha, \beta + \gamma)\epsilon(\beta, \gamma)$

- $\epsilon(\alpha, \beta) = -(-1)^{\alpha \cdot \beta + \alpha^2 \beta^2} \epsilon(\beta, \alpha)$ where $(-1)^{\alpha^2 \beta^2} = 1$ for even lattices.

If we want to construct an orbifold theory of a torus theory, in addition, we want to demand the invariance of the cocycle signs under the orbifold group action G

- $\epsilon(\Theta\alpha, \Theta\beta) = \epsilon(\alpha, \beta) \quad \forall \Theta \in G.$

A convenient choice of cocycle factor which obeys the above constraints is given by (see e.g. [88])

$$c_{P_2}(-P_1) = \exp \left[\frac{i}{2} \pi (p_2^t w_1 - p_1^t w_2) \right]. \quad (2.15)$$

For a holomorphic vertexoperator the right charge has to be (per definition) zero, i.e. $\mu - B^* \lambda = \lambda$, hence

$$(P_l, P_r) = (\sqrt{2}\lambda, 0) \quad \lambda \in \Lambda.$$

Inserting this into (2.15) yields a cocycle factor

$$\begin{aligned} c_{P_2}(-P_1) &= \exp \left[\frac{i}{4} \pi (P_{L_2}^t (1 - B^*) P_{L_1} - P_{L_1}^t (1 - B^*) P_{L_2}) \right] \\ &= \exp \left[\frac{i}{2} \pi P_{L_1}^t B^* P_{L_2} \right] \end{aligned} \quad (2.16)$$

and the corresponding cocycle sign $\epsilon(P_{L_1}, P_{L_2}) = c_{P_2}(-P_1)$.

Supersymmetric toroidal CFTs

This bosonic toroidal CFT can be extended to a supersymmetric theory by inclusion of d fermionic superpartners $\psi_i(z)$ of conformal weight $h = 1/2$ to the $U(1)$ currents j_i . Consequently, these obey the following OPE

$$\psi_i(z) \psi_j(w) \sim \frac{\delta_{ij}}{z - w}.$$

This supersymmetric extension yields a central charge of $c = 3d/2$. We now restrict the examination to theories of even dimension $d = 2D$ whose complex structure is more suitably expressed by the following choice of basis ($i = 1, \dots, D$)

$$\begin{aligned} X_{\pm}^{(i)} &= \frac{1}{\sqrt{2}} (X_i \pm i X_{i+D}) \\ j_{\pm}^{(i)} &= \frac{1}{\sqrt{2}} (j_i \pm i j_{i+D}) \\ \psi_{\pm}^{(i)} &= \frac{1}{\sqrt{2}} (\psi_i \pm i \psi_{i+D}). \end{aligned} \quad (2.17)$$

This set of fields yields the following non-vanishing OPEs

$$\begin{aligned} j_+^{(i)}(z) j_-^{(j)}(w) &\sim \frac{\delta^{ij}}{(z-w)^2} \\ \psi_+^{(i)}(z) \psi_-^{(j)}(w) &\sim \frac{\delta^{ij}}{z-w}. \end{aligned}$$

The superconformal toroidal theory compactified on an even dimensional torus exhibits $N = 2$ supersymmetry. The extended $N = 2$ supersymmetric Virasoro algebra is given in the above coordinates as [32]

$$\begin{aligned} T(z) &= \sum_{i=1}^{d/2} \left[:j_+^{(i)} j_-^{(i)} : (z) + \frac{1}{2} : \psi_+^{(i)} \partial \psi_-^{(i)} : (z) + \frac{1}{2} : \psi_-^{(i)} \partial \psi_+^{(i)} : (z) \right] \\ G^\pm(z) &= \sqrt{2} \sum_{i=1}^{d/2} : \psi_\pm^{(i)} j_\mp^{(i)} : (z) \\ J(z) &= \sum_{i=1}^{d/2} : \psi_+^{(i)} \psi_-^{(i)} : (z) \end{aligned} \quad (2.18)$$

as well as a similar antiholomorphic symmetry algebra. For the following let us signify such a supersymmetric toroidal theory with torus lattice Λ and B-field B by $\mathcal{T}(\Lambda, B)$.

The field content of these superconformal torus models is summarised in its partition functions. There are four different parts of the partition function corresponding to the four different sectors of the supersymmetric theory (as introduced in section 2.1)

$$\begin{aligned} Z_\Gamma^{NS}(\tau, z) &= Z_\Gamma^{\text{tor}}(\tau) \cdot \left| \frac{\theta_3(\tau, z)}{\eta(\tau)} \right|^d & Z_\Gamma^{\widetilde{NS}}(\tau, z) &= Z_\Gamma^{\text{tor}}(\tau) \cdot \left| \frac{\theta_4(\tau, z)}{\eta(\tau)} \right|^d \\ Z_\Gamma^R(\tau, z) &= Z_\Gamma^{\text{tor}}(\tau) \cdot \left| \frac{\theta_2(\tau, z)}{\eta(\tau)} \right|^d & Z_\Gamma^{\widetilde{R}}(\tau, z) &= Z_\Gamma^{\text{tor}}(\tau) \cdot \left| \frac{\theta_1(\tau, z)}{\eta(\tau)} \right|^d \end{aligned} \quad (2.19)$$

with the bosonic torus partition function $Z_\Gamma^{\text{tor}}(\tau)$ as in equation (2.14). The θ functions are given by (see e.g. [9, 32])

$$\begin{aligned} \theta_1(\tau, z) &= i \sum_{n=-\infty}^{\infty} (-1)^n q^{\frac{1}{2}(n-\frac{1}{2})^2} y^{n-\frac{1}{2}} \\ &= i q^{\frac{1}{8}} y^{-\frac{1}{2}} \prod_{n=1}^{\infty} (1-q^n)(1-q^{n-1}y)(1-q^n y^{-1}) \\ \theta_2(\tau, z) &= \sum_{n=-\infty}^{\infty} q^{\frac{1}{2}(n-\frac{1}{2})^2} y^{n-\frac{1}{2}} \end{aligned}$$

$$\begin{aligned}
&= q^{\frac{1}{8}} y^{-\frac{1}{2}} \prod_{n=1}^{\infty} (1 - q^n)(1 + q^{n-1}y)(1 + q^n y^{-1}) \\
\theta_3(\tau, z) &= \sum_{n=-\infty}^{\infty} q^{\frac{1}{2}n^2} y^n \\
&= \prod_{n=1}^{\infty} (1 - q^n)(1 + q^{n-\frac{1}{2}}y)(1 + q^{n-\frac{1}{2}}y^{-1}) \\
\theta_4(\tau, z) &= \sum_{n=-\infty}^{\infty} (-1)^n q^{\frac{1}{2}n^2} y^n \\
&= \prod_{n=1}^{\infty} (1 - q^n)(1 - q^{n-\frac{1}{2}}y)(1 - q^{n-\frac{1}{2}}y^{-1})
\end{aligned}$$

with $q = e^{2\pi i\tau}$ and $y = e^{2\pi iz}$. The additional modular parameter z describes the $U(1)$ charge of the respective fields which is coupled to their fermionic field contribution. But sometimes, we also like to express the bosonic part of the partition function in terms of θ functions. For this purpose, we only need the special Jacobi form $\theta_i(\tau) := \theta_i(\tau, 0)$.

In the following table we also note the transformation behaviour of the η as well as the θ functions under the two generators of the modular group $T : \tau \mapsto \tau + 1, z \mapsto z$ and $S : \tau \mapsto -1/\tau, z \mapsto -z/\tau$.

	T	S
$\theta_1(\tau, z)$	$e^{i\pi/4} \theta_1(\tau, z)$	$i e^{i\pi z^2/\tau} \sqrt{-i\tau} \theta_1(\tau, z)$
$\theta_2(\tau, z)$	$e^{i\pi/4} \theta_2(\tau, z)$	$e^{i\pi z^2/\tau} \sqrt{-i\tau} \theta_4(\tau, z)$
$\theta_3(\tau, z)$	$\theta_4(\tau, z)$	$e^{i\pi z^2/\tau} \sqrt{-i\tau} \theta_3(\tau, z)$
$\theta_4(\tau, z)$	$\theta_3(\tau, z)$	$e^{i\pi z^2/\tau} \sqrt{-i\tau} \theta_2(\tau, z)$
$\eta(\tau)$	$e^{i\pi/12} \eta(\tau)$	$\sqrt{-i\tau} \eta(\tau)$

The moduli space of toroidal CFTs

The moduli space of bosonic torus CFTs in dimension d is given by the Narain moduli space [89, 90]

$$\mathcal{M}_{\text{tor}} = \text{O}(\Gamma^{(d,d)}) \backslash \text{O}(d, d) / (\text{O}(d) \times \text{O}(d)).$$

This moduli space parameterises all possible even integer selfdual charge lattices $\Gamma^{d,d}$ in $\mathbb{R}^{d,d}$. Indeed, $\text{O}(d, d) / (\text{O}(d) \times \text{O}(d))$ is a Grassmannian space whose points can be

viewed as positive definite d -planes in $\mathbb{R}^{d,d}$. But a positive definite d -plane Π uniquely splits a vector $p \in \mathbb{R}^{d,d}$ into a sum $p = p_L + p_R$ with $p_L \in \Pi$ and $p_R \in \Pi^\perp$, the orthogonal complement of Π . Then, determining the maximal even selfdual lattice of such pairs (p_L, p_R) uniquely yields $\Gamma^{d,d}$. $O(\Gamma^{d,d})$ is the automorphism or duality group of this lattice. Its action simply re-arranges the charges and, hence, does not change the theory. Define the lattice $M = (\Lambda^T)^{-1}$. Then, the map from the description with lattice Λ and B-field B to the moduli space can easily be seen to be [32, 26]

$$v : O(d) \backslash (Gl(d) \times Skew(d)) \longmapsto O(d, d) / (O(d) \times O(d))$$

$$v(\Lambda, B) = \begin{pmatrix} M & 0 \\ 0 & \Lambda \end{pmatrix} \begin{pmatrix} \mathbb{1} & -B \\ 0 & \mathbb{1} \end{pmatrix}.$$

As the supersymmetric extension does not introduce further parameters into this theory the space of all supersymmetric torus CFTs is also given by the above moduli space \mathcal{M}_{tor} .

In chapter 3 we will only be interested in theories in $d = 4$ dimensions. As described in [31], one can actually apply the celebrated triality isomorphism to the moduli space in $d = 4$. The phenomenon of triality describes a set of automorphisms of $so(4, 4)$ which permute the basic and the two spin representations S^+ and S^- arbitrarily (the signature of the space does not matter for this result) [91]. In our case, the two spin representations are given by $SO^+(\mathcal{H}^{\text{odd}})$ and $SO^+(\mathcal{H}^{\text{even}})$ where \mathcal{H}^{odd} and $\mathcal{H}^{\text{even}}$ denote the spaces of odd respectively even cohomology of the target space torus.

Up to now, we have described the torus moduli space in terms of B and Λ , i.e. in terms of the torus one-cycles. Hence, we can use triality to achieve an equally well-defined description in terms of the even \mathbb{Z} cohomology of a torus T

$$\mathcal{H}^{\text{even}}(T, \mathbb{Z}) := \mathcal{H}^0(T, \mathbb{Z}) \oplus \mathcal{H}^2(T, \mathbb{Z}) \oplus \mathcal{H}^4(T, \mathbb{Z}).$$

This space is naturally endowed with the scalar product

$$(\omega_1, \omega_2) \mapsto \int_T \omega_1 \wedge \omega_2 \quad \forall \omega_1, \omega_2 \in \mathcal{H}^{\text{even}}(T, \mathbb{Z})$$

which is certainly 0 if $\omega_1 \wedge \omega_2$ is not a 4-form.

First, we need to transform the B-field to the second cohomology class. The skew-symmetric linear transformation $B \in Skew(\mathbb{R}^4)$ is mapped to $\Lambda^2(\mathbb{R}^4)$ via

$$b = \sum_{i < j} B_{ij} e_i \wedge e_j.$$

Its corresponding dual is defined to be

$$\check{b} = \sum_{kl, i < j} \frac{1}{2} \epsilon_{ijkl} B_{kl} e_i \wedge e_j.$$

Furthermore, let $V = \det(\Lambda)$ be the volume of the torus. Then, triality induces the parameterisation [31, 26]

$$s(\Lambda, B) = V^{1/2} \begin{pmatrix} V^{-1} & 0 & 0 \\ 0 & \Lambda^2(M) & 0 \\ 0 & 0 & 1 \end{pmatrix} \begin{pmatrix} 1 & \check{b} & -\frac{1}{2}\langle b, b \rangle \\ 0 & \mathbb{1} & -b \\ 0 & 0 & 1 \end{pmatrix}$$

where s maps again to the moduli space \mathcal{M}_{tor} .

This description of the moduli space in terms of the even cohomology of the target space is quite natural and important as soon as one wants to relate this to the moduli space of K3 compactification, the other possibility of $N = (4, 4)$ supersymmetric compactification in $d = 4$ dimensions. Indeed, K3 spaces only exhibit an even cohomology, their odd cohomology is trivial. Hence, one is forced to describe its moduli space in terms of even cohomology. We will come back to that in chapter 3.

2.3.3 Orbifold sigma models

Orbifolding torus models

The orbifold procedure is a method to obtain a new conformal field theory from an old one by dividing the latter by one of its finite symmetry (sub-)groups [92, 93, 94, 95]. In the following we want to restrict our attention to the construction of orbifold theories from torus theories. Our overview mainly sticks to the presentation in [95, 32].

The finite symmetry groups of interest in the torus case are the space and point groups. We regard space groups S which consist of a semi-direct product of a finite rotation group R and a translation group T

$$S = R \rtimes T .$$

The corresponding point group P , on the other hand, only consists of the finite rotation subgroup of S . As already described above, a torus can be thought of as the coset space \mathbb{R}^d/Λ ; but this is nothing more than an orbifold of the space \mathbb{R}^d by a space group with trivial rotation group and translation group Λ . As we have already used up the translational freedom we will only be interested in the point groups. Nevertheless, these point groups have to respect the isometry group of the torus. This restricts the point groups to the set of crystallographical groups which have already been classified in two and three dimensions.

From the field theoretic perspective the orbifold procedure reduces the field content inherited from the original theory to those fields which are invariant under the orbifold group G . On the other hand, new fields appear in the theory, so-called “twisted fields” or “twistfields”. Their origin can easily be understood from the torus point of view. Due to the identification of the identity with the orbifold group the periodicity conditions for the winding states have to be relaxed. Actually, the periodicity only requires the state to come back with the same boundary value modulo the action of some element of the orbifold group. This relaxation of conditions yields new states.

In order to see the exact field content of an orbifold theory let us regard how to construct the partition function of an orbifold. We introduce the projection operator which projects to the states which are invariant under the orbifold group G

$$P = \frac{1}{|G|} \sum_{h \in G} h .$$

Starting with the torus partition function (2.14) this yields its G -invariant part

$$\begin{aligned} \mathcal{Z}^G &= \frac{1}{|G|} \sum_{h \in G} \text{tr} \mathcal{H} \left(h q^{L_0 - \frac{c}{24}} \bar{q}^{\bar{L}_0 - \frac{c}{24}} \right) \\ &= \frac{1}{|G|} \sum_{h \in G} h \boxed{\square}_{\mathbb{I}} ; \end{aligned}$$

in the second line we introduce a useful notation which will become clearer in due course.

Taking into account that $q^{L_0 - \frac{c}{24}} \bar{q}^{\bar{L}_0 - \frac{c}{24}}$ induces a time translation we can think of $h \boxed{\square}_{\mathbb{I}}$ as describing fields which are twisted in time

$$X(\xi_0 + 1, \xi_1) = hX(\xi_0, \xi_1) \quad X(\xi_0, \xi_1 + 1) = X(\xi_0, \xi_1)$$

where ξ_0 and ξ_1 denote the time respectively space direction on the world sheet.

Now, we proceed demanding modular invariance of our new partition function. But as \mathcal{Z}^G is not yet modular invariant we are forced to include further traces into the partition function which describe states which are twisted in the spatial direction

$$X(\xi_0, \xi_1 + 1) = gX(\xi_0, \xi_1) ,$$

i.e. which fulfil the boundary conditions of periodicity only up to $g \in G$. We will denote the Hilbert space of spatially g twisted states by \mathcal{H}_g and the corresponding traces by

$$h \boxed{\square}_g$$

(with an h twist in the time direction). Indeed, the modular transformations of these trace are given by [95, 32]

$$\begin{aligned} h \boxed{\square}_g(\tau + 1) &= (g \circ h) \boxed{\square}_g(\tau) \\ h \boxed{\square}_g\left(-\frac{1}{\tau}\right) &= g \boxed{\square}_h(\tau) . \end{aligned}$$

But before we can write down the full orbifold partition function we need to note that G transformed fields behave as

$$hX(\xi_0, \xi_1 + 1) = (hgh^{-1}) hX(\xi_0, \xi_1) \quad \forall h \in G .$$

This identifies $\mathcal{H}_g \cong \mathcal{H}_{hgh^{-1}}$. Therefore, we only want to sum over the different cosets $\{hgh^{-1}, h \in G\}$ of G . This yields the following twisted part of the partition function

$$\begin{aligned} \mathcal{Z}_{\text{twist}}^G &= \frac{1}{|G|} \sum_{\substack{h, g \in G \\ hgh^{-1}=g, g \neq \mathbb{1}}} \text{tr } \mathcal{H}_g \left(hq^{L_0 - \frac{c}{24}} \bar{q}^{\bar{L}_0 - \frac{c}{24}} \right) \\ &= \frac{1}{|G|} \sum_{\substack{h, g \in G \\ hgh^{-1}=g, g \neq \mathbb{1}}} h \square_g \end{aligned}$$

and, finally, the full modular invariant partition function of an orbifold CFT

$$\mathcal{Z}_{\text{orb}}^G = \frac{1}{|G|} \sum_{\substack{h, g \in G \\ hgh^{-1}=g}} h \square_g. \quad (2.20)$$

The superconformal \mathbb{Z}_4 orbifold partition function

The motivation to our above derivation of the orbifold partition function was basically the bosonic torus partition function. But certainly the orbifold construction can easily be extended to superconformal torus models, simply applying equation (2.20) to the superconformal torus partition function (2.19).

In practice, the easiest way to obtain the orbifold partition function is simply applying the modular group to the G invariant part of the torus partition function until one has collected all contributions necessary for the whole partition function to close under the modular group. This is straight forward in the bosonic case, but for the superconformal case we have to take into account that the generators of the modular group S and T change the boundary conditions and, hence, map the different sectors into each other according to [73]

$$\begin{aligned} T : (A, A) &\longleftrightarrow (P, A) & (A, P), (P, P) \text{ invariant} \\ S : (P, A) &\longleftrightarrow (A, P) & (A, A), (P, P) \text{ invariant} \end{aligned}$$

where $(., .)$ signifies the either periodic (P) or antiperiodic (A) boundary conditions in time respectively space direction. The different sectors have boundary conditions as described in (2.9) This mixing of sectors by action of the modular group is actually the conformal field theoretic reason that we do need all four of these sectors; only $Z_{\tilde{R}}$ would be modular invariant for itself.

In chapter 3 we will need the twistfield content of the RR groundstates of a \mathbb{Z}_4 orbifold. We have, hence, performed the above programme and calculated the R-sector of the partition function of a \mathbb{Z}_4 orbifold to be

$$Z_{\mathbb{Z}_4}^{\Gamma, R} = \frac{1}{4} \left(\left(\frac{1}{|\eta(\sigma)|^8} \sum_{p \in \Gamma} q^{p_i^2/2} \bar{q}^{p_r^2/2} \right) \cdot \left| \frac{\theta_2(\sigma, z)}{\eta(\sigma)} \right|^4 + 8 \left| \frac{\eta(2\sigma)}{\theta_2(2\sigma)} \right|^2 \cdot \left| \frac{\theta_2(2\sigma, 2z)}{\eta(2\sigma)} \right|^2 \right)$$

$$\begin{aligned}
& + 16 \left| \frac{\eta(\sigma)}{\theta_2(\sigma)} \right|^4 \cdot \left| \frac{\theta_1(\sigma, z)}{\eta(\sigma)} \right|^4 + 16 \left| \frac{\eta(\sigma)}{\theta_4(\sigma)} \right|^4 \cdot \left| \frac{\theta_3(\sigma, z)}{\eta(\sigma)} \right|^4 + 16 \left| \frac{\eta(\sigma)}{\theta_3(\sigma)} \right|^4 \cdot \left| \frac{\theta_4(\sigma, z)}{\eta(\sigma)} \right|^4 \\
& + 8 \left| \frac{\eta(\frac{\sigma}{2})}{\theta_4(\frac{\sigma}{2})} \right|^4 \cdot \left| \frac{\theta_3(\frac{\sigma}{2}, z)}{\eta(\frac{\sigma}{2})} \right|^4 + 8 \left| \frac{(\eta(\sigma)\theta_3(\sigma))^{1/2}}{\theta_3(2\sigma) - i\theta_2(2\sigma)} \right|^2 \cdot \left| \frac{(\theta_3(2\sigma, 2z) + i\theta_2(2\sigma, 2z))}{(\eta(\sigma)\theta_3(\sigma))^{1/2}} \right|^2 \\
& + 8 \left| \frac{(\eta(\sigma)\theta_4(\sigma))^{1/2}}{\theta_3(2\sigma) + \theta_2(2\sigma)} \right|^2 \cdot \left| \frac{(\theta_3(2\sigma, 2z) - \theta_2(2\sigma, 2z))}{(\eta(\sigma)\theta_4(\sigma))^{1/2}} \right|^2 \\
& + 8 \left| \frac{(\eta(\sigma)\theta_3(\sigma))^{1/2}}{\theta_3(2\sigma) + i\theta_2(2\sigma)} \right|^2 \cdot \left| \frac{(\theta_3(2\sigma, 2z) - i\theta_2(2\sigma, 2z))}{(\eta(\sigma)\theta_3(\sigma))^{1/2}} \right|^2 \\
& + 8 \left(\left| \frac{(\eta(\sigma)\theta_2(\sigma))^{1/2}}{\theta_3(\frac{\sigma}{2}) + \theta_4(\frac{\sigma}{2})} \right|^2 \cdot \left| \frac{(\theta_3(\frac{\sigma}{2}, 2z) + \theta_4(\frac{\sigma}{2}, 2z))}{(\eta(\sigma)\theta_2(\sigma))^{1/2}} \right|^2 \right) ;
\end{aligned}$$

in each term the first factor gives the bosonic part, the second the fermionic. The first three terms constitute the untwisted sector, the other seven terms the different twisted sectors.

By keeping the bosonic and fermionic parts separate during the calculation we can actually see how much of the conformal weight is contributed from a bosonic and how much from a fermionic constituent of some field. This is a quite interesting question for twistfields as the non-trivial monodromy behaviour induces unusual bosonic and fermionic constituents. To see this for a useful example, we expand the terms six to nine each of which yields a leading contribution of

$$2 \left((q\bar{q})^{-1/6} (q\bar{q})^{3/16} \right) \cdot \left((q\bar{q})^{-1/12} (q\bar{q})^{1/16} \right) \cdot 1 .$$

The first big bracket gives the bosonic contribution, separating the overall modular factor first, the second bracket gives the fermionic contribution. Hence we find eight fields of overall conformal weight $(h, \tilde{h}) = (\frac{1}{4}, \frac{1}{4})$ where a $h_b = \frac{3}{16}$ part originates from bosonic degrees of freedom, a $h_f = \frac{1}{16}$ part from fermionic. This perfectly well coincides with the conformal weights of \mathbb{Z}_4 twistfields generating cuts for either bosonic or fermionic fields found in [95].

Similarly, we calculated the NS sector part of the \mathbb{Z}_4 orbifold partition function to be

$$\begin{aligned}
Z_{\mathbb{Z}_4}^{\Gamma, NS} &= \frac{1}{4} \left(\left(\frac{1}{|\eta(\sigma)|^8} \sum_{p \in \Gamma} q^{p_i^2/2} \bar{q}^{p_r^2/2} \right) \cdot \left| \frac{\theta_3(\sigma, z)}{\eta(\sigma)} \right|^4 + 8 \left| \frac{\eta(2\sigma)}{\theta_2(2\sigma)} \right|^2 \cdot \left| \frac{\theta_3(2\sigma, 2z)}{\eta(2\sigma)} \right|^2 \right. \\
& + 16 \left| \frac{\eta(\sigma)}{\theta_2(\sigma)} \right|^4 \cdot \left| \frac{\theta_4(\sigma, z)}{\eta(\sigma)} \right|^4 + 16 \left| \frac{\eta(\sigma)}{\theta_4(\sigma)} \right|^4 \cdot \left| \frac{\theta_2(\sigma, z)}{\eta(\sigma)} \right|^4 + 16 \left| \frac{\eta(\sigma)}{\theta_3(\sigma)} \right|^4 \cdot \left| \frac{\theta_1(\sigma, z)}{\eta(\sigma)} \right|^4 \\
& \left. + 8 \left| \frac{\eta(\frac{\sigma}{2})}{\theta_4(\frac{\sigma}{2})} \right|^4 \cdot \left| \frac{\theta_3(\frac{\sigma}{2}, z)}{\eta(\frac{\sigma}{2})} \right|^4 + 8 \left| \frac{(\eta(\sigma)\theta_3(\sigma))^{1/2}}{\theta_3(2\sigma) - i\theta_2(2\sigma)} \right|^2 \cdot \left| \frac{(\theta_3(2\sigma, 2z) + i\theta_2(2\sigma, 2z))}{(\eta(\sigma)\theta_3(\sigma))^{1/2}} \right|^2 \right)
\end{aligned}$$

$$\begin{aligned}
& + 8 \left| \frac{(\eta(\sigma)\theta_4(\sigma))^{1/2}}{\theta_3(2\sigma) + \theta_2(2\sigma)} \right|^2 \cdot \left| \frac{(\theta_3(2\sigma, 2z) - \theta_2(2\sigma, 2z))}{(\eta(\sigma)\theta_4(\sigma))^{1/2}} \right|^2 \\
& + 8 \left| \frac{(\eta(\sigma)\theta_3(\sigma))^{1/2}}{\theta_3(2\sigma) + i\theta_2(2\sigma)} \right|^2 \cdot \left| \frac{(\theta_3(2\sigma, 2z) + i\theta_2(2\sigma, 2z))}{(\eta(\sigma)\theta_3(\sigma))^{1/2}} \right|^2 \\
& + 8 \left(\left| \frac{(\eta(\sigma)\theta_2(\sigma))^{1/2}}{\theta_3(\frac{\sigma}{2}) + \theta_4(\frac{\sigma}{2})} \right|^2 \cdot \left| \frac{(\theta_3(\frac{\sigma}{2}, 2z) - \theta_4(\frac{\sigma}{2}, 2z))}{(\eta(\sigma)\theta_2(\sigma))^{1/2}} \right|^2 \right).
\end{aligned}$$

Again, the first three terms constitute the untwisted sector, the other seven terms the different twisted sectors. The parts of the partition function related to the other two sectors \widehat{NS} and \widehat{R} can be obtained in the same manner or as well by application of the spectral flow.

In this section, we have dissected the partition function of a very special superconformal orbifold model in order to obtain the special properties of twistfields. For a more general review of superconformal orbifold partition functions see [96].

The OPE of vertex operators with groundstate twistfields

There has already been quite some research about correlation functions and OPEs in orbifolds of torus theories [97, 95, 98, 99, 100, 101, 102, 88, 103, 26]. In chapter 3 we will, in particular, make use of the general OPE of a vertex operator of the original torus theory with a groundstate twistfield of a \mathbb{Z}_N orbifold theory. We will, hence, review this special OPE in the following.

Let us restrict our attention to the cyclic orbifold group $G = \mathbb{Z}_N$. Then the form of an OPE of a torus vertexoperator $V_p^{\text{torus}}(z)$ and a groundstate twistfield $T_f^l(w)$ is uniquely determined by the following properties:

- The monodromy around the orbifold fixed points, i.e.

$$V_p^{\text{torus}}(z) \longrightarrow V_{\theta p}^{\text{torus}}(z)$$

where we move the vertexoperator around a twistfield $T_f^l(w)$ which is located at such a fixed point f ; θ is the matrix of the representation of the orbifold group generator on the torus lattice. This determines the analytic behaviour of the OPE on the n fold covering space of \mathbb{C} .

- The known OPE of the torus vertexoperators.

In [26] these properties were used to show that this OPE looks like

$$V_{P(\mu,\lambda)}^{\text{torus}}(z) T_f^l(w) = (z-w)^h (\bar{z}-\bar{w})^{\bar{h}} g(P_L, P_R) \zeta_N^{\mu(Nx_f)l} T_{f'}^l(w) + \dots$$

with (h, \tilde{h}) the conformal dimension of $V_{P(\mu, \lambda)}^{\text{torus}}$, $\zeta_N := \exp 2\pi i/N$, and the translated fixpoint

$$x_{f'} = x_f + [(1 - \theta)^{-1} \lambda] = x_f \left[\frac{1}{n(f)} \sum_1^{n(f)-1} k \theta^k \lambda \right].$$

$f = (1 - \theta) x_f \in \Lambda$ signifies the fixpoint the twistfield lives at; $x_f \in I$ gives the location of that fixed point, where I can be taken as a subgroup of order $n(f)$ of $H_1(T, \mathbb{R})/H_1(T, \mathbb{Z})$ of the torus T which is orbifolded.

The same OPE has been calculated in [88] making use of the mode expansion of the fields. In this setting, a careful treatment of the zero modes allows for the calculation of the coupling parameter $g(P_L, P_R)$. This coupling parameter is independent of the position of the fixpoint and can be determined to be [88]

$$g(P_L, P_R) = e^{\pi i p^t (1-\theta)^{-1} w} g'_l(P_L, P_R)$$

with the vertex operator coupling constant ($d/2$ signifies the complex dimension)

$$\begin{aligned} g'_l(P_L, P_R) &= \prod_{\mu=1}^{d/2} \delta(l k_\mu)^{-(h^\mu + \tilde{h}^\mu)} \\ \delta(k_\mu) &= N^2 \prod_{a=1}^{N-1} \left(2 \sin \frac{\pi a}{N} \right)^{-2 \cos(2\pi a k_\mu)} \\ h^\mu &= \frac{1}{2} \|P_L^\mu\|^2, \quad \tilde{h}^\mu = \frac{1}{2} \|P_R^\mu\|^2. \end{aligned}$$

2.3.4 Supersymmetric minimal models and Gepner models

In this section we introduce a supersymmetric version of the minimal models and we show how tensor products of these can be used to construct consistent GSO projected models with a central charge $c \in 3\mathbb{Z}^+$. These so-called Gepner models are indeed interesting models for string theory compactifications. The presentation in this section is mainly based on the reviews [104, 105, 32].

The $N = 2$ supersymmetric Minimal Model

There is also a corresponding series of unitary minimal models wrt the $N = 2$ supersymmetric extension of the Virasoro algebra [106, 107, 108]. These models have central charges

$$c = \frac{3k}{k+2} \quad k = 2, \dots$$

They can be constructed either as a tensor product of the \mathbb{Z}_k parafermions and a free boson or as the following coset model

$$\frac{SU(2)_k \otimes U(1)_2}{U(1)_{k+2, \text{diag}}}.$$

The fields $\Phi_{m,s;\bar{m},\bar{s}}^l$ of the theory are labeled by the corresponding quantum numbers of this coset model with $l = \bar{l}$ referring to $SU(2)_k$. The spectrum of conformal weights and $U(1)$ charges of these fields is given by

$$h_{m,s}^l = \frac{l(l+2) - m^2}{4(k+2)} + \frac{s^2}{8} \bmod 1 \quad Q_{m,s}^l = \frac{m}{k+2} - \frac{s}{2} \bmod 2; \quad (2.21)$$

it is constraint by the following rules:

- The spectrum is restricted to the domain $0 \leq l \leq k$, $m = -k-1, \dots, k+2$ and $s = -1, \dots, 2$. Fields are, hence, identified according to $m \sim m \pm (2k+4)$ and $s \sim s \pm 4$.
- The sum of the three quantum numbers has to be even, i.e. $l + m + s \equiv 0 \bmod 2$.
- Fields are equivalent according to

$$\Phi_{m,s;\bar{m},\bar{s}}^l \sim \Phi_{m+k+2,s+2;\bar{m}+k+2,\bar{s}+2}^{k-l}.$$

The fields with odd s belong to the Ramond sector, the fields with even s to the Neveu-Schwarz sector of this $N = 2$ supersymmetric theory. The fields of left and right-handed spectral flow are given by $U_{\pm\frac{1}{2}} = \Phi_{\pm 1, \pm 1, 0, 0}^0$ respectively $\bar{U}_{\pm\frac{1}{2}} = \Phi_{0, 0, \pm 1, \pm 1}^0$.

For fields with $|m - s| \leq l$ the mod relations in (2.21) are irrelevant. However, to find the correct integer to be added for all fields one has to go back to the (holomorphic) characters of these supersymmetric models

$$\chi_{m,s}^l(\sigma, z) = \sum_{j=1}^k c_{4j+s-m}^l(\sigma) \Theta_{2m-(k+2)(4j+s), 2k(k+2)}(\sigma, \frac{z}{k+2})$$

and find the lowest weights appearing in their spectrum. The c_m^l signify the ‘‘string functions’’ of $SU(2)$ and $\Theta_{l,k}$, $|l| \leq k$, are the classical theta functions at level k . Now, we can also give the partition function of the NS-sector of the (k) supersymmetric minimal model

$$Z_{\text{NS}} = \frac{1}{2} \sum_{\substack{l=0, \dots, k \\ l=-k-1, \dots, k+2 \\ l+m \equiv 0(2)}} \left(\chi_{m,0}^l(\sigma, z) + \chi_{m,2}^l(\sigma, z) \right) \left(\chi_{m,0}^l(\bar{\sigma}, \bar{z}) + \chi_{m,2}^l(\bar{\sigma}, \bar{z}) \right).$$

The partition functions of the other sectors are obtained using spectral flow.

Due to the incorporation of the \mathbb{Z}_k parafermions into these models the statistics are quite complicated. In particular, it is not that easy to say when these fields behave as fermions. Especially when dealing with tensor products of these minimal models we need to use the following rule [109]

$$\Phi_{m_1, s_1; \bar{m}_1, \bar{s}_1}^{l_1} \otimes \Phi_{m_2, s_2; \bar{m}_2, \bar{s}_2}^{l_2} = (-1)^{\frac{1}{4}(s_1 - \bar{s}_1)(s_2 - \bar{s}_2)} \Phi_{m_2, s_2; \bar{m}_2, \bar{s}_2}^{l_2} \otimes \Phi_{m_1, s_1; \bar{m}_1, \bar{s}_1}^{l_1}$$

to track the negative signs due to fermionic behaviour.

The fusion rules for the holomorphic components of $\Phi_{m, s; \bar{m}, \bar{s}}^l(z, \bar{z}) = \psi_{m, s}^l(z) \bar{\psi}_{\bar{m}, \bar{s}}^l(\bar{z})$ are again given by a BPZ like set of rules

$$\left[\psi_{m, s}^l \right] \times \left[\psi_{m', s'}^{l'} \right] = \sum_{l''=|l-l'| \text{ step } 2}^{\min(l+l', 2k-l-l')} \left[\psi_{m+m', s+s'}^{l''} \right].$$

In the following, we will in particular need the (2) supersymmetric minimal model. This model at $c = 3/2$ can be identified with a tensor product of the Ising Model (the ordinary minimal model at $c_{4,3} = 1/2$ which is at the same time the $k = 2$ parafermionic theory) and the free boson at radius $\sqrt{2}$. This allows the following field identification

$$\Phi_{m, s; \bar{m}, \bar{s}}^l = \Xi_{m-s; \bar{m}-\bar{s}}^l(z, \bar{z}) e^{\frac{i}{2\sqrt{2}}(-m+2s)\phi(z)} e^{\frac{i}{2\sqrt{2}}(-\bar{m}+2\bar{s})\bar{\phi}(\bar{z})}$$

with

$$\Xi_{j; \bar{j}}^0(z, \bar{z}) = \Xi_{j \pm 2; \bar{j} \pm 2}^2(z, \bar{z}) = \xi_j^0(z) \xi_{\bar{j}}^0(\bar{z}) \quad \xi_0^0 = \mathbb{1}, \quad \xi_2^0 = \psi$$

and $\Xi_{1; \bar{1}}^1(z, \bar{z}) = \Xi_{-1; \bar{-1}}^1(z, \bar{z}) = \sigma(z, \bar{z})$ as well as $\Xi_{1; \bar{-1}}^1(z, \bar{z}) = \Xi_{-1; \bar{1}}^1(z, \bar{z}) = \mu(z, \bar{z})$; σ and μ are the generating groundstates of the two $(1/16, 1/16)$ representations of the Ising model with coupled holomorphic and antiholomorphic sectors (see e.g. [73, 9] for more details about this model). This field identification reduces the calculation of (2) model correlation functions to that of Ising and torus model correlation functions which are easy to do.

The construction of the $N = 2$ supersymmetric model as a tensor product of a \mathbb{Z}_k parafermion and a free boson yields the following representation of the $N = 2$ Super-Virasoro algebra

$$\begin{aligned} T(z) &= T_{\text{Pf}}(z) - \frac{1}{2} \partial\phi \partial\phi \\ G^-(z) &= \sqrt{\frac{2k}{k+2}} \psi_1 e^{i\sqrt{\frac{k+2}{k}}\phi(z)} \\ &= \psi(z) e^{i\sqrt{2}\phi(z)} \equiv \Phi_{0, 2; 0, 0}^0 \\ G^+(z) &= \sqrt{\frac{2k}{k+2}} \psi_{k-1} e^{-i\sqrt{\frac{k+2}{k}}\phi(z)} \\ &= \psi(z) e^{-i\sqrt{2}\phi(z)} \equiv \Phi_{0, -2; 0, 0}^0 \\ J(z) &= -i\sqrt{\frac{k}{k+2}} \partial\phi(z) = \frac{-i}{\sqrt{2}} \partial\phi(z); \end{aligned}$$

the first expression always refers to the holomorphic symmetry algebra of the general (k) supersymmetric minimal model, the second to the specialised version of $k = 2$. T_{Pf} signifies the energy momentum tensor of the respective parafermionic theory. The $U(1)$ charges given in (2.21) are indeed just the charges of the fields wrt $J(z)$. The normalisation of the algebra is consistent with

$$G^+(z)G^-(w) \sim \frac{2c}{3}(z-w)^{-3} + 2J(w)(z-w)^{-2} + \dots$$

Building Gepner models

For any set of positive integers k_i , $i = 1, \dots, r$, which yield a central charge of $c = \sum_{i=1}^r \frac{3k_i}{k_i+2} = 3d/2$ with $d \in 2\mathbb{Z}^+$ we can obtain a consistent CFT based on the tensor product $\bigotimes_{i=1}^r (k_i)$. Such a model is called a ‘‘Gepner model’’ [110, 111].

Let us first study the symmetry group of this tensor product. Each minimal model factor contributes a \mathbb{Z}_{k+2} symmetry

$$\Phi_{m,s;\bar{m},\bar{s}}^l \longmapsto e^{2\pi i \frac{m+\bar{m}}{2(k+2)}} \Phi_{m,s;\bar{m},\bar{s}}^l$$

which originates in its parafermionic subtheory. We will denote the elements of the resulting Abelian symmetry group $\prod_{i=1}^r \mathbb{Z}_{k_i+2}$ with $a = [a_1, \dots, a_r]$ and introduce the frequently used scalar product \bullet

$$a, b \in \prod_{i=1}^r \mathbb{Z}_{k_i+2} : \quad a \bullet b := \sum_{j=1}^r \frac{a_j b_j}{k_j + 2}.$$

In order to construct the Gepner model we need to implement a valid GSO projection on the above tensor product of supersymmetric minimal models. This can be done in the following two ways:

- One constructs an orbifold of the tensor product $\bigotimes_{i=1}^r (k_i)$ wrt the cyclic group generated by the element $\beta = [1, 1, \dots, 1] \in \prod_{i=1}^r \mathbb{Z}_{k_i+2}$.
- One enhances the \mathcal{W} -algebra with the current $U = \bigotimes_{i=1}^r \Phi_{2,2;0,0}^0$ and only keeps a maximal set of fields which are local to each other. This set certainly contains the \mathcal{W} -algebra.

This maximal set of the above second point has to be invariant under β as well. In practice it is, thus, useful to combine both methods. First, one enhances the \mathcal{W} -algebra with U and calculates all new fields which are obtained from OPEs with U . Then, one just keeps the fields which are invariant under the action of β .

Let us now turn to the model of special interest in this thesis, the Gepner model (2)⁴. In this model, the action of U on the holomorphic NS-sector characters of one constituent (2) model has several orbits

- $l = 1$: exchange of $m = 1 \leftrightarrow m = -1$;

- $l = 2$: $\chi_{0,0}^0 \rightarrow \chi_{2,2}^0 \rightarrow \chi_{0,2}^2 \rightarrow \chi_{2,0}^2 \rightarrow \chi_{0,0}^0$
- $l = 2$: $\chi_{0,2}^0 \rightarrow \chi_{2,0}^0 \rightarrow \chi_{0,0}^2 \rightarrow \chi_{2,2}^2 \rightarrow \chi_{0,2}^0$

while the antiholomorphic characters stay the same. On the other hand, the action of β produces four different phase factors on the constituent fields

ζ_m	$m \bmod 4$	fields
1	0	$\Phi_{0,0;0,0}^0, \Phi_{0,2;0,0}^0, \Phi_{0,0;0,2}^0, \Phi_{0,2;0,2}^0$ $\Phi_{0,0;0,0}^2, \Phi_{0,2;0,0}^2, \Phi_{0,0;0,2}^2, \Phi_{0,2;0,2}^2$
i	1	$\Phi_{1,0;1,0}^1, \Phi_{1,2;1,0}^1, \Phi_{1,0;1,2}^1, \Phi_{1,2;1,2}^1$
-1	2	$\Phi_{2,0;2,0}^2, \Phi_{2,2;2,0}^2, \Phi_{2,0;2,2}^2, \Phi_{2,2;2,2}^2$ $\Phi_{-2,0;-2,0}^2, \Phi_{-2,2;-2,0}^2, \Phi_{-2,0;-2,2}^2, \Phi_{-2,2;-2,2}^2$
$-i$	3	$\Phi_{-1,0;-1,0}^1, \Phi_{-1,2;-1,0}^1, \Phi_{-1,0;-1,2}^1, \Phi_{-1,2;-1,2}^1$

This table lists only the fields which have the same holomorphic and antiholomorphic field content. But as the phase factor ζ_m only depends on the holomorphic quantum numbers, the table is easily generalised to asymmetric fields generated via the action of U .

Now, we have collected all ingredients to construct $(2)^4$ Gepner fields along the lines of the above programme. In the following, we give a list of some typical examples:

$$\begin{aligned}
(\Phi_{1,0;1,0}^1)^{\otimes 4} &= \left(\sigma(z) e^{-\frac{i}{2\sqrt{2}}\varphi(z)} e^{-\frac{i}{2\sqrt{2}}\bar{\varphi}(\bar{z})} \right)^{\otimes 4} \\
(\Phi_{3,2;1,0}^1)^{\otimes 4} &= \left(\sigma(z) e^{\frac{i}{2\sqrt{2}}\varphi(z)} e^{-\frac{i}{2\sqrt{2}}\bar{\varphi}(\bar{z})} \right)^{\otimes 4} \\
\Phi_{0,0;0,0}^0 \otimes \Phi_{0,0;0,0}^0 \otimes \Phi_{2,0;2,0}^2 \otimes \Phi_{2,0;2,0}^2(z) \\
&= \mathbb{1} \otimes \mathbb{1} \otimes e^{-\frac{i}{\sqrt{2}}\varphi(z)} e^{-\frac{i}{\sqrt{2}}\bar{\varphi}(\bar{z})} \otimes e^{-\frac{i}{\sqrt{2}}\varphi(z)} e^{-\frac{i}{\sqrt{2}}\bar{\varphi}(\bar{z})} \\
\Phi_{0,2;0,0}^0 \otimes \Phi_{0,2;0,0}^0 \otimes \Phi_{2,0;2,0}^2 \otimes \Phi_{2,0;2,0}^2(z) \\
&= \psi(z) e^{i\sqrt{2}\varphi(z)} \otimes \psi(z) e^{i\sqrt{2}\varphi(z)} \otimes e^{-\frac{i}{\sqrt{2}}\varphi(z)} e^{-\frac{i}{\sqrt{2}}\bar{\varphi}(\bar{z})} \otimes e^{-\frac{i}{\sqrt{2}}\varphi(z)} e^{-\frac{i}{\sqrt{2}}\bar{\varphi}(\bar{z})} \\
\Phi_{-1,-2;1,0}^1 \otimes \Phi_{-3,-2;-1,0}^1 \otimes \Phi_{0,2;2,0}^2 \otimes \Phi_{4,2;-2,0}^0(z) \\
&= \sigma(z) e^{-\frac{3i}{2\sqrt{2}}\varphi(z)} e^{-\frac{i}{2\sqrt{2}}\bar{\varphi}(\bar{z})} \otimes \sigma(z) e^{-\frac{i}{2\sqrt{2}}\varphi(z)} e^{\frac{i}{2\sqrt{2}}\bar{\varphi}(\bar{z})} \otimes e^{i\sqrt{2}\varphi(z)} e^{-\frac{i}{\sqrt{2}}\bar{\varphi}(\bar{z})} \\
&\quad \otimes \psi(z) \bar{\psi}(\bar{z}) e^{\frac{i}{\sqrt{2}}\bar{\varphi}(\bar{z})} .
\end{aligned}$$

The fields of the holomorphic symmetry algebra in the Gepner model are constructed as the sum of fields which act as the respective generator in just one of the models and as the identity in all the other, e.g.

$$J(z) = \sum_{i=1}^4 \mathbb{1} \otimes \dots \otimes J_i \otimes \dots \otimes \mathbb{1} .$$

Orbifolds of Gepner models

A Gepner model possesses a large residual symmetry group

$$\mathcal{G}_{\text{ab}} = \left(\prod_{i=1}^r \mathbb{Z}_{k_i+2} \right) / \mathbb{Z}_M \quad M = \text{lcm} \{k_i + 2; i = 1, \dots, r\}$$

(which still has to be reduced further if we want to leave invariant the spectral flow and, hence, spacetime supersymmetry).

This symmetry group and its subgroups can be used to construct new CFTs via the orbifolding technique. As the whole symmetry group is Abelian let us, without loss of generality, regard a cyclic subgroup $H \simeq \mathbb{Z}_A$ generated by an element a . In order to construct the orbifold we enhance the \mathcal{W} -algebra with the current [32]

$$U^a = \bigotimes_{i=1}^r \Phi_{2a_j, 2a_j; 0, 0}^0,$$

add all fields which are results of OPEs with U^a , and only keep a maximal subset of fields which are local to each other. But similarly to the above described GSO projection, this maximal set of fields local to each other is identical to the set of fields which are invariant under H . In practice, the last of these two options is the more comfortable way to go. We will call an orbifold of a Gepner model a ‘‘Gepner like model’’.

There are two orbifolds of the Gepner model $(2)^4$ which are important in this thesis:

- The Gepner like model $(\hat{2})^4$ is obtained by an orbifold wrt the group $\mathbb{Z}_2 \equiv \langle [2, 2, 0, 0] \rangle \in \mathcal{G}_{\text{ab}}$. It can also be constructed via enhancing the \mathcal{W} -algebra of $(2)^4$ with the two currents [32]

$$\begin{aligned} \tilde{J}_{12} &= \Phi_{4,2;0,0}^0 \otimes \Phi_{4,2;0,0}^0 \otimes \Phi_{0,0;0,0}^0 \otimes \Phi_{0,0;0,0}^0 \\ \tilde{J}_{34} &= \Phi_{0,0;0,0}^0 \otimes \Phi_{0,0;0,0}^0 \otimes \Phi_{4,2;0,0}^0 \otimes \Phi_{4,2;0,0}^0. \end{aligned}$$

- The Gepner like model $(\tilde{2})^4$ denotes the orbifold wrt the group $\mathbb{Z}_2 \times \mathbb{Z}_2 \equiv \langle [2, 2, 0, 0], [2, 0, 2, 0] \rangle \in \mathcal{G}_{\text{ab}}$. This model can also be obtained by enhancing the \mathcal{W} -algebra of $(2)^4$ with the above simple current \tilde{J}_{12} as well as with all currents obtained from \tilde{J}_{12} by permutation of its factors [32].

Chapter 3

Observations on the moduli space of conformal sigma models compactified on K3

The moduli space of conformal field theory models with central charge $c = 6$ and $N = (4, 4)$ supersymmetry can be separated into two independent components. The first is given by the supersymmetric extension of the well explored 16-dimensional Narain moduli space of supersymmetric torus theories which is briefly discussed in section 2.3.2. The second component is given by the moduli space of conformal sigma models which are compactified on K3 surfaces, or rather of the moduli space of quantum extensions of these compactifications which also include the moduli of the important asymmetric background B-field. It is this second component which we still know very little about and which we want to uncover some new features about in this chapter.

The moduli space of K3 compactifications has already been studied in a series of publications [28, 112, 29, 30, 31, 32, 113, 33]. So far, this moduli space has been identified as an orbifold of a symmetric space by a maximal discrete symmetry group with Hausdorff quotient. Furthermore, it has been shown how to embed certain specific K3 surfaces, so-called orbifold surfaces, within this moduli space. This has led to a nice embedding picture of several conformal field theory models with a large symmetry algebra, \mathbb{Z}_n orbifold models and several Gepner models, within this moduli space. Due to their larger symmetry algebra, however, these models do not represent the generic inhabitant of this moduli space—about the generic models we know almost nothing.

In this chapter we want to examine several aspects of the K3 moduli space, which will hopefully bring us closer to the study of its generic points. After a short introduction to the geometry of the K3 component of the moduli space we will re-examine a very special point in this moduli space. This special point is the intersection point of the \mathbb{Z}_2 and \mathbb{Z}_4 orbifold subvarieties and has also been shown to be equal to a certain orbifold of the Gepner model $(2)^4$ [31, 32]. However, the proof of this identification has been rather indirect. We will give an explicit proof of this identification, on the geometric

side in section 3.2 as well as for the three different conformal field theory models in section 3.3. It is this explicit identification of the geometric points which enables us to relate the coordinates on the \mathbb{Z}_2 and \mathbb{Z}_4 orbifold subvarieties. In section 3.4 we then show how to use this coordinate transition in order to calculate a geometric geodesic between these two subvarieties as well as the generating matrix of this geodesic. We conclude this chapter by exploring the possibilities to describe such a geodesic on the conformal field theory side using conformal deformation theory.

The calculations presented in sections 3.2 and 3.3 have already been published in [114]. For further steps in the exploration of the K3 moduli space see e.g. [115].

3.1 Introduction to the geometry of the K3 moduli space

In the following we present the most important facts about the geometry of the K3 moduli space which are needed for the consequent sections. We try to stick to the conventions of [31, 32, 33], where a much more detailed presentation is given.

A classical K3 surface is defined to be a compact complex Kähler manifold of complex dimension 2. Its topology is summarised in its Hodge numbers, the dimensions of its Dolbeault cohomology classes,

$$\begin{array}{ccccccc}
 & & h^{0,0} & & & & 1 \\
 & h^{1,0} & & h^{0,1} & & 0 & 0 \\
 h^{2,0} & & h^{1,1} & & h^{0,2} & = & 1 & 20 & 1 & . \\
 & h^{2,1} & & h^{1,2} & & 0 & 0 & & & \\
 & & h^{2,2} & & & & 1 & & &
 \end{array}$$

It is a quite remarkable fact that a K3 surface only exhibits even cohomology. A more detailed introduction to K3 surfaces as well as their (complex) algebraic geometry can be found in [30] or in the mathematics literature, e.g. in [116].

The general structure of the K3 moduli space is given by

$$\mathrm{O}^+(\Gamma^{(4,20)}) \backslash \mathrm{O}^+(4,20) / \mathrm{SO}(4) \times \mathrm{O}(20) \cong \mathrm{O}^+(\Gamma^{(4,20)}) \backslash \mathrm{O}(4,20) / \mathrm{O}(4) \times \mathrm{O}(20)$$

where $\mathrm{O}^+(\Gamma^{(4,20)})$ signifies the discrete duality group. As we are only interested in local properties in this chapter, we will only deal with the unique smooth, simply connected covering space $\mathrm{O}(4,20)/\mathrm{O}(4) \times \mathrm{O}(20)$. This is a Grassmannian space whose points can be described by a four-plane in an even selfdual 24-dimensional lattice $\Gamma^{(4,20)}$ of signature (4, 20). Such even selfdual lattices are known to be unique up to isometries for a given signature (m, n) if $m > 0$ and $n > 0$ (see e.g. [30]).

But now we want to allocate specific conformal field theory models within this moduli space. In [31, 32] it has been deduced that the moduli spaces which can be generated from the torus moduli space via the \mathbb{Z}_n ($n = 2, 3, 4, 6$) orbifold procedure are actually embedded in the larger K3 moduli space. For each of these orbifold subvarieties [31, 32] describe an embedding and give the explicit coordinates within this

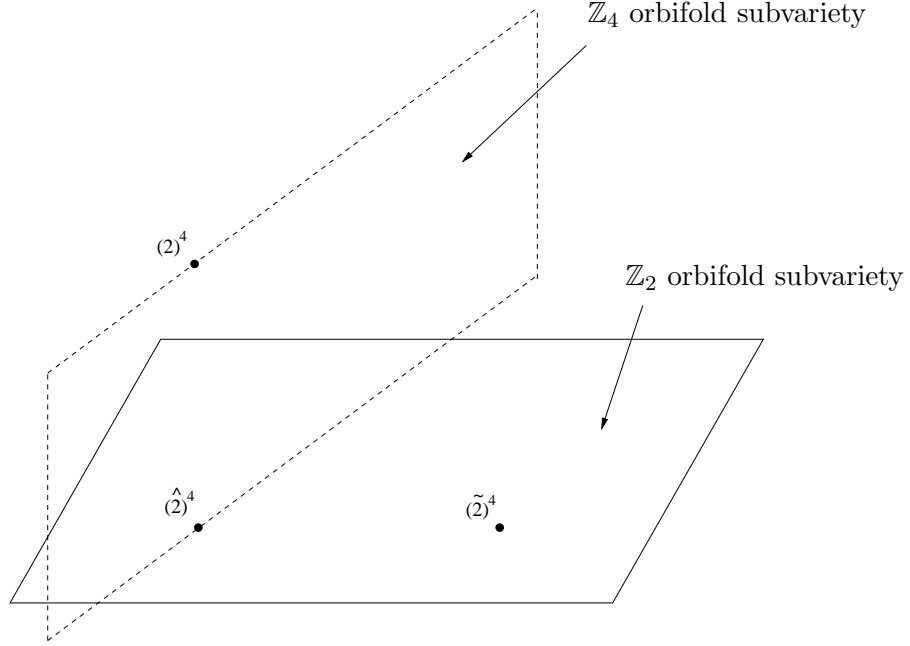


Figure 3.1: Snapshot of the relevant theories as embedded in K3 moduli space

embedding, i.e. they describe the four-planes within the corresponding reference lattices. The reference lattices, though, are different for different n as we will see below. It was an important insight of [31, 32] to show that the reference lattice is actually spanned by the whole even \mathbb{Z} cohomology

$$\mathcal{H}^{\text{even}}(X, \mathbb{Z}) := \mathcal{H}^0(X, \mathbb{Z}) \oplus \mathcal{H}^2(X, \mathbb{Z}) \oplus \mathcal{H}^4(X, \mathbb{Z})$$

of a K3 surface X . The four-plane within this reference lattice is then described by the geometric data of metric, B-field and volume. As for the torus moduli space in section 2.3.2 the cohomology lattice is endowed with the natural scalar product

$$(\omega_1, \omega_2) \mapsto \int_X \omega_1 \wedge \omega_2 \quad \forall \omega_1, \omega_2 \in \mathcal{H}^{\text{even}}(X, \mathbb{Z})$$

which vanishes if $\omega_1 \wedge \omega_2$ is not a 4-form.

In this chapter we are only concerned with two of the above orbifold subvarieties, the \mathbb{Z}_2 and \mathbb{Z}_4 orbifold subvarieties. These two subvarieties actually intersect in one point which is also isomorphic to another conformal field theory model, the Gepner like model $(\hat{2})^4$ which is described in section 2.3.4. The situation is depicted in figure 3.1. The other two points located in the picture, the Gepner model $(2)^4$ and the Gepner like model $(\tilde{2})^4$ will play a role in section 3.4. In the following section we will give the specific reference lattices as well as the prescription how to construct the four-plane from the data of the underlying torus model for both \mathbb{Z}_2 and \mathbb{Z}_4 orbifold models.

3.2 Geometric intersection of the \mathbb{Z}_2 and \mathbb{Z}_4 subvarieties

Let us perform the orbifolding procedure of section 2.3.2 on all tori in the torus moduli space wrt the discrete symmetry groups \mathbb{Z}_2 and \mathbb{Z}_4 . In this manner we achieve two further moduli spaces which are 16- respectively 8-dimensional. These two orbifold moduli spaces have been shown to be embedded into the K3 moduli space as \mathbb{Z}_2 and \mathbb{Z}_4 (orbifold) subvarieties [31, 32].

It has also been shown by conformal field theory arguments that these two subvarieties intersect in one specific point. Unfortunately, however, the reference lattices have to be chosen quite differently for the two embeddings of the \mathbb{Z}_2 and \mathbb{Z}_4 subvarieties such that the geometric identification of that specific point is definitely not clear. Given the high dimensionality of the lattice as well as its nontrivial signature it is also not obvious from inspection that both lattices actually have the same structure.

In this section we will prove the geometric identification of these two points by giving an explicit isomorphism between the two bases of the two embedding spaces which maps both lattices and four-planes into each other.

3.2.1 Reference lattices and four-planes for \mathbb{Z}_2 and \mathbb{Z}_4 orbifold models

First we need to review the reference lattices and the construction of the embedded four-plane for both \mathbb{Z}_2 and \mathbb{Z}_4 orbifold models as described in [31, 32, 33].

Let us start with the torus model $\mathcal{T}(\Lambda, B)$. From section 2.3.2 we know that using the triality isomorphism the torus moduli space can equally well be described by rotations in its even cohomology class $\mathcal{H}^{\text{even}}(\mathcal{T}, \mathbb{R})$. This is the perfect starting point to find a suitable embedding of orbifolds of these tori into the K3 moduli space bearing in mind that the K3 moduli space actually only exhibits even cohomology.

If we take an orbifold of a torus model by some group G only the part of the cohomology survives which is invariant under G . This trivially accounts for the fact that \mathbb{Z}_2 and \mathbb{Z}_4 orbifolds do not have any nontrivial odd cohomology. On the other hand, performing this orbifold procedure we produce singularities, the fixpoints of the G action on the torus. In order to get a mathematically well-defined surface we need to blow-up these singularities to locally projective circles (as described in [30] or in [116] p.182 in more detail). This introduces new cohomology cycles, so-called exceptional divisors $E_i \in \mathcal{H}^2(X, \mathbb{Z})$. In the orbifold limit they have zero volume and, most importantly, self-intersection number $||E_i||^2 = -2$. These additional elements of the second cohomology class account for the much higher dimensionality of $h^{1,1}$ in the K3 case in contrast to the torus case. We call such a surface with blown-up orbifold singularities an orbifold surface.

Usually, one needs more than one exceptional divisor to blow-up an orbifold singularity. The case of a \mathbb{Z}_2 singularity is just the exception where we indeed need only one such exceptional divisor E with $\langle E, E \rangle = -2$. The case of a \mathbb{Z}_4 singularity is already more complicated; we need three exceptional divisors $E^{(+)}$, $E^{(0)}$ and $E^{(-)}$ with

intersection matrix

$$\langle E_i, E_j \rangle_{i,j=+,0,-} = \begin{pmatrix} -2 & 1 & 0 \\ 1 & -2 & 1 \\ 0 & 1 & -2 \end{pmatrix}.$$

In general, the singularities of a complex two-dimensional surface can be classified by the A , D , E groups. The singularities produced by cyclic groups \mathbb{Z}_n , which are interesting for our purposes, are resolved by exceptional divisors with an intersection matrix which is the negative of the Cartan matrix of A_{n-1} .

Furthermore, for any such orbifold surface X , let $v^\circ \in \mathcal{H}^0(X, \mathbb{Z})$ and $v \in \mathcal{H}^4(X, \mathbb{Z})$ be the generators of the respective one-dimensional cohomology groups, with $\langle v^\circ, v \rangle = 1$, $\|v^\circ\|^2 = \|v\|^2 = 0$. Also let $P_{jk} := \text{span}_{\mathbb{F}_2}(f_j, f_k)$ with $j, k \in \{1, \dots, 4\}$ and f_j the j th standard basis vector. And, let μ_i be the dual vectors to the generators λ_i of Λ .

We can now give the reference lattice of a \mathbb{Z}_2 orbifold of $\mathcal{T}(\Lambda, B)$, which we call $\mathcal{K}(\Lambda, B)$. The orbifold group acts via multiplication by -1 on \mathbb{R}^4 . The lattice of even cohomology $\Gamma = \mathcal{H}^{\text{even}}(X, \mathbb{Z})$ of the K3 surface X corresponding to $\mathcal{K}(\Lambda, B)$ is generated by

$$\begin{aligned} \hat{v} &= \sqrt{2} v, \\ \hat{v}^\circ &= \frac{1}{\sqrt{2}} v^\circ - \frac{1}{4} \sum_{i \in I} E_i + \sqrt{2} v \end{aligned} \quad (3.1)$$

and the sublattice $\hat{\Gamma}_{\mathbb{Z}_2}$ (using $\hat{E}_i := -\frac{1}{\sqrt{2}}v + E_i$)

$$\hat{\Gamma}_{\mathbb{Z}_2} := \text{span}_{\mathbb{Z}} \left(\frac{1}{\sqrt{2}} \mu_j \wedge \mu_k + \frac{1}{2} \sum_{i \in P_{jk}} \hat{E}_{i+l}, \hat{E}_m; l, m \in I \right). \quad (3.2)$$

$I = (\mathbb{F}_2)^4$ parametrises the sixteen \mathbb{Z}_2 orbifold fixpoints which have been blown up with one exceptional divisor each.

Similarly let $\mathbb{Z}_4(\Lambda, B)$ signify the \mathbb{Z}_4 orbifold of $\mathcal{T}(\Lambda, B)$, where the orbifold group acts like $\mu_1 \mapsto \mu_2, \mu_2 \mapsto -\mu_1, \mu_3 \mapsto -\mu_4, \mu_4 \mapsto \mu_3$. The lattice of the even cohomology $\Gamma = \mathcal{H}^{\text{even}}(Y, \mathbb{Z})$ of the corresponding K3 surface Y is generated by¹

$$\begin{aligned} \hat{v} &= 2 v, \\ \hat{v}^\circ &= \frac{1}{2} v^\circ - \frac{1}{4} \sum_{i \in I^{(2)}} E_i - \frac{1}{8} \sum_{i \in I^{(4)}} (3E_i^{(+)} + 4E_i^{(0)} + 3E_i^{(-)}) + 2 v \end{aligned}$$

and the sublattice $\hat{\Gamma}_{\mathbb{Z}_4}$ spanned by (using $\hat{E}_i := -\langle E_i, \hat{v}^\circ \rangle \hat{v} + E_i$)

$$\frac{1}{2} \mu_1 \wedge \mu_2 + \frac{1}{2} \hat{E}_{(0,0,1,0)+\epsilon(1,1,0,0)} + \frac{1}{4} \sum_{i \in P_{34} \cap I^{(4)}} \hat{E}_{i+\epsilon(1,1,0,0)} \quad \text{with } \epsilon \in \{0, 1\},$$

¹We apologise for the abuse of notation using the same symbols \hat{E} etc. as in the $\mathcal{K}(\Lambda, B)$ models in order to prevent a proliferation of indices. We hope that a distinction between the different models is clearly visible from the context.

$$\begin{aligned}
& \frac{1}{2} \mu_3 \wedge \mu_4 - \frac{1}{2} \hat{E}_{(1,0,0,0)+\epsilon(0,0,1,1)} - \frac{1}{4} \sum_{i \in P_{12} \cap I^{(4)}} \hat{E}_{i+\epsilon(0,0,1,1)} \quad \text{with } \epsilon \in \{0, 1\}, \\
& \frac{1}{2} (\mu_1 \wedge \mu_3 + \mu_4 \wedge \mu_2) - \frac{1}{2} \sum_{i \in P_{13}} \hat{E}_{i+j} + \hat{E}_j \quad \text{with } j \in I^{(4)}, \\
& \frac{1}{2} (\mu_1 \wedge \mu_4 + \mu_2 \wedge \mu_3) - \frac{1}{2} \sum_{i \in P_{14}} \hat{E}_{i+j} + \hat{E}_j \quad \text{with } j \in I^{(4)}, \\
& \hat{E}_k \quad \text{with } k \in I^{(2)} \cup I^{(4)}.
\end{aligned}$$

$I^{(4)} = \{0000, 0011, 1100, 1111\}$ parametrises the four \mathbb{Z}_4 orbifold fixpoints whose blow-up produces three exceptional divisors each, $I^{(2)} = \{0100, 0001, 0111, 1101, 0110, 0101\}$ the six \mathbb{Z}_2 orbifold fixpoints.

The four-plane which is embedded into these reference lattices is then described by the geometric data of the underlying torus model (see section 2.3.2)

- the metric described by the three-plane $\Sigma_T = \langle \sigma_i \rangle_{i=1,2,3}$,
- the B-field, in its description $b = \sum_{i < j} B_{ij} e_i \wedge e_j$ mapped to the second cohomology class,
- and the volume V_T .

The resulting four-plane x is spanned by the four vectors

$$\begin{aligned}
\Xi_i &= \sigma_i - \langle b, \sigma_i \rangle v \quad \forall i = 1, 2, 3 \\
\Xi_4 &= v^\circ + b + \left(V_T - \frac{\langle b, b \rangle}{2} \right) v.
\end{aligned} \tag{3.3}$$

The \mathbb{Z}_2 orbifold $\mathcal{K}(\mathbb{Z}^4, \mathbf{0})$

The geometric data of the torus model with lattice $\Lambda = \mathbb{Z}^4$ and vanishing B-field $B = 0$ is easily summarised to be

$$\begin{aligned}
\Sigma_T &= \left\langle e_1 \wedge e_2 + e_3 \wedge e_4, e_1 \wedge e_3 + e_4 \wedge e_2, e_1 \wedge e_4 + e_2 \wedge e_3 \right\rangle \\
V_T &= 1 \\
B_T &= 0 \quad \implies \quad b = 0.
\end{aligned}$$

This yields the following positive definite four-plane representing the special model $\mathcal{K}(\mathbb{Z}^4, \mathbf{0})$, the \mathbb{Z}_2 orbifold of $\mathcal{T}(\mathbb{Z}^4, \mathbf{0})$. The given lattice vectors A_i lie within the above described lattice of signature $(4, 20)$ for \mathbb{Z}_2 orbifold surfaces and are pairwise orthogonal and of norm $\|A_i\| = 4$:

$$\begin{aligned}
A_{21} &= \sqrt{2} (e_1 \wedge e_2 + e_3 \wedge e_4) \\
A_{22} &= \sqrt{2} (e_1 \wedge e_3 + e_4 \wedge e_2)
\end{aligned}$$

$$\begin{aligned} A_{23} &= \sqrt{2} (e_1 \wedge e_4 + e_2 \wedge e_3) \\ A_{24} &= 2\hat{v}^\circ + \frac{1}{2} \sum_{i \in I^{(2)}} \hat{E}_i + 3\hat{v}. \end{aligned}$$

The space orthogonal to this four-plane is likewise spanned by the following pairwise orthogonal lattice vectors of norm $\|A_i\| = -4$

$$\begin{aligned} A_1 &= \sqrt{2} (e_1 \wedge e_2 - e_3 \wedge e_4) \\ A_2 &= \sqrt{2} (e_1 \wedge e_3 - e_4 \wedge e_2) \\ A_3 &= \sqrt{2} (e_1 \wedge e_4 - e_2 \wedge e_3) \\ A_4 &= 2\hat{v}^\circ + \frac{1}{2} \sum_{i \in I^{(2)}} \hat{E}_i + \hat{v} \\ A_5 &= \frac{1}{2} (\hat{E}_{0000} - \hat{E}_{1100} - \hat{E}_{0011} + \hat{E}_{1111} - \hat{E}_{1010} - \hat{E}_{1001} - \hat{E}_{0110} - \hat{E}_{0101}) - \hat{v} \\ A_6 &= \frac{1}{2} (\hat{E}_{0000} - \hat{E}_{1100} - \hat{E}_{0011} + \hat{E}_{1111} + \hat{E}_{1010} + \hat{E}_{1001} + \hat{E}_{0110} + \hat{E}_{0101}) + \hat{v} \\ A_7 &= \frac{1}{2} (\hat{E}_{0000} + \hat{E}_{1100} + \hat{E}_{0011} + \hat{E}_{1111} - \hat{E}_{1010} + \hat{E}_{1001} + \hat{E}_{0110} - \hat{E}_{0101}) + \hat{v} \\ A_8 &= \frac{1}{2} (\hat{E}_{0000} + \hat{E}_{1100} + \hat{E}_{0011} + \hat{E}_{1111} + \hat{E}_{1010} - \hat{E}_{1001} - \hat{E}_{0110} + \hat{E}_{0101}) + \hat{v} \\ A_9 &= \frac{1}{2} (\hat{E}_{1000} + \hat{E}_{0100} + \hat{E}_{0010} + \hat{E}_{0001} - \hat{E}_{1110} - \hat{E}_{1101} - \hat{E}_{1011} - \hat{E}_{0111}) \\ A_{10} &= \frac{1}{2} (\hat{E}_{1000} + \hat{E}_{0100} - \hat{E}_{0010} - \hat{E}_{0001} + \hat{E}_{1110} + \hat{E}_{1101} - \hat{E}_{1011} - \hat{E}_{0111}) \\ A_{11} &= \frac{1}{2} (\hat{E}_{1000} - \hat{E}_{0100} + \hat{E}_{0010} - \hat{E}_{0001} + \hat{E}_{1110} - \hat{E}_{1101} + \hat{E}_{1011} - \hat{E}_{0111}) \\ A_{12} &= \frac{1}{2} (\hat{E}_{1000} - \hat{E}_{0100} - \hat{E}_{0010} + \hat{E}_{0001} - \hat{E}_{1110} + \hat{E}_{1101} + \hat{E}_{1011} - \hat{E}_{0111}) \\ A_{13} &= \frac{1}{2} (\hat{E}_{0000} - \hat{E}_{1100} + \hat{E}_{0011} - \hat{E}_{1111} - \hat{E}_{1010} + \hat{E}_{1001} - \hat{E}_{0110} + \hat{E}_{0101}) \\ A_{14} &= \frac{1}{2} (\hat{E}_{0000} - \hat{E}_{1100} + \hat{E}_{0011} - \hat{E}_{1111} + \hat{E}_{1010} - \hat{E}_{1001} + \hat{E}_{0110} - \hat{E}_{0101}) \\ A_{15} &= \frac{1}{2} (\hat{E}_{0000} + \hat{E}_{1100} - \hat{E}_{0011} - \hat{E}_{1111} - \hat{E}_{1010} - \hat{E}_{1001} + \hat{E}_{0110} + \hat{E}_{0101}) \\ A_{16} &= \frac{1}{2} (\hat{E}_{0000} + \hat{E}_{1100} - \hat{E}_{0011} - \hat{E}_{1111} + \hat{E}_{1010} + \hat{E}_{1001} - \hat{E}_{0110} - \hat{E}_{0101}) \\ A_{17} &= \frac{1}{2} (\hat{E}_{1000} + \hat{E}_{0100} + \hat{E}_{0010} - \hat{E}_{0001} - \hat{E}_{1110} + \hat{E}_{1101} + \hat{E}_{1011} + \hat{E}_{0111}) + \hat{v} \\ A_{18} &= \frac{1}{2} (\hat{E}_{1000} + \hat{E}_{0100} - \hat{E}_{0010} + \hat{E}_{0001} + \hat{E}_{1110} - \hat{E}_{1101} + \hat{E}_{1011} + \hat{E}_{0111}) + \hat{v} \\ A_{19} &= \frac{1}{2} (\hat{E}_{1000} - \hat{E}_{0100} + \hat{E}_{0010} + \hat{E}_{0001} + \hat{E}_{1110} + \hat{E}_{1101} - \hat{E}_{1011} + \hat{E}_{0111}) + \hat{v} \\ A_{20} &= \frac{1}{2} (\hat{E}_{1000} - \hat{E}_{0100} - \hat{E}_{0010} - \hat{E}_{0001} - \hat{E}_{1110} - \hat{E}_{1101} - \hat{E}_{1011} + \hat{E}_{0111}) - \hat{v}. \end{aligned}$$

The \mathbb{Z}_4 orbifold $\mathbb{Z}_4(\frac{1}{\sqrt{2}}D_4, B^*)$

Now we want to look at the special theory $\mathbb{Z}_4(\frac{1}{\sqrt{2}}D_4, B^*)$, with the lattice $D_4 = \{x \in \mathbb{Z}_4 | \sum x_i \equiv 0 \pmod{2}\}$. The geometric data of the corresponding torus model is given by

$$\begin{aligned} \Sigma_T &= \left\langle 2e_1 \wedge e_2 + (e_1 \wedge e_3 + e_4 \wedge e_2) - (e_1 \wedge e_4 + e_2 \wedge e_3), \right. \\ &\quad (e_1 \wedge e_3 + e_4 \wedge e_2) + (e_1 \wedge e_4 + e_2 \wedge e_3), \\ &\quad \left. 2e_3 \wedge e_4 - (e_1 \wedge e_3 + e_4 \wedge e_2) + (e_1 \wedge e_4 + e_2 \wedge e_3) \right\rangle \\ V_T &= \frac{1}{2} \\ B_T &= \tilde{B}^* \implies b = e_1 \wedge e_2 + \frac{1}{2}(e_1 \wedge e_3 + e_4 \wedge e_2) - \frac{1}{2}(e_1 \wedge e_4 + e_2 \wedge e_3) \end{aligned}$$

where the B field in this theory is given as the $\Lambda^* \otimes \mathbb{R} \rightarrow \Lambda \otimes \mathbb{R}$ map

$$B^* = \begin{pmatrix} 0 & 1 & 0 & 0 \\ -1 & 0 & 0 & 0 \\ 0 & 0 & 0 & 1 \\ 0 & 0 & -1 & 0 \end{pmatrix}. \quad (3.4)$$

In this model the positive definite four-plane representing this point in moduli space is spanned by the following pairwise orthogonal lattice vectors of norm $\|B_i\| = 4$ (within the above described lattice of signature $(4, 20)$ for \mathbb{Z}_4 orbifold surfaces)

$$\begin{aligned} B_{21} &= 2e_1 \wedge e_2 + (e_1 \wedge e_3 + e_4 \wedge e_2) - (e_1 \wedge e_4 + e_2 \wedge e_3) - \hat{v} \\ B_{22} &= (e_1 \wedge e_3 + e_4 \wedge e_2) + (e_1 \wedge e_4 + e_2 \wedge e_3) \\ B_{23} &= 2e_3 \wedge e_4 - (e_1 \wedge e_3 + e_4 \wedge e_2) + (e_1 \wedge e_4 + e_2 \wedge e_3) \\ B_{24} &= 4\hat{v}^\circ + 2e_1 \wedge e_2 + (e_1 \wedge e_3 + e_4 \wedge e_2) - (e_1 \wedge e_4 + e_2 \wedge e_3) \\ &\quad + \sum_{i \in I^{(2)}} \hat{E}_i + \frac{1}{2} \sum_{i \in I^{(4)}} (3\hat{E}_i^{(+)} + 4\hat{E}_i^{(0)} + 3\hat{E}_i^{(-)}) + 4\hat{v}. \end{aligned}$$

The space orthogonal to this four-plane is likewise spanned by the following pairwise orthogonal lattice vectors of norm $\|B_i\| = -4$

$$\begin{aligned} B_1 &= 2(e_1 \wedge e_2 - e_3 \wedge e_4) + (e_1 \wedge e_3 + e_4 \wedge e_2) - (e_1 \wedge e_4 + e_2 \wedge e_3) \\ B_2 &= 4\hat{v}^\circ + 2e_1 \wedge e_2 + (e_1 \wedge e_3 + e_4 \wedge e_2) - (e_1 \wedge e_4 + e_2 \wedge e_3) \\ &\quad + \sum_{i \in I^{(2)}} \hat{E}_i + \frac{1}{2} \sum_{i \in I^{(4)}} (3\hat{E}_i^{(+)} + 4\hat{E}_i^{(0)} + 3\hat{E}_i^{(-)}) + 3\hat{v} \\ B_3 &= \hat{E}_{0100} - \hat{E}_{0111} \\ B_4 &= \hat{E}_{0001} - \hat{E}_{1101} \\ B_5 &= \hat{E}_{0110} - \hat{E}_{1010} \end{aligned}$$

$$\begin{aligned}
B_6 &= \hat{E}_{0100} + \hat{E}_{0111} + \hat{v} \\
B_7 &= \hat{E}_{0001} + \hat{E}_{1101} + \hat{v} \\
B_8 &= \hat{E}_{0110} + \hat{E}_{1010} + \hat{v} \\
B_9 &= \frac{1}{2}(\hat{E}_{0000}^{(+)} + 2\hat{E}_{0000}^{(0)} + \hat{E}_{0000}^{(-)} + \hat{E}_{1100}^{(+)} + 2\hat{E}_{1100}^{(0)} + \hat{E}_{1100}^{(-)} + \hat{E}_{0011}^{(+)} - \hat{E}_{0011}^{(-)} \\
&\quad - \hat{E}_{1111}^{(+)} + \hat{E}_{1111}^{(-)}) + \hat{v} \\
B_{10} &= \frac{1}{2}(\hat{E}_{0000}^{(+)} + 2\hat{E}_{0000}^{(0)} + \hat{E}_{0000}^{(-)} + \hat{E}_{1100}^{(+)} + 2\hat{E}_{1100}^{(0)} + \hat{E}_{1100}^{(-)} - \hat{E}_{0011}^{(+)} + \hat{E}_{0011}^{(-)} \\
&\quad + \hat{E}_{1111}^{(+)} - \hat{E}_{1111}^{(-)}) + \hat{v} \\
B_{11} &= \frac{1}{2}(\hat{E}_{0000}^{(+)} + 2\hat{E}_{0000}^{(0)} + \hat{E}_{0000}^{(-)} - \hat{E}_{1100}^{(+)} - 2\hat{E}_{1100}^{(0)} - \hat{E}_{1100}^{(-)} - \hat{E}_{0011}^{(+)} + \hat{E}_{0011}^{(-)} \\
&\quad - \hat{E}_{1111}^{(+)} + \hat{E}_{1111}^{(-)}) \\
B_{12} &= \frac{1}{2}(\hat{E}_{0000}^{(+)} + 2\hat{E}_{0000}^{(0)} + \hat{E}_{0000}^{(-)} - \hat{E}_{1100}^{(+)} - 2\hat{E}_{1100}^{(0)} - \hat{E}_{1100}^{(-)} + \hat{E}_{0011}^{(+)} - \hat{E}_{0011}^{(-)} \\
&\quad + \hat{E}_{1111}^{(+)} - \hat{E}_{1111}^{(-)}) \\
B_{13} &= \frac{1}{2}(\hat{E}_{0000}^{(+)} + \hat{E}_{0000}^{(-)} + \hat{E}_{1100}^{(+)} + \hat{E}_{1100}^{(-)} + \hat{E}_{0011}^{(+)} + \hat{E}_{0011}^{(-)} + \hat{E}_{1111}^{(+)} + \hat{E}_{1111}^{(-)}) + \hat{v} \\
B_{14} &= \frac{1}{2}(\hat{E}_{0000}^{(+)} + \hat{E}_{0000}^{(-)} - \hat{E}_{1100}^{(+)} - \hat{E}_{1100}^{(-)} + \hat{E}_{0011}^{(+)} + \hat{E}_{0011}^{(-)} - \hat{E}_{1111}^{(+)} - \hat{E}_{1111}^{(-)}) \\
B_{15} &= \frac{1}{2}(\hat{E}_{0000}^{(+)} + \hat{E}_{0000}^{(-)} + \hat{E}_{1100}^{(+)} + \hat{E}_{1100}^{(-)} - \hat{E}_{0011}^{(+)} - \hat{E}_{0011}^{(-)} - \hat{E}_{1111}^{(+)} - \hat{E}_{1111}^{(-)}) \\
B_{16} &= \frac{1}{2}(\hat{E}_{0000}^{(+)} + \hat{E}_{0000}^{(-)} - \hat{E}_{1100}^{(+)} - \hat{E}_{1100}^{(-)} - \hat{E}_{0011}^{(+)} - \hat{E}_{0011}^{(-)} + \hat{E}_{1111}^{(+)} + \hat{E}_{1111}^{(-)}) \\
B_{17} &= \frac{1}{2}(\hat{E}_{0000}^{(+)} - \hat{E}_{0000}^{(-)} + \hat{E}_{1100}^{(+)} - \hat{E}_{1100}^{(-)} - \hat{E}_{0011}^{(+)} - 2\hat{E}_{0011}^{(0)} - \hat{E}_{0011}^{(-)} \\
&\quad + \hat{E}_{1111}^{(+)} + 2\hat{E}_{1111}^{(0)} + \hat{E}_{1111}^{(-)}) \\
B_{18} &= \frac{1}{2}(\hat{E}_{0000}^{(+)} - \hat{E}_{0000}^{(-)} + \hat{E}_{1100}^{(+)} - \hat{E}_{1100}^{(-)} + \hat{E}_{0011}^{(+)} + 2\hat{E}_{0011}^{(0)} + \hat{E}_{0011}^{(-)} \\
&\quad - \hat{E}_{1111}^{(+)} - 2\hat{E}_{1111}^{(0)} - \hat{E}_{1111}^{(-)}) \\
B_{19} &= \frac{1}{2}(\hat{E}_{0000}^{(+)} - \hat{E}_{0000}^{(-)} - \hat{E}_{1100}^{(+)} + \hat{E}_{1100}^{(-)} + \hat{E}_{0011}^{(+)} + 2\hat{E}_{0011}^{(0)} + \hat{E}_{0011}^{(-)} \\
&\quad + \hat{E}_{1111}^{(+)} + 2\hat{E}_{1111}^{(0)} + \hat{E}_{1111}^{(-)}) + \hat{v} \\
B_{20} &= \frac{1}{2}(\hat{E}_{0000}^{(+)} - \hat{E}_{0000}^{(-)} - \hat{E}_{1100}^{(+)} + \hat{E}_{1100}^{(-)} - \hat{E}_{0011}^{(+)} - 2\hat{E}_{0011}^{(0)} - \hat{E}_{0011}^{(-)} \\
&\quad - \hat{E}_{1111}^{(+)} - 2\hat{E}_{1111}^{(0)} - \hat{E}_{1111}^{(-)}) - \hat{v}.
\end{aligned}$$

3.2.2 Identification of lattice vectors at the intersection point

In [31] it was shown by indirect arguments that the conformal field theories associated with the K3 geometries at $\mathcal{K}(\mathbb{Z}^4, 0)$ and $\mathbb{Z}_4(\frac{1}{\sqrt{2}}D_4, B^*)$ can be identified and therefore signify the same point in K3 moduli space. Here, we want to give a direct proof that

the geometries associated with these theories are indeed the same. It is given by the following identification of the respective lattices of both theories which also identifies the four-planes placed within these lattices

$$\begin{array}{ll}
A_1 \cong B_6 & A_2 \cong -B_5 \\
A_3 \cong -B_4 & A_4 \cong -B_{15} \\
A_5 \cong B_2 & A_6 \cong -B_{13} \\
A_7 \cong B_{14} & A_8 \cong B_{16} \\
A_9 \cong -B_1 & A_{10} \cong B_3 \\
A_{11} \cong B_8 & A_{12} \cong B_7 \\
A_{13} \cong -B_9 & A_{14} \cong -B_{10} \\
A_{15} \cong B_{11} & A_{16} \cong B_{12} \\
A_{17} \cong -B_{17} & A_{18} \cong -B_{18} \\
A_{19} \cong B_{19} & A_{20} \cong -B_{20} \\
A_{21} \cong -B_{21} & A_{22} \cong B_{22} \\
A_{23} \cong B_{23} & A_{24} \cong B_{24} .
\end{array} \tag{3.5}$$

As this is a highly symmetric point in moduli space this identification is certainly only one of a great variety of possible ones.

Proof. In order to prove the above statement (3.5) we first need to express the generators of one lattice in terms of the respective basis. We choose to take the generators of the lattice $\Gamma(\mathcal{K}(\mathbb{Z}^4, 0))$ of $\mathcal{K}(\mathbb{Z}^4, 0)$ and express them in terms of the A_i , $i = 1, \dots, 24$. Using the above equivalence we can, hence, find the vectors equivalent to these generators in the \mathbb{R} -span of the other lattice, $\text{span}_{\mathbb{R}}(B_i; i = 1, \dots, 24)$. These vectors have to be shown to be lattice vectors in $\Gamma(\mathbb{Z}_4(\frac{1}{\sqrt{2}}D_4, B^*))$ again. Now, as already explained in the beginning of section 3.1, both lattices are known to be even selfdual of signature $(4, 20)$ and are, hence, unique up to isometries. As both bases A_i and B_j consist of pairwise orthogonal vectors and as the identification (3.5) preserves the norm of these basis vectors, the identification preserves the scalar product on the whole lattice. Thus, as this set of vectors is known to be generators for one of the two lattices, it has to generate the other as well.

On the other hand, the four-planes are spanned by A_{21} , A_{22} , A_{23} , and A_{24} in $\Gamma(\mathcal{K}(\mathbb{Z}^4, 0))$ and B_{21} , B_{22} , B_{23} , and B_{24} in $\Gamma(\mathbb{Z}_4(\frac{1}{\sqrt{2}}D_4, B^*))$, and are thus identified. Hence, we have given a simultaneous isomorphism of both lattices and both four-planes which describe the two theories $\mathcal{K}(\mathbb{Z}^4, 0)$ and $\mathbb{Z}_4(\frac{1}{\sqrt{2}}D_4, B^*)$. This proves that both these theories signify the same point in K3 moduli space.

We have performed the explicit calculation for all generators of $\Gamma(\mathcal{K}(\mathbb{Z}^4, 0))$ as given in (3.1) and (3.2). We want to present a choice of typical examples of this calculation. Each time we first express a generator of $\Gamma(\mathcal{K}(\mathbb{Z}^4, 0))$ in terms of the orthogonal basis of A_i , then we use the identification given in equation (3.5) to rewrite this expression in terms of the B_j , and finally we express the result in terms of a sum of lattice vectors of $\Gamma(\mathbb{Z}_4(\frac{1}{\sqrt{2}}D_4, B^*))$ (either given as single vectors or collected in big brackets):

$$\begin{aligned}
\hat{E}_{0000} &= \frac{1}{4}(A_5 + A_6 + A_7 + A_8 + A_{13} + A_{14} + A_{15} + A_{16} + A_4 - A_{24}) \\
&\hat{=} \frac{1}{4}(B_2 - B_{13} + B_{14} + B_{16} - B_9 - B_{10} + B_{11} + B_{12} - B_{15} - B_{24}) \\
&= -\hat{v} - \hat{E}_{1100}^{(+)} - \hat{E}_{1100}^{(0)} - \hat{E}_{1100}^{(-)} \\
\hat{E}_{1000} &= \frac{1}{4}(A_9 + A_{10} + A_{11} + A_{12} + A_{17} + A_{18} + A_{19} + A_{20} + A_4 - A_{24}) \\
&\hat{=} \frac{1}{4}(-B_1 + B_3 + B_8 + B_7 - B_{17} - B_{18} + B_{19} - B_{20} - B_{15} - B_{24}) \\
&= \left(-e_1 \wedge e_2 + \frac{1}{2}(\hat{E}_{0000}^{(+)} + \hat{E}_{0000}^{(-)} + \hat{E}_{0011}^{(+)} + \hat{E}_{0011}^{(-)}) \right) \\
&\quad + \left(\frac{1}{2}e_3 \wedge e_4 - \frac{1}{2}\hat{E}_{0100} - \frac{1}{4}(-\hat{E}_{0000}^{(+)} - 2\hat{E}_{0000}^{(0)} - 3\hat{E}_{0000}^{(-)} \right. \\
&\quad \quad \left. - \hat{E}_{1100}^{(+)} - 2\hat{E}_{1100}^{(0)} - 3\hat{E}_{1100}^{(-)}) \right) \\
&\quad + \left(-\frac{1}{2}(e_1 \wedge e_3 + e_4 \wedge e_2) - \frac{1}{2}(\hat{E}_{0000}^{(+)} + \hat{E}_{0000}^{(-)}) + \frac{1}{2}(\hat{E}_{0100} + \hat{E}_{0001} + \hat{E}_{0101}) \right) \\
&\quad + \left(\frac{1}{2}(e_1 \wedge e_4 + e_2 \wedge e_3) + \frac{1}{2}(\hat{E}_{0011}^{(+)} + \hat{E}_{0011}^{(-)}) + \frac{1}{2}(-\hat{E}_{0111} - \hat{E}_{0001} - \hat{E}_{0101}) \right) \\
&\quad - \hat{v}^\circ - \hat{E}_{0000}^{(+)} - \hat{E}_{0000}^{(0)} - \hat{E}_{0000}^{(-)} - \hat{E}_{1100}^{(+)} - \hat{E}_{1100}^{(0)} - \hat{E}_{1100}^{(-)} - \hat{E}_{0011}^{(+)} - \hat{E}_{0011}^{(-)} \\
\frac{1}{\sqrt{2}}e_1 \wedge e_2 + \frac{1}{2}(\hat{E}_{0000} - \hat{E}_{0010} - \hat{E}_{0001} + \hat{E}_{0011}) \\
&= \frac{1}{4}(A_1 + A_{21} + A_7 + A_8 + A_{13} + A_{14} - A_{19} + A_{20} - A_9 + A_{10}) \\
&\hat{=} \frac{1}{4}(B_6 - B_{21} + B_{14} + B_{16} - B_9 - B_{10} - B_{19} - B_{20} + B_1 + B_3) \\
&= \left(-\frac{1}{2}e_3 \wedge e_4 + \frac{1}{2}\hat{E}_{0100} + \frac{1}{4}(-\hat{E}_{0000}^{(+)} - 2\hat{E}_{0000}^{(0)} - 3\hat{E}_{0000}^{(-)} \right. \\
&\quad \left. - \hat{E}_{1100}^{(+)} - 2\hat{E}_{1100}^{(0)} - 3\hat{E}_{1100}^{(-)}) \right) + \hat{E}_{0000}^{(-)} \\
\hat{v} &= \frac{1}{2}(-A_4 + A_{24}) \cong \frac{1}{2}(B_{15} + B_{24}) \\
&\hat{=} \left(e_1 \wedge e_2 + \frac{1}{2}(\hat{E}_{0000}^{(+)} + \hat{E}_{0000}^{(-)} + \hat{E}_{0011}^{(+)} + \hat{E}_{0011}^{(-)}) \right) \\
&\quad + \left(\frac{1}{2}(e_1 \wedge e_3 + e_4 \wedge e_2) - \frac{1}{2}(\hat{E}_{0000}^{(+)} + \hat{E}_{0000}^{(-)}) + \frac{1}{2}(\hat{E}_{0100} + \hat{E}_{0001} + \hat{E}_{0101}) \right) \\
&\quad + \left(-\frac{1}{2}(e_1 \wedge e_4 + e_2 \wedge e_3) + \frac{1}{2}(\hat{E}_{1111}^{(+)} + \hat{E}_{1111}^{(-)}) + \frac{1}{2}(\hat{E}_{0111} + \hat{E}_{1110} + \hat{E}_{0110}) \right) \\
&\quad + 2\hat{v}^\circ + 2\hat{v} + \sum_{i \in \{0000, 1100\}} (\hat{E}_i^{(+)} + \hat{E}_i^{(0)} + \hat{E}_i^{(-)}) + \hat{E}_{0011}^{(0)} + \hat{E}_{1111}^{(0)}
\end{aligned}$$

$$\begin{aligned}
\hat{v}^\circ &= \frac{1}{4}(-A_4 + A_5 - A_6 - A_7 - A_8 - A_{17} - A_{18} - A_{19} + A_{20} + 3A_{24}) \\
&\cong \frac{1}{4}(B_{15} + B_2 + B_{13} - B_{14} - B_{16} + B_{17} + B_{18} - B_{19} - B_{20} + 3B_{24}) \\
&= 4\hat{v}^\circ + 4\hat{v} + 2e_1 \wedge e_2 + (e_1 \wedge e_3 + e_4 \wedge e_2) - (e_1 \wedge e_4 + e_2 \wedge e_3) + \sum_{i \in I^{(2)}} \hat{E}_i \\
&\quad + 2 \sum_{i \in I^{(4)}} \left(\hat{E}_i^{(+)} + \hat{E}_i^{(0)} + \hat{E}_i^{(-)} \right) - \frac{1}{2} \sum_{i \in I^{(4)}} \left(\hat{E}_i^{(+)} + \hat{E}_i^{(-)} \right) + \hat{E}_{1100} .
\end{aligned}$$

□

3.3 Identification of CFTs at the $(\hat{2})^4$ Gepner point

Let us now turn to the conformal field theoretic identification at the $(\hat{2})^4$ Gepner point. [31, 32] have shown that two orbifold CFTs, the \mathbb{Z}_2 orbifold $\mathcal{K}(\mathbb{Z}^4, 0)$ and the \mathbb{Z}_4 orbifold $\mathbb{Z}_4(\frac{1}{\sqrt{2}}D_4, B^*)$ (now regarded as CFTs), coincide with the same Gepner like theory $(\hat{2})^4$, a \mathbb{Z}_2 orbifold of the Gepner model $(2)^4$ as described in section 2.3.4. The last identification has been achieved via first identifying the two theories $\mathcal{K}(\frac{1}{\sqrt{2}}D_4, B^*)$ and $(\hat{2})^4$ (a $(\mathbb{Z}_2)^2$ orbifold of $(2)^4$ as described in section 2.3.4) and then showing that the same \mathbb{Z}_2 orbifold action transforms both theories to the above two theories $\mathbb{Z}_4(\frac{1}{\sqrt{2}}D_4, B^*)$ and $(\hat{2})^4$. In this section we want to present the explicit identification of these three CFT models.

First recall that certain superconformal field theories at $c = 6$ can be identified using the following steps if they have a specifically enlarged symmetry algebra ([31, 32]):

- The partition function has to agree in each sector.
- The current part of the holomorphic symmetry algebra \mathcal{A}_h , i.e. the algebra of the fields with $(h, \tilde{h}) = (1, 0)$ has to agree. The $su(2)_1^2$ part of the symmetry algebra which originates in the $N = 4$ supersymmetry structure has to be enhanced by at least a $u(1)^4$. Hence, we need $u(1)^6 \subset \mathcal{A}_h$ for this argument to work. The same applies to the antiholomorphic symmetry algebra $\mathcal{A}_{\tilde{h}}$.
- Denote the $U(1)$ currents in $su(2)_1^2$ as $J^{(1)}, J^{(2)}$, the $U(1)$ currents in $u(1)^4$ as j^1, \dots, j^4 . Define the “bosonic” Hilbert subspace

$$\mathcal{H}_b := \left\{ |\varphi\rangle \in \mathcal{H} \mid J_0^{(k)} |\varphi\rangle = 0 \quad \forall k \in \{1, 2\} \right\} .$$

Then the charge lattice w.r.t. the subalgebra $u(1)^4$

$$\Gamma_b := \left\{ \gamma \in \mathbb{R}^{d,d} \mid \exists |\varphi\rangle \in \mathcal{H}_b : j_0^k |\varphi\rangle = \gamma^k |\varphi\rangle \quad \forall k \in \{1, \dots, 4\} \right\}$$

has to be isomorphic to the same selfdual lattice in both theories as well. It suffices to show this agreement for a set of generators $|\varphi\rangle$ of this selfdual lattice.

The main idea of the proof of this statement ([31, 32]) is that w.r.t. the $u(1)^4$ subalgebra the bosonic part of these theories can be viewed as a toroidal theory in $d = 4$ dimensions, which is uniquely determined by its charge lattice. The identification of the partition function and the supersymmetry algebra then determine the complete supersymmetric theories to be isomorphic.

In the special case of our three theories the partition functions have already been shown to agree in [31]. For example, the NS sector part of the partition function of $\mathcal{K}(\mathbb{Z}^4, 0)$ is given by [31, 32]

$$Z_{\Gamma(\mathbb{Z}^4, 0)}^{NS}(\sigma, z) = \frac{1}{2} \left[\frac{1}{4} \left(\left| \frac{\theta_2(\sigma)}{\eta(\sigma)} \right|^4 + \left| \frac{\theta_3(\sigma)}{\eta(\sigma)} \right|^4 + \left| \frac{\theta_4(\sigma)}{\eta(\sigma)} \right|^4 \right)^2 + \left| \frac{\theta_3(\sigma)\theta_4(\sigma)}{\eta(\sigma)^2} \right|^4 + \left| \frac{\theta_2(\sigma)\theta_3(\sigma)}{\eta(\sigma)^2} \right|^4 + \left| \frac{\theta_2(\sigma)\theta_4(\sigma)}{\eta(\sigma)^2} \right|^4 \right] \cdot \left| \frac{\theta_3(\sigma, z)}{\eta(\sigma)} \right|^4 .$$

We now elaborate the enhanced symmetry algebras for the three theories as well as the lattices of $(1/4, 1/4)$ Ramond groundstate fields explicitly. The $(1/4, 1/4)$ Ramond groundstate fields generate \mathcal{H}_b as they are the lowest components of the supersymmetric groundstate fields.

3.3.1 The symmetry algebra of $\mathcal{K}(\mathbb{Z}^4, 0)$

We already know the supersymmetric generators in the symmetry algebra of $\mathcal{K}(\mathbb{Z}^4, 0)$ from section 2.3.2. Thus, we still need to extract the additional holomorphic vertex operators with $(h, \tilde{h}) = (1, 0)$. The charge lattice of $\mathcal{K}(\mathbb{Z}^4, 0)$ is given by

$$(P_r(\mu, \lambda), P_l(\mu, \lambda)) = \frac{1}{\sqrt{2}}(\mu + \lambda, \mu - \lambda) = \left(p + \frac{1}{2}w, p - \frac{1}{2}w \right) ,$$

with $w = \sqrt{2}\lambda \in \sqrt{2}\Lambda = \sqrt{2}\mathbb{Z}^4$ and $p = \frac{1}{\sqrt{2}}\mu \in \frac{1}{\sqrt{2}}\Lambda^* = \frac{1}{\sqrt{2}}\mathbb{Z}^4$.

Hence we get four additional holomorphic $U(1)$ currents which are invariant under \mathbb{Z}_2 action $e_i \mapsto -e_i$ $i \in \{1, \dots, 4\}$ (using the convention $V_P = V_{\lambda, \mu}$)

$$U_i = V_{e_i, e_i}^{\text{inv}} = V_{e_i, e_i}^t + V_{-e_i, -e_i}^t \quad i = 1, \dots, 4 .$$

The cocycle factors for a $u(1)^4$ algebra of holomorphic vertex operators are naturally 1. Hence we get the OPE

$$U_i(z)U_j(w) = 2\delta_{ij}(z-w)^{-2} + O(1) .$$

The total, enhanced holomorphic symmetry algebra can be diagonalised as (with the complexified toroidal bosonic currents $j_{\pm}^{(k)}$ and their superpartners $\psi_{\pm}^{(k)}$ as given in

section 2.3.2)

$$\begin{aligned}
J' &:= (\psi_+^{(1)}\psi_-^{(1)} + \psi_+^{(2)}\psi_-^{(2)}) & J'^+ &:= \sqrt{2}\psi_+^{(1)}\psi_+^{(2)} & J'^- &:= \sqrt{2}\psi_-^{(2)}\psi_-^{(1)} \\
A' &:= (\psi_+^{(1)}\psi_-^{(1)} - \psi_+^{(2)}\psi_-^{(2)}) & A'^+ &:= \sqrt{2}\psi_+^{(1)}\psi_-^{(2)} & A'^- &:= \sqrt{2}\psi_+^{(2)}\psi_-^{(1)} \\
\hline
P' &= \frac{1}{2}(U_1 + U_2 + U_3 + U_4) \\
Q' &= \frac{1}{2}(U_1 + U_2 - U_3 - U_4) \\
R' &= \frac{1}{2}(U_1 - U_2 + U_3 - U_4) \\
S' &= \frac{1}{2}(U_1 - U_2 - U_3 + U_4).
\end{aligned}$$

This diagonalisation of the $U(1)$ currents has the advantage that P' and Q' are already invariant under the \mathbb{Z}_4 operation

$$\begin{aligned}
e_1 &\mapsto e_2 & e_2 &\mapsto -e_1 \\
e_3 &\mapsto -e_4 & e_4 &\mapsto e_3.
\end{aligned} \tag{3.6}$$

This \mathbb{Z}_4 operation acts the same way on the currents j^i and their superpartners ψ^i .

3.3.2 The symmetry algebra of $\mathbb{Z}_4(\frac{1}{\sqrt{2}}D_4, B^*)$

Remember the definition of D_4 and B^* in (3.4). It is now easier to study the symmetry algebra of the \mathbb{Z}_2 orbifold $\mathcal{K}(\frac{1}{\sqrt{2}}D_4, B^*)$ first and to get the symmetry algebra of $\mathbb{Z}_4(\frac{1}{\sqrt{2}}D_4, B^*)$ by an explicit orbifold action thereafter.

Hence, let us first look for additional holomorphic vertex operators in $\mathcal{K}(\frac{1}{\sqrt{2}}D_4, B^*)$. Due to $\Lambda = \frac{1}{\sqrt{2}}D_4$ the left charges of these are given as roots out of the root system of D_4

$$(P_l, P_r) = \frac{1}{\sqrt{2}}(\mu - B^*\lambda + \lambda, \mu - B^*\lambda - \lambda) = (\alpha_i, 0) \quad \alpha_i \in D_4,$$

which leads to the following cocycle factor on the root system of D_4 (derived in (2.16))

$$c_{\alpha_2}(-\alpha_1) = \exp\left[\frac{i}{2}\pi\alpha_1^t B^* \alpha_2\right].$$

The roots of D_4 are given as linear combinations of the unit vectors $\alpha = e_i \pm e_j$. Hence, we can change the basis of the vertex operators in the holomorphic algebra to the more useful linear combination (following [31])

$$W_{ij}^\pm := \frac{1}{2}\left(V_{e_i+e_j}^{\text{inv}} \pm V_{e_i-e_j}^{\text{inv}}\right),$$

where

$$V_\alpha^{\text{inv}}(z) = (V_\alpha^{\text{torus}} + V_{-\alpha}^{\text{torus}})$$

is the \mathbb{Z}_2 invariant linear combination of the torus vertex operators V^{torus} . We directly observe the symmetry of the indices $W_{ij}^\pm = W_{ji}^\pm$.

One can now calculate the OPEs of all the W_{ij}^\pm . In order to make the full $su(2)_1^6$ symmetry visible we re-write them in the following form

$$\begin{aligned}
J &:= (\psi_+^{(1)}\psi_-^{(1)} + \psi_+^{(2)}\psi_-^{(2)}) & J^+ &:= \sqrt{2}\psi_+^{(1)}\psi_+^{(2)} & J^- &:= \sqrt{2}\psi_-^{(2)}\psi_-^{(1)} \\
A &:= (\psi_+^{(1)}\psi_-^{(1)} - \psi_+^{(2)}\psi_-^{(2)}) & A^+ &:= \sqrt{2}\psi_+^{(1)}\psi_-^{(2)} & A^- &:= \sqrt{2}\psi_+^{(2)}\psi_-^{(1)} \\
P &:= W_{14}^- + W_{23}^- & P^\pm &:= \frac{1}{\sqrt{2}}((W_{12}^+ + W_{34}^+) \pm i(W_{24}^- - W_{13}^-)) \\
Q &:= W_{12}^+ - W_{34}^+ & Q^\pm &:= \frac{1}{\sqrt{2}}((W_{24}^- + W_{13}^-) \pm i(W_{14}^- - W_{23}^-)) \\
R &:= W_{14}^+ + W_{23}^+ & R^\pm &:= \frac{1}{\sqrt{2}}((W_{24}^+ - W_{13}^+) \pm i(W_{12}^- + W_{34}^-)) \\
S &:= W_{24}^+ + W_{13}^+ & S^\pm &:= \frac{1}{\sqrt{2}}((W_{12}^- - W_{34}^-) \pm i(W_{14}^+ - W_{23}^+))
\end{aligned} \tag{3.7}$$

where the $su(2)_1$ currents $\mathcal{J}, \mathcal{J}^\pm$ are normalised to fulfil the following OPEs

$$\begin{aligned}
\mathcal{J}(z)\mathcal{J}^\pm(w) &\sim \pm 2(z-w)^{-1}\mathcal{J}^\pm(w) \\
\mathcal{J}^+(z)\mathcal{J}^-(w) &\sim \pm 2(z-w)^{-2} + 2(z-w)^{-1}\mathcal{J}(w) \\
\mathcal{J}(z)\mathcal{J}(w) &\sim \pm 2(z-w)^{-2}.
\end{aligned} \tag{3.8}$$

Let us now turn to the symmetry algebra of the $\mathbb{Z}_4(\frac{1}{\sqrt{2}}D_4, B^*)$ model. [31] have shown that it is enhanced to $su(2)^2 \otimes u(1)^4$ which is just given by the symmetry currents of (3.7) which are invariant under the \mathbb{Z}_4 operation (3.6). These are

$$J, J^\pm; \quad P, P^\pm; \quad A; Q; R; S.$$

There are no new holomorphic $(1, 0)$ currents in the twisted sectors.

3.3.3 Non-twisted groundstate $(\frac{1}{4}, \frac{1}{4})$ fields

The torus theory contains eight groundstate $(\frac{1}{4}, \frac{1}{4})$ fields in the Ramond sector. These generate the Clifford algebra of groundstates for the Ramond sector. They can be diagonalised to have charges which are non-vanishing only wrt to one of the currents J, A (as in (3.7)) and its respective antiholomorphic counterpart

- E_J^\pm having charges $(\pm 1, \pm 1)$ w.r.t. J, \bar{J}
- F_J^\pm having charges $(\pm 1, \mp 1)$ w.r.t. J, \bar{J}
- E_A^\pm having charges $(\pm 1, \pm 1)$ w.r.t. A, \bar{A}
- F_A^\pm having charges $(\pm 1, \mp 1)$ w.r.t. A, \bar{A} .

All of these fields survive the \mathbb{Z}_2 orbifolding, but only six of them,

$$E_J^\pm, \quad F_J^\pm, \quad E_A^\pm,$$

survive the above \mathbb{Z}_4 orbifolding with the action of equation (3.6). As the two torus symmetry fields J and A are made up of free fermions (the superpartners of the bosonic currents of the torus theory) a representation for these eight groundstate fields can be written down in terms of a suitable bosonisation.

3.3.4 Twisted groundstate $(\frac{1}{4}, \frac{1}{4})$ fields in $\mathbb{Z}_4(\frac{1}{\sqrt{2}}\mathbf{D}_4, \mathbf{B}^*)$

The other groundstate $(\frac{1}{4}, \frac{1}{4})$ fields have to come from the twisted sectors. Let us first regard the action of the additional symmetry generators on the groundstate twistfields of this theory. For $\mathbb{Z}_4(\frac{1}{\sqrt{2}}\mathbf{D}_4, \mathbf{B}^*)$ we have the lattice $\Lambda = \frac{1}{\sqrt{2}}\mathbf{D}_4 = \frac{1}{\sqrt{2}}\Lambda_d$ where Λ_d will be the lattice numbering our fixpoints, i.e. $f \in \Lambda_d$. The representation of the orbifold group generator is given by

$$\theta_4 = \begin{pmatrix} 0 & -1 & 0 & 0 \\ 1 & 0 & 0 & 0 \\ 0 & 0 & 0 & 1 \\ 0 & 0 & -1 & 0 \end{pmatrix} \quad \theta_2 = \theta_4^2 = \begin{pmatrix} -1 & 0 & 0 & 0 \\ 0 & -1 & 0 & 0 \\ 0 & 0 & -1 & 0 \\ 0 & 0 & 0 & -1 \end{pmatrix}. \quad (3.9)$$

\mathbb{Z}_2 twistfields

For \mathbb{Z}_2 twistfields we have a coupling of (see section 2.3.3)

$$g^{(N=2)}(\alpha, 0) = \frac{1}{4} e^{\frac{1}{2}\pi i(\alpha+B^*\alpha)^t(1-\theta_2)^{-1}\alpha} = \frac{i}{4}$$

due to $\|\alpha\|^2 = 2$ and the antisymmetry of B^* . Furthermore, the translation of the fixpoint in the OPE of the holomorphic vertex operator and the twistfield is given by

$$x_f \mapsto x_f + (1 - \theta_2)^{-1}\lambda = x_f + \frac{1}{2} \frac{\alpha}{\sqrt{2}}.$$

Hence we get an OPE of

$$\begin{aligned} V_{e_i+e_j}(z) T_f^{(N=2)}(w) &= (V_{e_i+e_j}^t(z) + V_{-e_i-e_j}^t(z)) T_f^{(N=2)}(w) \\ &= g^{(N=2)}(\alpha, 0)(z-w)^{-1} \\ &\quad \left(e^{i\pi(\alpha+B^*\alpha)^t(\sqrt{2}x_f)} + e^{-i\pi(\alpha+B^*\alpha)^t(\sqrt{2}x_f)} \right) T_{f'}^{(N=2)}(w) \\ &= \frac{i}{2} e^{i\pi(\alpha+B^*\alpha)^t(\sqrt{2}x_f)} T_{[x_f+\frac{1}{2\sqrt{2}}\alpha]}^{(N=2)}(w). \end{aligned}$$

Now using this OPE, we can diagonalise the groundstate twistfields wrt the action of the enhanced symmetry generators

$$\begin{aligned}
E_P^\pm &= \sum_{\substack{\delta_1=\delta_2 \\ \delta_3=\delta_4}} (-1)^{\delta_3} T_{\underline{\delta}}^{(N=2)} \pm i \sum_{\substack{\delta_1 \neq \delta_2 \\ \delta_3 \neq \delta_4}} (-1)^{\delta_2+\delta_3} T_{\underline{\delta}}^{(N=2)} \\
F_P^\pm &= \sum_{\substack{\delta_1 \neq \delta_2 \\ \delta_3=\delta_4}} T_{\underline{\delta}}^{(N=2)} \pm i \sum_{\substack{\delta_1=\delta_2 \\ \delta_3 \neq \delta_4}} (-1)^{\delta_1} T_{\underline{\delta}}^{(N=2)} \\
E_Q^\pm &= \sum_{\substack{\delta_1=\delta_2 \\ \delta_3=\delta_4}} T_{\underline{\delta}}^{(N=2)} \pm i \sum_{\substack{\delta_1 \neq \delta_2 \\ \delta_3=\delta_4}} (-1)^{\delta_3} T_{\underline{\delta}}^{(N=2)} \\
F_Q^\pm &= \sum_{\substack{\delta_1=\delta_2 \\ \delta_3 \neq \delta_4}} (-1)^{\delta_1+\delta_3} T_{\underline{\delta}}^{(N=2)} \pm i \sum_{\substack{\delta_1 \neq \delta_2 \\ \delta_3 \neq \delta_4}} (-1)^{\delta_2} T_{\underline{\delta}}^{(N=2)} \\
E_R^\pm &= \sum_{\substack{\delta_1=\delta_2 \\ \delta_3=\delta_4}} (-1)^{\delta_1} T_{\underline{\delta}}^{(N=2)} \pm i \sum_{\substack{\delta_1 \neq \delta_2 \\ \delta_3 \neq \delta_4}} T_{\underline{\delta}}^{(N=2)} \\
F_R^\pm &= \sum_{\substack{\delta_1 \neq \delta_2 \\ \delta_3=\delta_4}} (-1)^{\delta_2+\delta_3} T_{\underline{\delta}}^{(N=2)} \pm i \sum_{\substack{\delta_1=\delta_2 \\ \delta_3 \neq \delta_4}} (-1)^{\delta_3} T_{\underline{\delta}}^{(N=2)} \\
E_S^\pm &= \sum_{\substack{\delta_1=\delta_2 \\ \delta_3=\delta_4}} (-1)^{\delta_1+\delta_3} T_{\underline{\delta}}^{(N=2)} \pm i \sum_{\substack{\delta_1=\delta_2 \\ \delta_3 \neq \delta_4}} T_{\underline{\delta}}^{(N=2)} \\
F_S^\pm &= \sum_{\substack{\delta_1 \neq \delta_2 \\ \delta_3=\delta_4}} (-1)^{\delta_1} T_{\underline{\delta}}^{(N=2)} \pm i \sum_{\substack{\delta_1 \neq \delta_2 \\ \delta_3 \neq \delta_4}} (-1)^{\delta_3} T_{\underline{\delta}}^{(N=2)},
\end{aligned}$$

where the index indicates the $U(1)$ current (P , Q , R or S) this field is charged with. The respective holomorphic and antiholomorphic charges are $(\pm 1, \pm 1)$ for fields E^\pm and $(\pm 1, \mp 1)$ for fields F^\pm . The charges wrt the respective other three currents as well as J and A vanish. The following ten fields are invariant under the \mathbb{Z}_4 action (3.6) and are, hence, contained in $\mathbb{Z}_4(\frac{1}{\sqrt{2}}D_4, B^*)$ as well

$$E_P^\pm, F_P^\pm; E_Q^\pm; E_R^\pm; E_S^\pm.$$

\mathbb{Z}_4 twistfields

In the case of \mathbb{Z}_4 twistfields the vertex operator coupling amounts to (see section 2.3.3)

$$g_l^{(N=4)}(\alpha, 0) = \frac{1}{8} \quad \forall l = 1, 3.$$

The total coupling constant $g^{(N=4)}(\alpha, 0)$ still depends on the order of the twist as we will see below. The fixpoint of the twistfield is translated due to the action of the vertex operator

$$x_f \mapsto x_{f'} = x_f + (1 - \theta_4^l)^{-1} \lambda = x_f + \frac{1}{2}(1 + \theta_4^l) \frac{\alpha}{\sqrt{2}}.$$

Hence we get an OPE for $l = 1$ of

$$\begin{aligned}
V_{e_i+e_j}(z) T_f^{(N=4) l=1}(w) &= (V_{e_i+e_j}^t(z) + V_{-e_i-e_j}^t(z)) T_f^{(N=4) l=1}(w) \\
&= g^{(N=4)'}(\alpha, 0) e^{\frac{1}{2}\pi i(\alpha+B^*\alpha)^t \frac{1}{2}(1+\theta_4)\alpha} (z-w)^{-1} \\
&\quad \left(e^{i\pi(\alpha+B^*\alpha)^t(\sqrt{2}x_f)} + e^{-i\pi(\alpha+B^*\alpha)^t(\sqrt{2}x_f)} \right) T_{f'}^{(N=4) l=1}(w) \\
&= \frac{1}{4} e^{i\pi(\alpha+B^*\alpha)^t(\sqrt{2}x_f)} e^{\frac{i\pi}{2}\alpha^t L_1 \alpha} T_{[x_f + \frac{1}{2\sqrt{2}}(1+\theta_4)\alpha]}^{(N=4) l=1}(w)
\end{aligned}$$

as well as for $l = 3$ of

$$\begin{aligned}
V_{e_i+e_j}(z) T_f^{(N=4) l=3}(w) &= (V_{e_i+e_j}^t(z) + V_{-e_i-e_j}^t(z)) T_f^{(N=4) l=3}(w) \\
&= g^{(N=4)'}(\alpha, 0) e^{\frac{1}{2}\pi i(\alpha+B^*\alpha)^t \frac{1}{2}(1+\theta_4)\alpha} (z-w)^{-1} \\
&\quad \left(e^{3i\pi(\alpha+B^*\alpha)^t(\sqrt{2}x_f)} + e^{-3i\pi(\alpha+B^*\alpha)^t(\sqrt{2}x_f)} \right) T_{f'}^{(N=4) l=3}(w) \\
&= \frac{1}{4} e^{3i\pi(\alpha+B^*\alpha)^t(\sqrt{2}x_f)} e^{\frac{i\pi}{2}\alpha^t L_3 \alpha} T_{[x_f + \frac{1}{2\sqrt{2}}(1-\theta_4)\alpha]}^{(N=4) l=3}(w)
\end{aligned}$$

with

$$L_1 = \begin{pmatrix} 0 & -1 & 0 & 0 \\ 1 & 0 & 0 & 0 \\ 0 & 0 & 1 & 0 \\ 0 & 0 & 0 & 1 \end{pmatrix} \quad L_3 = \begin{pmatrix} 1 & 0 & 0 & 0 \\ 0 & 1 & 0 & 0 \\ 0 & 0 & 0 & -1 \\ 0 & 0 & 1 & 0 \end{pmatrix}.$$

Using this OPE one can diagonalise the twistfields according to

	q_A	q_Q	q_R	q_S
$N_1 := (T_{0000}^1 + T_{1100}^1) + i(T_{1111}^1 - T_{0011}^1)$	$+\frac{1}{2}$	$+\frac{1}{2}$	$+\frac{1}{2}$	$-\frac{1}{2}$
$N_2 := (T_{0000}^1 + T_{1100}^1) - i(T_{1111}^1 - T_{0011}^1)$	$+\frac{1}{2}$	$+\frac{1}{2}$	$-\frac{1}{2}$	$+\frac{1}{2}$
$N_3 := (T_{0000}^1 - T_{1100}^1) + i(T_{1111}^1 + T_{0011}^1)$	$+\frac{1}{2}$	$-\frac{1}{2}$	$+\frac{1}{2}$	$+\frac{1}{2}$
$N_4 := (T_{0000}^1 - T_{1100}^1) - i(T_{1111}^1 + T_{0011}^1)$	$+\frac{1}{2}$	$-\frac{1}{2}$	$-\frac{1}{2}$	$-\frac{1}{2}$
$N_5 := (T_{0000}^3 + T_{1100}^3) + i(T_{1111}^3 - T_{0011}^3)$	$-\frac{1}{2}$	$-\frac{1}{2}$	$+\frac{1}{2}$	$-\frac{1}{2}$
$N_6 := (T_{0000}^3 + T_{1100}^3) - i(T_{1111}^3 - T_{0011}^3)$	$-\frac{1}{2}$	$-\frac{1}{2}$	$-\frac{1}{2}$	$+\frac{1}{2}$
$N_7 := (T_{0000}^3 - T_{1100}^3) + i(T_{1111}^3 + T_{0011}^3)$	$-\frac{1}{2}$	$+\frac{1}{2}$	$+\frac{1}{2}$	$+\frac{1}{2}$
$N_8 := (T_{0000}^3 - T_{1100}^3) - i(T_{1111}^3 + T_{0011}^3)$	$-\frac{1}{2}$	$+\frac{1}{2}$	$-\frac{1}{2}$	$-\frac{1}{2}$

where all of these are not charged under J and P and the antiholomorphic charges are just the same as the holomorphic ones. The charge wrt A cannot be derived from the

above OPE, as it is a current made up of the $(\frac{1}{2}, 0)$ fermions of the torus theory. In section 2.3.3 we show that a very careful calculation of the R-Sector partition function — keeping the factors originating from the bosonic and fermionic characters well apart — reveals that the \mathbb{Z}_4 groundstate twistfields are made up of a bosonic twistfield of conformal weight $h_b = \frac{3}{16}$ and a fermionic twistfield of conformal weight $h_f = \frac{1}{16}$. This perfectly well corresponds to the general formulae for bosonic twistfields $h_b = \frac{1}{2} \frac{k}{N} (1 - \frac{k}{N})$ and the one for fermionic twistfields $h_f = \frac{1}{2} \frac{k}{N}$ derived in [95] by CFT methods. But one also observes, inspecting the partition function, that these fields are uncharged wrt the other current J made up of $(\frac{1}{2}, 0)$ fermions. Hence, they have to be charged under A . To see this we translate our specific orbifold action (3.9) to the complexified torus fields of (2.17). Then the orbifold action acts on both complex dimensions of the torus in just the opposite way, i.e. with multiplication with phases which are complex conjugate to each other. (This corresponds to the fact that the first two real dimensions are rotated just the opposite way as the last two by (3.9).) However, following the derivation in [95], this means that in the above formula for the twisted fermionic conformal weights h_f we have to take k for the first dimension and $-k$ for the second. But J and A , as defined in (3.7), measure the fermionic content in both complex dimensions independently (with currents of the form $\psi_+^{(i)} \psi_-^{(i)}$ in the complex dimension i). J adds the fermionic content, A subtracts it. Knowing that (by convention) l in T^l refers to the first complex dimension the claimed charges follow.

3.3.5 Twisted groundstate $(\frac{1}{4}, \frac{1}{4})$ fields in $\mathcal{K}(\mathbb{Z}_4, \mathbf{0})$

This time we only have \mathbb{Z}_2 twistfields with generator θ_2 (3.9). The lattice vectors are given by e_i , and hence the fixpoint of the twistfield is translated due to the action of the vertex operator (see section 2.3.3)

$$x_f \mapsto x_{f'} = x_f + (1 - \theta_2)^{-1} e_i = x_f + \frac{1}{2} e_i .$$

The fixpoints are elements of the finite group $x_f \in \frac{1}{2} \mathbb{Z}^4 / \mathbb{Z}^4$. The coupling is given as above

$$g^{(N=2)}(\alpha, 0) = \frac{1}{4} e^{\frac{1}{2} \pi i (\sqrt{2} e_i)^t \frac{1}{2} (\sqrt{2} e_i)} = \frac{i}{4} .$$

It follows an OPE (with $\Sigma_f = T_f^{(N=2)}$)

$$\begin{aligned} U_i(z) \Sigma_f(w) &= (V_{e_i, e_i}^t(z) + V_{-e_i, -e_i}^t(z)) \Sigma_f(w) \\ &= g^{(N=2)}(\alpha, 0) (\sqrt{2} e_i, 0) (z - w)^{-1} \\ &\quad \left(e^{2\pi i (\frac{1}{\sqrt{2}} e_i)^t (\sqrt{2} x_f)} + e^{2\pi i (-\frac{1}{\sqrt{2}} e_i)^t (\sqrt{2} x_f)} \right) \Sigma_{f'}(w) \\ &= \frac{i}{2} e^{i\pi e_i^t x_f} \Sigma_{[x_f + \frac{1}{2} e_i]}(w) . \end{aligned}$$

This OPE yields the following diagonalisation of the twistfields ($N'_{i/j}$ means: N'_i respectively N'_j)

	q_P	q_Q	q_R	q_S
$E'_P{}^\pm := (\Sigma_{0000} - \Sigma_{1100} - \Sigma_{0011} + \Sigma_{1111} - \Sigma_{1010} - \Sigma_{1001} - \Sigma_{0110} - \Sigma_{0101}) \pm i(\Sigma_{1000} + \Sigma_{0100} + \Sigma_{0010} + \Sigma_{0001} - \Sigma_{1110} - \Sigma_{1101} - \Sigma_{1011} - \Sigma_{0111})$	± 1	0	0	0
$E'_Q{}^\pm := (\Sigma_{0000} - \Sigma_{1100} - \Sigma_{0011} + \Sigma_{1111} + \Sigma_{1010} + \Sigma_{1001} + \Sigma_{0110} + \Sigma_{0101}) \pm i(\Sigma_{1000} + \Sigma_{0100} - \Sigma_{0010} - \Sigma_{0001} + \Sigma_{1110} + \Sigma_{1101} - \Sigma_{1011} - \Sigma_{0111})$	0	± 1	0	0
$E'_R{}^\pm := (\Sigma_{0000} + \Sigma_{1100} + \Sigma_{0011} + \Sigma_{1111} - \Sigma_{1010} + \Sigma_{1001} + \Sigma_{0110} - \Sigma_{0101}) \pm i(\Sigma_{1000} - \Sigma_{0100} + \Sigma_{0010} - \Sigma_{0001} + \Sigma_{1110} - \Sigma_{1101} + \Sigma_{1011} - \Sigma_{0111})$	0	0	± 1	0
$E'_S{}^\pm := (\Sigma_{0000} + \Sigma_{1100} + \Sigma_{0011} + \Sigma_{1111} + \Sigma_{1010} - \Sigma_{1001} - \Sigma_{0110} + \Sigma_{0101}) \pm i(\Sigma_{1000} - \Sigma_{0100} - \Sigma_{0010} + \Sigma_{0001} - \Sigma_{1110} + \Sigma_{1101} + \Sigma_{1011} - \Sigma_{0111})$	0	0	0	± 1
$N'_{1/6} := (\Sigma_{0000} - \Sigma_{1100} + \Sigma_{0011} - \Sigma_{1111} - \Sigma_{1010} + \Sigma_{1001} - \Sigma_{0110} + \Sigma_{0101}) \pm i(\Sigma_{1000} + \Sigma_{0100} + \Sigma_{0010} - \Sigma_{0001} - \Sigma_{1110} + \Sigma_{1101} + \Sigma_{1011} + \Sigma_{0111})$	$\pm \frac{1}{2}$	$\pm \frac{1}{2}$	$\pm \frac{1}{2}$	$\mp \frac{1}{2}$
$N'_{3/8} := (\Sigma_{0000} + \Sigma_{1100} - \Sigma_{0011} - \Sigma_{1111} - \Sigma_{1010} - \Sigma_{1001} + \Sigma_{0110} + \Sigma_{0101}) \pm i(\Sigma_{1000} - \Sigma_{0100} + \Sigma_{0010} + \Sigma_{0001} + \Sigma_{1110} + \Sigma_{1101} - \Sigma_{1011} + \Sigma_{0111})$	$\pm \frac{1}{2}$	$\mp \frac{1}{2}$	$\pm \frac{1}{2}$	$\pm \frac{1}{2}$
$N'_{2/5} := (\Sigma_{0000} - \Sigma_{1100} + \Sigma_{0011} - \Sigma_{1111} + \Sigma_{1010} - \Sigma_{1001} + \Sigma_{0110} - \Sigma_{0101}) \pm i(\Sigma_{1000} + \Sigma_{0100} - \Sigma_{0010} + \Sigma_{0001} + \Sigma_{1110} - \Sigma_{1101} + \Sigma_{1011} + \Sigma_{0111})$	$\pm \frac{1}{2}$	$\pm \frac{1}{2}$	$\mp \frac{1}{2}$	$\pm \frac{1}{2}$
$N'_{4/7} := (\Sigma_{0000} + \Sigma_{1100} - \Sigma_{0011} - \Sigma_{1111} + \Sigma_{1010} + \Sigma_{1001} - \Sigma_{0110} - \Sigma_{0101}) \pm i(-\Sigma_{1000} + \Sigma_{0100} + \Sigma_{0010} + \Sigma_{0001} + \Sigma_{1110} + \Sigma_{1101} + \Sigma_{1011} - \Sigma_{0111})$	$\pm \frac{1}{2}$	$\mp \frac{1}{2}$	$\mp \frac{1}{2}$	$\mp \frac{1}{2}$

where all of these are not charged under J and A and the antiholomorphic charges are just the same as the holomorphic ones.

3.3.6 Fields of the Gepner model $(\widehat{2})^4$

It is easier to describe the field content of the more symmetric Gepner model $(\widehat{2})^4$ with $\widehat{su}(2)_1^6$ symmetry algebra first and then to derive the field content of $(\widehat{2})^4$ by orbifolding. Details about the calculations in Gepner models and especially about how to compute the (2) superminimal model as a tensor product of a $c = 1$ theory and an Ising model are summarised in section 2.3.4. Following [31], we define X_{ij} to be the Gepner model field with $\Phi_{4,2;0,0}^0$ as the i th and j th tensor factors and $\Phi_{0,0;0,0}^0$ elsewhere, and Y_{ij} to be the Gepner Model field with $\Phi_{-2,2;0,0}^0$ as the i th and j th tensor factors and $\Phi_{2,2;0,0}^0$ elsewhere. Furthermore, let J_i be the $U(1)$ current of the i th minimal model. Then,

the complete $\widehat{su}(2)_1^6$ symmetry algebra of $(\widehat{2})^4$ is given by

$$\begin{aligned}
J'' &:= J_1 + J_2 + J_3 + J_4 & J''^\pm &:= \sqrt{2} (\Phi_{\mp 2,2;0,0}^0)^{\otimes 4} \\
A'' &:= J_1 + J_2 - J_3 - J_4 & A''^+ &:= \sqrt{2} Y_{12} & A''^- &:= \sqrt{2} Y_{34} \\
\hline
P'' &:= J_1 - J_2 + J_3 - J_4 & P''^+ &:= \sqrt{2} Y_{13} & P''^- &:= \sqrt{2} Y_{24} \\
Q'' &:= J_1 - J_2 - J_3 + J_4 & Q''^+ &:= \sqrt{2} Y_{14} & Q''^- &:= \sqrt{2} Y_{23} \\
R'' &:= i(X_{13} - X_{24}) & R''^\pm &:= \frac{i}{\sqrt{2}}(X_{14} + X_{23}) \pm \frac{1}{\sqrt{2}}(X_{12} + X_{34}) \\
S'' &:= i(X_{13} + X_{24}) & S''^\pm &:= \frac{i}{\sqrt{2}}(X_{14} - X_{23}) \mp \frac{1}{\sqrt{2}}(X_{12} - X_{34}),
\end{aligned} \tag{3.10}$$

with the $\widehat{su}(2)_1$ normalised as in equation (3.8).

The $(\frac{1}{4}, \frac{1}{4})$ fields corresponding to Ramond groundstates can thus be diagonalised wrt the action of the above currents

$$\begin{aligned}
E_J''^\pm &= (\Phi_{\mp 1, \mp 1; \mp 1, \mp 1}^0)^{\otimes 4} \\
F_J''^\pm &= (\Phi_{\mp 1, \mp 1; \pm 1, \pm 1}^0)^{\otimes 4} \\
E_A''^\pm &= (\Phi_{\mp 1, \mp 1; \mp 1, \mp 1}^0)^{\otimes 2} \otimes (\Phi_{\pm 1, \pm 1; \pm 1, \pm 1}^0)^{\otimes 2} \\
F_A''^\pm &= (\Phi_{\mp 1, \mp 1; \pm 1, \pm 1}^0)^{\otimes 2} \otimes (\Phi_{\pm 1, \pm 1; \mp 1, \mp 1}^0)^{\otimes 2} \\
E_P''^\pm &= \Phi_{\mp 1, \mp 1; \mp 1, \mp 1}^0 \otimes \Phi_{\pm 1, \pm 1; \pm 1, \pm 1}^0 \otimes \Phi_{\mp 1, \mp 1; \mp 1, \mp 1}^0 \otimes \Phi_{\pm 1, \pm 1; \pm 1, \pm 1}^0 \\
F_P''^\pm &= \Phi_{\mp 1, \mp 1; \pm 1, \pm 1}^0 \otimes \Phi_{\pm 1, \pm 1; \mp 1, \mp 1}^0 \otimes \Phi_{\mp 1, \mp 1; \pm 1, \pm 1}^0 \otimes \Phi_{\pm 1, \pm 1; \mp 1, \mp 1}^0 \\
E_Q''^\pm &= \Phi_{\mp 1, \mp 1; \mp 1, \mp 1}^0 \otimes \Phi_{\pm 1, \pm 1; \pm 1, \pm 1}^0 \otimes \Phi_{\mp 1, \mp 1; \pm 1, \pm 1}^0 \otimes \Phi_{\pm 1, \pm 1; \mp 1, \mp 1}^0 \\
F_Q''^\pm &= \Phi_{\mp 1, \mp 1; \pm 1, \pm 1}^0 \otimes \Phi_{\pm 1, \pm 1; \mp 1, \mp 1}^0 \otimes \Phi_{\mp 1, \mp 1; \mp 1, \mp 1}^0 \otimes \Phi_{\pm 1, \pm 1; \pm 1, \pm 1}^0 \\
E_R''^\pm &= (\Phi_{2,1;2,1}^1)^{\otimes 4} + (\Phi_{2,1;-2,-1}^1)^{\otimes 4} \\
&\quad \pm [(\Phi_{2,1;2,1}^1 \otimes \Phi_{2,1;-2,-1}^1)^{\otimes 2} - (\Phi_{2,1;-2,-1}^1 \otimes \Phi_{2,1;2,1}^1)^{\otimes 2}] \\
F_R''^\pm &= (\Phi_{2,1;2,1}^1)^{\otimes 2} \otimes (\Phi_{2,1;-2,-1}^1)^{\otimes 2} + (\Phi_{2,1;-2,-1}^1)^{\otimes 2} \otimes (\Phi_{2,1;2,1}^1)^{\otimes 2} \\
&\quad \pm i [\Phi_{2,1;-2,-1}^1 \otimes \Phi_{2,1;2,1}^1 \otimes \Phi_{2,1;2,1}^1 \otimes \Phi_{2,1;-2,-1}^1 \\
&\quad \quad + \Phi_{2,1;2,1}^1 \otimes \Phi_{2,1;-2,-1}^1 \otimes \Phi_{2,1;-2,-1}^1 \otimes \Phi_{2,1;2,1}^1] \\
E_S''^\pm &= (\Phi_{2,1;2,1}^1)^{\otimes 4} - (\Phi_{2,1;-2,-1}^1)^{\otimes 4} \\
&\quad \mp [(\Phi_{2,1;2,1}^1 \otimes \Phi_{2,1;-2,-1}^1)^{\otimes 2} + (\Phi_{2,1;-2,-1}^1 \otimes \Phi_{2,1;2,1}^1)^{\otimes 2}] \\
F_S''^\pm &= (\Phi_{2,1;2,1}^1)^{\otimes 2} \otimes (\Phi_{2,1;-2,-1}^1)^{\otimes 2} - (\Phi_{2,1;-2,-1}^1)^{\otimes 2} \otimes (\Phi_{2,1;2,1}^1)^{\otimes 2} \\
&\quad \pm i [\Phi_{2,1;-2,-1}^1 \otimes \Phi_{2,1;2,1}^1 \otimes \Phi_{2,1;2,1}^1 \otimes \Phi_{2,1;-2,-1}^1 \\
&\quad \quad - \Phi_{2,1;2,1}^1 \otimes \Phi_{2,1;-2,-1}^1 \otimes \Phi_{2,1;-2,-1}^1 \otimes \Phi_{2,1;2,1}^1] .
\end{aligned}$$

As in section 3.3.4 the index indicates the $U(1)$ current this field is charged with, holomorphic respectively antiholomorphic charges $(\pm 1, \pm 1)$ for E^\pm and $(\pm 1, \mp 1)$ for F^\pm .

Now, as $(\widehat{2})^4$ is gained from $(\widetilde{2})^4$ by an \mathbb{Z}_2 orbifold generated by

$$[2', 2', 0, 0] : \bigotimes_{i=1}^4 \Phi_{m_i, s_i; \bar{m}_i, \bar{s}_i}^{l_i} \mapsto e^{\frac{2\pi i}{8}(\bar{m}_1 - m_1 - \bar{m}_3 + m_3)} \bigotimes_{i=1}^4 \Phi_{m_i, s_i; \bar{m}_i, \bar{s}_i}^{l_i},$$

the surviving $\hat{su}(2)_1^2 \otimes \hat{u}^4$ symmetry algebra of $(\widehat{2})^4$ is given by the currents

$$J, J^\pm; \quad A; \quad P, P^\pm; \quad Q; \quad R; \quad S.$$

Of the above Ramond groundstate fields the following are invariant under the orbifold group action

$$E_J''^\pm, F_J''^\pm; \quad E_A''^\pm; \quad E_P''^\pm, F_P''^\pm; \quad E_Q''^\pm; \quad E_R''^\pm; \quad E_S''^\pm.$$

The list of $(\frac{1}{4}, \frac{1}{4})$ fields in $(\widehat{2})^4$ has to be completed by the following twistfields (wrt the above orbifold construction as described in the end of section 2.3.4)

$$\begin{aligned} T_1 &= \Phi_{2,1;2,1}^1 \otimes \Phi_{-1,-1;-1,-1}^0 \otimes \Phi_{2,1;2,1}^1 \otimes \Phi_{1,1;1,1}^0 \\ T_2 &= \Phi_{2,1;2,1}^1 \otimes \Phi_{1,1;1,1}^0 \otimes \Phi_{2,1;2,1}^1 \otimes \Phi_{-1,-1;-1,-1}^0 \\ T_3 &= \Phi_{-1,-1;-1,-1}^0 \otimes \Phi_{2,1;2,1}^1 \otimes \Phi_{1,1;1,1}^0 \otimes \Phi_{2,1;2,1}^1 \\ T_4 &= \Phi_{1,1;1,1}^0 \otimes \Phi_{2,1;2,1}^1 \otimes \Phi_{-1,-1;-1,-1}^0 \otimes \Phi_{2,1;2,1}^1 \\ T_5 &= \Phi_{2,1;-2,-1}^1 \otimes \Phi_{-1,-1;-1,-1}^0 \otimes \Phi_{2,1;-2,-1}^1 \otimes \Phi_{1,1;1,1}^0 \\ T_6 &= \Phi_{2,1;-2,-1}^1 \otimes \Phi_{1,1;1,1}^0 \otimes \Phi_{2,1;-2,-1}^1 \otimes \Phi_{-1,-1;-1,-1}^0 \\ T_7 &= \Phi_{-1,-1;-1,-1}^0 \otimes \Phi_{2,1;-2,-1}^1 \otimes \Phi_{1,1;1,1}^0 \otimes \Phi_{2,1;-2,-1}^1 \\ T_8 &= \Phi_{1,1;1,1}^0 \otimes \Phi_{2,1;-2,-1}^1 \otimes \Phi_{-1,-1;-1,-1}^0 \otimes \Phi_{2,1;-2,-1}^1. \end{aligned}$$

These can be diagonalised wrt to the action of the invariant $U(1)$ currents

	q_J	q_A	q_P	q_Q	q_R	q_S
$N_{1/2}'' = T_3 \pm T_7$	0	$+\frac{1}{2}$	0	$+\frac{1}{2}$	$\pm\frac{1}{2}$	$\pm\frac{1}{2}$
$N_{3/4}'' = T_1 \mp T_5$	0	$+\frac{1}{2}$	0	$-\frac{1}{2}$	$\pm\frac{1}{2}$	$\pm\frac{1}{2}$
$N_{5/6}'' = T_4 \pm T_8$	0	$-\frac{1}{2}$	0	$-\frac{1}{2}$	$\pm\frac{1}{2}$	$\pm\frac{1}{2}$
$N_{7/8}'' = T_2 \mp T_6$	0	$-\frac{1}{2}$	0	$+\frac{1}{2}$	$\pm\frac{1}{2}$	$\pm\frac{1}{2}$

3.3.7 Explicit identification of the three theories

We can now explicitly identify the three CFTs $(\widehat{2})^4$, $\mathcal{K}(\mathbb{Z}^4, 0)$ and $\mathbb{Z}_4(\frac{1}{\sqrt{2}}D_4, B^*)$ wrt their the symmetry algebras and their lattices of $(\frac{1}{4}, \frac{1}{4})$ fields. The identification of the

symmetry algebra is not totally fixed (this reflects the high amount of symmetry of these theories); one possible way of identifying the currents is

$$\begin{aligned}
J &\simeq J'' \simeq J' & J^\pm &\simeq J''^\pm \simeq J'^\pm \\
A &\simeq A'' \simeq P' \\
P &\simeq P'' \simeq A' & P^\pm &\simeq P''^\pm \simeq A'^\pm \\
Q &\simeq Q'' \simeq Q' \\
R &\simeq R'' \simeq R' \\
S &\simeq S'' \simeq S' .
\end{aligned}$$

Comparing the charges wrt the above currents this leads to the following identification of $(\frac{1}{4}, \frac{1}{4})$ fields

$$\begin{aligned}
E_J^\pm &\simeq E_J''^\pm \simeq E_J'^\pm & F_J^\pm &\simeq F_J''^\pm \simeq F_J'^\pm \\
E_A^\pm &\simeq E_A''^\pm \simeq E_P'^\pm \\
E_P^\pm &\simeq E_P''^\pm \simeq E_A'^\pm & F_P^\pm &\simeq F_P''^\pm \simeq F_A'^\pm \\
E_Q^\pm &\simeq E_Q''^\pm \simeq E_Q'^\pm \\
E_R^\pm &\simeq E_R''^\pm \simeq E_R'^\pm \\
E_S^\pm &\simeq E_S''^\pm \simeq E_S'^\pm \\
N_i &= N_i' = N_i'' \quad \forall i \in \{1, \dots, 8\} .
\end{aligned} \tag{3.11}$$

This identification implies the important observation that the \mathbb{Z}_2 and \mathbb{Z}_4 orbifold subvarieties in K3 moduli space, which intersect in only one point as described earlier, are orthogonal to each other. In order to see this it is important to recall some facts about conformal deformation theory (see section 3.5 and [34, 95, 31, 32]). The possible exact marginal deformation fields in these $c = 6$ theories are not charged under the $U(1)$ current J of the SUSY algebra and can be generated as the $(1, 1)$ superpartners of $(\frac{1}{2}, \frac{1}{2})$ NS fields which again can be generated via spectral flow from $(\frac{1}{4}, \frac{1}{4})$ Ramond fields. Now we have two types of deformation fields within our orbifold theories. Deformation fields which originate from the original torus theory generate all the deformations along the orbifold subvarieties and are well understood. The corresponding $(\frac{1}{4}, \frac{1}{4})$ Ramond fields in $\mathcal{K}(\mathbb{Z}^4, 0)$ are $E_A'^\pm$ and $F_A'^\pm$, the ones in $\mathbb{Z}_4(\frac{1}{\sqrt{2}}D_4, B^*)$ are E_A^\pm . On the other hand, we do not understand very much about deformations with twistfields. The $(\frac{1}{4}, \frac{1}{4})$ Ramond fields corresponding to these deformations are given by $E_P'^\pm, E_Q'^\pm, E_R'^\pm, E_S'^\pm, N_i'$ in $\mathcal{K}(\mathbb{Z}^4, 0)$, and $E_P^\pm, F_P^\pm, E_Q^\pm, E_R^\pm, E_S^\pm, N_i$ in $\mathbb{Z}_4(\frac{1}{\sqrt{2}}D_4, B^*)$. Now the orbifold group selection rules imply that the deformation fields originating from the torus theory and the twisted deformation fields are orthogonal wrt the Zamolodchikov metric as any two point function of the two types has to vanish. Now the identification in (3.11) implies that torus deformations of one theory are identified with twistfield deformations of the respective other. This, the fact that deformations along the orbifold subvarieties are generated by torus deformations and the orthogonality of the two types of deformation fields prove the above stated orthogonality of the \mathbb{Z}_2 and \mathbb{Z}_4 orbifold subvarieties.

3.4 A geometric geodesic in K3 moduli space

In the following we want to present one example of how to calculate a geodesic between two different points in moduli space. We choose the geodesic between the two points which are related to the two Gepner models $(2)^4$ and $(\tilde{2})^4$ and which, hence, lie on the \mathbb{Z}_4 respectively \mathbb{Z}_2 subvarieties of the K3 moduli space. The situation is depicted in figure 3.1.

We first need to find the transition matrix between these two points and then dissect this transition matrix in order to find the generator of the geodesic.

3.4.1 Finding the transition matrix

In section 3.2 the transition between the \mathbb{Z}_2 and \mathbb{Z}_4 subvarieties in K3 moduli space has been given in terms of the two bases A_i respectively B_i , $i = 1, \dots, 24$. For our current purpose it is more efficient to first switch to yet two other bases. For models in the \mathbb{Z}_2 subvariety we introduce the basis

$$\begin{aligned}
a_1 &= \frac{1}{\sqrt{2}}(e_1 \wedge e_2 + e_3 \wedge e_4) = \frac{1}{2} A_{21} \\
a_2 &= \frac{1}{\sqrt{2}}(e_1 \wedge e_3 + e_4 \wedge e_2) = \frac{1}{2} A_{22} \\
a_3 &= \frac{1}{\sqrt{2}}(e_1 \wedge e_4 + e_2 \wedge e_3) = \frac{1}{2} A_{23} \\
a_4 &= \hat{v}^\circ + \frac{1}{4} \sum_{i \in I(2)} \hat{E}_i + \frac{3}{2} \hat{v} = \frac{1}{2} A_{24} \\
a_5 &= -\frac{1}{2} A_9 \quad a_9 = -\frac{1}{2} A_2 \quad a_{13} = -\frac{1}{2} A_{13} \quad a_{17} = -\frac{1}{2} A_6 \quad a_{21} = -\frac{1}{2} A_{17} \\
a_6 &= \frac{1}{2} A_5 \quad a_{10} = \frac{1}{2} A_1 \quad a_{14} = -\frac{1}{2} A_{14} \quad a_{18} = \frac{1}{2} A_7 \quad a_{22} = -\frac{1}{2} A_{18} \\
a_7 &= \frac{1}{2} A_{10} \quad a_{11} = \frac{1}{2} A_{12} \quad a_{15} = \frac{1}{2} A_{15} \quad a_{19} = -\frac{1}{2} A_4 \quad a_{23} = \frac{1}{2} A_{19} \\
a_8 &= -\frac{1}{2} A_3 \quad a_{12} = \frac{1}{2} A_{11} \quad a_{16} = \frac{1}{2} A_{16} \quad a_{20} = \frac{1}{2} A_8 \quad a_{24} = -\frac{1}{2} A_{20}
\end{aligned}$$

and for models in the \mathbb{Z}_4 subvariety the following one

$$\begin{aligned}
b_1 &= \frac{1}{\sqrt{2}}(e_1 \wedge e_2 + e_3 \wedge e_4) \\
b_2 &= \frac{1}{\sqrt{2}}(e_1 \wedge e_3 + e_4 \wedge e_2) \\
b_3 &= \frac{1}{\sqrt{2}}(e_1 \wedge e_4 + e_2 \wedge e_3) \\
b_4 &= \sqrt{2} \hat{v}^\circ + \frac{\sqrt{2}}{4} \left(\sum_{i \in I(2)} \hat{E}_i + \frac{1}{2} \sum_{i \in I(4)} (3\hat{E}_i^{(+)} + 4\hat{E}_i^{(0)} + 3\hat{E}_i^{(-)}) \right) + \frac{5\sqrt{2}}{4} \hat{v} \\
b_5 &= \frac{1}{\sqrt{2}}(e_1 \wedge e_2 - e_3 \wedge e_4) \\
b_6 &= \sqrt{2} \hat{v}^\circ + \frac{\sqrt{2}}{4} \left(\sum_{i \in I(2)} \hat{E}_i + \frac{1}{2} \sum_{i \in I(4)} (3\hat{E}_i^{(+)} + 4\hat{E}_i^{(0)} + 3\hat{E}_i^{(-)}) \right) + \frac{3\sqrt{2}}{4} \hat{v}
\end{aligned}$$

This is a block diagonal matrix with a nontrivial 8×8 block

$$M := \begin{pmatrix} -\frac{3}{2} & \frac{1}{2} & 0 & -\frac{1}{2} & 0 & \frac{1}{2}\sqrt{2} & -\frac{1}{2} & -1 \\ 0 & 0 & -\frac{3}{2} & 1 & \frac{1}{2}\sqrt{2} & \frac{1}{2}\sqrt{2} & 1 & \frac{1}{2} \\ 1 & 1 & \frac{1}{2} & 0 & -\frac{1}{2}\sqrt{2} & -\frac{1}{2}\sqrt{2} & 0 & \frac{1}{2} \\ 0 & 0 & \frac{1}{2} & 1 & 0 & 0 & 0 & \frac{1}{2} \\ -\frac{1}{2} & -\frac{1}{2} & -1 & \frac{1}{2} & \sqrt{2} & \frac{1}{2}\sqrt{2} & \frac{1}{2} & 0 \\ -1 & 0 & -\frac{1}{2} & 0 & 0 & \sqrt{2} & 0 & -\frac{1}{2} \\ \frac{1}{2}\sqrt{2} & 0 & -\frac{1}{2}\sqrt{2} & \frac{1}{2}\sqrt{2} & 0 & 0 & \sqrt{2} & \frac{1}{2}\sqrt{2} \\ -\frac{1}{2}\sqrt{2} & 0 & 0 & -\frac{1}{2}\sqrt{2} & 0 & 0 & 0 & -\sqrt{2} \end{pmatrix}$$

of signature $(4, 4)$ and the identity in the rest of the space. For the further discussion it is sufficient to analyse this block M and to find the Lie algebra element which generates this block as the identity is trivially generated. We will, hence, also use M to signify the special element $O_{(\tilde{2})^4}$ of $O(4, 20)$ in the further discussion as long as the mathematics is not effected by this additional identity block; we apologise for this abuse of notation but hope that this choice actually contributes to a clearer presentation.

3.4.2 Calculating the generator of the geodesic

Due to the fact that we deal with a symmetric space $O(4, 20)/O(4) \times O(20)$ the tangent spaces at all points are isomorphic to that one of the identity. Hence, our choice of where to put the identity in $O(4, 20)$ and, thus, what coordinates we use does not affect the calculation of the generator of the geodesic as the generator is an element of the tangent space. This justifies our nice choice of coordinates in section 3.4.1. We have actually placed the $(\tilde{2})^4$ model at the identity point and only need to dissect the transition matrix M to $(\tilde{2})^4$.

Before we proceed we note that we still calculate in the covering space $O(4, 20)/(O(4) \times O(20))$ of the K3 moduli space. We do not take into account the maximal discrete symmetry group which we have to divide the covering space by to gain the proper K3 moduli space. Certainly, the effects of this group action have to be considered after a geodesic has been calculated in the covering space; this is probably done most efficiently knowing the corresponding CFT deformation.

Let us denote the geodesic by

$$\gamma : t \longrightarrow \exp(At) \quad t \in [0, 1]$$

with $\exp(A) = M$. Our task is, hence, to find A , the logarithm of M . Usually the functions \exp and \log are defined for matrices just by formally applying the respective Taylor series of these functions. But neither is this a numerically very practicable way nor do we have a sufficiently large domain of definition, in particular for \log . On the

other hand, it is possible to diagonalise the matrix M over \mathbb{C} as it is an orthogonal matrix (with signature). Our strategy in calculating \exp as well as \log will thus be to diagonalise the matrix, to apply the respective function to its diagonal matrix of eigenvalues and to perform the change of basis back to the undiagonalised coordinates. It is easily seen that this procedure is indeed equivalent to the Taylor series, where defined, as the matrix of change of basis which diagonalises a polynomial A^m is the same as the one for the diagonalisation of A itself. This works perfectly well for \exp , but for \log we have to be careful in the determination of the branch in \mathbb{C} if some eigenvalues are not positive real.

To see how we can overcome this problem with \log let us have a closer look at the Lie algebra of our specific symmetric space (see e.g. [117] for more details). The Lie algebra $\mathfrak{o}(p, q)$ of $O(p, q)$ has a Cartan decomposition

$$\mathfrak{o}(p, q) = \mathfrak{k} + \mathfrak{p}$$

such that each matrix can be split according to

$$\mathfrak{o}(p, q) \ni X = \begin{pmatrix} T_1 & K \\ K^t & T_2 \end{pmatrix} \quad (3.13)$$

with T_1 and T_2 skew symmetric. Then, \mathfrak{k} is the subalgebra of $\mathfrak{o}(p, q)$ spanned by the skew symmetric matrices T_1 and T_2 and \mathfrak{p} is the subspace of symmetric matrices of form

$$\begin{pmatrix} 0 & K \\ K^t & 0 \end{pmatrix}.$$

The component \mathfrak{k} is also the Lie algebra of the factor group $O(p) \times O(q)$. But unfortunately, the crucial component \mathfrak{p} is not a subalgebra and, hence, the Lie algebra of $O(p, q)/O(p) \times O(q)$ cannot be taken to be \mathfrak{p} . Nevertheless, for each conjugacy class $[M] \in O(p, q)/O(p) \times O(q)$ there is always one element of the conjugacy class $N := \exp(B) \in [M]$ for which the generator B is in \mathfrak{p} , i.e. for which B is symmetric.

Taking the logarithm of such an N is pretty easy as the eigenvalues of the symmetric matrix B have to be real and, thus, the logarithm of the eigenvalues of N has to be real as well; the question of which branch to take vanishes. But on the level of a group manifold with high dimensionality it is very hard to solve the respective constraints to find such an element of a conjugacy class; and the split of the Lie algebra element A , which can be easily performed on the Lie algebra level as in (3.13), does not transfer to the group level (via \exp) because \mathfrak{p} is not a subalgebra.

We can, however, use this split on the Lie algebra level to devise the following iterative procedure to get a symmetric generator B starting with M . Define a matrix M_{inter} with initial value M and an orthogonal matrix T , initially taken to be the identity. Then perform iteratively:

1. Take the logarithm of the matrix M_{inter} as described above; the result is called a .

2. Perform a Cartan decomposition of a as in (3.13); the element of \mathfrak{k} is called t .
3. Calculate the corresponding group element $T_{\text{inter}} = \exp(t)$.
4. M_{inter} is rotated to $M_{\text{inter}} \mapsto M_{\text{inter}} T_{\text{inter}}^{-1}$. Similarly $T \mapsto T_{\text{inter}} T$.

This iteration quickly leads to a separation of M into an element $M_{\text{inter}} \in [M]$ which is generated by a symmetric generator and a rotation $T = M_{\text{inter}}^{-1} M$ of very high accuracy. In our example hundred iterations were enough for an accuracy of at least 10^{-10} .

The only elements of the factor group which this algorithm does not “detect” are sign flips in an even number of columns, i.e. elements of the form

$$\begin{pmatrix} (-1)^{i_1} & 0 & & 0 \\ 0 & (-1)^{i_2} & & 0 \\ & & \ddots & \\ 0 & 0 & & (-1)^{i_d} \end{pmatrix}$$

with $i_1 + i_2 + \dots + i_d \equiv 0 \pmod{2}$. These can easily be corrected by hand inspecting the signs of the eigenvalues of the resulting M_{inter} .

Due to the size of the involved matrices this iteration cannot be performed with exact numbers. Turning back to our specific example we find the numerical solution

$$M_{\text{inter}} = \begin{pmatrix} 1.6058 & -0.16903 & -0.33806 & -0.16903 & 0.084520 & 0.84515 & -0.71714 & 0.71714 \\ -0.16903 & 1.7748 & -0.25355 & 0.084520 & 1.0142 & 0.42258 & 0.95618 & -0.35857 \\ -0.33806 & -0.25355 & 1.4368 & 0.084520 & -0.84515 & -0.59161 & 0.23905 & -0.35857 \\ -0.16903 & 0.084520 & 0.084520 & 1.0987 & 0.0 & -0.084520 & 0.11952 & -0.47809 \\ 0.084520 & 1.0142 & -0.84515 & 0.0 & 1.6058 & 0.33806 & 0.23905 & 0.0 \\ 0.84515 & 0.42258 & -0.59161 & -0.084520 & 0.33806 & 1.4368 & -0.11952 & 0.23905 \\ -0.71714 & 0.95618 & 0.23905 & 0.11952 & 0.23905 & -0.11952 & 1.5213 & -0.33806 \\ 0.71714 & -0.35857 & -0.35857 & -0.47809 & 0.0 & 0.23905 & -0.33806 & 1.3522 \end{pmatrix}$$

(rounded to five digits for a better display).

But, as this matrix should only involve rational numbers and roots of these, that is to say pretty easy numbers, we can try to get the exact answer using the method of continued fractions. Continued fractions are a popular tool in number theory (see e.g. [118]). They choose a different hierarchy of displaying numbers instead of the additive hierarchy of e.g. the decimal system in the following form

$$x_0 + \frac{1}{x_1 + \frac{1}{x_2 + \frac{1}{x_3 + \dots}}} .$$

The nice thing about this style of displaying real numbers is that rational numbers and fractions are very easily recognisable:

- Rational numbers have a continued fraction representation which definitely terminates.
- Roots of quadratic equations with rational coefficients have a continued fraction representation which becomes periodic at some point.

Now, if one knows a real number to a quite high accuracy and if this number is supposed to be either a rational number or a root of a quadratic equation, one usually observes either the break up of the continued fraction (i.e. the appearance of a very large number x_i) or the first few periods in the continued fraction representation of its approximation. In this way one can guess the continued fraction representation of the exact number and retrieve this number by re-calculating it from its exact continued fraction representation.

Applying this method to the above M_{inter} yields

$$N = \begin{pmatrix} \frac{19}{70} \sqrt{35} & -1/35 \sqrt{35} & -\frac{2}{35} \sqrt{35} & -1/35 \sqrt{35} & \frac{1}{70} \sqrt{35} & 1/7 \sqrt{35} & -\frac{3}{35} \sqrt{70} & \frac{3}{35} \sqrt{70} \\ -1/35 \sqrt{35} & 3/10 \sqrt{35} & -\frac{3}{70} \sqrt{35} & \frac{1}{70} \sqrt{35} & \frac{6}{35} \sqrt{35} & 1/14 \sqrt{35} & \frac{4}{35} \sqrt{70} & -\frac{3}{70} \sqrt{70} \\ -\frac{2}{35} \sqrt{35} & -\frac{3}{70} \sqrt{35} & \frac{17}{70} \sqrt{35} & \frac{1}{70} \sqrt{35} & -1/7 \sqrt{35} & -1/10 \sqrt{35} & 1/35 \sqrt{70} & -\frac{3}{70} \sqrt{70} \\ -1/35 \sqrt{35} & \frac{1}{70} \sqrt{35} & \frac{1}{70} \sqrt{35} & \frac{13}{70} \sqrt{35} & 0 & -\frac{1}{70} \sqrt{35} & \frac{1}{70} \sqrt{70} & -\frac{2}{35} \sqrt{70} \\ \frac{1}{70} \sqrt{35} & \frac{6}{35} \sqrt{35} & -1/7 \sqrt{35} & 0 & \frac{19}{70} \sqrt{35} & \frac{2}{35} \sqrt{35} & 1/35 \sqrt{70} & 0 \\ 1/7 \sqrt{35} & 1/14 \sqrt{35} & -1/10 \sqrt{35} & -\frac{1}{70} \sqrt{35} & \frac{2}{35} \sqrt{35} & \frac{17}{70} \sqrt{35} & -\frac{1}{70} \sqrt{70} & 1/35 \sqrt{70} \\ -\frac{3}{35} \sqrt{70} & \frac{4}{35} \sqrt{70} & 1/35 \sqrt{70} & \frac{1}{70} \sqrt{70} & 1/35 \sqrt{70} & -\frac{1}{70} \sqrt{70} & \frac{9}{35} \sqrt{35} & -\frac{2}{35} \sqrt{35} \\ \frac{3}{35} \sqrt{70} & -\frac{3}{70} \sqrt{70} & -\frac{3}{70} \sqrt{70} & -\frac{2}{35} \sqrt{70} & 0 & 1/35 \sqrt{70} & -\frac{2}{35} \sqrt{35} & \frac{8}{35} \sqrt{35} \end{pmatrix}.$$

We have checked that this N is indeed an element of $O(4, 4)$ and that $T = N^{-1} M$ is an element of the orthogonal factor group. The eigenvalues of N are

$$\begin{aligned} n_1 &= 1/4 \sqrt{35} + 1/4 \sqrt{3} + 1/4 \sqrt{22 + 2 \sqrt{35} \sqrt{3}} \\ n_2 &= 1/4 \sqrt{35} + 1/4 \sqrt{3} - 1/4 \sqrt{22 + 2 \sqrt{35} \sqrt{3}} \\ n_3 &= 1/4 \sqrt{35} - 1/4 \sqrt{3} + 1/4 \sqrt{22 - 2 \sqrt{35} \sqrt{3}} \\ n_4 &= 1/4 \sqrt{35} - 1/4 \sqrt{3} - 1/4 \sqrt{22 - 2 \sqrt{35} \sqrt{3}} \\ n_5 &= 1/4 \sqrt{35} + 1/4 \sqrt{3} + 1/4 \sqrt{22 + 2 \sqrt{35} \sqrt{3}} \\ n_6 &= 1/4 \sqrt{35} + 1/4 \sqrt{3} - 1/4 \sqrt{22 + 2 \sqrt{35} \sqrt{3}} \\ n_7 &= 1/4 \sqrt{35} - 1/4 \sqrt{3} + 1/4 \sqrt{22 - 2 \sqrt{35} \sqrt{3}} \\ n_8 &= 1/4 \sqrt{35} - 1/4 \sqrt{3} - 1/4 \sqrt{22 - 2 \sqrt{35} \sqrt{3}}. \end{aligned}$$

The symmetric Lie algebra element B , however, is not describable by such easy numbers

as it involves logarithms. We, hence, only give a numerical approximation here

$$B = \begin{pmatrix} 0.0 & 0.0 & 0.0 & 0.0 & 0.044250 & 0.68381 & -0.54611 & 0.54611 \\ 0.0 & 0.0 & 0.0 & 0.0 & 0.77231 & 0.34190 & 0.75658 & -0.27305 \\ 0.0 & 0.0 & 0.0 & 0.0 & -0.68381 & -0.43041 & 0.21047 & -0.27305 \\ 0.0 & 0.0 & 0.0 & 0.0 & 0.0 & -0.044250 & 0.062580 & -0.42094 \\ 0.044250 & 0.77231 & -0.68381 & 0.0 & 0.0 & 0.0 & 0.0 & 0.0 \\ 0.68381 & 0.34190 & -0.43041 & -0.044250 & 0.0 & 0.0 & 0.0 & 0.0 \\ -0.54611 & 0.75658 & 0.21047 & 0.062580 & 0.0 & 0.0 & 0.0 & 0.0 \\ 0.54611 & -0.27305 & -0.27305 & -0.42094 & 0.0 & 0.0 & 0.0 & 0.0 \end{pmatrix}.$$

Thus, we have finally achieved to calculate the exact element N in the conjugacy class $[M]$ of the transition from $(2)^4$ to $(\tilde{2})^4$ which is generated by a completely symmetric element B of the Lie algebra. In this situation, B can be determined exactly as a matrix of entries which at worst contain logarithms of square roots, or, as above, as a numerical approximation to arbitrary precision. B is, indeed, the generator of the geodesic between $(2)^4$ and $(\tilde{2})^4$. The calculations in this section have been performed with the help of the computer algebra system Maple.

3.5 Deforming CFT along a geodesic

How can we describe the conformal field theory of a generic point in the K3 moduli space? We have already seen how to span geodesics in the geometric picture of the moduli space which start and/or end at points which correspond to known theories. The most promising way to describe a generic model in moduli space is to take a geodesic between that point and a point of a known model and to find a corresponding deformation of the conformal field theories along this geodesic. Finding such a deformation of CFTs is certainly the hardest challenge of such a project and has not been solved yet. Nevertheless, we want to describe the current state of our research on this point and comment on the possibilities of how to proceed further.

3.5.1 Conformal deformation theory

Infinitesimally, this deformation is described by the conformal deformation theory [34]. Its main idea is to add a (first) small perturbation to the action functional of the form

$$\delta S = \sum_i g_i \int d^2z O_i(z, \bar{z}); \quad (3.14)$$

the g_i signify the coupling constants of that perturbation and the $O_i(z, \bar{z})$ the perturbing fields. In order to keep the theory conformal and, in particular, scale invariant the coupling constants have to be dimensionless. Counting dimensions in δS restricts the perturbing fields to be of conformal dimension $(h, \tilde{h}) = (1, 1)$. Perturbations of this sort are called “marginal” in contrast to relevant and irrelevant perturbations which both introduce scales into the theory. However, in order to guaranty globally that

the new perturbed theories are again conformal one has to require even more. The marginal operators have to stay marginal in the perturbed theories and even should not mix with other marginal operators; otherwise, they would introduce a scale as soon as one would integrate the local deformation to a global one. Marginal operators with such a property are called “exact marginal”. This specific condition is elaborated in more detail below. In addition we also demand that the perturbing fields $O_i(z, \bar{z})$ are hermitian in order to keep the real structure of the CFT.

Let us start to work out the deformation of the two-point-function to lowest order. We choose a basis of marginal operators normalised as

$$\langle O_i(z, \bar{z}) O_j(w, \bar{w}) \rangle = \frac{\delta_{ij}}{(z-w)^2}. \quad (3.15)$$

The first order deformation is simply given by the derivative of the new perturbed theory wrt the coupling constant. There are two possible ways to calculate the derivative. First we can take it of the general CFT form of a two-point-function as given in (2.4)

$$\frac{\partial}{\partial g_i} \langle \Phi_\alpha(x, \bar{x}) \Phi_\beta(0, 0) \rangle = \left(-2 \frac{\partial h}{\partial g_i} \log(x) - 2 \frac{\partial \tilde{h}}{\partial g_i} \log(\bar{x}) \right) \langle \Phi_\alpha(x, \bar{x}) \Phi_\beta(0, 0) \rangle \quad (3.16)$$

using for simplicity translational invariance in order to set the second coordinate equal to zero. The second way of taking the derivative exploits the deformed action functional as

$$\begin{aligned} \frac{\partial}{\partial g_i} \langle \Phi_\alpha(x, \bar{x}) \Phi_\beta(0, 0) \rangle &= \int d^2w \langle O_i(w, \bar{w}) \Phi_\alpha(x, \bar{x}) \Phi_\beta(0, 0) \rangle \\ &= C_{III}^{i\alpha\beta} x^{-2h_\alpha} \bar{x}^{-2\tilde{h}_\alpha} \int d^2w \frac{|x|^2}{|w-x|^2 |w|^2} \end{aligned} \quad (3.17)$$

where in the second line we have used the general CFT form of a three-point-function with coupling constant $C_{III}^{i\alpha\beta}$ (2.4) as well as the known conformal weight of $O_i(w, \bar{w})$. We need to regularise the last integral, e.g. by the cutoff ϵ . This reduces the integral to the integration domain

$$\tilde{G}_\epsilon(x) = \{w \in \mathbb{C} \mid |w-x| > \epsilon, |w| > \epsilon\}.$$

But, using $Sl(2, \mathbb{C})$ invariance of the correlation function, we can simplify the integral performing the $Sl(2, \mathbb{C})$ transformation

$$\gamma: \quad z(z') = \frac{xz'}{z'+x}$$

to primed coordinates. In particular, this transformation maps 0 to 0 and x to $x' \rightarrow \infty$. For small $\epsilon \rightarrow 0$ the integration domain is mapped to

$$G_\epsilon(x) = \{w \in \mathbb{C} \mid \epsilon < |w| < \frac{|x|^2}{\epsilon}\}.$$

This, finally, leads to the following result for (3.17)

$$\begin{aligned} \frac{\partial}{\partial g_i} \langle \Phi_\alpha(x, \bar{x}) \Phi_\beta(0, 0) \rangle &= C_{III}^{i\alpha\beta} x^{-2h_\alpha} \bar{x}^{-2\tilde{h}_\alpha} \int_{G_\epsilon(x)} d^2w \frac{1}{|w|^2} \\ &= C_{III}^{i\alpha\beta} x^{-2h_\alpha} \bar{x}^{-2\tilde{h}_\alpha} 2\pi \log \frac{|x|^2}{\epsilon^2}. \end{aligned} \quad (3.18)$$

The infinities at the $\epsilon \rightarrow 0$ singularity of this result are eliminated by the usual renormalisation programme of field theory. The fields $\Phi_\alpha(x, \bar{x})$ have to be renormalised by the subtraction of the corresponding infinite parts in order to get a finite result in 3.18. This finite result, however, can be compared to our first way of calculating the perturbation in equation (3.16). In this manner we get the first order perturbation of the conformal weight

$$\frac{\partial h}{\partial g_i} = -\pi C_{III}^{i\alpha\alpha} \quad \frac{\partial \tilde{h}}{\partial g_i} = -\pi C_{III}^{i\alpha\alpha}. \quad (3.19)$$

Now we can proceed to explain the integrability conditions of exact marginality. The crucial point is to examine the renormalisation of the marginal operators $O_i(z, \bar{z})$ themselves during the perturbation. This renormalisation is given by [119]

$$O_i \longmapsto O_i + g_i \pi \log \epsilon^2 \left(C_{III}^{iii} O_i + \sum_j C_{III}^{ijj} O_j \right). \quad (3.20)$$

But a marginal operator is only exact if its conformal weight is not changed during the perturbation and, secondly, if it does not mix with other marginal operators. According to equation (3.19) the first of these two conditions amounts to the vanishing of $C_{III}^{iii} = 0$, the second to that of $C_{III}^{ijj} = 0$ for all O_j in the theory.

This can be generalised to higher orders. In case that we know that all derivatives of the conformal weight $\frac{\partial^l h}{\partial g_i^l}$ vanish up to order n we get analogously to equation (3.16)

$$\begin{aligned} \frac{\partial^{n+1}}{\partial g_i^{n+1}} \langle \Phi_\alpha(x, \bar{x}) \Phi_\alpha(0, 0) \rangle &= \\ &= \left(-2 \frac{\partial^{n+1} h}{\partial g_i^{n+1}} \log(x) - 2 \frac{\partial^{n+1} \tilde{h}}{\partial g_i^{n+1}} \log(\bar{x}) \right) \langle \Phi_\alpha(x, \bar{x}) \Phi_\beta(0, 0) \rangle. \end{aligned} \quad (3.21)$$

Inductively, we can conclude that the conformal weight of a field does not change to all orders if the following perturbation integrals

$$\int d^2w_1 \dots \int d^2w_{n+1} \langle \Phi_\alpha(x, \bar{x}) \Phi_\alpha(0, 0) O_i(w_1) \dots O_i(w_{n+1}) \rangle_c, \quad (3.22)$$

regularised by a cutoff ϵ , do not exhibit logarithmic divergencies.

These considerations lead to the following necessary conditions for exact marginality [32]:

- The integrals over n -point-functions in (3.22) do not exhibit logarithmic divergencies; in particular, we have $C_{III}^{iii} = 0$ to first order.
- $C_{III}^{ij} = 0$, i.e. the exact marginal operators do not mix with any other $(h, \tilde{h}) = (1, 1)$ operator.

These conditions are not linear. Consequently, linear combinations of exact marginal operators are not necessarily exact marginal again. The most prominent example of such a behaviour can be found in the moduli space of $c = 1$ bosonic torus theories at the meeting point of the ordinary torus and the orbifold line [120]. For supersymmetric theories, though, we do not know of any case of such peculiar behaviour.

Above, we have only described the perturbation of the two-point-function which yields the perturbation of the conformal weights and, hence, the new spectrum. In order to see how the whole CFT evolves under the perturbation one also needs to inspect the perturbation of the three-point-functions and, thus, the structure constants of the theory. The procedure follows the same lines as above, only that the integrals to be calculated become even more complicated. Let us, hence, stick to the easier (and still very difficult) problem to find the perturbed conformal weights.

3.5.2 Conformal deformations in K3 moduli space

The K3 moduli space is an 80-dimensional parameter space which is naturally endowed with 80 exact marginal operators at each of its points. These are given as the $(h, \tilde{h}) = (1, 1)$ supersymmetric partners of the 80 $(h, \tilde{h}) = (1/2, 1/2)$ groundstates [31]. This supersymmetry relation has actually been used by Dixon to argue that these $(1, 1)$ fields are exact marginal to all orders [95]; the argument uses a re-ordering of the contours as well as the OPE of the supercurrents in the superconformal algebra.

In order to describe a deformation of conformal field theories along a geodesic it would be sufficient to know the first non-trivial order of the deformation. The first order deformation would be by far the easiest to calculate as seen in the previous section. Unfortunately, the symmetry of the known theories in moduli space, which could be used as a starting point for the deformation, is so high that almost all three-point-functions which contain only one marginal field and which are, hence, relevant for perturbations to first order vanish. This has been observed for \mathbb{Z}_2 orbifolds in [103] and the analysis of respective correlation functions in the Gepner model yields a similar picture.

Hence, it is necessary to calculate perturbations at least to second order. This means that we have to be able to perform double volume integrals over four-point-functions. One can try to handle these integrals with a cut-off regularisation. This is certainly well-defined, but leads to a hard case by case study of the integrals which has only been performed for a few examples (see e.g. [121, 103]). This method is certainly not suitable for the large number of integrals which have to be evaluated when calculating in a Gepner model framework.

On the other hand, these integrals are nicely manageable with complex calculus methods as in [122, 123, 124, 125, 126, 127, 128], but only if the integral is regularised in some analytic way; a cut-off cuts away pieces of the complex plane and is, thus, not suitable for complex calculus arguments. The method of analytic regularisation has been introduced by Speer [129, 130] as a generalisation of dimensional regularisation. The theory is simply regularised by the analytic continuation of one or some of its physical parameters to the complex regime. After such a consistent regularisation, the renormalisation is performed by the usual BPHZ subtraction and the physical limit.

However, it has not yet been possible to identify such an analytic continuation which is at the same time effective and well-defined:²

- Continuation in the dimension, i.e. dimensional regularisation, yields contradictory results already for such a simple theory as the bosonic $c = 1$ model; part of the second order perturbation simply contradicts the first order perturbation. The reason for this failure should simply be that all these conformal field theory models are very specific to dimension two. Changing the dimension one would at least have to change the basis of fields drastically (from vertexoperators to polynomials) in order to get physically meaningful results.
- A continuation in the conformal weights seems arbitrary. One can actually choose the manner of continuation in such a way that there is no contradiction between first and second order. But this does not yield an obviously favoured continuation, and worse, the way of doing this changes uncontrollably from integral to integral.
- A continuation of the central charge is probably the most well-defined method from a conformal field theoretic standpoint. The only problem is that it is usually not possible! In particular, the theories which are studied in this chapter are very specific, especially the Gepner models, and do not belong to a continuum of conformal field theories with respect to the central charge. There is, however, the conjecture and hope that all CFTs are describable by a free field construction. If we were able to describe one of our theories by a free field construction, this way of continuing the central charge should be feasible.

For the time being, however, the question of how to consistently regularise the appearing complex volume integrals remains the main unsolved question of the deformation project. A smaller question which also needs to be resolved after a successful renormalisation is how to identify the marginal operator with a geometric generator of a geodesic. This question should be solvable by exploring the plentitude of symmetries in K3 moduli space, although it might be a tedious quest due to the high dimensionality of the space in question.

In the next section we present the way of calculating a quite general class of double volume integrals which we used to analyse the possibility of the different analytic

²We thank A.B. Zamolodchikov for enlightening discussions about the following points.

continuations. The results of these calculations can be written in terms of hypergeometric functions. As the continuation variable appears within the parameters of these hypergeometric functions we need to expand these with respect to their parameters in order to be able to continue the renormalisation process, in particular, to get the correct subtractions. This is most efficiently done by methods developed in [131] where infinite sums of ratios of gamma functions are expanded into generalised Euler Zagier sums. We have adapted the corresponding programme of [132] to our needs, especially implementing the expansion around parameters at rational numbers along the lines of [133]. All these calculations have been implemented using C++ and the computer algebra package GiNaC [134].

3.5.3 Calculation of the two-loop integral

In the following we want to present one very promising way of calculating the double volume integrals. Our elaboration is based on ideas of [122] and [124] how to use the Stokes theorem in order to separate complex volume integrals into products of contour integrals.

How to calculate complex volume integrals

In CFT any physical correlation function C can be written as monodromy invariant real bilinear product of the holomorphic and antiholomorphic conformal blocks, f_α resp. \bar{f}_α ,

$$C(w_1, \dots, w_n) = f_\alpha(w_1, \dots, w_n) Q_{\alpha\beta} \bar{f}_\beta(\bar{w}_1, \dots, \bar{w}_n).$$

The reality condition requires the matrix $Q_{\alpha\beta}$ to be hermitian. We introduce the following shorthand for the above hermitian quadratic form

$$(f, g)_Q = f_\alpha Q_{\alpha\beta} \bar{g}_\beta.$$

In the following we want to calculate the complex volume integral

$$I = \int d^2w (f_\alpha(w, z_0, \dots, z_m), \bar{f}_\beta(\bar{w}, \bar{z}_0, \dots, \bar{z}_m))_Q.$$

The calculation of multiple complex volume integrals can be reduced to this case inductively as we will show for an example in the next section.

For any fixed point P on the complex w plane define

$$\hat{f}(w) = \int_P^w dz f(z).$$

Then, for any domain A in the complex w plane we can now use the complex Stokes theorem (see e.g. [9])

$$\int_A d^2z \partial_z F(z, \bar{z}) = \frac{i}{2} \int_{\partial A} d\bar{z} F(z, \bar{z})$$

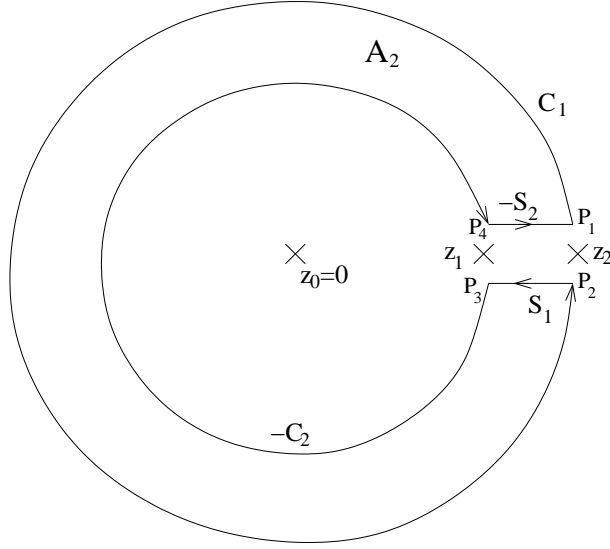


Figure 3.2: Separation of the complex plane into annuli

in order to rewrite the complex volume integral over A according to

$$\int_A d^2w (f, f)_Q = \int_A d^2w \partial_w (\hat{f}, f)_Q = \frac{i}{2} \int_{\partial A} d\bar{z} (\hat{f}, f)_Q. \quad (3.23)$$

The w plane contains $m + 2$ possible singular points z_0, \dots, z_{m+1} where we can deliberately put $z_0 = 0$ and where z_{m+1} signifies the point at infinity. We now split the complex w plane into $m + 1$ annuli $A_l = \{w \in \mathbb{C} \mid |z_{l-1}| < |w| < |z_l|\}$, $l \in \{1, \dots, m+1\}$. This induces a split of the integral into

$$I = \sum_{l=1}^{m+1} I_{A_l}.$$

Let us first regard the annulus A_2 as an example how to calculate these integrals. We choose the contour of A_2 to run as given in figure 3.2: C_1 , from P_1 to P_2 , the circle $|w| = |z_2|$; S_1 , from P_2 to P_3 , the line between z_2 and z_1 just below the cut between the two points; $-C_2$, from P_3 to P_4 , the circle $|w| = |z_1|$ in opposite direction; $-S_2$, from P_4 to P_1 , the line between z_1 and z_2 just above the cut between the two points. In the picture we have put the singular points onto the real line for simplicity. In general one has to deform the contours suitably. We now define two further shorthands

$$J_C \equiv \int_C d\bar{z} (\hat{f}, f)_Q(z, \bar{z})$$

$$(I_C)_\alpha \equiv \int_C dz f_\alpha(z),$$

where, in the definition of J_C , we choose the fixed point P of \hat{f} to be the starting point of the contour C . Using (3.23) we find the four contributions to I_{A_2}

- C_1 : $\frac{i}{2} \int_{P_1}^{P_2} d\bar{w} \left(\int_{P_1}^w dz f(z), f \right)_Q = \frac{i}{2} J_{C_1}$
- S_1 : $\frac{i}{2} \int_{P_2}^{P_3} d\bar{w} \left(\int_{P_1}^{P_2} dz f(z) + \int_{P_2}^w dz f(z), f \right)_Q = \frac{i}{2} [(I_{C_1}, I_{S_1})_Q + J_{S_1}]$
- $-C_2$: $-\frac{i}{2} \int_{P_3}^{P_4} d\bar{w} \left(\int_{P_1}^{P_4} dz f(z) + \int_{P_4}^w dz f(z), f \right)_Q = -\frac{i}{2} [(I_{S_2}, I_{C_2})_Q + J_{C_2}]$
- $-S_2$: $-\frac{i}{2} \int_{P_1}^{P_4} d\bar{w} \left(\int_{P_1}^w dz f(z), f \right)_Q = -\frac{i}{2} J_{S_2}$.

The fact that each annulus does not contain any singular points leads to the identity

$$I_{C_1} + I_{S_1} - I_{C_2} - I_{S_2} = 0. \quad (3.24)$$

Furthermore, knowing the monodromy behaviour across the cut between the fixed points z_{l-1} and z_l allows us to relate the two integrals I_{S_1} and I_{S_2} via the monodromy matrix M_l

$$(I_{S_1})_\alpha = (M_l)_{\alpha\beta} (I_{S_2})_\beta. \quad (3.25)$$

Due to the monodromy invariance and, hence, single valuedness of $(f, f)_Q$ around any singular points and across any cuts, J_{S_1} has to equal J_{S_2} and, thus, these contributions cancel. Analogously, the J_{C_1} contribution of annulus A_l has to cancel the $-J_{C_2}$ contribution of annulus A_{l+1} . Hence, we are only left with products of contour integrals.

Concerning the singular points at $z_0 = 0$ and $z_{m+1} = \infty$ we assume that contours around these points vanish if we take the radius of the contour to 0 (for z_0) or to ∞ (for z_{m+1}). This corresponds to the assumption that these singular points are not of integral type.

Now we can use (3.24) and (3.25) in order to express the I_{S_i} contributions by I_{C_1} and I_{C_2} . We hence reach the total contribution of the annulus A_l to I (already neglecting the J_C terms)

$$\begin{aligned} I_{A_l} &= \frac{i}{2} ((I_{C_1}, I_{S_1})_Q - (I_{S_2}, I_{C_2})_Q) \\ &= \frac{i}{2} ((I_{C_1}, I_{C_2} - I_{C_1})_{Q(\mathbb{1} - M_l)^{-1}} - (I_{C_1} - I_{C_2}, I_{C_2})_{(\mathbb{1} - M_l)^{-1}Q}) \\ &= \frac{i}{2} ((I_{C_2}, I_{C_2})_{(\mathbb{1} - M_l)^{-1}Q} - (I_{C_1}, I_{C_1})_{(\mathbb{1} - M_l)^{-1}Q}), \end{aligned}$$

where we have used the unitarity of Q in the second equality and the invariance of Q under monodromy transformations in the third. Defining I_l to be the integral on the contour $|w| = |z_l|$ and summing up all contributions we finally get

$$\begin{aligned} I &= \sum_l I_{A_l} = \frac{i}{2} \sum_{l=1}^{m+1} [(I_{l-1}, I_{l-1})_{(\mathbb{1} - M_l)^{-1}Q} - (I_l, I_l)_{(\mathbb{1} - M_l)^{-1}Q}] \\ &= \frac{i}{2} \sum_{k=1}^m (I_k, I_k)_{[(\mathbb{1} - M_{k+1})^{-1} - (\mathbb{1} - M_k)^{-1}]Q}. \end{aligned}$$

Calculation of a specific two-loop integral

We want to study the following special example, the integral

$$J(z, w) = (z - w)^f (\bar{z} - \bar{w})^{\bar{f}} \int d^2x d^2y (x - w)^a (\bar{x} - \bar{w})^{\bar{a}} (z - x)^b (\bar{z} - \bar{x})^{\bar{b}} (y - w)^d (\bar{y} - \bar{w})^{\bar{d}} (z - y)^e (\bar{z} - \bar{y})^{\bar{e}} (x - y)^c (\bar{x} - \bar{y})^{\bar{c}}. \quad (3.26)$$

Without loss of generality we can set $w = 0$ and drag z out of the integral by a change of coordinates

$$x' = \frac{x}{z} \quad y' = \frac{y}{z}.$$

This results in

$$J(z, 0) = z^{a+b+c+d+e+f+2} \bar{z}^{\bar{a}+\bar{b}+\bar{c}+\bar{d}+\bar{e}+\bar{f}+2} J(1, 0).$$

Hence we need to investigate

$$J(1, 0) = \int d^2x d^2y x^a \bar{x}^{\bar{a}} (1 - x)^b (1 - \bar{x})^{\bar{b}} y^d \bar{y}^{\bar{d}} (1 - y)^e (1 - \bar{y})^{\bar{e}} (x - y)^c (\bar{x} - \bar{y})^{\bar{c}}.$$

The relevant conformal block functions are given by

$$f_{abdec}(x, y) = x^a (1 - x)^b y^d (1 - y)^e (x - y)^c.$$

For the following calculations we put $q_a := \exp(\pi i a)$ and use the conventions that contours are taken to be positive in a counterclockwise direction as well as that we will always start with the identity on the sheet above the cut closest to the identity (in order to keep track of phase factors).

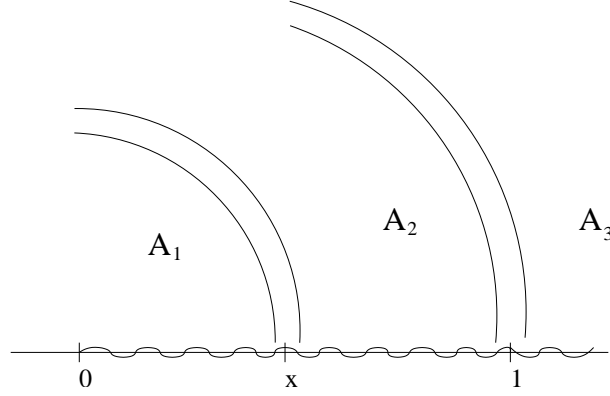
The diagonal case

Let us first study the easiest version of $J(1, 0)$, the diagonal case. This means that $Q = \mathbb{1}$, that we have equal holomorphic and antiholomorphic exponents, $a = \bar{a}$ etc., and that we only deal with $f(x, y) := f_{abdec}(x, y)$.

The outer x integration has singular points at 0, 1 and ∞ . Hence we need to regard the two annuli $0 < |x| < 1$ and $1 < |x| < \infty$.

Case 1: $0 < |x| < 1$

In order to perform the y integration we can just apply the algorithm of section 3.5.3 one to one. The situation of this integral with singular points at 0, x , 1 and ∞ is depicted in figure 3.3. We choose the cuts to run from 0 to x to 1 to ∞ . Although

Figure 3.3: Singular points and the choice of cuts in the y plane

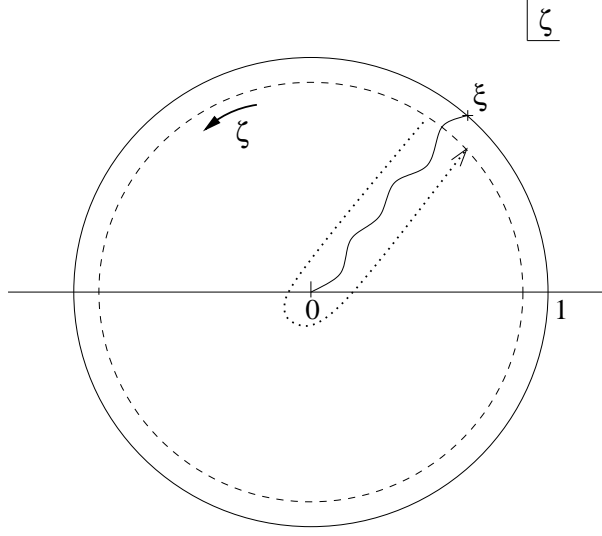
we have depicted x on the real axis in figure 3.3 for simplicity, it is only bound to the above constraint $0 < |x| < 1$. We get

$$\int_{0 < |x| < 1} d^2 y |f(x, y)|^2 = -\frac{i}{2} [(1 - q_a^2)^{-1} - (1 - q_c^2 q_a^2)^{-1}] \left| \int_{\substack{|\zeta|=|x| \\ (|\zeta|=|x|-\epsilon)}} d\zeta f(x, \zeta) \right|^2 \\ - \frac{i}{2} [(1 - q_c^2 q_a^2)^{-1} - (1 - q_c^2 q_a^2 q_e^2)^{-1}] \left| \int_{\substack{|\zeta|=1 \\ (|\zeta|=1-\epsilon)}} d\zeta f(x, \zeta) \right|^2. \quad (3.27)$$

Here we introduced an infinitesimal $\epsilon > 0$ in order to keep track of sign factors when calculating a stack of contours later on. The first term corresponds to the $|y| = |x|$ contributions of the annuli A_1 and A_2 , the second to the $|y| = 1$ contributions of the annuli A_2 and A_3 (see figure 3.3). The contributions at 0 and ∞ vanish by assumption. The monodromy factor M_2 e.g. can be calculated taking y around x and 0, which amounts to a phase of $q_c^2 q_a^2$.

Now we want to perform the x integration in the region $0 < |x| < 1$. In section 3.5.3 we argued that any J_C type contribution of an annulus will cancel against a respective term of another annulus due to single valuedness of the physical correlator. Hence, we will present the following calculation up to these J_C terms as we do not need to calculate them. As by assumption the contributions at 0 and ∞ vanish, the only contribution will come from the contour at $|x| = 1$ (obviously from the annulus $A_1 = 0 < |x| < 1$). The integral over the first term in (3.27) yields

$$\int_{0 < |x| < 1} d^2 x \left| \int_{\substack{|\zeta|=|x| \\ (|\zeta|=|x|-\epsilon)}} d\zeta f(x, \zeta) \right|^2 = \\ = -\frac{i}{2} (1 - q_a^2 q_c^2 q_a^2)^{-1} \left| \int_{\substack{|\xi|=1 \\ (|\xi|=1-\epsilon)}} d\xi \int_{\substack{|\zeta|=|\xi| \\ (|\zeta|=|\xi|-\epsilon)}} d\zeta f(\xi, \zeta) \right|^2$$

Figure 3.4: Cuts and contours in the ζ plane

$$\begin{aligned}
&= -\frac{i}{2}(1 - q_a^2 q_c^2 q_d^2)^{-1} \left| (-1 + q_a^2 q_c^2 q_d^2) \int_0^1 d\xi (-1 + q_d^2) \int_0^\xi d\zeta f(\xi, \zeta) \right|^2 \\
&= -\frac{i}{2}(1 - q_a^{-2} q_c^{-2} q_d^{-2}) |1 - q_d^2|^2 \left| \int_0^1 d\xi \int_0^\xi d\zeta \xi^a (1 - \xi)^b \zeta^d (1 - \zeta)^e (\xi - \zeta)^c \right|^2 \\
&= -\frac{i}{2}(1 - q_a^{-2} q_c^{-2} q_d^{-2}) |1 - q_d^2|^2 \\
&\quad \left| \int_0^1 d\xi \int_0^1 dt \xi^{a+c+d+1} (1 - \xi)^b t^d (1 - t)^c (1 - \xi t)^e \right|^2 \\
&= -\frac{i}{2}(1 - q_a^{-2} q_c^{-2} q_d^{-2}) |1 - q_d^2|^2 |F(a + c + d + 1, b, d, c, e)|^2, \tag{3.28}
\end{aligned}$$

where we use the shorthand

$$F(a, b, d, e, c) := \int_0^1 dx \int_0^1 dy x^a (1 - x)^b y^d (1 - y)^e (1 - xy)^c.$$

Two important comments are due concerning this calculation:

- When calculating the monodromy factor in the first equality of (3.28) we have to take into account that together with x we have to take the whole ζ integral around 0. That means that we have to take x and ζ around 0 and, very importantly, also x around ζ during this process as we have imposed the condition $|\zeta| = |x| - \epsilon$.
- The second equality in (3.28) is a result of the contraction of the contours around the cuts. In figure 3.4 the cuts of the ζ plane are depicted as chosen earlier on, together with the ζ contour (dashed line), the contracted ζ contour (dotted

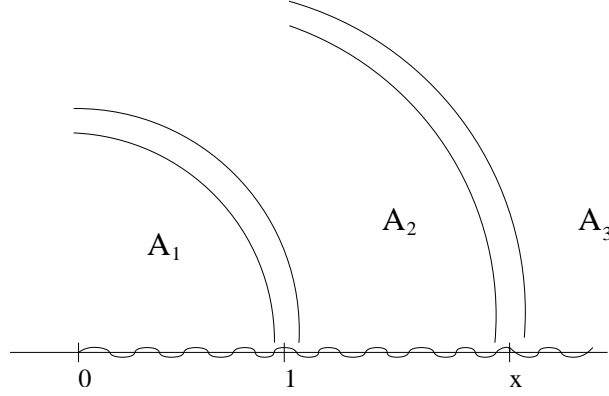
line) as well as the ξ contour (solid line). The cuts in the ξ plane run from 0 to 1 to ∞ . Hence, contracting the ξ integral around the cut on the real line, we automatically take the contracted contour of the ζ integral to the real line as well, from above for ξ in the upper halfplane, from below for ξ in the lower halfplane. But the difference in phases between these two cases amounts to exactly the same phasefactor as just calculated for the monodromy factor. The difference in phases between the two segments of the ζ integration is just given by taking ζ around 0 (and certainly the opposite direction along the real line).

The integral over the second term in (3.27) yields

$$\begin{aligned}
& \int_{0 < |x| < 1} d^2x \left| \int_{\substack{|\zeta|=1 \\ (|\zeta|=1-\epsilon)}} d\zeta f(x, \zeta) \right|^2 = \\
&= -\frac{i}{2} (1 - q_a^2)^{-1} \left| \int_{\substack{|\xi|=1 \\ (|\xi|=|\zeta|-\epsilon)}} d\xi \int_{\substack{|\zeta|=1 \\ (|\zeta|=1-\epsilon)}} d\zeta f(\xi, \zeta) \right|^2 \\
&= -\frac{i}{2} (1 - q_a^2)^{-1} \left| (-1 + q_a^2) \int_0^1 d\xi \left[- \int_\xi^1 d\zeta f(\xi, \zeta) - \int_0^\xi d\zeta f(\xi, \zeta) \right. \right. \\
&\quad \left. \left. + q_d^2 \int_0^\xi d\zeta f(\xi, \zeta) + q_c^2 q_d^2 \int_\xi^1 d\zeta f(\xi, \zeta) \right] \right|^2 \\
&= -\frac{i}{2} (1 - q_a^{-2}) \left| (1 - q_c^2 q_d^2) \int_0^1 d\xi \int_\xi^1 d\zeta f(\xi, \zeta) + (1 - q_d^2) \int_0^1 d\xi \int_0^\xi d\zeta f(\xi, \zeta) \right|^2 \\
&= -\frac{i}{2} (1 - q_a^{-2}) \left| q_c^{-1} (1 - q_c^2 q_d^2) F(a + c + d + 1, e, a, c, b) \right. \\
&\quad \left. + (1 - q_d^2) F(a + c + d + 1, b, d, c, e) \right|^2. \tag{3.29}
\end{aligned}$$

This time we have to add the following remarks:

- The monodromy factor in the first equality of (3.29) is calculated just taking x around 0. This time the ζ integral does not depend on x .
- The cut structure in the ζ plane (see figure 3.3, take $y = \zeta$) determines the ordering between the two contours. As x is encircled by the contour of ζ , the ξ contour has to lie within the ζ contour.
- The second equality is again a result of the contraction of the contours around the cuts. The difference in phase factor between the ξ integration above and below the cut is again given by the same factor as the one in the monodromy calculation, q_a^2 . This time, the ζ integration also starts and ends at 1, going around 0. But as the ζ plane contains the singular point ξ on the cut between 0 and 1, we have to split the integration at ξ .

Figure 3.5: Singular points and the choice of cuts in the y plane

- Going around ξ on a tiny half-circle between the integration \int_0^ξ and \int_ξ^1 amounts to an additional phase of q_c . But this phase drops out of the calculation naturally if we arrange for the difference $\pm(\xi - \zeta)$ in $f(\xi, \zeta)$ to be always positive. Only if we go around the full circle from \int_1^ξ (on the upper halfplane) to \int_ξ^1 (on the lower halfplane) the function does not know about the sheet any more and we have to add an additional monodromy factor of q_c^2 . Furthermore, our convention about the orientation of contours always dictates whether to take q_C or q_C^{-1} .
- The fourth equality uses the following calculational trick for the first term

$$\begin{aligned}
 \int_0^1 d\xi \int_\xi^1 d\zeta f(\xi, \zeta) &= \int_0^1 d\zeta \int_0^\zeta d\xi f(\xi, \zeta) \\
 &= q_c^{-1} \int_0^1 d\zeta \int_0^\zeta d\xi \zeta^d (1 - \zeta)^e x i^a (1 - \xi)^b (\zeta - \xi)^c \\
 &= q_c^{-1} F(a + c + d + 1, b, d, c, e) .
 \end{aligned}$$

Otherwise, it proceeds the same way as in (3.28).

Case 2: $1 < |x| < \infty$

In the second case, $1 < |x| < \infty$, the calculation works very much the same way as in the first. Hence, we are only going to point out the major differences. We have depicted the position of the singular points 0, x , 1 and ∞ , cuts and the annuli within the y plane in figure 3.5. We choose the cuts to run from 0 to 1 to x to ∞ . Again remember that although we have depicted x on the real axis in figure 3.5 for simplicity, it is only bound to the above constraint $1 < |x| < \infty$. We get

$$\int_{1 < |x| < \infty} d^2y |f(x, y)|^2 = -\frac{i}{2} [(1 - q_a^2)^{-1} - (1 - q_a^2 q_e^2)^{-1}] \left| \int_{\substack{|\zeta|=1 \\ (|\zeta|=1+\epsilon)}} d\zeta f(x, \zeta) \right|^2$$

$$- \frac{i}{2} [(1 - q_d^2 q_e^2)^{-1} - (1 - q_c^2 q_d^2 q_e^2)^{-1}] \left| \int_{\substack{|\zeta|=|x| \\ (|\zeta|=|x|-\epsilon)}} d\zeta f(x, \zeta) \right|^2, \quad (3.30)$$

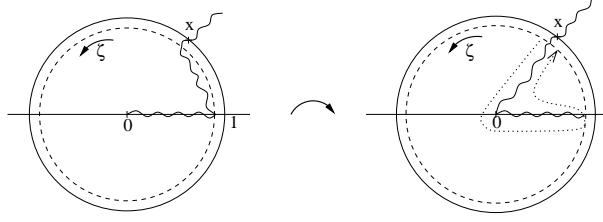
where again we have introduced an infinitesimal ϵ in order to keep track of the order of multiple contours.

Now, the integral over the first term in (3.30) is similar to the second x integration in the $0 < |x| < 1$ case. We have

$$\begin{aligned} & \int_{1 < |x| < \infty} d^2x \left| \int_{\substack{|\zeta|=1 \\ (|\zeta|=1+\epsilon)}} d\zeta f(x, \zeta) \right|^2 = \\ &= \frac{i}{2} (1 - q_a^2 q_b^2 q_c^2)^{-1} \left| \int_{\substack{|\xi|=1 \\ (|\xi|=|\zeta|+\epsilon)}} d\xi \int_{\substack{|\zeta|=1 \\ (|\zeta|=1+\epsilon)}} d\zeta f(\xi, \zeta) \right|^2 \\ &= \frac{i}{2} (1 - q_a^2 q_b^2 q_c^2)^{-1} \left| \int_{\substack{|\zeta|=1 \\ (|\zeta|=1+\epsilon)}} d\zeta \int_{\substack{|\xi|=1 \\ (|\xi|=|\zeta|+\epsilon)}} d\xi f(\xi, \zeta) \right|^2 \\ &= \frac{i}{2} (1 - q_a^2 q_b^2 q_c^2)^{-1} \left| (-1 + q_d^2) \int_0^1 d\zeta \left[- \int_{\zeta}^1 d\xi f(\xi, \zeta) - \int_0^{\zeta} d\xi f(\xi, \zeta) \right. \right. \\ &\quad \left. \left. + q_a^2 \int_0^{\zeta} d\xi f(\xi, \zeta) + q_a^2 q_c^2 \int_{\zeta}^1 d\xi f(\xi, \zeta) \right] \right|^2 \\ &= \frac{i}{2} (1 - q_a^2 q_b^2 q_c^2)^{-1} |1 - q_d^2|^2 \left| (1 - q_a^2 q_c^2) \int_0^1 d\zeta \int_{\zeta}^1 d\xi f(\xi, \zeta) \right. \\ &\quad \left. + (1 - q_a^2) \int_0^1 d\zeta \int_0^{\zeta} d\xi f(\xi, \zeta) \right|^2 \\ &= \frac{i}{2} (1 - q_a^2 q_b^2 q_c^2)^{-1} |1 - q_d^2|^2 \left| (1 - q_a^2 q_c^2) F(a + c + d + 1, b, d, c, e) \right. \\ &\quad \left. + q_c (1 - q_a^2) F(a + c + d + 1, e, a, c, b) \right|^2. \quad (3.31) \end{aligned}$$

The only differences to the calculation in (3.29) are slightly different monodromy factors due to the changed singular structure and the additional step in the second equality of (3.31) where we interchanged the order of the integrals and, hence, changed the cut structure. As we approach the circle $|x| = 1$ from above this time, the ξ and ζ contours are interchanged in comparison to the calculation in (3.29). But as we want to use the same argument as in (3.29), a change of the integrations seems reasonable. We are allowed to do this as both contours are independent of each other (in contrast to the calculation in (3.28)) as long as we keep the same ordering.

The integral over the second term in (3.30) is quite similar to the first x integration in the $0 < |x| < 1$ case. The situation of the cuts in the ζ plane in this case is shown in the first picture of figure 3.6. As this cut structure is not very useful for our calculation, we change it to a linear combination of these cuts, depicted in the second picture of

Figure 3.6: Change of cuts in the ζ plane

3.6. This change of basis for the cuts is allowed as it does not cross any of our contours. Hence, we have

$$\begin{aligned}
& \int_{1 < |x| < \infty} d^2x \left| \int_{\substack{|\zeta|=|x| \\ (|\zeta|=|x|-\epsilon)}} d\zeta f(x, \zeta) \right|^2 = \\
&= \frac{i}{2} (1 - q_a^2 q_b^2 q_c^2 q_d^2 q_e^2)^{-1} \left| \int_{\substack{|\xi|=1 \\ (|\xi|=1+2\epsilon)}} d\xi \int_{\substack{|\zeta|=|\xi| \\ (|\zeta|=|\xi|-\epsilon)}} d\zeta f(\xi, \zeta) \right|^2 \\
&= \frac{i}{2} (1 - q_a^2 q_b^2 q_c^2 q_d^2 q_e^2)^{-1} \left| - \int_0^1 d\xi \left(- \int_0^\xi d\zeta f(\xi, \zeta) + q_a^2 \int_0^\xi d\zeta f(\xi, \zeta) \right. \right. \\
&\quad \left. \left. + q_a^2 \int_\xi^1 d\zeta q_c \tilde{f}(\xi, \zeta) - q_d^2 q_e^2 \int_\xi^1 d\zeta q_c \tilde{f}(\xi, \zeta) \right) \right. \\
&\quad \left. + q_a^2 q_c^2 q_d^2 \int_0^1 d\xi \left(\int_\xi^1 d\zeta q_c^{-1} \tilde{f}(\xi, \zeta) - q_e^2 \int_\xi^1 d\zeta q_c^{-1} \tilde{f}(\xi, \zeta) \right. \right. \\
&\quad \left. \left. - q_e^2 \int_0^\xi d\zeta f(\xi, \zeta) + q_d^2 q_e^2 \int_0^\xi d\zeta f(\xi, \zeta) \right) \right|^2 \\
&= \frac{i}{2} (1 - q_a^2 q_b^2 q_c^2 q_d^2 q_e^2)^{-1} \left| (1 - q_d^2) (1 - q_a^2 q_c^2 q_d^2 q_e^2) \int_0^1 d\xi \int_0^\xi d\zeta f(\xi, \zeta) \right. \\
&\quad \left. - q_c q_d^2 (1 - q_e^2) (1 - q_a^2) \int_0^1 d\xi \int_\xi^1 d\zeta \tilde{f}(\xi, \zeta) \right|^2 \\
&= \frac{i}{2} (1 - q_a^2 q_b^2 q_c^2 q_d^2 q_e^2)^{-1} \left| (1 - q_d^2) (1 - q_a^2 q_c^2 q_d^2 q_e^2) F(a + c + d + 1, b, d, c, e) \right. \\
&\quad \left. - q_c q_d^2 (1 - q_e^2) (1 - q_a^2) F(a + c + d + 1, e, a, c, b) \right|^2. \tag{3.32}
\end{aligned}$$

Three important remarks are due:

- Calculating the monodromy factor for the first equality of (3.32) we have to take the whole ζ integral around 0 together with x , as in (3.28). Hence, we get contributions from taking x around 0 and 1, from taking ζ around 0 and 1 and from taking x around ζ (due to the ϵ assignment which orders the contours).
- The second equality is reached by contraction of the contours around the cuts.



Figure 3.7: Contours in the ζ plane after the contraction of the ξ contour

The contraction in the ζ plane is shown in the second picture of figure 3.6. Figure 3.7 shows the situation after we have also contracted ξ . Doing this we have taken both contours to the real line simultaneously. The two cases of ξ being in the upper and the lower halfplane are depicted. In the calculation, accordingly, we have first written down the contribution to the ξ integration in the upper halfplane, then the one in the lower. Both contributions contain four separate terms of the ζ integration which has to be split according to figure 3.7. Note that by our convention we always start on the sheet in the upper halfplane to the very right.

- One has to be careful to give the phase factor which separates the $0 < \zeta < 1$ integration at ξ the right orientation. We have depicted the right phase factors in figure 3.7 as well.

Summing up the contributions

Now we need to sum up the contributions. In particular, this means that we have to multiply the four contributions of (3.28), (3.29), (3.31) and (3.32) with the correct monodromy factors given in the equations (3.27) and (3.30). This sums up to

$$\begin{aligned}
J &= \left(-\frac{1}{4}\right) \left((1 - q_d^2)^{-1} - (1 - q_c^2 q_d^2)^{-1}\right) (1 - q_a^{-2} q_c^{-2} q_d^{-2}) |1 - q_d^2|^2 \\
&\quad |F(a + c + d + 1, b, d, c, e)|^2 \\
&+ \left(-\frac{1}{4}\right) \left((1 - q_c^2 q_d^2)^{-1} - (1 - q_c^2 q_d^2 q_e^2)^{-1}\right) (1 - q_a^{-2}) \\
&\quad |q_c^{-1} (1 - q_c^2 q_d^2) F(a + c + d + 1, e, a, c, b) + (1 - q_d^2) F(a + c + d + 1, b, d, c, e)|^2 \\
&+ \frac{1}{4} \left((1 - q_d^2)^{-1} - (1 - q_d^2 q_e^2)^{-1}\right) (1 - q_a^2 q_b^2 q_c^2)^{-1} |1 - q_d^2|^2 \\
&\quad |q_c^{-1} (1 - q_a^2 q_c^2) F(a + c + d + 1, b, d, c, e) + (1 - q_a^2) F(a + c + d + 1, e, a, c, b)|^2 \\
&+ \frac{1}{4} \left((1 - q_d^2 q_e^2)^{-1} - (1 - q_c^2 q_d^2 q_e^2)^{-1}\right) (1 - q_a^2 q_b^2 q_c^2 q_d^2 q_e^2)^{-1} \\
&\quad |(1 - q_d^2) (1 - q_a^2 q_c^2 q_d^2 q_e^2) F(a + c + d + 1, b, d, c, e) \\
&\quad - q_c q_d^2 (1 - q_e^2) (1 - q_a^2) F(a + c + d + 1, e, a, c, b)|^2
\end{aligned}$$

$$\begin{aligned}
&= \left(-\frac{1}{4}\right) [((1 - q_d^2)^{-1} - (1 - q_c^2 q_d^2)^{-1}) (1 - q_a^{-2} q_c^{-2} q_d^{-2}) |1 - q_d^2|^2 \\
&\quad + ((1 - q_c^2 q_d^2)^{-1} - (1 - q_c^2 q_d^2 q_e^2)^{-1}) (1 - q_a^{-2}) |1 - q_d^2|^2 \\
&\quad - ((1 - q_d^2)^{-1} - (1 - q_d^2 q_e^2)^{-1}) (1 - q_a^2 q_b^2 q_c^2)^{-1} |1 - q_d^2|^2 |1 - q_a^2 q_c^2|^2 \\
&\quad - ((1 - q_d^2 q_e^2)^{-1} - (1 - q_c^2 q_d^2 q_e^2)^{-1}) (1 - q_a^2 q_b^2 q_c^2 q_d^2 q_e^2)^{-1} |1 - q_d^2|^2 |1 - q_a^2 q_c^2 q_d^2 q_e^2|^2] \\
&\quad \quad \quad F(a + c + d + 1, b, d, c, e)^2 \\
&- \left(\frac{1}{4}\right) [((1 - q_c^2 q_d^2)^{-1} - (1 - q_c^2 q_d^2 q_e^2)^{-1}) (1 - q_a^{-2}) |1 - q_c^2 q_d^2|^2 \\
&\quad - ((1 - q_d^2)^{-1} - (1 - q_d^2 q_e^2)^{-1}) (1 - q_a^2 q_b^2 q_c^2)^{-1} |1 - q_d^2|^2 |1 - q_a^2|^2 \\
&\quad - ((1 - q_d^2 q_e^2)^{-1} - (1 - q_c^2 q_d^2 q_e^2)^{-1}) (1 - q_a^2 q_b^2 q_c^2 q_d^2 q_e^2)^{-1} |1 - q_e^2|^2 |1 - q_a^2|^2] \\
&\quad \quad \quad F(a + c + d + 1, e, a, c, b)^2 \\
&- \left(\frac{1}{4}\right) [((1 - q_c^2 q_d^2)^{-1} - (1 - q_c^2 q_d^2 q_e^2)^{-1}) (1 - q_a^{-2}) \\
&\quad \quad \quad (q_c^{-1} (1 - q_c^2 q_d^2) (1 - q_d^{-2}) + q_c (1 - q_c^{-2} q_d^{-2}) (1 - q_d^2)) \\
&\quad \quad \quad - ((1 - q_d^2)^{-1} - (1 - q_d^2 q_e^2)^{-1}) (1 - q_a^2 q_b^2 q_c^2)^{-1} |1 - q_d^2|^2 \\
&\quad \quad \quad (q_c^{-1} (1 - q_d^2 q_c^2) (1 - q_a^{-2}) + q_c (1 - q_a^{-2} q_c^{-2}) (1 - q_d^2)) \\
&\quad \quad \quad + ((1 - q_d^2 q_e^2)^{-1} - (1 - q_c^2 q_d^2 q_e^2)^{-1}) (1 - q_a^2 q_b^2 q_c^2 q_d^2 q_e^2)^{-1} \\
&\quad \quad \quad ((1 - q_d^2) (1 - q_a^2 q_c^2 q_d^2 q_e^2) q_c^{-1} q_d^{-2} (1 - q_e^{-2}) (1 - q_a^{-2}) \\
&\quad \quad \quad + (1 - q_d^{-2}) (1 - q_a^{-2} q_c^{-2} q_d^{-2} q_e^{-2}) q_c q_d^2 (1 - q_e^2) (1 - q_a^2))] \\
&\quad \quad \quad F(a + c + d + 1, b, d, c, e) F(a + c + d + 1, e, a, c, b) .
\end{aligned}$$

Here we have used the reality of $F(a + c + d + 1, b, d, c, e)$ and $F(a + c + d + 1, e, a, c, b)$. This can be evaluated to

$$\begin{aligned}
J &= -\frac{1}{4} (\sin(\pi(a + b + c)) \sin(\pi(c + d + e)) \sin(\pi(a + b + c + d + e)))^{-1} \\
&\quad \times [\sin(\pi b) \sin(\pi d) (\sin(\pi(2a + b + 3c + d + 2e)) - \sin(\pi(b + c + d + 2e))) \\
&\quad \quad - \sin(\pi(2a + b + c + d)) + \sin(\pi(b + c + d)) + \sin(\pi(b - c - d)) \\
&\quad \quad + \sin(\pi(-b - c + d))] F(a + c + d + 1, b, d, c, e)^2 \\
&\quad + \sin(\pi a) \sin(\pi e) (\sin(\pi(a + 2b + 3c + 2d + e)) - \sin(\pi(a + c + 2d + e))) \\
&\quad \quad - \sin(\pi(a + 2b + c + e)) + \sin(\pi(a + c + e)) + \sin(\pi(a - c - e)) \\
&\quad \quad + \sin(\pi(-a - c + e))] F(a + c + d + 1, e, a, c, b)^2 \\
&\quad - 8 \sin(\pi a) \sin(\pi b) \sin(\pi d) \sin(\pi e) \sin(\pi(a + b + 2c + d + e)) \\
&\quad \quad \quad F(a + c + d + 1, b, d, c, e) F(a + c + d + 1, e, a, c, b) .
\end{aligned}$$

This result is now manifestly real and invariant under the exchange $a \leftrightarrow d$, $b \leftrightarrow e$, which amounts to changing the order of the integration (or the exchange of x and y) in the original integral.

The off-diagonal case

Demanding that $J(1,0)$ originates from a physical correlator puts strict constraints on the possible off-diagonal cases. First the difference between the holomorphic and the antiholomorphic exponents (e.g. $a - \bar{a}$) has to be an integer, second for each $J(1,0)$ we have to find the same integral with holomorphic and antiholomorphic exponents exchanged and the prefactor complex conjugated. Hence, assuming real prefactors the only possible off-diagonal case amounts to the hermitian form given by

$$Q = p \cdot \begin{pmatrix} 0 & 1 \\ 1 & 0 \end{pmatrix} \quad p \in \mathbb{R} ,$$

with the two functions

$$\begin{aligned} f_1(x, y) &= x^a (1-x)^b y^d (1-y)^e (x-y)^c . \\ f_2(x, y) &= x^{a+n_a} (1-x)^{b+n_b} y^{d+n_d} (1-y)^{e+n_e} (x-y)^{c+n_c} \quad n_i \in \mathbb{Z} . \end{aligned}$$

But as all prefactors only depend on phases the changes in the calculation are not very severe, because the difference between the holomorphic and the antiholomorphic exponents is integer (i.e. they produce the same phases, almost always!). Thus, let us just enumerate the changes which have to be made:

- All monodromy factors are the same as in the diagonal case.
- The calculation of the integrals stays the same as long as only 2π phases, i.e. squares of $q_s = \exp(\pi i s)$ factors, are involved. The only other factor appearing is q_c . This produces an extra minus-sign in some places if n_c is odd.
- We have to distinguish which of the functions $F(a+c+d+1, b, d, c, e)$ etc. originates from integrals with holomorphic or antiholomorphic exponents.
- As we now sum up two off-diagonal products of block-functions the result is doubled in most places, in comparison to the diagonal case.

Hence we reach a total result for the off-diagonal case of

$$\begin{aligned} J(f_1, f_2) &= \\ &= \left(-\frac{1}{2}\right) \left[\left((1-q_d^2)^{-1} - (1-q_c^2 q_d^2)^{-1} \right) (1-q_a^{-2} q_c^{-2} q_d^{-2}) |1-q_d^2|^2 \right. \\ &\quad + \left((1-q_c^2 q_d^2)^{-1} - (1-q_c^2 q_d^2 q_e^2)^{-1} \right) (1-q_a^{-2}) |1-q_d^2|^2 \\ &\quad - \left((1-q_d^2)^{-1} - (1-q_d^2 q_e^2)^{-1} \right) (1-q_a^2 q_b^2 q_c^2)^{-1} |1-q_d^2|^2 |1-q_a^2 q_c^2|^2 \\ &\quad \left. - \left((1-q_d^2 q_e^2)^{-1} - (1-q_c^2 q_d^2 q_e^2)^{-1} \right) (1-q_a^2 q_b^2 q_c^2 q_d^2 q_e^2)^{-1} |1-q_d^2|^2 |1-q_a^2 q_c^2 q_d^2 q_e^2|^2 \right] \\ &\quad F(a+c+d+1, b, d, c, e) F(\bar{a} + \bar{c} + \bar{d} + 1, \bar{b}, \bar{d}, \bar{c}, \bar{e}) \\ &- \left(\frac{1}{2}\right) q_{n_c} \left[\left((1-q_c^2 q_d^2)^{-1} - (1-q_c^2 q_d^2 q_e^2)^{-1} \right) (1-q_a^{-2}) |1-q_c^2 q_d^2|^2 \right. \end{aligned}$$

$$\begin{aligned}
& - \left((1 - q_d^2)^{-1} - (1 - q_d^2 q_e^2)^{-1} \right) (1 - q_a^2 q_b^2 q_c^2)^{-1} |1 - q_d^2|^2 |1 - q_a^2|^2 \\
& - \left((1 - q_d^2 q_e^2)^{-1} - (1 - q_c^2 q_d^2 q_e^2)^{-1} \right) (1 - q_a^2 q_b^2 q_c^2 q_d^2 q_e^2)^{-1} |1 - q_e^2|^2 |1 - q_a^2|^2 \Big] \\
& \quad F(a + c + d + 1, e, a, c, b) F(\bar{a} + \bar{c} + \bar{d} + 1, \bar{e}, \bar{a}, \bar{c}, \bar{b}) \\
- & \left(\frac{1}{4} \right) \left[\left((1 - q_c^2 q_d^2)^{-1} - (1 - q_c^2 q_d^2 q_e^2)^{-1} \right) (1 - q_a^{-2}) \right. \\
& \quad \left(q_c^{-1} (1 - q_c^2 q_d^2) (1 - q_d^{-2}) + q_c (1 - q_c^{-2} q_d^{-2}) (1 - q_d^2) \right) \\
& - \left((1 - q_d^2)^{-1} - (1 - q_d^2 q_e^2)^{-1} \right) (1 - q_a^2 q_b^2 q_c^2)^{-1} |1 - q_d^2|^2 \\
& \quad \left(q_c^{-1} (1 - q_a^2 q_c^2) (1 - q_a^{-2}) + q_c (1 - q_a^{-2} q_c^{-2}) (1 - q_a^2) \right) \\
& + \left((1 - q_d^2 q_e^2)^{-1} - (1 - q_c^2 q_d^2 q_e^2)^{-1} \right) (1 - q_a^2 q_b^2 q_c^2 q_d^2 q_e^2)^{-1} \\
& \quad \left((1 - q_d^2) (1 - q_a^2 q_c^2 q_d^2 q_e^2) q_c^{-1} q_d^{-2} (1 - q_e^{-2}) (1 - q_a^{-2}) \right. \\
& \quad \left. + (1 - q_d^{-2}) (1 - q_a^{-2} q_c^{-2} q_d^{-2} q_e^{-2}) q_c q_d^2 (1 - q_e^2) (1 - q_a^2) \right) \Big] \\
& \quad \left(F(a + c + d + 1, e, a, c, b) F(\bar{a} + \bar{c} + \bar{d} + 1, \bar{b}, \bar{d}, \bar{c}, \bar{e}) \right. \\
& \quad \left. + q_{n_c} F(a + c + d + 1, b, d, c, e) F(\bar{a} + \bar{c} + \bar{d} + 1, \bar{e}, \bar{a}, \bar{c}, \bar{b}) \right) \\
= & -\frac{1}{2} (\sin(\pi(a + b + c)) \sin(\pi(c + d + e)) \sin(\pi(a + b + c + d + e)))^{-1} \\
& \times [\sin(\pi b) \sin(\pi d) (\sin(\pi(2a + b + 3c + d + 2e)) - \sin(\pi(b + c + d + 2e))) \\
& \quad - \sin(\pi(2a + b + c + d)) + \sin(\pi(b + c + d)) + \sin(\pi(b - c - d)) \\
& \quad + \sin(\pi(-b - c + d))] F(a + c + d + 1, b, d, c, e) F(\bar{a} + \bar{c} + \bar{d} + 1, \bar{b}, \bar{d}, \bar{c}, \bar{e}) \\
& + q_{n_c} \sin(\pi a) \sin(\pi e) (\sin(\pi(a + 2b + 3c + 2d + e)) - \sin(\pi(a + c + 2d + e))) \\
& \quad - \sin(\pi(a + 2b + c + e)) + \sin(\pi(a + c + e)) + \sin(\pi(a - c - e)) \\
& \quad + \sin(\pi(-a - c + e))] F(a + c + d + 1, e, a, c, b) F(\bar{a} + \bar{c} + \bar{d} + 1, \bar{e}, \bar{a}, \bar{c}, \bar{b}) \\
& - 4 \sin(\pi a) \sin(\pi b) \sin(\pi d) \sin(\pi e) \sin(\pi(a + b + 2c + d + e)) \\
& \quad \left(F(a + c + d + 1, e, a, c, b) F(\bar{a} + \bar{c} + \bar{d} + 1, \bar{b}, \bar{d}, \bar{c}, \bar{e}) \right. \\
& \quad \left. + q_{n_c} F(a + c + d + 1, b, d, c, e) F(\bar{a} + \bar{c} + \bar{d} + 1, \bar{e}, \bar{a}, \bar{c}, \bar{b}) \right) \Big] .
\end{aligned}$$

It is apparent that the possible minus-signs q_{n_c} only effect the relation between the four major terms. Furthermore, we notice that the result is symmetric wrt the exchange of the holomorphic and antiholomorphic part.

This completes our calculation of the specific integral (3.26). Almost all integrals which appear in the second order deformation of two point functions in the $(2)^4$ Gepner model and orbifolds thereof are of this still relatively simple form. Hence, we were able to calculate the relevant integrals for the second order perturbation in these models for a given analytic regularisation. But, as already discussed in section 3.5.2, we have not succeeded in finding a suitable regularisation scheme which is at the same time effective and well-defined within the whole model and which would, thus, allow for a consistent renormalisation of the perturbed fields. This problem still remains to be solved.

Chapter 4

Higher rank indecomposable structures in augmented minimal models

The key feature of logarithmic conformal field theories as described in section 2.2 is the appearance of non-irreducible but indecomposable representations. Indeed, the action of the L_0 operator on the states of these representations can be cast in the indecomposable form of Jordan cells.

The logarithmic CFT models which are best understood up to now are certainly given by the extension of the minimal model series which we will introduce as “augmented $c_{p,1}$ minimal models” below [48, 49, 50, 45, 46, 47]. These models exhibit Virasoro representations with indecomposable structures up to rank 2 which have been constructed explicitly in [45].

In this chapter, we will show that these augmented $c_{p,1}$ minimal models are only special cases of the extension of general $c_{p,q}$ minimal models. These so-called “augmented $c_{p,q}$ minimal models” generically exhibit a much richer structure than the augmented $c_{p,1}$ models. In particular, they contain representations with Jordan cells up to rank 3 as well as several new types of rank 2 representations.

After an introduction to the terminology in section 4.1 we will investigate the augmented $c_{p,q}$ minimal models as representations of the Virasoro algebra using two different tools. First, we will explore the possibility of having nullvectors in higher rank indecomposable representations in section 4.2. Then, we will introduce the second tool in section 4.3, the explicit construction of the fusion product of two representations. In sections 4.4 and 4.5 we will apply this most powerful second tool to two special models, the augmented $c_{2,3} = 0$ and the augmented $c_{2,5} = -22/5$ model, respectively. This, finally, leads us to conjecturing the representation content and the fusion algebra for general augmented $c_{p,q}$ models in section 4.6. The appendices contain material to several explicit calculations in this chapter. Appendix A presents the explicit Jordan diagonalisation of L_0 in the three rank 3 representations which we discuss in this

chapter. Appendix B collects the explicitly calculated fusion rules in both models, the augmented $c_{2,3} = 0$ and $c_{2,5} = -22/5$ model. Finally, we present several examples of higher rank logarithmic nullvectors in appendix C.

4.1 What are augmented minimal models?

In this section we want to introduce the notion of “augmented minimal models” as one possible extension of the minimal model series. Thereby, we will keep our focus mainly on representations of only the Virasoro algebra.

Introducing augmented minimal models

In section 2.3.1 we have seen that already a small standard cell $\{(r, s) | 1 \leq r < q, 1 \leq s < p\}$ of the whole infinite Kac table suffices in order to describe the finite number of representations of a minimal model. In particular, this standard cell does not include weights on its border, i.e. weights which obey either $r = q$ or $s = p$. Furthermore, these weights on the border do not appear in any higher embedding structure of nullvectors in this minimal set of representations—they are simply ignored for minimal models.

Hence, the question arises what happens if we include states of weights on the border of the standard cell as irreducible representations in our theory. This, indeed, leads to consistent conformal field theory models, but with regard to representations of the Virasoro algebra the inclusion of these weights actually forces us to include representations of weights in the whole infinite Kac table into our model. We only retain the relation (2.12) which identifies two equal weights across the diagonal of the Kac table. Such models we call “augmented minimal models”.

Let us first make the terminology more precise. We will call weights whose indices obey $r = iq$ and $s = jp$ ($i, j \in \mathbb{Z}$) “on the corners of the Kac table” and weights whose indices obey (exclusively) either $r = iq$ or $s = jp$ ($i, j \in \mathbb{Z}$) “on the border of the Kac table”. All other weights which already appear in the minimal models we call “in the bulk of the Kac table”. An extract of the (infinite) Kac table for $c_{2,3} = 0$ is given in table 4.1. In this table we have indicated the border as areas with lighter shade and the corners as areas with darker shade; the bulk consists of the unshaded areas.

We also need to introduce the notion of a “weight chain” for conformal weights on the border or in the bulk. These weight chains are supposed to be a handy storage of information about the weights on successive embedding levels in the embedding structures of figure 2.1. A weight chain for weights on the border is a list of all weights which differ just by integers, ordered by size without multiplicity (see figure 2.1a):

$$\begin{aligned} W_{(r,p)}^{\text{border}} &:= \{h_{r,p}, h_{q-r,2p}, h_{r,3p}, \dots\} & \forall r < q, \\ W_{(q,s)}^{\text{border}} &:= \{h_{q,s}, h_{2q,p-s}, h_{3q,s}, \dots\} & \forall s < p. \end{aligned}$$

To form a weight chain for weights in the bulk we take a likewise list of weights differing just by integers, ordered by size without multiplicity. Then we map this list into a list

Table 4.1: Kac table for $c_{2,3} = 0$

		s				
		1	2	3	4	5
r	1	0	$\frac{5}{8}$	2	$\frac{33}{8}$	7
	2	0	$\frac{1}{8}$	1	$\frac{21}{8}$	5
	3	$\frac{1}{3}$	$-\frac{1}{24}$	$\frac{1}{3}$	$\frac{35}{24}$	$\frac{10}{3}$
	4	1	$\frac{1}{8}$	0	$\frac{5}{8}$	2
	5	2	$\frac{5}{8}$	0	$\frac{1}{8}$	1
	6	$\frac{10}{3}$	$\frac{35}{24}$	$\frac{1}{3}$	$-\frac{1}{24}$	$\frac{1}{3}$
	7	5	$\frac{21}{8}$	1	$\frac{1}{8}$	0
	8	7	$\frac{33}{8}$	2	$\frac{5}{8}$	0
	9	$\frac{28}{3}$	$\frac{143}{24}$	$\frac{10}{3}$	$\frac{35}{24}$	$\frac{1}{3}$
	10	12	$\frac{65}{8}$	5	$\frac{21}{8}$	1
	11	15	$\frac{85}{8}$	7	$\frac{33}{8}$	2

of sets, the first set just consisting of the lowest weight, then every next set consisting of the next two weights. Regarding figure 2.1b we get

$$W_{(r,s)}^{\text{bulk}} := \{h_{r,s}, \{h_{r,2p-s}, h_{q+r,p-s}\}, \{h_{r,2p+s}, h_{2q+r,s}\}, \dots\} \quad \forall r < q, s < p.$$

Of course, the nullvector embedding structure for irreducible representations corresponding to weights in the bulk stays the same as for the corresponding representations in the proper minimal models of section 2.3.1; one retains the same two string twisted picture of figure 2.1b. However, as already explained in [45] the nullvector embedding structure actually collapses to a string for representations with weights on the corners or the border—as depicted in figure 2.1a.

It is very important to keep in mind that the nullvectors corresponding to these higher weights in figure 2.1 are only true nullvectors within representations that are generated as a Virasoro module from one (!) singular vector, i.e. irreducible representations. This picture changes as soon as there appears indecomposable structure within the representation, as we will see shortly. Nevertheless, these vectors keep their prominent role even within higher rank representations.

Augmented $c_{p,1}$ models

The only well studied augmented models up to now are contained in the series $c_{p,1}$, $p = 2, 3, \dots$ (see e.g. [82, 45, 46, 44, 47, 49, 50]). These models have been observed to

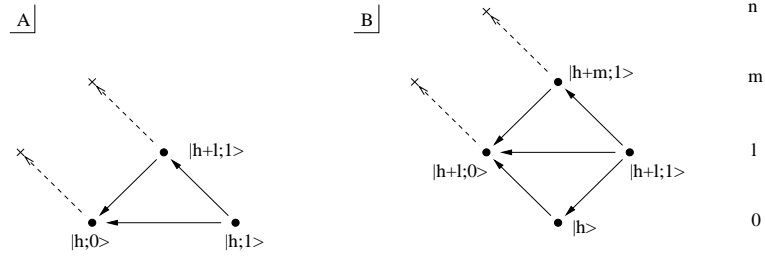


Figure 4.1: Rank 2 representations for weights on the border

contain representations with non-trivial Jordan blocks up to rank 2 and, thus, belong to the few examples of logarithmic CFTs. We just want to give a quick introduction to the higher rank representations appearing in these models.

First we need to observe that the $c_{p,1}$ models are quite exceptional representatives of the general augmented minimal models as they do not have any weights in their Kac table bulk. As described in [45], they consistently contain irreducible representations to all their weights on the corners and the border as well as two possible types of rank 2 Virasoro representations which, though, only appear for weights on the border.

We have depicted these two types of rank 2 representations in figure 4.1 following the graphical conventions of [45]. The black dots correspond either to generating fields, i.e. fields which are not describable as descendants of some other field, or to singular descendants of these which, although they are null in the module of their parent field, have a non-vanishing Shapovalov form with some other field of the whole higher rank representation. The crosses, on the other hand, represent true nullvectors of the whole higher rank representation. Finally, we take horizontal arrows to denote indecomposable action (of L_0), arrows pointing upwards to denote a descendant relation and arrows pointing downwards to denote a non-trivial action of positive Virasoro modes. Arrows towards a true nullvector are usually depicted as dashed. But as explained more thoroughly in section 4.2, nullvectors which are built in part on a Jordan cell field with higher Jordan level always have to contain contributions from descendants of fields with lower Jordan level as well, especially from descendants of the primary field. The corresponding arrows have to be understood in this way. Furthermore, we indicate the levels on the right or left hand side of each picture. The naming of the fields follows our convention of section 2.2.

Let us first describe the generic rank 2 representation which is shown as case **B** in figure 4.1. This representation is realised for every weight h on the border of the Kac table. The levels l , m and n given in the picture are just the successive levels of the respective weight chain of h . In order to see the translation to the notation of [45] let us denote (r, s) to be the Kac labels of the weight $h + l$. Now, the representation of type **B** has a primary groundstate $|h\rangle = \xi_{r,s}$. The first Jordan cell, however, only appears at the next weight in the weight chain at level l . This Jordan cell consists of the singular descendant of $|h\rangle$ at level l which we call $|h + l; 0\rangle = \phi_{r,s}$ as well as the

so-called “logarithmic partner” $|h+l;1\rangle = \psi_{r,s}$. As the notation already suggests, both fields are related by the indecomposable L_0 action

$$\begin{aligned} L_0 |h+l;1\rangle &= (h+l) |h+l;1\rangle + |h+l;0\rangle \\ L_0 |h+l;0\rangle &= (h+l) |h+l;0\rangle . \end{aligned}$$

Although the singular descendant $|h+l;0\rangle$ is a nullvector within the module generated by its parent field $|h\rangle$, it is promoted to be non-null by the inclusion of its logarithmic partner. Hence, $|h\rangle$ does not generate a proper irreducible (sub)representation, but $|h+l;0\rangle$ does—the next nullvector on $|h\rangle$, which appears at the next level m in the weight chain, is a proper one. There is, however, no nullvector yet at level m which incorporates descendants from the logarithmic partner $|h+l;1\rangle$. The first such nullvector is encountered even one level further up the weight chain, at level n .

Hence, we need two fields to generate this representation, the groundstate $|h\rangle$ and the logarithmic partner $|h+l;1\rangle$. The logarithmic partner, however, is not a primary state but is mapped to $|h\rangle$ by some polynomial of positive Virasoro modes. As argued in [45], if there is no additional singular vector on $|h\rangle$ on a level lower than l , this polynomial can be chosen as monomial such that

$$(L_1)^l |h+l;1\rangle = \beta |h\rangle \quad L_p |h+l;1\rangle = 0 \quad \forall p \geq 2 \quad (4.1)$$

for a constant β depending on the representation. Indeed, as there is only one singular descendant at level l we can use the freedom to redefine $|h+l;1\rangle$ by the addition of level l descendants of $|h\rangle$ to make the L_p action on $|h+l;1\rangle$ vanish for all $p \geq 2$. But, due to the fact that the first singular vector appears at level l , there is a unique $l-1$ descendant ξ^D of $|h\rangle = \xi_{r,s}$ with

$$(L_1)^{l-1} \xi^D = |h\rangle \quad L_p \xi^D = 0 \quad \forall p \geq 2 ; \quad (4.2)$$

these vanishing conditions reduce the number of length $l-1$ positive Virasoro monoms supposed to map this state to zero by one (actually $(L_1)^{l-1}$ is excluded). Hence, we have exactly as many vanishing conditions as free parameters for a possible descendant field, not counting the overall normalisation. As there is no singular state at this level, the equations have only one solution. The freedom of normalisation can then be used to fix the $(L_1)^{l-1}$ action. On the other hand, the state $L_1 |h+l;1\rangle$ also fulfils the requirement that it vanishes under the action of L_p for all $p \geq 2$. We have just seen that such a state is unique and, thus, it follows that

$$L_1 |h+l;1\rangle = \beta \xi^D$$

for some constant β . Now, we have used up all freedom to define $|h+l;1\rangle$ with the exception of adding multiples of $|h+l;0\rangle$. But as $|h+l;0\rangle$ is a singular descendant this does not effect any of the mappings with positive Virasoro modes. Therefore, β is the unique and defining parameter of the representation.

The second type of rank 2 representation is depicted in figure 4.1 **A**. It is a degenerate version of case **B** where the Jordan cell appears at the first weight of a border weight chain. In this case, we cannot have a groundstate at a lower weight, but the two generating states of the representation are just the two Jordan cell states $|h; 0\rangle = \phi_{1,s}$ and $|h; 1\rangle = \psi_{1,s}$. Hence, we also do not need an additional parameter β . $|h; 0\rangle$ is primary and generates an irreducible subrepresentation; $|h; 1\rangle = \psi_{1,s}$ is now what we call “logarithmic primary”, i.e. primary with the exception of the indecomposable action of L_0 (see section 2.2).

But as these $c_{p,1}$ models do not contain any bulk in their Kac table, we do not expect them to be generic. In order to understand the generic features of general augmented $c_{p,q}$ models we will study the two easiest candidates for augmented models with non-empty bulk of the Kac table in the following sections of this chapter, the augmented $c_{2,3} = 0$ model as well as the augmented Yang-Lee model with $c_{2,5} = -22/5$. And indeed, the existence of representations with weights in the Kac table bulk induces an even richer structure with indecomposable representations up to rank 3.

For the $c_{p,1}$ models it was shown that they actually have a larger \mathcal{W} algebra as symmetry algebra, the triplet algebra $\mathcal{W}(2, 2p - 1, 2p - 1, 2p - 1)$. We have strong hints that such a larger \mathcal{W} algebra is also the underlying symmetry algebra of the generic augmented $c_{p,q}$ models [135]. The effective Kac table of these theories with enlarged symmetry algebra can then again be reduced to a standard cell, which is larger than their minimal model counterpart, though. This standard cell is given by $\{(r, s) | 1 \leq r < nq, 1 \leq s < np\}$ with n usually an odd integer larger than 1, e.g. 3 for the above mentioned triplet algebras of the $c_{p,1}$ models. In this thesis, however, we want to concentrate mainly on the pure Virasoro representation theory and, hence, do not restrict our Kac table in any way if not stated otherwise.

4.2 Exploring logarithmic nullvectors

In this section we explain how to calculate logarithmic nullvectors, i.e. nullvectors in higher rank representations which also involve descendants of higher Jordan levels. We present logarithmic nullvectors in different kinds of higher rank representations.

We first review logarithmic nullvectors in representations of arbitrary rank where the Jordan cell lies on the lowest weight level and give a clarifying proof of the equations present in the literature [82]. We then discuss and give explicit new results for rank 2 logarithmic nullvectors in augmented $c_{p,1}$ models with the more general setup of a first Jordan cell at arbitrary level. This is shown to be in accordance with the rank 2 representations of the augmented $c_{p,1}$ models known in the literature. We finally present a survey of logarithmic nullvectors in possible rank 2 representations of the above mentioned types in the general augmented $c_{2,3} = 0$ model. In this way, we can put severe constraints on the possible rank 2 representations appearing in the augmented $c_{2,3} = 0$ model which we show to be in accordance with the findings of the fusion calculation in section 4.4.

The results of this section as well as the corresponding appendix C have already been published in [136].

4.2.1 Jordan cells on lowest weight level

Let us recall the construction of nullvectors in a logarithmic representation in which the states of the Jordan cell are all lowest weight states [57, 58, 82]. We will especially clarify the respective procedure in [82] and give a proof of the proposed logarithmic nullvector conditions.

We want to construct vectors which are null on the whole logarithmic representation. Following [82] we choose the general ansatz

$$|\chi_{h,c}^{(n)}\rangle = \sum_{j=0}^{r-1} \sum_{|\mathbf{n}|=n} b_j^{\mathbf{n}}(h, c) L_{-\mathbf{n}} |h; \partial_\theta^j a(\theta)\rangle \quad (4.3)$$

with $a(\theta) = \sum_{i=0}^{r-1} a_i \frac{1}{i!} \theta^i$ and the usual multi-index notation for the modes $L_{\mathbf{n}}$. Choosing the states $|h; j\rangle$ instead of $|h; \partial_\theta^j a(\theta)\rangle$ on the right hand side would have yielded the same generality of the ansatz and in the end the same set of solutions. We prefer this special ansatz, however, for two reasons. First of all it already incorporates our knowledge that in this form of logarithmic representations there will only be a non-trivial action of the L_0 modes in the end of the nullvector calculation and that this is given by derivatives wrt θ onto lower ranks. This justifies the ∂_θ^j part of the ansatz. On the other hand, by including lower orders of θ^i into $a(\theta)$ we solve for nullvectors of lower rank subrepresentations at the same time. For this we will always treat the a_m as arbitrary parameters.

Now, we can calculate the level n nullvector conditions for arbitrary k and \mathbf{n}_l , $|\mathbf{n}_l| = n$, as follows (the index l indicates a suitable enumeration of the multi-indices \mathbf{n}):

$$\begin{aligned} & \langle h; r-1-k | L_{\mathbf{n}_l} |\chi_{h,c}^{(n)}\rangle \\ &= \sum_{j=0}^{r-1} \sum_{|\mathbf{n}|=n} b_j^{\mathbf{n}}(h, c) \sum_{m=j}^{r-1} a_m \langle h; r-1-k | L_{\mathbf{n}_l} L_{-\mathbf{n}} |h; m-j\rangle \\ &= \sum_{j=0}^{r-1} \sum_{|\mathbf{n}|=n} \sum_{m=j}^{r-1} a_m b_j^{\mathbf{n}}(h, c) \langle h; r-1-k | \sum_{t=0}^{m-j} \frac{1}{t!} \left(\frac{\partial^t}{\partial h^t} f_{\mathbf{n}_l, \mathbf{n}}(h, c) \right) |h; m-j-t\rangle \\ &= \sum_{m=0}^{r-1} a_m \sum_{j=0}^m \sum_{|\mathbf{n}|=n} \sum_{t=0}^{m-j} b_j^{\mathbf{n}}(h, c) \frac{1}{t!} \left(\frac{\partial^t}{\partial h^t} f_{\mathbf{n}_l, \mathbf{n}}(h, c) \right) \\ & \quad \times \left(\delta_{t, m-j-k} + \sum_{s=0}^{m-j-k-1} \delta_{s,t} D_{m-j-k-s} \right) \end{aligned}$$

$$=: \sum_{m=0}^{r-1} a_m \mathcal{A}'_{\mathbf{n}_l}(m, k), \quad (4.4)$$

where in the second step we used (2.11) due to the logarithmic primarity of the Jordan cell ground states $|h; m\rangle$ as well as in the third step the Shapovalov form (2.10). As we want to keep the a_m as arbitrary parameters the nullvector conditions on $|\chi_{h,c}^{(n)}\rangle$ are equivalent to the identical vanishing of all $\mathcal{A}'_{\mathbf{n}_l}(m, k)$.

Let us calculate the terms proportional to $\delta_{t,m-j-k}$ in $\mathcal{A}'_{\mathbf{n}_l}(m, k)$ first:

$$\begin{aligned} & \sum_{j=0}^m \sum_{|\mathbf{n}|=n} \sum_{t=0}^{m-j} b_j^{\mathbf{n}}(h, c) \frac{1}{t!} \left(\frac{\partial^t}{\partial h^t} f_{\mathbf{n}_l, \mathbf{n}}(h, c) \right) \delta_{t,m-j-k} \\ &= \sum_{j=0}^{m-k} \sum_{|\mathbf{n}|=n} b_j^{\mathbf{n}}(h, c) \frac{1}{(m-k-j)!} \left(\frac{\partial^{m-k-j}}{\partial h^{m-k-j}} f_{\mathbf{n}_l, \mathbf{n}}(h, c) \right) \\ &=: \mathcal{A}_{\mathbf{n}_l}(m-k). \end{aligned}$$

It is important to notice that the $\mathcal{A}_{\mathbf{n}_l}(m-k)$ indeed only depend on the difference $m-k$.

We now show that the vanishing of the $\mathcal{A}_{\mathbf{n}_l}(m-k)$ is necessary and already sufficient for the vanishing of the nullvector conditions in (4.4) by using complete induction over $m-k$. For $m-k=0$ we trivially find $\mathcal{A}'_{\mathbf{n}_l}(m, k) = \mathcal{A}_{\mathbf{n}_l}(m-k)$. This can easily be inferred from (4.4) noting that in the fourth line the summation over t actually only runs from 0 to $m-j-k$, consequently the one over j only from 0 to $m-k$. On the other hand we find for general $m-k$

$$\begin{aligned} & \mathcal{A}'_{\mathbf{n}_l}(m, k) - \mathcal{A}_{\mathbf{n}_l}(m-k) \\ &= \sum_{j=0}^m \sum_{|\mathbf{n}|=n} \sum_{t=0}^{m-j-k-1} b_j^{\mathbf{n}}(h, c) \frac{1}{t!} \left(\frac{\partial^t}{\partial h^t} f_{\mathbf{n}_l, \mathbf{n}}(h, c) \right) D_{m-j-k-t} \\ &= \sum_{j=0}^{m-k-1} \sum_{|\mathbf{n}|=n} \sum_{t=j}^{m-k-1} b_j^{\mathbf{n}}(h, c) \frac{1}{(t-j)!} \left(\frac{\partial^{t-j}}{\partial h^{t-j}} f_{\mathbf{n}_l, \mathbf{n}}(h, c) \right) D_{m-k-t} \\ &= \sum_{t=0}^{m-k-1} D_{m-k-t} \sum_{|\mathbf{n}|=n} \sum_{j=0}^t b_j^{\mathbf{n}}(h, c) \frac{1}{(t-j)!} \left(\frac{\partial^{t-j}}{\partial h^{t-j}} f_{\mathbf{n}_l, \mathbf{n}}(h, c) \right) \\ &= \sum_{t=0}^{m-k-1} D_{m-k-t} \mathcal{A}_{\mathbf{n}_l}(t). \end{aligned}$$

But this vanishes due to the induction assumption $\mathcal{A}_{\mathbf{n}_l}(t) = 0$ for all $t < m-k$. Hence, the vanishing of $\mathcal{A}'_{\mathbf{n}_l}(m, k)$ is equivalent to the vanishing of $\mathcal{A}_{\mathbf{n}_l}(m-k)$ and therefore the statement is proven.

Now, if we regard these calculations with a_{r-1} as the only non-vanishing parameter, we see that we still retain the whole set of conditions, $\mathcal{A}_{\mathbf{n}_l}(r-1-k) = 0$ for all $k = 0, \dots, r-1$. On the other hand, taking another a_i with $i < r-1$ as the only non-vanishing parameter automatically yields the respective set of conditions for a rank $i+1$ nullvector, a nullvector of a rank $i+1$ logarithmic subrepresentation. This indeed justifies our chosen ansatz as well as keeping the parameters a_m arbitrary.

Furthermore, this calculation shows that any nullvector wrt a (logarithmic or irreducible) representation is automatically a nullvector to any larger logarithmic representation containing the former one as a subrepresentation.

The third fact we would like to stress is that, generically, the nullvector of some rank r logarithmic representation is not a pure descendant of the Jordan cell state with rank index r , but always contains descendants of the other Jordan cell states with lower rank index, including the groundstate of the irreducible representation.

4.2.2 Logarithmic nullvectors for $c_{p,1}$

Already for the well-studied $c_{p,1}$ models, however, the representations with Jordan cells on the lowest level analysed in the preceding section are not the end of the story but rather only very special cases [45]. For the generic rank 2 logarithmic representations in these models one needs a generalised way of calculating logarithmic nullvectors, which we will develop in the following.

The ansatz

As described in section 4.1 there are two possible types of rank 2 Virasoro representations appearing in the augmented $c_{p,1}$ models which we depict in figure 4.1.

The case of a Jordan cell built solely on logarithmic primary fields which we discussed in section 4.2.1 corresponds to case **A** in figure 4.1. This case is, though, just the exceptional case for the lowest rank 2 representation of a border weight chain; it only appears with a Jordan cell on the lowest weight of this chain.

The generic rank 2 representation which is shown as case **B** in figure 4.1, however, requires a more general ansatz of logarithmic nullvectors. Loosing the prerequisite of logarithmic primarity of all Jordan cell fields we cannot assume that only polynomials in the Virasoro null-mode and the central charge operator contribute to the matrix elements in the calculation of the nullvector conditions — we now have to take into account operators $(L_{-1}L_1)^j$, $j > 0$, as well. Hence, the relation between the nullvector polynomials on the different Jordan cell states is not governed by the action of L_0 and, thus, derivatives by θ alone. An ansatz of the form (4.3) is not reasonable any more.

Instead, we propose the more general ansatz for the generic rank 2 representation

$$|\chi_{h,c}^{(n)}\rangle = \sum_{|\mathbf{n}|=n-l} b_1^{\mathbf{n}}(h,c) L_{-\mathbf{n}} |h+l;1\rangle + \sum_{|\mathbf{m}|=n} b_0^{\mathbf{m}}(h,c) L_{-\mathbf{m}} |h\rangle. \quad (4.5)$$

Here we choose a notation close to section 4.2.1 describing a state by its weight and enumerating Jordan cell states according to the L_0 action

$$L_0|h;n\rangle = h|h;n\rangle + (1 - \delta_{n,0})|h;n-1\rangle .$$

The ansatz (4.5) certainly incorporates general level $n-l$ descendants of $|h+l;0\rangle$ as $|h+l;0\rangle$ is just a level l singular descendant of $|h\rangle$ itself. However, we need this more general ansatz (4.5) because building descendants only on the Jordan cell states we would miss out several states of the rank 2 representation which are descendants of level n of $|h\rangle$, but cannot be written as descendants of $|h+l;0\rangle$.

This ansatz leads to the following complete set of nullvector conditions

$$\begin{aligned} 0 &\stackrel{!}{=} \langle h+l;1|L_{\mathbf{n}_i}|\chi_{h,c}^{(n)}\rangle \\ &= \sum_{|\mathbf{n}|=n-l} b_1^{\mathbf{n}}(h,c) \langle h+l;1|L_{\mathbf{n}_i}L_{-\mathbf{n}}|h+l;1\rangle + \sum_{|\mathbf{m}|=n} b_0^{\mathbf{m}}(h,c) \langle h+l;1|L_{\mathbf{n}_i}L_{-\mathbf{m}}|h\rangle \\ &= \sum_{|\mathbf{n}|=n-l} b_1^{\mathbf{n}}(h,c) \langle h+l;1|F_{\mathbf{n}_i,\mathbf{n}}^{(1)}(L_{-1}^l L_1^l, L_0, C)|h+l;1\rangle \\ &\quad + \sum_{|\mathbf{m}|=n} b_0^{\mathbf{m}}(h,c) \langle h+l;1|F_{\mathbf{n}_i,\mathbf{n}}^{(2)}(L_{-1}^l, L_{-1}^l L_0^s, L_{-1}^l C^t)|h\rangle \end{aligned} \quad (4.6)$$

as well as

$$\begin{aligned} 0 &\stackrel{!}{=} \langle h|L_{\mathbf{m}_j}|\chi_{h,c}^{(n)}\rangle \\ &= \sum_{|\mathbf{n}|=n-l} b_1^{\mathbf{n}}(h,c) \langle h|L_{\mathbf{m}_j}L_{-\mathbf{n}}|h+l;1\rangle + \sum_{|\mathbf{m}|=n} b_0^{\mathbf{m}}(h,c) \langle h|L_{\mathbf{m}_j}L_{-\mathbf{m}}|h\rangle \\ &= \sum_{|\mathbf{n}|=n-l} b_1^{\mathbf{n}}(h,c) \langle h|F_{\mathbf{m}_j,\mathbf{n}}^{(3)}(L_1^l, L_0^s L_1^l, C^t L_1^l)|h+l;1\rangle \\ &\quad + \sum_{|\mathbf{m}|=n} b_0^{\mathbf{m}}(h,c) \langle h+l;1|F_{\mathbf{m}_j,\mathbf{n}}^{(4)}(L_0, C)|h\rangle , \end{aligned} \quad (4.7)$$

for any $s, t > 0$. Several remarks are necessary. The functions $F^{(1)}, \dots, F^{(4)}$ indicate what polynomials of Virasoro generators we can reduce the interior of the above matrix elements to by successively using the Virasoro algebra, the level matching condition as well as properties of the states which these modes are applied to. Although we are not able to reduce these to polynomials solely of L_0 and C as in section 4.2.1, these properties make possible a fair amount of reduction to functions which are polynomials only of specific combinations of the four operators L_{-1}, L_0, L_1 and C . More specifically the function $F^{(2)}$ actually only depends on terms proportional to $L_{-1}^l, L_{-1}^l L_0, L_{-1}^l L_0^2, \dots$ as well as $L_{-1}^l C, L_{-1}^l C^2, \dots$. This follows from the fact that to the right this function acts on a primary field, to the left however on a field which vanishes under the action of $L_p, p \geq 2$, and whose weight is just at level l above $|h\rangle$.

As discussed earlier, we do not retain such nice interrelations between the nullvector polynomials as in section 4.2.1 which could be cast into the θ calculus. But we can still find remnants of such relations as e.g. by looking at the nullvector conditions given by the application of level n descendants of $|h+l;0\rangle$ onto the nullvector ansatz

$$\begin{aligned}
0 &\stackrel{!}{=} \langle h+l;0|L_{\mathbf{n}_j}|\chi_{h,c}^{(n)}\rangle \\
&= \sum_{|\mathbf{n}|=n-l} b_1^{\mathbf{n}}(h,c) \langle h+l;0|L_{\mathbf{n}_j} L_{-\mathbf{n}}|h+l;1\rangle + \sum_{|\mathbf{m}|=n} b_0^{\mathbf{m}}(h,c) \langle h+l;0|L_{\mathbf{n}_j} L_{-\mathbf{m}}|h\rangle \\
&= \sum_{|\mathbf{n}|=n-l} b_1^{\mathbf{n}}(h,c) \langle h+l;0|F_{\mathbf{n}_j,\mathbf{n}}^{(1)}(L_{-1}^l L_1^l, L_0, C)|h+l;1\rangle \\
&\quad + \sum_{|\mathbf{m}|=n} b_0^{\mathbf{m}}(h,c) \langle h+l;0|F_{\mathbf{n}_j,\mathbf{n}}^{(2)}(L_{-1}^l, L_{-1}^l L_0^s, L_{-1}^l C^t)|h\rangle \\
&= \sum_{|\mathbf{n}|=n-l} b_1^{\mathbf{n}}(h,c) \langle h+l;0|F_{\mathbf{n}_j,\mathbf{n}}^{(1)}(L_{-1}^l L_1^l, L_0, C)|h+l;1\rangle. \tag{4.8}
\end{aligned}$$

These conditions are clearly a subset of the conditions (4.7) as $|h+l;0\rangle$ is just a descendant of $|h\rangle$. Now we make use of the Shapovalov form (2.10) to deduce that the only terms contributing to the matrix elements in (4.8) can come from contributions of $F_{\mathbf{n}_j,\mathbf{n}}^{(1)}(L_{-1}^l L_1^l, L_0, C)|h+l;1\rangle$ which are proportional to $|h+l;1\rangle$. But then we can insert these vanishing equations back into (4.6) concluding that the terms in (4.6) proportional to D_1 (of the Shapovalov form) already vanish on their own — a consequence of a subset of the relations (4.7). This is a reminiscence of the fact that in section 4.2.1 the conditions $\mathcal{A}'_{\mathbf{n}_i}(m,k)$ can be split into the conditions $\mathcal{A}_{\mathbf{n}_i}(m-k)$ which only depend on the difference $m-k$. Hence, we can conclude that any logarithmic nullvector of the proposed kind does not depend on the constants of the Shapovalov form.

Implementation on the computer

Now, one can put the Virasoro-algebraic calculations on the computer and solve the resulting equations for possible logarithmic nullvectors.

We have implemented these calculations in C++ using the computer algebra package GiNaC [134]. We constructed new classes for the algebraic objects fields, fieldmodes, products of fieldmodes as well as descendant fields. The implemented Virasoro relations (as well as possibly further commutation relations) are used for direct simplification of descendant fields towards the normal ordered standard form as soon as these are constructed. It is important to note that within the procedure the application of modes to the field has priority to the commutation of modes in order to reduce the blow-up of the number of terms within the calculation.

The calculation of matrix elements is performed in two steps. First, all fieldmodes within the matrix elements are used to construct a descendant state on the ket-state which is then automatically simplified (see above). Then the correct coefficients are picked using the properties of the bra-state as well as the Shapovalov form.

The main property which has to be implemented into the fields, besides their conformal weight (and possibly fermion number), is their behaviour under the action of non-negative Virasoro modes. We picked conformal primary as the standard and implemented deviations from that in a list which is pointed to by a member of each instance. E.g. for calculations of representation type **B** (see figure 4.1) we had to implement the indecomposable L_0 action as well as the non-vanishing L_1 action which maps $|h; 1\rangle$ to the unique level $(l - 1)$ descendant of $|h - l\rangle$ with properties (4.2).

Results

We have calculated the above logarithmic nullvector equations for the $c_{2,1} = -2$ representation $\mathcal{R}_{2,1}$ with lowest lying vector $\xi_{2,1}$ at $h = 0$ and Jordan cell $(\phi_{2,1} = L_{-1}\xi_{2,1}, \psi_{2,1})$ at $h = 1$, a representation of type **B** (see figure 4.1). We found the following first nontrivial logarithmic nullvector at level 6 (above the lowest lying vector)

$$\begin{aligned} & \left(m_1 L_{-1}^6 + m_2 L_{-2} L_{-1}^4 + m_3 L_{-3} L_{-1}^3 + \left(\frac{16}{3} - 4m_1 + \frac{16}{3}\beta - 2m_2 \right) L_{-2}^2 L_{-1}^2 \right. \\ & \quad \left. + (-12 - 12m_1 + 6\beta) L_{-4} L_{-1}^2 + \left(-\frac{20}{3} - 2m_3 - 16m_1 - \frac{56}{3}\beta - 2m_2 \right) L_{-3} L_{-2} L_{-1} \right. \\ & \quad \left. + \left(\frac{4}{3} - 16m_1 + \frac{10}{3}\beta - 2m_2 \right) L_{-5} L_{-1} - 8\beta L_{-4} L_{-2} + 6\beta L_{-3}^2 - 4\beta L_{-6} \right) \xi_{2,1} \\ & + \left(L_{-1}^5 - 10L_{-2} L_{-1}^3 + 6L_{-3} L_{-1}^2 + 16L_{-2}^2 L_{-1} - 12L_{-4} L_{-1} - 8L_{-3} L_{-2} + 4L_{-5} \right) \psi_{2,1}. \end{aligned}$$

This level is indeed the expected one as the Kac table of $c_{2,1} = -2$ gives us a third nullvector condition for $h = 0$ exactly at level 6 as well as a corresponding second nullvector condition for $h = 1$ at level 5. Hence, we confirm the existence of a further nontrivial nullvector at the expected level in the logarithmic rank 2 representation $\mathcal{R}_{2,1}$ derived by different means in [45].

We notice that up to the overall normalisation of this state the nullvector polynomial applied to the second Jordan cell state $\psi_{2,1}$ is unique. On the other hand, the nullvector polynomial on $\xi_{2,1}$, which serves as a correction to the effects of the indecomposable action on $\psi_{2,1}$, still exhibits three degrees of freedom. But, we know that there is an ordinary nullvector at level 2 above $h = 1$ in the irreducible subrepresentation whose descendants span a parameter space of dimension three at level 5 (above $h = 1$). Adding such a descendant of this nullvector will certainly not alter our equations and, hence, accounts for the additional three degrees of freedom m_i , $i = 1, 2, 3$.

In the same manner, one can calculate logarithmic nullvectors in all rank 2 logarithmic representations in the $c_{p,1}$ models, limited only by computer power and memory. We give a second example for a type **B** logarithmic nullvector in appendix C.1.

4.2.3 Possible logarithmic nullvectors for $c_{2,3} = 0$

The $c_{p,1}$ models might be the best-studied logarithmically conformal models but they still are quite special cases of the general augmented $c_{p,q}$ models, which we still know

much less about. Hence, an even more exciting question than the above construction of predicted logarithmic nullvectors surely is whether one can use these techniques to explore the shapes of the supposedly more complicated logarithmic representations in general augmented CFTs. In the following we will attack this question for the augmented model $c_{2,3} = 0$ which seems sufficiently generic to show all the features of general augmented $c_{p,q}$ models.

Due to the underlying enhanced \mathcal{W} symmetry all possible types of representations can already be found within the restricted Kac table area $\{(r, s) | 1 \leq r < 3q, 1 \leq s < 3\}$ in the augmented $c_{p,1}$ case. For the remaining part of this section it, thus, seems useful to restrict our attention to the restricted Kac table area $\{(r, s) | 1 \leq r < 3q, 1 \leq s < 3p\}$ for the general augmented $c_{p,q}$ models as well.

Weights on the corners and borders of the augmented Kac table of $c_{2,3} = 0$

We propose that fields associated to weights on the corner and the borders of the augmented Kac table of $c_{2,3} = 0$ are contained in the same types of representations as the corresponding ones in the $c_{p,1}$ models.

Within the above restricted Kac table area the weights on the corners, $h = -1/24, 35/24$, only appear once modulo the relations (2.12) and accordingly only exhibit the usual two nullvector conditions. Hence, there are no new (logarithmic) representations to be expected besides the ordinary irreducible Virasoro representation built on ground-states with these weights. Indeed, these weights give exactly the prelogarithmic fields which have been shown to be primary and to generate an irreducible representation, but not to admit an embedding into any larger indecomposable representation [137].

The weights on the borders of the Kac table actually appear in the same kind of triplets of two equal conformal weights and one which is shifted by some positive integer as we know it from the $c_{p,1}$ models (again modulo the relations (2.12)). The triplets are $T_1 := \{1/8, 1/8, 33/8\}$, $T_2 := \{5/8, 5/8, 21/8\}$ and $T_3 := \{1/3, 1/3, 10/3\}$. We also find the same nullvector structure concerning these weights within the Kac table as we know it from the corresponding representations of the $c_{p,1}$ models. Hence, we have checked the existence of the typical logarithmic nullvectors for all cases which were accessible to computer power and memory.

First we have checked for the first logarithmic nullvector in representation type **A** (see figure 4.1) and found the expected ones for all three triplets, on level 8 for T_1 , on level 10 for T_2 as well as on level 9 for T_3 . The result for T_1 can be found in appendix C.2.

A check for the first logarithmic nullvector in representation type **B** was only possible for the triplet T_2 . In this case, we have a Jordan cell for $h = 21/8$ with a lower lying field at $h = 1/8$. We find the first nontrivial logarithmic nullvector at level 16 which seems to be just at the limit of our current computing power and ability. The first logarithmic nullvectors for type **B** representations corresponding to the other two triplets are expected at even higher levels, at 18 and 20 for T_3 resp. T_1 .

These results are indeed compatible with our above proposition and a nice and

nontrivial check for its validity.

Weights in the bulk of the augmented Kac table of $c_{2,3} = 0$

For possible logarithmic representations corresponding to weights in the bulk of the Kac table, however, we do not have any prototypes yet. Hence, we are now going to explore the main candidates for such representations and elaborate constraints on their shapes using our techniques of constructing logarithmic nullvectors. We notice two main differences to the situation on the borders.

First of all, the bulk of the augmented Kac table of $c_{2,3} = 0$ (see table 4.1) exhibits an even higher abundance of equal numbers (up to integer shift) than in the $c_{p,1}$ models, which is a clear sign of logarithmic representations there. Up to the relations (2.12) and within the restricted Kac table area of consideration we find a nonuplet $N = \{0, 0, 0, 1, 1, 2, 2, 5, 7\}$ of weights which are equal up to integer shift and which contain one weight with triple degeneracy, $h = 0$. It does not seem very likely that this nonuplet just splits into three triplets of the types analysed above. On the contrary, the analysis of the corresponding modular functions even suggests the possibility of a rank 3 logarithmic representation, and certainly predicts the existence of several more complicated rank 2 logarithmic representations constructed with weights within this set [135].

On the other hand, we have to notice that the embedding structure for nullvectors is different in the bulk in contrast to the linear embedding structure on the border (discussed in [45]). In the bulk the embedding structure is given by the more generic two string twisted picture, depicted in figure 2.1b.

Now, inspecting the nonuplet N of bulk weights we expect the usual irreducible representations to the integer weights $h = 0, 1, 2, 5, 7$ as well as rank 2 representations corresponding to Jordan cells at weight $h = 0, 1, 2$. We have depicted a list of possible candidates for rank 2 representations corresponding to these bulk weights in figure 4.2. These pictures represent the low lying embedding structure of these candidates using the same symbols as in section 4.2.2. Additionally, we have indicated the conformal weight on the different levels to the left of each picture as well as the unknown higher embedding structure by question marks (“?”). We have checked for the lowest nontrivial logarithmic nullvectors for all these candidates and summarise the results in table 4.2.

Type C. The calculations for the type **C** representations have been performed using the methods of section 4.2.1. For this type we even managed to calculate one rank 3 logarithmic nullvector; i.e. the first rank 3 logarithmic nullvector with lowest weight Jordan cell at $h = 0$ appears at level 12.

Type E. We were able to apply the procedure of section 4.2.2 directly to the type **E** representation because we do not encounter any additional nullvector below the level of the Jordan cell and because we can take $(L_0 - 1)$ to map $|1; 1\rangle$ to a proper singular descendant of $|0\rangle$, i.e. $L_{-1}|0\rangle$.

Type F. In case of the type **F** representation we actually encounter an additional

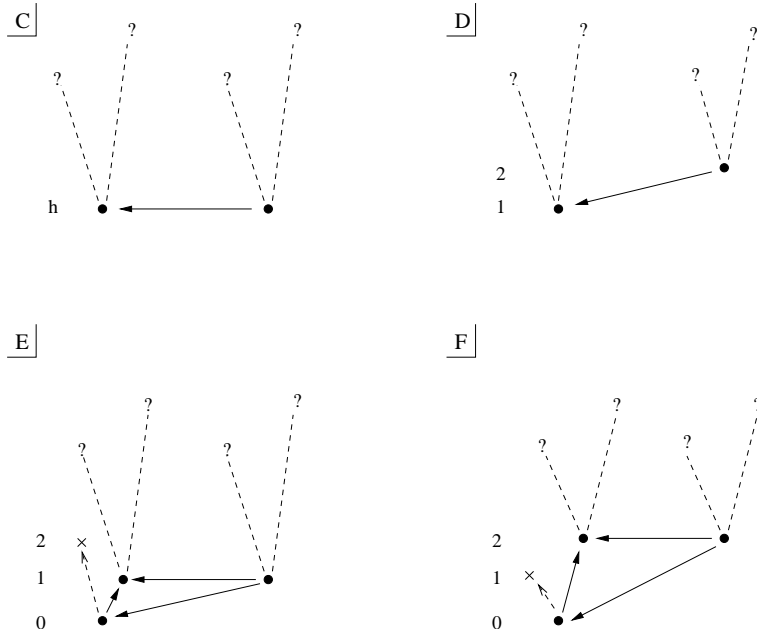


Figure 4.2: Candidates for rank 2 representations for weights in the bulk of $c = 0$

Table 4.2: Lowest logarithmic nullvectors of candidates for bulk representations

type	lowest weight	rank	level of lowest logarithmic nullvector
C	0	2	5
C	1	2	11
C	2	2	10
C	0	3	12
D	1	2	> 14
E	0	2	12
F	0	2	12

nullvector below the level of the Jordan cell. This can, however, be remedied quite easily. Due to the lower lying nullvector at level 1 there is no state which L_1 could map $|2; 1\rangle$ to. But certainly L_2 can take the job to map $|2; 1\rangle$ directly down to $|0\rangle$, a mapping unique up to normalisation. This yields the new conditions

$$L_2|2; 1\rangle = \beta |0\rangle \quad L_p|2; 1\rangle = 0 \quad \text{for } p = 1 \text{ and } p \geq 3.$$

The singular descendant in the Jordan cell is therefore given by $|2; 0\rangle = L_{-2}|0\rangle$.

This feature of an additional nullvector below the level of the Jordan cell clearly shows the novelty of the bulk representations in contrast to the ones on the border described in [45]; it arises due to the more intricate embedding structure for these bulk representations compared to the embedding structure for representations on the border. A generalisation to similar cases with additional nullvectors on levels lower than the Jordan cell seems straightforward though more tedious due to the more complex embedding structure of nullvectors which are not on the “nice” level 1.

Type D. The case of the type **D** representation is more questionable. Here, we actually do not have a singular descendant of $|1\rangle$ on the level of the Jordan cell, hence no primary state which $(L_0 - 2)$ could map $|2; 1\rangle$ to. A priori it is not clear whether it is necessary for L_0 to map $|2; 1\rangle$ to a singular descendant of $|1\rangle$. Hence we took $(L_0 - 2)$ to map $|2; 1\rangle$ to the only existing descendant of $|1\rangle$ at level 1 which is though not singular, i.e. $L_{-1}|1\rangle$. The results of possible logarithmic nullvectors, however, do not seem to offer a particular rich structure up to the accessible levels (see table 4.2).

We include the explicit results for the two cases **E** and **F** in appendix C.3. It is quite interesting to inspect e.g. the result for type **F**. Although we actually did not impose the relation $L_{-1}|0\rangle = 0$ into the computer programme, the result incorporates such a nullvector or, to be a bit more cautious, at least the independence of the result from this particular descendant; indeed, all descendants of $L_{-1}|0\rangle$ just appear with free parameters. This corresponds to the additional freedom due to lower nullvectors in the irreducible subrepresentation discussed in the end of section 4.2.2. On the other hand, the second singular vector on $|0\rangle$ on level 2 does not pop up in the same manner as a possible nullvector in this result; rather, the result is consistent with our ansatz where we actually impose that the level 2 singular vector on $|0\rangle$ is not a nullvector for the whole rank 2 representation. Hence, we take the first observation of the independence from $L_{-1}|0\rangle$ as a strong hint that a representation where both these singular descendants are not null in the whole logarithmic representation is not favoured by our calculations.

4.3 How to calculate fusion products

An even more powerful tool to gain information about a consistent set of representations which form a conformal field theory model is given by the fusion product analysis. Our calculation of fusion products is based on an algorithm first developed by W. Nahm [67] to prove that the fusion of quasirational representations contains only finitely

many quasirational subrepresentations and, hence, that the category of quasirational representations is stable. In [45] this algorithm was generalised. They also described a procedure how one can use this algorithm to get (computationally usually sufficient) constraints to fix the field content of the fusion product at a given level.

In this section we want to give a short summary of the Nahm algorithm and the procedure described in [45]. We will then present the specific properties of our particular implementation. The next three sections will apply this method to the two general augmented models at central charge $c_{2,3} = 0$ and $c_{2,5} = -22/5$ and give a conjectured generalisation of the resulting higher rank representations and fusion rules to arbitrary augmented $c_{p,q}$ models.

Most of the results in sections 4.3 to 4.6 as well as the corresponding appendices A and B are based on work already published in [138].

4.3.1 The Nahm algorithm

The nice and short presentation of the Nahm algorithm in [45] relies on the coproduct formula. For a holomorphic field of conformal weight h and mode expansion

$$S(w) = \sum_{l \in \mathbb{Z}+h} w^{l-h} S_{-l}$$

it is given by [64, 139]

$$\begin{aligned} \Delta_{z,\zeta}(S_n) &= \sum_{m=1-h}^n \binom{n+h-1}{m+h-1} \zeta^{n-m} (S_m \otimes \mathbb{1}) \\ &\quad + \epsilon \sum_{l=1-h}^n \binom{n+h-1}{l+h-1} z^{n-l} (\mathbb{1} \otimes S_l) \\ &= \tilde{\Delta}_{z,\zeta}(S_n) \quad \forall n \geq 1-h \\ \Delta_{z,\zeta}(S_{-n}) &= \sum_{m=1-h}^{\infty} \binom{n+m-1}{m+h-1} (-1)^{m+h-1} \zeta^{-(n+m)} (S_m \otimes \mathbb{1}) \\ &\quad + \epsilon \sum_{l=n}^{\infty} \binom{l-h}{n-h} (-z)^{l-n} (\mathbb{1} \otimes S_{-l}) \quad \forall n \geq h \\ \tilde{\Delta}_{z,\zeta}(S_{-n}) &= \sum_{m=n}^{\infty} \binom{m-h}{n-h} (-\zeta)^{m-n} (S_{-m} \otimes \mathbb{1}) \\ &\quad + \epsilon \sum_{l=1-h}^{\infty} \binom{n+l-1}{l+h-1} (-1)^{l+h-1} z^{-(n+l)} (\mathbb{1} \otimes S_l) \quad \forall n \geq h, \end{aligned}$$

where $\epsilon = -1$ if both S_m and the first field in the tensor product it is applied to are fermionic and $\epsilon = +1$ otherwise. Furthermore, z and ζ are the positions of the two fields of the tensor product which this fused operator is applied to. Due to the symmetry

of the fusion product there are two alternative ways of writing the comultiplication, denoted $\Delta_{z,\zeta}$ and $\tilde{\Delta}_{z,\zeta}$. Demanding that both $\Delta_{z,\zeta}$ and $\tilde{\Delta}_{z,\zeta}$ actually yield the same result we get the fusion space of two representations \mathcal{H}_i at positions z_i , $i = 1, 2$,

$$\mathcal{H}_1 \otimes_f \mathcal{H}_2 := (\mathcal{H}_1 \otimes \mathcal{H}_2) / (\Delta_{z_1, z_2} - \tilde{\Delta}_{z_1, z_2}).$$

Remember that \otimes_f denotes the fusion product of two representations.

In this chapter we will only look at representations wrt the Virasoro algebra $\mathcal{A}(L)$ which is generated by the modes L_n of the $h(L) = 2$ Virasoro field L . We need the following subalgebras

$$\begin{aligned} \mathcal{A}_-^0(L) &:= \langle L_{-n} | 0 < n < h(L) \rangle \\ \mathcal{A}_{--}(L) &:= \langle L_{-n} | n \geq h(L) \rangle \\ \mathcal{A}_{\pm}(L) &:= \langle L_n | \pm n > 0 \rangle \end{aligned}$$

as well as the subalgebra of words with length of at least n

$$\mathcal{A}_n(L) = \left\langle \prod_{j=1}^m L_{-l_j}^{k_j} \mid \sum_{j=1}^m k_j l_j \geq n \right\rangle.$$

The essential information about a representation \mathcal{H} is already encoded in its “special subspace”, the quotient space

$$\mathcal{H}^s := \mathcal{H} / (\mathcal{A}_{--}(L) \mathcal{H}).$$

We also need the family of filtrations of \mathcal{H} given as quotient spaces

$$\mathcal{H}^n := \mathcal{H} / (\mathcal{A}_{n+1}(L) \mathcal{H}).$$

Especially for irreducible \mathcal{H} this space is equal to the set of descendants up to level n .

We want to restrict to a certain type of representations, the “quasirational representations”. We use the definition of a quasirational representation that it is a representation with finite special subspace. For quasirational representations of the Virasoro algebra it has been shown that [67, 45]

$$(\mathcal{H}_1 \otimes_f \mathcal{H}_2)^n \subset \mathcal{H}_1^s \otimes \mathcal{H}_2^n \quad \wedge \quad (\mathcal{H}_1 \otimes_f \mathcal{H}_2)^n \subset \mathcal{H}_1^n \otimes \mathcal{H}_2^s. \quad (4.9)$$

The proof uses the following Nahm algorithm which can be shown to map every state of the tensor product $\mathcal{H}_1^i \otimes \mathcal{H}_2^j$ to a state in the respective right hand side in (4.9) in a finite number of steps.

We present the algorithm only for the first equation in (4.9) as the other version works the same way by symmetry of the fusion product. In the following, we regard the states of the tensor product to be at positions $(z_1, z_2) = (1, 0)$. The two steps of the Nahm algorithm are then given by:

(A1) A vector $\psi_1 \otimes \psi_2 \in \mathcal{H}_1 \otimes \mathcal{H}_2$ is rewritten in the form

$$\psi_1 \otimes \psi_2 = \sum_i \psi_1^i \otimes \psi_2^i + \Delta_{1,0}(\mathcal{A}_{n+1}(L)) (\mathcal{H}_1 \otimes \mathcal{H}_2)$$

with $\psi_1^i \in \mathcal{H}_1^s$. This can be achieved by the following recursive procedure.

The crucial step is to use the nullvector conditions on ψ_1 to re-express it in the form

$$\psi_1 = \sum_j \psi_j^s + \sum_k \mathcal{A}_{--} \chi_k^s,$$

with $\psi_j^s, \chi_k^s \in \mathcal{H}_1^s$. We still need to get rid of the \mathcal{A}_{--} action on the χ_k^s . We use the following formula derived from the comultiplication formula and its translation properties for $m \leq n$ [45]

$$\begin{aligned} (L_{-m} \otimes \mathbb{1}) &= \sum_{l=m}^n \binom{l-h}{m-h} \Delta_{1,0}(L_{-l}) \\ &\quad - \epsilon \sum_{l=1-h}^{\infty} \binom{m+l-1}{m-h} (-1)^{h-m-1} (\mathbb{1} \otimes L_l) + \Delta_{1,0}(\mathcal{A}_{n+1}(L)). \end{aligned}$$

This formula actually enables us to replace the $(L_{-m} \otimes \mathbb{1})$ action in $\mathcal{A}_{--} \chi_k^s \otimes \psi_2$ by terms where \mathcal{A}_- or even the identity acts on the left hand vector of the tensor product. This is true as in the range $m \leq l \leq n$ the comultiplication $\Delta_{1,0}(L_{-l})$ is actually of the simple form $\mathcal{A}_-^0 \otimes \mathbb{1} + \mathbb{1} \otimes \mathcal{A}_{--}$. Now we have to take the result and repeat this procedure starting again with the re-expression of the first fields ψ_1 in the tensor product. A simple count of the strictly decreasing level of modes during the iteration shows that this algorithm has to terminate [67].

(A2) This step has to be applied to each term of the resulting sum from step (A1) separately. The input, a resulting tensor product from (A1) $\psi_1 \otimes \psi_2 \in \mathcal{H}_1^s \otimes \mathcal{H}_2$, is rewritten as

$$\psi_1 \otimes \psi_2 = \sum_t \psi_1^t \otimes \psi_2^t + \Delta_{1,0}(\mathcal{A}_{n+1}(L)) (\mathcal{H}_1 \otimes \mathcal{H}_2),$$

where now $\psi_1^t \in \mathcal{A}_-^0 \mathcal{H}_1^s$ and $\psi_2^t \in \mathcal{H}_2^n$.

This is achieved by repeatedly using

$$\Delta_{1,0}(L_{-I}) = (\mathbb{1} \otimes L_{-I}) + \sum_k c_k (\mathcal{A}_-^0 \otimes L_{-I_k})$$

for a word $L_{-I} = L_{-i_1} L_{-i_2} \dots$ of negative Virasoro modes with level $|I|$ and constant c_k . This recursion has to finish as the Virasoro monomials L_{-I_k} are of strictly lower level $|I_k| < |I|$. This formula is just the result of repeated use of the comultiplication formula for a monomial of modes of the same field and for the special coordinates $(z, \zeta) = (1, 0)$.

As we want to have the states in the fusion product which are projected to the subspace $(\mathcal{H}_1 \otimes_f \mathcal{H}_2)^n$ we do not have to care about contributions $\Delta_{1,0}(\mathcal{A}_{n+1}(L))(\mathcal{H}_1 \otimes \mathcal{H}_2)$. It is then easy to see that iterated application of steps (A1) and (A2) will finally yield the required result (4.9). This algorithm terminates in a finite number of steps as the number of modes on both fields strictly decreases when re-expressing ψ_1 in step (A1) using its nullvector condition and does not increase in step (A2).

4.3.2 Constraints for the fusion algebra

By (4.9) we know that $(\mathcal{H}_1 \otimes_f \mathcal{H}_2)^n$ is actually embedded in the easily constructed space $\mathcal{F} := \mathcal{H}_1^s \otimes \mathcal{H}_2^n$. Hence, we want to find the full set of constraints which describes $(\mathcal{H}_1 \otimes_f \mathcal{H}_2)^n$ in \mathcal{F} .

The important idea of [45] was that one can find nontrivial constraints by applying \mathcal{A}_{n+1} to states in \mathcal{F} . We then have to use the Nahm algorithm in order to map the resulting descendant states into our “standard” space \mathcal{F} . By definition these descendant states are divided out of $(\mathcal{H}_1 \otimes_f \mathcal{H}_2)^n$ and, hence, are supposed to vanish. Thus, their mapping to \mathcal{F} should evaluate to zero—if we acquire non-trivial expressions this simply yields the desired constraints by imposing their vanishing.

This procedure is even improved if we use the nontrivial nullvector conditions on the second field to replace the action of certain Virasoro monomials before performing the Nahm algorithm. This introduces the information about the nullvector structure on the second representation of the tensor product into the game; the information about the nullvector structure on the first representation of the tensor product has already been used in the Nahm algorithm itself.

As we noticed during our calculation it even improves the situation to include the nullvector conditions on the tensor factors in the space \mathcal{F} itself.

In the following we will denote the level n at which we perform the computation with L . Certainly, one cannot perform this calculation for all of \mathcal{A}_{L+1} . We, hence, restricted our computation to the application of Virasoro monomials

$$\left\langle \prod_{j=1}^m L_{-l_j}^{k_j} \mid \sum_{j=1}^m k_j l_j = \tilde{L} \right\rangle.$$

of equal level \tilde{L} . Usually we performed the calculation from $\tilde{L} = L + 1$ up to a maximal \tilde{L}_{\max} . Both L and \tilde{L}_{\max} are given for the respective calculations in the appendix.

As we are limited to the calculation of a finite number of constraints this procedure is only able to give a lower bound on the number of constraints and, hence, an upper bound on the number of states in the fusion product at that level. On the other hand, these constraints seem to be highly non-trivial such that already a very low $\tilde{L}_{\max} > L$, often even $\tilde{L}_{\max} = L + 1$, is sufficient to gain all constraints which yield representations in a consistent fusion algebra. This already worked very well in [45] for the $c_{p,1}$ model case and as we will see it also works very well in the general augmented $c_{p,q}$ model case.

Now, it is especially interesting to observe the action of positive Virasoro modes on $(\mathcal{H}_1 \otimes_f \mathcal{H}_2)^L$. The positive Virasoro modes, however, induce an action

$$L_m : (\mathcal{H}_1 \otimes_f \mathcal{H}_2)^L \rightarrow (\mathcal{H}_1 \otimes_f \mathcal{H}_2)^{L-m} \quad \forall m \leq L .$$

It is important to note that the L_m map to a space of respective lower maximal level. Hence, we need to construct all spaces of lower maximal level $0 \leq n < L$. To achieve this we start with $(\mathcal{H}_1 \otimes_f \mathcal{H}_2)^L$ and successively impose the constraints which arise in the above described way from the vanishing of the action of Virasoro monomials of level m with $n < m \leq L$ on \mathcal{F} .

4.3.3 Implementation for the $c_{p,q}$ models

As in section 4.2.2 we have implemented the main calculational tasks, especially the Nahm algorithm and the calculation of the constraints, in C++ using the computer algebra package GiNaC [134]. As basic ingredients in this algorithm we could again use the classes for the algebraic objects fields, fieldmodes, products of fieldmodes and descendant fields as well as the automatic evaluation method of the descendant fields described in section 4.2.2. We also constructed a new class for tensor products of fields.

As GiNaC does not support factorisation we used the JordanForm package of the computer algebra system Maple in order to get the Jordan diagonal form of the L_0 matrix on the resulting space as well as the matrices of base change. This Maple calculation is performed via command-line during the run of the C++ programme.

As we see in section 4.1 some irreducible representations in the general augmented $c_{p,q}$ models have more than one nullvector (two, to be precise) which are completely independent, i.e. such that none of these nullvectors can be written as a descendant of the others. Hence, it is important to include both independent nullvectors into the nullvector lists which are used for replacements in the calculation as explained above. This is needed to provide the full information about the nullvector structure of the original representations which are to be fused. Sometimes one even needs to choose an \tilde{L}_{\max} large enough such that the second nullvector can also become effective. The special subspace, however, is nevertheless determined by the level l of the lowest nullvector

$$\langle \psi, L_{-1}\psi, L_{-1}^2\psi, \dots, L_{-1}^{l-1}\psi \rangle .$$

Besides the fusion of two irreducible representations we also implemented the possibility of fusing an irreducible representation with a rank 2 representation. Actually, this generalisation is quite straight forward. Instead of one state which generates an irreducible representation we now need two generating states. However, we have to be careful because the second generating state, the logarithmic partner, is not primary. Hence, we implemented the indecomposable action on this second generating field as additional conditions proprietary to that field (as already done in section 4.2). We also have to be careful to calculate the correct nullvector structure which includes besides

an ordinary nullvector on the primary field the first logarithmic nullvector of the whole indecomposable representation. We have calculated these logarithmic nullvectors using the algorithm of section 4.2.

In order to speed up the algorithm we widely used hashing tables. This measure actually resulted in a quite equal use of computing time and memory (on a standard PC with up to 4GB memory); calculations which are on the edge of using up the memory have run times between half a day and a few days.

The performance of the implemented algorithm is, however, quite hard to benchmark as it varies very much with different input and output. Concerning the input the computing time rises with the level of the nullvectors—especially, the nullvector level of the first tensor factor is crucial. We also need much more time to compute fusion products with representations on weights that are strictly rational than corresponding ones with integer weights. And then, the performance of course depends exponentially on L as well as \tilde{L} , although the dependence on L is much stronger. Concerning the output the computational power of Maple is frequently the limiting factor if we have a large resulting L_0 matrix.

We have also checked the correct implementation of the algorithm by reproducing quite some fusion rules of the $c_{p,1}$ models given in [45]. In particular, we reproduced the Virasoro matrices for the example given in the appendix of [45]. We also noted that the algorithm is very sensitive and fragile such that an only small change in the parameters or the programme yields completely unreasonable results.

In contrast to the lowest $c_{p,1}$ models we have to cover a much larger parameter space with states of higher nullvectors already for the easiest general augmented $c_{p,q}$ model, the augmented $c_{2,3} = 0$ model. We, hence, decided to calculate the fusion of the lowest representations at $L = 6$ in order to be able to get results at the same L for a large parameter space. For the higher fusion as well as the fusion with rank 2 representations we had to reduce L . Details as well as the results are given in appendix B.

4.4 Fusion analysis of the augmented $c_{2,3} = 0$ model

In this section we explicitly discuss our calculations of the fusion product of representations in the $c_{2,3} = 0$ augmented model which lead us to the conjectured general fusion rules of section 4.6. We present examples for the newly appearing higher rank representations and also elaborate the consistency conditions for the fusion product in this case.

4.4.1 Higher rank representations

Representations of rank 2

Table 4.3 presents an overview over the specific properties of all rank 2 representations we have calculated for this model. In our notation, the two parameters of the rank 2

Table 4.3: Specific properties of rank 2 representations in $c_{2,3} = 0$

	β_1	β_2	level of log. partner	level of first nullvector	level of first log. nullvector	type
$\mathcal{R}^{(2)}(5/8, 5/8)$	–	–	0	2	10	A
$\mathcal{R}^{(2)}(1/3, 1/3)$	–	–	0	3	9	A
$\mathcal{R}^{(2)}(1/8, 1/8)$	–	–	0	4	8	A
$\mathcal{R}^{(2)}(5/8, 21/8)$	–5	–	2	10	16	B
$\mathcal{R}^{(2)}(1/3, 10/3)$	140/27	–	3	9	18	B
$\mathcal{R}^{(2)}(1/8, 33/8)$	–700/81	–	4	8	20	B
$\mathcal{R}^{(2)}(0, 1)_5$	1/3	–	1	2	7	G
$\mathcal{R}^{(2)}(0, 1)_7$	–1/2	–	1	2	5	H
$\mathcal{R}^{(2)}(0, 2)_5$	–	–5/8	2	1	7	I
$\mathcal{R}^{(2)}(0, 2)_7$	–	5/6	2	1	5	K
$\mathcal{R}^{(2)}(1, 5)$	2800/9	–	4	6	14	G
$\mathcal{R}^{(2)}(1, 7)$	30800/27	1100/9	6	4	14	I
$\mathcal{R}^{(2)}(2, 5)$	–420	–	3	5	10	H
$\mathcal{R}^{(2)}(2, 7)$	–880	–440/3	5	3	10	K

representation $\mathcal{R}^{(2)}$ give the lowest weight and the weight of the logarithmic partner in this representation, i.e. the weights of the two states which generate this representation. The additional index will be explained when we discuss these particular representations (see p. 122). Analogously, we denote an irreducible representation generated by a highest weight state of weight h by $\mathcal{V}(h)$.

The first block contains the rank 2 representations to the three different weight chains lying on the border of the Kac table, i.e. $W_{(1,2)}^{\text{border}} := \{5/8, 21/8, 85/8, \dots\}$, $W_{(3,1)}^{\text{border}} := \{1/3, 10/3, 28/3, \dots\}$ and $W_{(2,2)}^{\text{border}} := \{1/8, 33/8, 65/8, \dots\}$. There are two different types of rank 2 representations which exhibit precisely the same structure as the rank 2 representations of the augmented $c_{p,1}$ models described in section 4.1. They can, hence, be described by the same pictures in figure 4.1 **A** and **B**. This has already been conjectured in section 4.2 by calculation of their first logarithmic nullvectors.

The first three representations in table 4.3 are the groundstate rank 2 representation visualised in figure 4.1 **A**. They exhibit an indecomposable Jordan cell already on the zeroth level. In this case the logarithmic partner state $|h; 1\rangle$ of the irreducible ground state $|h; 0\rangle$ is logarithmic primary, i.e. it is primary with the exception of an indecomposable action of L_0

$$L_0|h; 1\rangle = h|h; 1\rangle + |h; 0\rangle .$$

$|h; 0\rangle$ actually spans an irreducible subrepresentation; its first nullvector (depicted as a cross in the figure) is hence found on the level of the next weight $h+l$ in the corresponding weight chain. The descendants of $|h; 1\rangle$, however, do not form to give a nullvector

at $h+l$. In order to find the first nullvector involving descendants of $|h; 1\rangle$ we have to go one weight further in the weight chain. These representations are uniquely generated by the two groundstates $|h; i\rangle$, $i = 0, 1$; there is no need of an additional parameter to describe them.

The next three representations in table 4.3 are the first excited representations of these three weight chains depicted in figure 4.1 **B**. The logarithmic partner state $|h+l; 1\rangle$ lies on that level l at which we would expect the first nullvector of the groundstate $|h\rangle$ if the groundstate were to span an irreducible representation. Hence, the subrepresentation generated by $|h\rangle$ is not irreducible, but only indecomposable. Actually the indecomposable action of L_0 just maps $|h+l; 1\rangle$ to the singular l descendant of $|h\rangle$ which we call $|h+l; 0\rangle$ and which normally would be the first nullvector of an irreducible h representation

$$L_0|h+l; 1\rangle = (h+l)|h+l; 1\rangle + |h+l; 0\rangle.$$

$|h+l; 0\rangle$, on the other hand, spans an irreducible subrepresentation and yields its first nullvector on the level of the second weight after h in the weight chain, called $h+m$. In order to find the first logarithmic nullvector we have to go even one weight further in the weight chain to $h+n$. Certainly, the logarithmic partner field cannot be logarithmic primary; but as discussed in [45] it can still be made to at least vanish under all L_p , $p > 2$. This induces one characteristic parameter $\beta = \beta_1$ in this representation due to the action of L_1 ; we take β to parameterise the following equation (see section 4.1 for a more detailed explanation)

$$(L_1)^l |h+l; 1\rangle = \beta |h\rangle.$$

The structure visualised in figure 4.1 **B** is actually thought to be the generic type of rank 2 representation for weights on the border. It should be found for every two adjacent weights in a border weight chain. As in the $c_{p,1}$ model case the representations of the type depicted in figure 4.1 **A** can only be found for the first and hence lowest weight of a weight chain. We have also successfully checked for the existence of the first logarithmic nullvectors at the levels given in table 4.3 using the algorithm of [136]. Even the level 20 logarithmic nullvector was now accessible to our computational power due to our explicit knowledge of β .

The second block of table 4.3 contains the specific properties of the lowest rank 2 representations which we found for weights in the weight chain of the Kac table bulk, i.e. $W_{(1,1)}^{\text{bulk}} := \{\{0\}, \{1, 2\}, \{5, 7\}, \dots\}$. There are four different types of rank 2 representations depicted in figure 4.3 which appear to be a generalisation of the situation on the border for the case of figure 4.1 **B**. This generalisation has to take into account the more complicated embedding structure of representations with weights in the bulk—the linear picture of figure 2.1a has to be replaced by the two string twisted picture of figure 2.1b. As we now have two possible nullvectors on every step of the weight chain, of which only one is rendered non-null by the existence of a logarithmic partner state of the same level, we actually also encounter cases **I** and **K** where there is

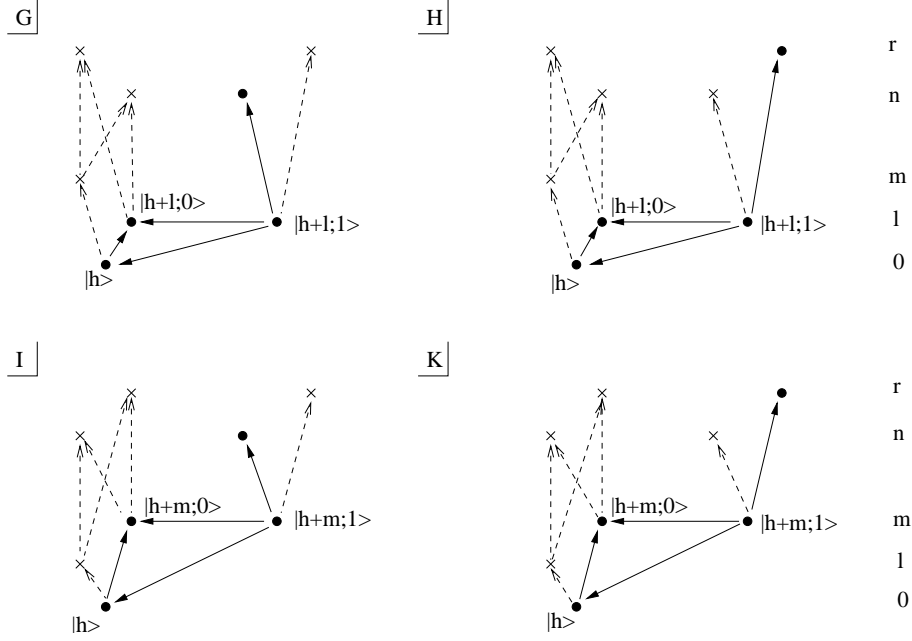


Figure 4.3: Rank 2 representations for weights in the bulk

a true nullvector on a level lower than the logarithmic partner state. This is new and makes the description of these particular cases more complicated.

Let us first describe the cases **G** and **H**. Starting with the lowest weight state $|h\rangle$ the first possible nullvectors are given by the next set in the weight chain at levels l and m . In the present cases the corresponding singular descendant $|h+l;0\rangle$ on $|h\rangle$ at the lower of these two levels l is rendered to be non-null by the existence of a logarithmic partner state $|h+l;1\rangle$. The indecomposable action of L_0 on $|h+l;1\rangle$ is again given by

$$L_0|h+l;1\rangle = (h+l)|h+l;1\rangle + |h+l;0\rangle.$$

Furthermore, the argument of section 4.1 still applies that due to the absence of a nullvector on $|h\rangle$ on a level lower than the Jordan cell we can transform $|h+l;1\rangle$ by the addition of level l descendants of $|h\rangle$ such that it is annihilated by $L_p \forall p \geq 2$. Then L_1 maps $|h+l;1\rangle$ to the unique level $l-1$ descendant of $|h\rangle$ which is annihilated by $L_p \forall p \geq 2$. As for representations with weights on the border we take the resulting one parameter $\beta = \beta_1$ to parameterise the equation

$$(L_1)^l |h+l;1\rangle = \beta |h\rangle.$$

The second state corresponding to this set in the weight chain, the one at level m , actually stays null in the rank 2 representation. This fixes the nullvector structure on $|h\rangle$ as the embedding structure of figure 2.1 b tells us that the nullvectors of the next set in the weight chain, at levels n and r , are joint descendants of the states corresponding

to the previous set of weights. But as the singular state at level m is already a nullvector the singular states at level n and r have to be null as well. The situation is somewhat different for the descendants of the logarithmic partner as $|h+l; 1\rangle$ is the starting point of its embedding structure. The cases **G** and **H** correspond to the two possibilities of having the first logarithmic nullvector on level r respectively n . There is, however, no additional nullvector at the respective other weight. Examples for the case **G** are $\mathcal{R}^{(2)}(0, 1)_5$ and $\mathcal{R}^{(2)}(1, 5)$, for the case **H** $\mathcal{R}^{(2)}(0, 1)_7$ and $\mathcal{R}^{(2)}(2, 5)$. Again, the lowest representations play a special role as both cases are realised for lowest weight 0. Hence, we indicate the level of the logarithmic descendant which is promoted to be non-null as an index. It is important to note, however, that both cases are already distinguished by their different β values.

Let us turn to the cases **I** and **K**. These exhibit very much the same structure as the cases **G** and **H**. The crucial difference is the existence of a nullvector already on a level lower than the level of the logarithmic partner. This fact prevents us from applying the above argument how to describe the representation by only one parameter. The special cases of $\mathcal{R}^{(2)}(0, 2)_5$ and $\mathcal{R}^{(2)}(0, 2)_7$ can nevertheless be reduced to one parameter quite easily. As there is no non-null descendant of the lowest weight state $|0\rangle$ at level 1 the only positive Virasoro mode which can map the logarithmic partner $|2; 1\rangle$ to a non-zero state is L_2 . Hence, we take the one parameter $\beta = \beta_2$ to parameterise the equation

$$L_2 |2; 1\rangle = \beta |0\rangle .$$

This behaviour is, however, not generic. We find that we need at least two parameters to describe these two kinds of rank 2 representations in general. To see this let us regard all normal ordered monomials in Virasoro modes of length m . We are able to transform $|h+m; 1\rangle$ by addition of level m descendants of $|h\rangle$ in such a way that only the application of two such Virasoro monomials does not annihilate $|h+m; 1\rangle$. In particular we have:

- For $\mathcal{R}^{(2)}(1, 7)$ we find the two parameters $\beta_1 = 30800/27$ and $\beta_2 = 1100/9$ parameterising

$$\begin{aligned} (L_1)^6 |7; 1\rangle &= \beta_1 |1\rangle \\ (L_1)^3 L_3 |7; 1\rangle &= \beta_2 |1\rangle . \end{aligned}$$

$\mathcal{R}^{(2)}(1, 7)$ has been parameterised in such a way that the monomials $(L_1)^6$ and $(L_1)^3 L_3$ are the only ones with a non-trivial action on $|7; 1\rangle$. This yields the following mappings of single Virasoro modes

$$\begin{aligned} L_1 |7; 1\rangle &= \frac{11}{729} \left(\frac{857}{2} L_{-5} - 473 L_{-4} L_{-1} - 721 L_{-3} L_{-2} + \frac{4279}{12} L_{-3} L_{-1}^2 \right. \\ &\quad \left. + \frac{809}{2} L_{-2}^2 L_{-1} - \frac{1295}{12} L_{-2} L_{-1}^3 \right) |1\rangle \\ L_2 |7; 1\rangle &= 0 \end{aligned}$$

$$\begin{aligned} L_3 |7; 1\rangle &= \frac{275}{324} (L_{-1}^3 + 12 L_{-2} L_{-1} - 24 L_{-3}) |1\rangle \\ L_p |7; 1\rangle &= 0 \quad \forall p \geq 4. \end{aligned}$$

- For $\mathcal{R}^{(2)}(2, 7)$ the two parameters are $\beta_1 = -880$ and $\beta_2 = -440/3$ parameterising

$$\begin{aligned} (L_1)^5 |7; 1\rangle &= \beta_1 |2\rangle \\ (L_1)^2 L_3 |7; 1\rangle &= \beta_2 |2\rangle. \end{aligned}$$

This yields the following mappings of single Virasoro modes

$$\begin{aligned} L_1 |7; 1\rangle &= \frac{5}{17} \left(-\frac{143}{3} L_{-4} + \frac{44}{3} L_{-3} L_{-1} + \frac{49}{3} L_{-2}^2 - 6 L_{-2} L_{-1}^2 \right) |2\rangle \\ L_2 |7; 1\rangle &= 0 \\ L_3 |7; 1\rangle &= -\frac{20}{3} \left(L_{-1}^2 - \frac{3}{2} L_{-2} \right) |2\rangle \\ L_p |7; 1\rangle &= 0 \quad \forall p \geq 4. \end{aligned}$$

In both cases L_3 maps $|h + m; 1\rangle$ to a multiple of the unique descendant of $|h\rangle$ on level $l - 1$ which is annihilated by $L_p \forall p \geq 2$.

We conjecture that it actually suffices to have two parameters in order to characterise rank 2 representations of type **I** and **K**. As we have a nullvector already on the lower level l this unique state on level $m - 1$ which is annihilated by $L_p \forall p \geq 2$ is a descendant of this nullvector. Hence, we want to lift the restrictions by incorporating one further non-zero mapping, the mapping by $L_{m-(l-1)}$ to the unique state on level $l - 1$ which is annihilated by $L_p \forall p \geq 2$, in order to ensure that we do not map into pure descendants of the lower nullvector. This is, indeed, equivalent to demanding that the application of all normal ordered positive Virasoro monomials of length m annihilates $|h + m; 1\rangle$ except for L_1^m and $L_1^{l-1} L_{m-(l-1)}$.

For all bulk rank 2 representations listed in table 4.3 we were able to see the level of the first logarithmic nullvector already in the calculated fusion spectrum. We also confirmed this lowest logarithmic nullvector using the algorithm of section 4.2. It is remarkable to see that for the bulk rank 2 representations $\mathcal{R}^{(2)}(0, 1)_i$ and $\mathcal{R}^{(2)}(0, 2)_i$, $i = 5, 7$, we encounter the first nullvectors already on lower levels than the ones proposed in section 4.2.3. However, the solutions in section 4.2.3 are given for general β ; it is only for the special β s in table 4.3 that we encounter solutions even on lower levels.

Representations of rank 3

Representations of rank 3 only appear for weights in the bulk. In the following we will discuss the four lowest examples explicitly.

$\mathcal{R}^{(3)}(\mathbf{0}, \mathbf{0}, \mathbf{1}, \mathbf{1})$: Although we only encounter a rank 3 indecomposable structure in this representation, we nevertheless need four states to generate it. We will see that this is

Table 4.4: Number of states for $\mathcal{R}^{(3)}(0, 0, 1, 1)$

level	number of states			total number of state	new null subrepresentations
	Jordan level 0	Jordan level 1	Jordan level 2		
0	1	1	–	2	–
1	2	1	1	4	–
2	3	1	1	5	1
3	5	2	2	9	–
4	8	3	3	14	–
5	11	5	4	20	2
6	17	7	6	30	–
7	23?	11?	8?	42?	2

necessary and natural by two different ways of visualising the nullvector structure of $\mathcal{R}^{(3)}(0, 0, 1, 1)$. The explicit Jordan form of the L_0 action on $\mathcal{R}^{(3)}(0, 0, 1, 1)$ is given in appendix A.1.

The first way starts out with the Jordan diagonalisation of the representation and is shown in figure 4.4 \mathbf{L}_1 . We have two groundstates $|0; i\rangle$, $i = 0, 1$, at level 0 which are interrelated by the rank 2 indecomposable action of L_0

$$L_0 |0; 1\rangle = |0; 0\rangle \quad L_0 |0; 0\rangle = 0 .$$

On level 1, the level of the first possible nullvector on $|0; i\rangle$, the Jordan cell is enhanced to rank 3

$$\begin{aligned} L_0 |1; 2\rangle &= |1; 2\rangle + |1; 1\rangle \\ L_0 |1; 1\rangle &= |1; 1\rangle + |1; 0\rangle \\ L_0 |1; 0\rangle &= |1; 0\rangle . \end{aligned}$$

A further fourth state of weight 1 decouples in the L_0 action

$$L_0 |1; 3\rangle' = |1; 3\rangle' ;$$

but this seeming decoupling is deceiving as the singular descendant of $|0; 1\rangle$ is actually composed of the sum of the Jordan cell state $|1; 1\rangle$ and the “decoupling” state $|1; 3\rangle'$; indeed the action of L_{-1} on $|0; i\rangle$, $i = 0, 1$, is given by

$$\begin{aligned} L_{-1} |0; 0\rangle &= |1; 0\rangle \\ L_{-1} |0; 1\rangle &= |1; 1\rangle + |1; 3\rangle' . \end{aligned}$$

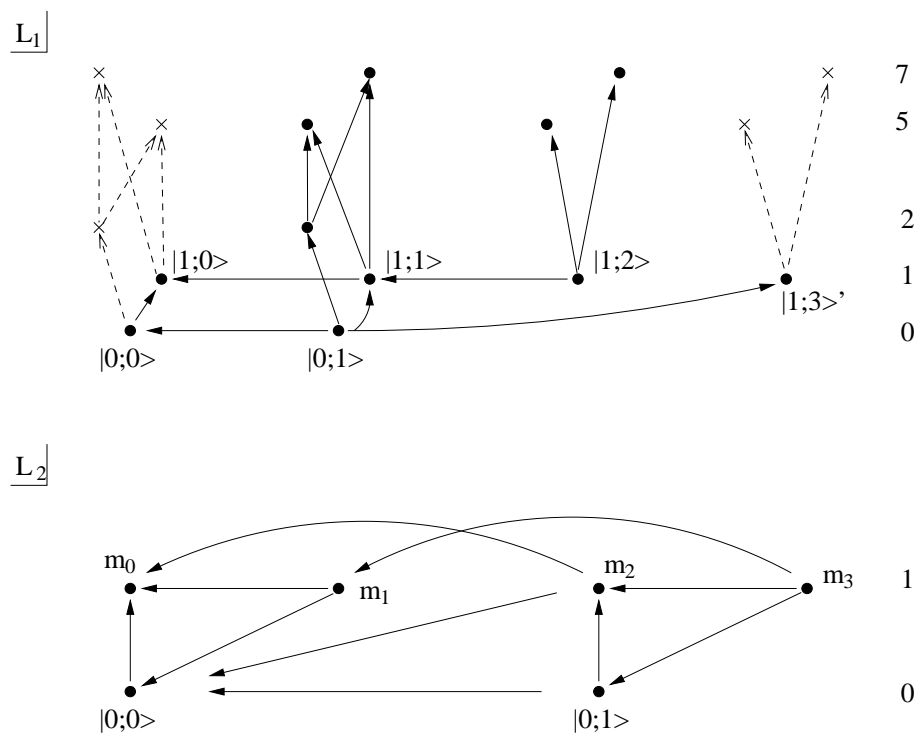


Figure 4.4: Two ways to visualise $\mathcal{R}^{(3)}(0, 0, 1, 1)$

The further nullvector structure is also depicted in figure 4.4 **L**₁. We were able to calculate all states up to level 6 explicitly. The total number of states is also attainable for level 7, but in an indirect way via the second view on this representation to be discussed below. We give a list of the total number of states in table 4.4; we split the number according to the position of the state in the Jordan cell, which we also call the “Jordan level” of that state as introduced in section 2.2. E.g. for level 5 there are four rank 3 Jordan cells, one additional rank 2 Jordan cell plus the four which are subcells of a rank 3 cell as well as six additional single eigenvalues.

Now we find one nullvector on level 2, the singular descendant $L_{-2}|0;0\rangle$. This nullvector has two singular descendants on level 5 and 7 which are also nullvectors of $|1;0\rangle = L_{-1}|0;0\rangle$ due to the bulk embedding structure. The “decoupling” state $|1;3\rangle'$ generates an irreducible representation with null singular vectors on level 5 and 7. These vectors as well as their descendants are the only nullvectors up to level 7. We do not yet encounter a logarithmic nullvector up to this level.

In a second way of visualising this representation we can actually view it as an indecomposable combination of rank 2 representations whose structure is given in much the same way as in figure 4.1 **A**; we only have to replace the two lowest black dots by the two rank 2 representations $\mathcal{R}^{(2)}(0,1)_5$ and the higher by $\mathcal{R}^{(2)}(2,7)$. Surprisingly, we can also put $\mathcal{R}^{(3)}(0,0,1,1)$ in a likewise form with the lower two black dots replaced by $\mathcal{R}^{(2)}(0,1)_7$ and the higher with $\mathcal{R}^{(2)}(2,5)$. Let us see how this comes about.

We choose the setup for the lowest levels as depicted in figure 4.4 **L**₂: we have two separate rank 2 representations with lowest states $|0;0\rangle$ respectively $|0;1\rangle$. $|0;0\rangle$ has a logarithmic partner at level 1, called m_1 , to its singular descendant $m_0 := L_{-1}|0;0\rangle = |1;0\rangle$. Likewise, $|0;1\rangle$ has a logarithmic partner at level 1, called m_3 , to its singular descendant $m_2 := L_{-1}|0;1\rangle = |1;1\rangle + |1;3\rangle'$. Furthermore, both representations are connected by the indecomposable L_0 action on $|0;1\rangle$. This directly promotes to the indecomposable action of L_0 on their L_{-1} descendants

$$L_0 m_0 = |1;0\rangle \quad L_0 m_2 = |1;2\rangle + |1;0\rangle$$

as well as the consistent L_1 action

$$L_1 m_0 = 0 \quad L_1 m_2 = 2|0;0\rangle.$$

Now we still have to check whether we can find m_1 and m_3 which fit this setup. We express m_1 and m_3 as linear combinations of the level 1 states $|1;j\rangle$, $j = 1, 2, 3$ and impose the following conditions and parameters:

- $L_0 m_1 = m_1 + m_0$,
- $L_1 m_1 = \xi_1|0;0\rangle$,
- $L_0 m_3 = m_3 + m_2 + r m_1 + s m_0$,
- $L_1 m_3 = \xi_2|0;1\rangle + \xi_3|0;0\rangle$.

We find that s and ξ_3 are actually irrelevant parameters which can be set to 0 using the residual freedom. r and ξ_2 are functions of ξ_1 . Hence, there is one free parameter in this representation. It is most useful to just express r in terms of ξ_1 and then study the relation between ξ_1 and ξ_2 as these parameters are the defining parameters of the rank 2 representations we started with. The relation is given by

$$(12\xi_1 + 1)(12\xi_2 + 1) = 25.$$

There are only two solutions which fit the bulk rank 2 spectrum discussed above; they also seem to be the most natural ones

$$\begin{aligned}\xi_1 = \xi_2 &= -\frac{1}{2} \\ \xi_1 = \xi_2 &= \frac{1}{3}.\end{aligned}$$

These two solutions exactly give the lower level rank 2 representations which we proposed above to be the two lower dots in the figure 4.1 **A** like setup. In order to get the respective representation corresponding to the higher dot of 4.1 **A** we just have to count the number of states and compare these. As this higher rank 2 representation only “fills up” states which would be null in a pure rank 2 setting, but are not null in this rank 3 setting (e.g. $L_{-2}|0; 1\rangle$) we do not need any further parameters to describe this representation.

Therefore there is only the one additional parameter r besides the parameters of the ingredient rank 2 representations which we need to describe $\mathcal{R}^{(3)}(0, 0, 1, 1)$. It is given in terms of ξ_1 as

$$r = \frac{-25}{12\xi_1 + 1}.$$

Finally, we still need to explain how to determine the number of states for level 7 (as in table 4.4). If we want to use the total number of states to determine this higher black dot in the above setting we can decide this question knowing the total number of states of $\mathcal{R}^{(3)}(0, 0, 1, 1)$ up to level 5 ($\mathcal{R}^{(2)}(2, 5)$ and $\mathcal{R}^{(2)}(2, 5)$ already differ at their third level). But then, we can, in turn, easily use this setting in order to determine the number of states for any higher level.

$\mathcal{R}^{(3)}(\mathbf{0}, \mathbf{0}, \mathbf{2}, \mathbf{2})$: The rank 3 representation $\mathcal{R}^{(3)}(0, 0, 2, 2)$ looks much the same as the previous one.

Again the first way to visualise the representation starts out with its Jordan diagonalisation and is shown in figure 4.5 **M**₁. We have two groundstates $|0; i\rangle$, $i = 0, 1$, at level 0 which are interrelated by the rank 2 indecomposable action of L_0

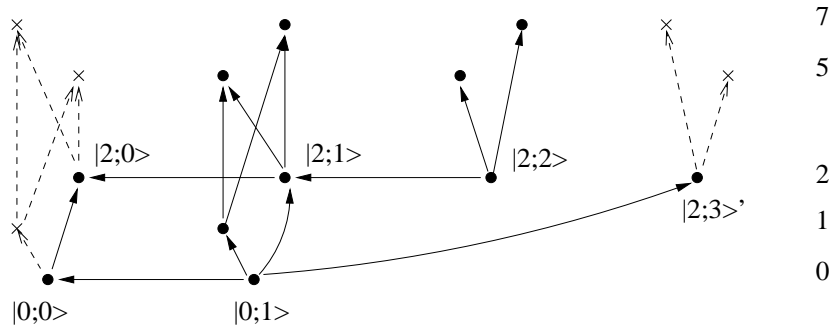
$$L_0|0; 1\rangle = |0; 0\rangle \quad L_0|0; 0\rangle = 0.$$

On level 1 we encounter the first nullvector $L_{-1}|0; 0\rangle$. The level 1 descendant of $|0; 1\rangle$ is not null, though, due to the rank 2 indecomposable structure. On level 2 the Jordan

Table 4.5: Number of states for $\mathcal{R}^{(3)}(0, 0, 2, 2)$

level	number of states			total number of state	new null subrepresentations
	Jordan level 0	Jordan level 1	Jordan level 2		
0	1	1	–	2	–
1	1	–	–	1	1
2	3	1	1	5	–
3	4	1	1	6	–
4	7	2	2	11	–
5	9	3	2	14	2
6	15?	5?	4?	24?	–
7	19?	7?	4?	30?	2

M_1



M_2

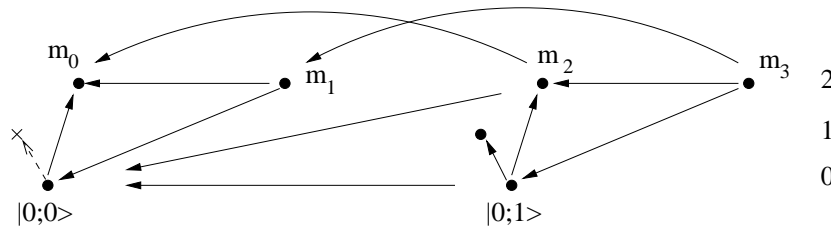


Figure 4.5: Two ways to visualise $\mathcal{R}^{(3)}(0, 0, 2, 2)$

cell is enhanced to rank 3

$$\begin{aligned} L_0 |2; 2\rangle &= 2 |2; 2\rangle + |2; 1\rangle \\ L_0 |2; 1\rangle &= 2 |2; 1\rangle + |2; 0\rangle \\ L_0 |2; 0\rangle &= 2 |2; 0\rangle . \end{aligned}$$

We find two further states on level 2: One of these is just the level 1 descendant of $L_{-1}|0; 1\rangle$, i.e. $L_{-1}^2|0; 1\rangle$. The other one is a new state $|2; 3\rangle'$ which again seemingly decouples in the L_0 action

$$L_0 |2; 3\rangle' = 2 |2; 3\rangle'$$

but which is connected to the rank 3 cell by the descendant equations

$$\begin{aligned} L_{-2} |0; 0\rangle &= |2; 0\rangle \\ L_{-2} |0; 1\rangle &= |2; 1\rangle + |2; 3\rangle' . \end{aligned}$$

The further nullvector structure is as depicted in figure 4.5 \mathbf{M}_1 . We also give the total number of states on the different levels in table 4.5. These numbers have been calculated explicitly up to level 5 and extrapolated by a similar argument as in the $\mathcal{R}^{(3)}(0, 0, 1, 1)$ case up to level 7.

Let us come to the second way of visualising $\mathcal{R}^{(3)}(0, 0, 2, 2)$. Again we can view this representation as an indecomposable combination of rank 2 representations whose structure is given in much the same way as in figure 4.1 \mathbf{A} ; this time we have to replace the two lowest black dots by two rank 2 representations $\mathcal{R}^{(2)}(0, 2)_5$ and the higher by $\mathcal{R}^{(2)}(1, 7)$. And as in the $\mathcal{R}^{(3)}(0, 0, 1, 1)$ case we obtain the rank 3 representation in a second way taking the lower two black dots to be $\mathcal{R}^{(2)}(0, 2)_7$ and the higher one to be $\mathcal{R}^{(2)}(1, 5)$.

This comes about in almost the same way as in the $\mathcal{R}^{(3)}(0, 0, 1, 1)$ case. The important difference is that the existence of a nullvector on a level lower than the Jordan cell in the constituent representations, e.g. $\mathcal{R}^{(2)}(0, 2)_7$, leads to a shift in the true singular vectors as soon as we combine them to the rank 3 representation. To see this let us choose the setup for the lowest levels as depicted in figure 4.5 \mathbf{M}_2 : we have two separate rank 2 representations with lowest states $|0; 0\rangle$ respectively $|0; 1\rangle$. On level 1 we have an ordinary nullvector descendant on $|0; 0\rangle$. The level 1 descendant on $|0; 1\rangle$, however, is rendered non-null by the rank 2 structure; $L_{-1}|0; 1\rangle$ is actually the lowest state of the third rank 2 representation $\mathcal{R}^{(2)}(1, h)$ which we also have to fill in to indecomposably combine these rank 2 representations to $\mathcal{R}^{(3)}(0, 0, 2, 2)$. Due to this non-vanishing L_{-1} action on $|0; 1\rangle$ the singular vector on $|0; 1\rangle$ is shifted to

$$m_2 := \left(L_{-2} - \frac{3}{2} L_{-1}^2 \right) |0; 1\rangle .$$

We have to change our ansatz accordingly. We assume that both level 2 singular descendants $m_0 := L_{-2} |0; 0\rangle$ and m_2 have logarithmic partners m_1 and m_3 respectively.

Furthermore, both separate rank 2 representations are connected by the indecomposable L_0 action on $|0; 1\rangle$. This directly promotes to the indecomposable action of L_0 on their level 2 descendants

$$L_0 m_0 = 2 m_0 \quad L_0 m_2 = 2 m_2 + m_0$$

as well as the consistent L_2 action

$$L_2 m_0 = 0 \quad L_2 m_2 = -5 |0; 0\rangle .$$

In order to fit m_1 and m_3 to this setting we express them as linear combinations of the level 2 states $|2; j\rangle$, $j = 1, 2, 3$ as well as $L_{-1}^2 |0; 1\rangle$ and impose the following conditions and parameters:

- $L_0 m_1 = 2 m_1 + m_0$,
- $L_1 m_1 = 0$,
- $L_2 m_1 = \xi_1 |0; 0\rangle$,
- $L_0 m_3 = 2 m_3 + m_2 + r m_1 + s m_0$,
- $L_1 m_3 = 0$,
- $L_2 m_3 = \xi_2 |0; 1\rangle$.

The two parameters ξ_1 and ξ_2 are the defining parameters of the constituent rank 2 representations. We find that s is actually an irrelevant parameter which can be set to 0 using the residual freedom. r and ξ_2 are functions of ξ_1 . We express r in terms of ξ_1 and then study the relation between ξ_1 and ξ_2

$$\left(1 - \frac{48}{5} \xi_1\right) \left(1 - \frac{48}{5} \xi_2\right) = 49 .$$

As in the $\mathcal{R}^{(3)}(0, 0, 1, 1)$ case we find two solutions which at the same time fit the bulk rank 2 spectrum and also seem to be the most natural ones

$$\begin{aligned} \xi_1 = \xi_2 &= -\frac{5}{8} \\ \xi_1 = \xi_2 &= \frac{5}{6} . \end{aligned}$$

These two solutions give just the lower level rank 2 representations proposed in the setup above. Again, counting the number of states up to level 5 we uniquely determine the third representation needed to complete this setup.

Besides the parameters ξ_i of the ingredient rank 2 representations we need one additional parameter r to describe this construction of $\mathcal{R}^{(3)}(0, 0, 2, 2)$. It is given by

$$r = \frac{49}{\frac{48}{5} \xi_1 - 1} .$$

Table 4.6: Number of states for $\mathcal{R}^{(3)}(0, 1, 2, 5)$

level	number of states			total number of state	new null subrepresentations
	Jordan level 0	Jordan level 1	Jordan level 2		
0	1	–	–	1	–
1	1	1	–	2	–
2	2	2	–	4	–
3	3	3	–	6	–
4	5	5	–	10	–
5	8	7	1	16	–

$\mathcal{R}^{(3)}(\mathbf{0}, \mathbf{1}, \mathbf{2}, \mathbf{5})$: The rank 3 representation $\mathcal{R}^{(3)}(0, 1, 2, 5)$ is the only higher rank 3 representation which was accessible to our calculations up to that level at which the rank 3 structure appears. From our knowledge of the other towers of representations it should nevertheless be fair to conjecture that most of the generic features of rank 3 representations in these $c_{p,q}$ models are already visible in this example.

In table 4.6 we list the number of states as calculated. We have also included the basis of states which brings L_0 into Jordan diagonal form in appendix A.3.

Again we find two ways to visualise the embedding structure. The Jordan diagonalisation of L_0 gives an embedding structure of the form depicted in figure 4.6 \mathbf{N}_1 . As the situation is even more complicated as for $\mathcal{R}^{(3)}(0, 0, 1, 1)$ and $\mathcal{R}^{(3)}(0, 0, 2, 2)$ we have labeled the states according to the indexed basis which is chosen by the computer and listed in appendix A.3. We can see that both singular vectors on n_0 , i.e. n_4 at level 1 and n_{23} at level 2, are incorporated into rank 2 Jordan cells. But nevertheless we do not encounter a first rank 3 cell until level 5. The first vector of this rank 3 Jordan cell, n_{16} , which is a true eigenvector, is given by the joint singular vector on n_4 and n_{23} . As in the $\mathcal{R}^{(3)}(0, 0, 1, 1)$ case there is a vector at level 5 which seems to decouple from the representation. But again this decoupling in terms of the L_0 action is deceiving as this vector is a sum of descendants of n_5 and n_{24} (see appendix A.3 for the explicit expressions). Hence, as for $\mathcal{R}^{(3)}(0, 0, 1, 1)$ this rank 3 representation needs four generating states.

As a second way to visualise this representation we conjecture that we can construct this representation by an indecomposable combination of the four rank 2 representations $\mathcal{R}^{(2)}(0, 1)_7$, twice $\mathcal{R}^{(2)}(2, 5)$ and $\mathcal{R}^{(2)}(7, 12)$ assembled as in figure 4.1 \mathbf{B} ; as before we replace the black dots in figure 4.1 \mathbf{B} by the respective rank 2 representations. The picture that emerges is depicted in figure 4.6 \mathbf{N}_2 . What are the hints at such a

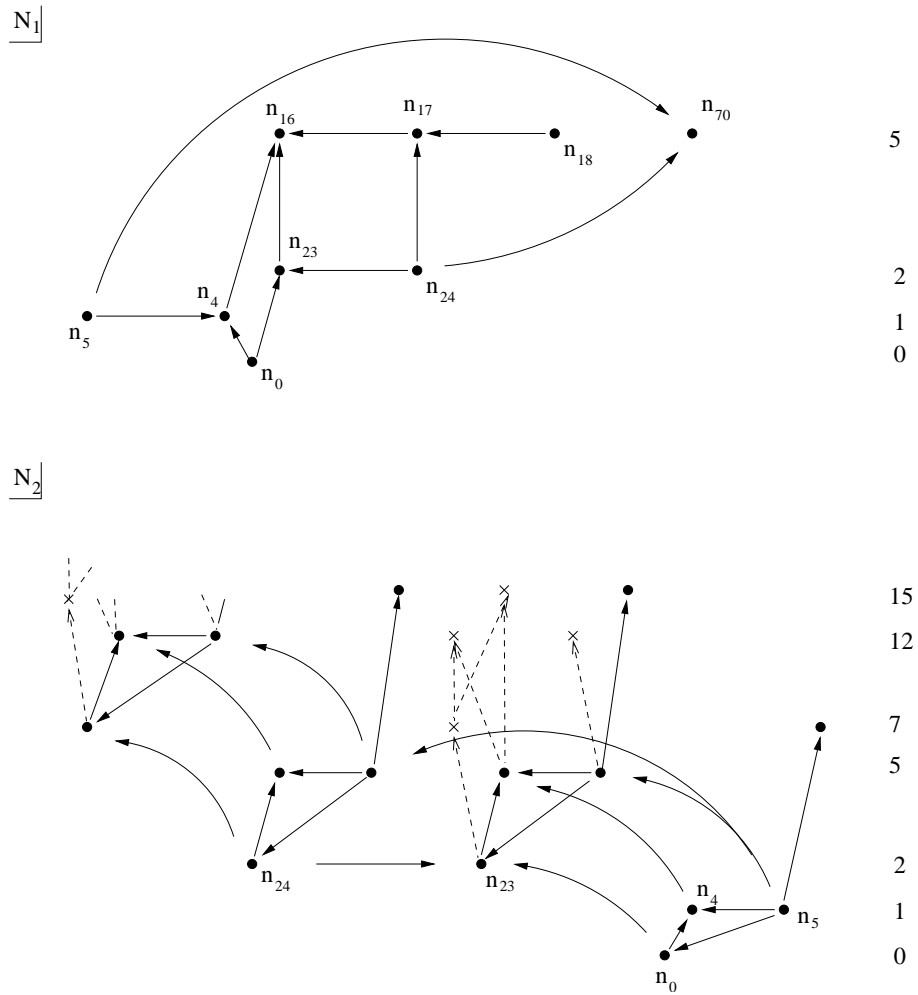


Figure 4.6: Two ways to visualise $\mathcal{R}^{(3)}(0, 1, 2, 5)$

deconstruction of $\mathcal{R}^{(3)}(0, 1, 2, 5)$? First of all we find that

$$L_1 n_5 = -\frac{1}{2}n_0 ;$$

this equation reproduces the defining β parameter of $\mathcal{R}^{(2)}(0, 1)_7$. Hence, the two lowest generating states of $\mathcal{R}^{(3)}(0, 1, 2, 5)$, n_0 and n_5 , generate a tower of states which resembles the rank 2 representation $\mathcal{R}^{(2)}(0, 1)_7$. The only difference to a true subrepresentation $\mathcal{R}^{(2)}(0, 1)_7$ is that the usual first nullvector on n_0 , $n_{23} = L_{-2} n_0$, is rendered non-null by its inclusion into an indecomposable rank 2 cell with

$$\begin{aligned} L_0 n_{23} &= 2n_{23} \\ L_0 n_{24} &= 2n_{24} + n_{23} . \end{aligned} \tag{4.10}$$

In the $\mathcal{R}^{(3)}(0, 0, 1, 1)$ and $\mathcal{R}^{(3)}(0, 0, 2, 2)$ cases we have seen examples that the indecomposable connection of two rank 2 cells of the same type of rank 2 representation produces a rank 3 cell and a seemingly decoupling further state. But this is exactly the structure we discover in this case at level 5—a rank 3 cell

$$\begin{aligned} L_0 n_{16} &= 2n_{16} \\ L_0 n_{17} &= 2n_{17} + n_{16} \\ L_0 n_{18} &= 2n_{18} + n_{17} \end{aligned}$$

as well as a seemingly decoupling state n_{70} . Hence, we conjecture that n_{23} and n_{24} are actually both the lower generators of towers of states which both resemble $\mathcal{R}^{(2)}(2, 5)$, but which are indecomposably connected according to equation (4.10). This structure up to level 5 is in perfect agreement with the total count of states given in table 4.6. Unfortunately, we cannot say anything about the embedding structure or the count of states for higher levels and, thus, the inclusion of the fourth rank 2 representation $\mathcal{R}^{(2)}(7, 12)$ is highly conjectural. It is only lead by the intuition that in any rank 2 structure the first nullvectors on the true eigenstate have to have non-null corresponding states on the side of the logarithmic partner due to the non-degeneracy of the Shapovalov form.

There is, however, one further way of looking at the situation. Let us regard the fusion equation of the irreducible representation of weight $h = 1/3$ and the rank 2 representation $\mathcal{R}^{(2)}(1, 5)$

$$\mathcal{V}(1/3) \otimes_f \mathcal{R}^{(2)}(1, 5) = \mathcal{R}^{(3)}(0, 1, 2, 5) .$$

But, as described before, we can also view $\mathcal{R}^{(2)}(1, 5)$ as a combination of four towers of states which resemble its irreducible counterparts in terms of numbers of states and singular vectors but which are indecomposably connected to form $\mathcal{R}^{(2)}(1, 5)$. In this case, we can think of $\mathcal{R}^{(2)}(1, 5)$ as being constructed by indecomposably connecting $\mathcal{V}(1)$, twice $\mathcal{V}(5)$ as well as $\mathcal{V}(12)$. But the fusion of its single constituents should be

consistent with the fusion of $\mathcal{R}^{(2)}(1, 5)$ itself. Therefore, inspecting the fusion rules (the first two calculated, see appendix B.1, the third inferred from the fusion rules of section 4.6)

$$\begin{aligned}\mathcal{V}(1/3) \otimes_f \mathcal{V}(1) &= \mathcal{R}^{(2)}(0, 1)_7 \\ \mathcal{V}(1/3) \otimes_f \mathcal{V}(5) &= \mathcal{R}^{(2)}(2, 5) \\ \mathcal{V}(1/3) \otimes_f \mathcal{V}(12) &= \mathcal{R}^{(2)}(7, 12)\end{aligned}$$

we are again lead to the conjecture that we can build $\mathcal{R}^{(3)}(0, 1, 2, 5)$ by indecomposably connecting $\mathcal{R}^{(2)}(0, 1)_7$, twice $\mathcal{R}^{(2)}(2, 5)$ and $\mathcal{R}^{(2)}(7, 12)$.

Like the previous two rank 3 representations $\mathcal{R}^{(3)}(0, 1, 2, 5)$ can also be composed of rank 2 representations in a second way. Indeed, an inspection of the fusion equation

$$\mathcal{V}(5/8) \otimes_f \mathcal{R}^{(2)}(5/8, 21/8) = \mathcal{R}^{(3)}(0, 1, 2, 5)$$

leads to the conjecture that we can also construct $\mathcal{R}^{(3)}(0, 1, 2, 5)$ by indecomposably connecting $\mathcal{R}^{(2)}(0, 2)_7$, twice $\mathcal{R}^{(2)}(1, 5)$ and $\mathcal{R}^{(2)}(7, 15)$. This is also in perfect agreement with the total count of states up to the accessible level 5. To see the defining parameter of the lowest rank 2 representation $\mathcal{R}^{(2)}(0, 2)_7$ we have to keep in mind that as in the $\mathcal{R}^{(3)}(0, 0, 2, 2)$ case the absence of nullvectors can change the singular vectors. And indeed, as L_{-1} does not annihilate n_0 due to the indecomposable structure the level 2 singular descendant on n_0 is shifted to

$$n'_{23} = n_{23} - \frac{3}{2} n_4 .$$

Taking into account the non-trivial action of the positive Virasoro modes on the new state n_{24} at level 2 (after removal of some residual freedom)

$$\begin{aligned}L_1 n_{24} &= 3 n_5 \\ L_2 n_{24} &= -\frac{17}{12} n_0\end{aligned}\tag{4.11}$$

we find a suitable logarithmic partner of n'_{23} as

$$n'_{24} = n_{24} + \frac{9}{8} n_4 - \frac{3}{2} n_5 .$$

This actually exhibits the desired properties

$$\begin{aligned}L_1 n'_{24} &= 0 \\ L_2 n'_{24} &= \frac{5}{6} n_0 ,\end{aligned}$$

especially the correct defining parameter $\beta = 5/6$ for $\mathcal{R}^{(2)}(0, 2)_7$.

$\mathcal{R}^{(3)}(0, 1, 2, 7)$: Although the rank 3 representation $\mathcal{R}^{(3)}(0, 1, 2, 7)$ is not accessible to our computational power we can nevertheless tackle its decomposition in the same way

as the fusion decomposition method in the preceding case. For this argument we take the appearances of $\mathcal{R}^{(3)}(0, 1, 2, 7)$ for granted as conjectured in appendix B.1. Then looking at the fusion equation

$$\mathcal{V}(5/8) \otimes_f \mathcal{R}^{(2)}(1/8, 33/8) = \mathcal{R}^{(3)}(0, 1, 2, 7)$$

we conjecture that $\mathcal{R}^{(3)}(0, 1, 2, 7)$ can be constructed by indecomposably connecting the four rank 2 representations $\mathcal{R}^{(2)}(0, 1)_5$, twice $\mathcal{R}^{(2)}(2, 7)$ and $\mathcal{R}^{(2)}(5, 12)$. Similarly, looking at

$$\mathcal{V}(1/3) \otimes_f \mathcal{R}^{(2)}(1/3, 10/3) = \mathcal{R}^{(3)}(0, 1, 2, 7) \oplus \mathcal{R}^{(2)}(1/3, 10/3)$$

we can think of $\mathcal{R}^{(3)}(0, 1, 2, 7)$ to be composed of $\mathcal{R}^{(2)}(0, 2)_5$, twice $\mathcal{R}^{(2)}(1, 7)$ and $\mathcal{R}^{(2)}(5, 15)$.

4.4.2 Explicit calculation of the fusion products

We have calculated the fusion product of a large variety of representations in the augmented $c_{2,3} = 0$ model. To do this we have used the Nahm algorithm described in section 4.3 to determine the fusion product of irreducible and rank 1 representations with themselves as well as with the lowest lying and first excited rank 2 representations. In order to show that the fusion algebra indeed closes we have used the symmetry and associativity of the fusion product to calculate the fusion of higher rank representations. We have also used these conditions in order to perform consistency checks as described in the next subsection. The results itself are listed in appendix B.1.

In section 4.6 we want to propose a generalisation of the BPZ and $c_{p,1}$ fusion rules which is applicable to all augmented $c_{p,q}$ models and, hence, also describes in a unifying way the fusion of this model. But as these general rules look quite complex it is also possible to find simplified versions for the augmented $c_{2,3} = 0$ model, e.g.

$$\mathcal{V}(5/8) \otimes_f \mathcal{W}(1/3|i) = \mathcal{W}(-1/24|i) ,$$

where $\mathcal{W}(h|i)$ signifies the i th element in the weight chain starting with h .

4.4.3 Consistency of fusion products

A consistent fusion product has to obey two main properties, symmetry and associativity. We have used both these properties for consistency checks for the chosen spectrum and the performed calculation as well as for the determination of the fusion product of higher rank representations.

The main implication of this consistency, however, is the absence of an irreducible representation of weight $h = 0$ in the spectrum, call it $\mathcal{V}(0)$. The representation $\mathcal{V}(0)$ would be endowed with nullvectors on level 1 and 2 and would, hence, only consist of

the one groundstate. Performing the Nahm algorithm of section 4.3 we get the following fusion products

$$\mathcal{V}(0) \otimes_f \mathcal{V}(0) = \mathcal{V}(0) \quad (4.12)$$

$$\mathcal{V}(0) \otimes_f \mathcal{V}(h) = 0 \quad \forall h \in \left\{ \frac{5}{8}, \frac{1}{3}, \frac{1}{8}, \frac{-1}{24}, \frac{33}{8}, \frac{10}{3}, \frac{21}{8}, 2, 1, 7, 5 \right\}. \quad (4.13)$$

On the other hand, using just the equations (4.13) and the fusion rules of appendix B.1 we arrive at

$$\begin{aligned} (\mathcal{V}(0) \otimes_f (\mathcal{V}(2) \otimes_f \mathcal{V}(2))) &= (\mathcal{V}(0) \otimes_f \mathcal{V}(0)) \oplus (\mathcal{V}(0) \otimes_f \mathcal{V}(2)) \\ &= \mathcal{V}(0) \otimes_f \mathcal{V}(0) \end{aligned}$$

as well as by associativity at

$$\begin{aligned} ((\mathcal{V}(0) \otimes_f \mathcal{V}(2)) \otimes_f \mathcal{V}(2)) &= 0 \otimes_f \mathcal{V}(2) \\ &= 0. \end{aligned}$$

(Similar equations can be obtained involving the other $\mathcal{V}(h)$ with h from (4.13).) This argument thus implies

$$\mathcal{V}(0) \otimes_f \mathcal{V}(0) = 0.$$

But this is in clear contradiction to (4.12). Fortunately, however, $\mathcal{V}(0)$ completely decouples from the rest of the fusion (as one can see in appendix B.1). Hence, the contradiction is easily solved by simply excluding $\mathcal{V}(0)$ from the spectrum.

On the other hand the representations $\mathcal{R}^{(2)}(0, 1)_5$ and $\mathcal{R}^{(2)}(0, 1)_7$ contain a state with weight 0 which generates a subrepresentation $\mathcal{R}^{(1)}(0)_1$. This subrepresentation is indecomposable but neither is it irreducible nor does it exhibit any higher rank behaviour. It only exists as a subrepresentation as it needs the embedding into the rank 2 representation in order not to have nullvectors at both levels 1 and 2. But nevertheless, being a subrepresentation of a representation in the spectrum it has to be included into the spectrum, too. Similarly, the representations $\mathcal{R}^{(2)}(0, 2)_5$ and $\mathcal{R}^{(2)}(0, 2)_7$ contain a rank 1 subrepresentation $\mathcal{R}^{(1)}(0)_2$. However, looking at the fusion rules which we calculate for these two rank 1 representations (see appendix B.1), especially

$$\mathcal{R}^{(1)}(0)_2 \otimes_f \mathcal{V}(h) = \mathcal{V}(h) \quad \forall h \in \left\{ \frac{5}{8}, \frac{1}{3}, \frac{1}{8}, \frac{-1}{24}, \frac{33}{8}, \frac{10}{3}, \frac{21}{8}, 2, 1, 7, 5 \right\},$$

we see that the situation is after all not really too bad: $\mathcal{R}^{(1)}(0)_2$ behaves much more like the true vacuum representation as the expected $\mathcal{V}(0)$ (only regard the behaviour in (4.13)).

We now want to present one nice example how to use the symmetry and associativity of the fusion product in order to determine the higher rank fusion. Let us assume that we already know the fusion of irreducible representations with themselves as well as

with rank 2 representations, i.e. the results we actually calculated using the Nahm algorithm (see appendix B.1). Then we start off with

$$\left(\left(\mathcal{V}(1/8) \otimes_f \mathcal{V}(1/3) \right) \otimes_f \mathcal{R}^{(2)}(1/3, 1/3) \right) = \mathcal{R}^{(2)}(1/8, 1/8) \otimes_f \mathcal{R}^{(2)}(1/3, 1/3) .$$

Using associativity we can also calculate

$$\begin{aligned} & \left(\mathcal{V}(1/8) \otimes_f \left(\mathcal{V}(1/3) \otimes_f \mathcal{R}^{(2)}(1/3, 1/3) \right) \right) \\ &= \left(\mathcal{V}(1/8) \otimes_f \left(\mathcal{R}^{(3)}(0, 0, 2, 2) \oplus \mathcal{R}^{(2)}(1/3, 1/3) \right) \right) \\ &= 2 \mathcal{R}^{(2)}(1/8, 1/8) \oplus \mathcal{R}^{(2)}(5/8, 21/8) \oplus \left(\mathcal{V}(1/8) \otimes_f \mathcal{R}^{(3)}(0, 0, 2, 2) \right) . \end{aligned}$$

On the other hand we can use the symmetry as well as the associativity once more to get

$$\begin{aligned} & \left(\mathcal{V}(1/3) \otimes_f \left(\mathcal{V}(1/8) \otimes_f \mathcal{R}^{(2)}(1/3, 1/3) \right) \right) \\ &= \left(\mathcal{V}(1/3) \otimes_f \left(2 \mathcal{R}^{(2)}(1/8, 1/8) \oplus \mathcal{R}^{(2)}(5/8, 21/8) \right) \right) \\ &= 4 \mathcal{R}^{(2)}(1/8, 1/8) \oplus 2 \mathcal{R}^{(2)}(5/8, 21/8) \oplus \mathcal{V}(-1/24) \oplus 2 \mathcal{V}(35/24) \oplus \mathcal{V}(143/24) . \end{aligned}$$

By comparison we thus arrive at already two new higher rank fusion products

$$\begin{aligned} & \mathcal{R}^{(2)}(1/8, 1/8) \otimes_f \mathcal{R}^{(2)}(1/3, 1/3) \\ &= 4 \mathcal{R}^{(2)}(1/8, 1/8) \oplus 2 \mathcal{R}^{(2)}(5/8, 21/8) \oplus \mathcal{V}(-1/24) \oplus 2 \mathcal{V}(35/24) \oplus \mathcal{V}(143/24) \\ & \mathcal{V}(1/8) \otimes_f \mathcal{R}^{(3)}(0, 0, 2, 2) \\ &= 2 \mathcal{R}^{(2)}(1/8, 1/8) \oplus \mathcal{R}^{(2)}(5/8, 21/8) \oplus \mathcal{V}(-1/24) \oplus 2 \mathcal{V}(35/24) \oplus \mathcal{V}(143/24) . \end{aligned}$$

The complete list of the higher rank fusion products which we calculated is given in appendix B.1.

4.4.4 An unexpected connection to quantum spin chains

Inspecting the field content of the augmented $c_{2,3} = 0$ model as calculated in this section, we actually find that the numerical results of [41], table 1, which are supposed to give the low level state content of CFT representations at $c = 0$ for an XXZ quantum spin chain, perfectly match our representations $\mathcal{R}^{(1)}(0)_2$, $\mathcal{R}^{(1)}(0)_1$ and $\mathcal{V}(1/3)$, respectively. Although the numerical results give only relatively few levels we conjecture that they are correctly described by the above mentioned $c_{2,3} = 0$ representations.

Regarding the fusion product of these representations (as given in appendix B.1), it is interesting to see that the two representations $\mathcal{R}^{(1)}(0)_2$ and $\mathcal{R}^{(1)}(0)_1$ already induce the existence of the irreducible $\mathcal{V}(1/3)$. Furthermore, these three representations belong to a subalgebra of the fusion algebra of the augmented $c_{2,3} = 0$ model. Besides these three representations this subalgebra comprises the two rank 2 representations

$\mathcal{R}^{(2)}(0, 2)_5$ and $\mathcal{R}^{(2)}(0, 1)_7$, of which $\mathcal{R}^{(1)}(0)_2$ and $\mathcal{R}^{(1)}(0)_1$ are subrepresentations, as well as excited irreducible representations with weights in the weight chain of $h = 1/3$ and half of the excited rank 2 representations associated to the bulk weight chain of $h = 0$. We obtain this subalgebra by restricting spectrum and fusion to the left column of the Kac table in table 4.1, i.e. $s = 1$. This yields a simplified spectrum of conformal weights of

$$h_{r,1} = \frac{r^2 - 3r + 2}{6}. \quad (4.14)$$

Thus, the subalgebra is given by the following Hilbert space

$$\mathcal{H}' = \bigoplus_{\rho=1}^{\infty} \mathcal{V}(h_{3\rho,1}) \oplus \bigoplus_{\rho=1}^{\infty} \left(\mathcal{R}^{(2)}(h_{3\rho-2,1}, h_{3\rho+2,1}) \oplus \mathcal{R}^{(2)}(h_{3\rho-1,1}, h_{3\rho+1,1}) \right)$$

where the $\rho = 1$ terms of the rank 2 representations are given by $\mathcal{R}^{(2)}(0, 2)_5$ respectively $\mathcal{R}^{(2)}(0, 1)_7$ (for the correct indices). Certainly, this Hilbert space \mathcal{H}' also contains all (ir)reducible subrepresentations of its rank 2 representations. The spectrum of irreducible as well as reducible rank 1 (sub)representations within this subalgebra is compatible with the spectrum of equation (5.1) in [41]; our variable r in (4.14) has to be identified with $2s + 1$ of [41]. Indeed, the characters given in equation (5.2) of [41] agree with the state content of representations in \mathcal{H}' , i.e. with the irreducible representations for the weights $h_{3\rho,1} = \frac{1}{3}, \frac{10}{3}, \frac{28}{3}, \dots$ and with the rank 1 reducible but indecomposable subrepresentations of the rank 2 representations for integer weights $h = 0, 1, 2, 5, 7, \dots$. Hence, this subalgebra is compatible with the spectrum, the characters, and the available numerical results presented in [41].

This is an unexpected and very exciting connection of logarithmic CFT and, in particular, the augmented $c_{2,3} = 0$ model to quantum spin chains.

4.5 Fusion analysis of the augmented Yang–Lee model

Unfortunately, a complete exploration of the low lying spectrum of the next easiest general augmented model, the augmented Yang–Lee model at $c_{2,5} = -22/5$, is not yet possible due to limitations on the computational power. Nevertheless, we were able to compute most of the crucial features which we observed in the fusion of the augmented $c_{2,3} = 0$ model, including the lowest rank 2 and rank 3 representations as well as the absence of irreducible representations corresponding to the original minimal model. We also give various examples of fusion products which confirm the general fusion rules conjectured in section 4.6. The explicit results are listed in appendix B.2.

The Kac table of $c_{2,5} = -22/5$ is depicted in table 4.7. We encounter two bulk weight chains

$$\begin{aligned} W_{(1,1)}^{\text{bulk, YL}} &:= \{ \{0\}, \{1, 4\}, \{7, 13\}, \dots \} \\ W_{(2,1)}^{\text{bulk, YL}} &:= \left\{ \left\{ -\frac{1}{5} \right\}, \left\{ \frac{9}{5}, \frac{14}{5} \right\}, \left\{ \frac{44}{5}, \frac{54}{5} \right\}, \dots \right\} \end{aligned}$$

Table 4.7: Kac table for $c_{2,5} = -22/5$

		s				
		1	2	3	4	5
r	1	0	$\frac{11}{8}$	4	$\frac{63}{8}$	13
	2	$-\frac{1}{5}$	$\frac{27}{40}$	$\frac{14}{5}$	$\frac{247}{40}$	$\frac{54}{5}$
	3	$-\frac{1}{5}$	$\frac{7}{40}$	$\frac{9}{5}$	$\frac{187}{40}$	$\frac{44}{5}$
	4	0	$-\frac{1}{8}$	1	$\frac{27}{8}$	7
	5	$\frac{2}{5}$	$-\frac{9}{40}$	$\frac{2}{5}$	$\frac{91}{40}$	$\frac{27}{5}$
	6	1	$-\frac{1}{8}$	0	$\frac{11}{8}$	4
	7	$\frac{9}{5}$	$\frac{7}{40}$	$-\frac{1}{5}$	$\frac{27}{40}$	$\frac{14}{5}$
	8	$\frac{14}{5}$	$\frac{27}{40}$	$-\frac{1}{5}$	$\frac{7}{40}$	$\frac{9}{5}$
	9	4	$\frac{11}{8}$	0	$-\frac{1}{8}$	1
	10	$\frac{27}{5}$	$\frac{91}{40}$	$\frac{2}{5}$	$-\frac{9}{40}$	$\frac{2}{5}$
	11	7	$\frac{27}{8}$	1	$-\frac{1}{8}$	0
	12	$\frac{44}{5}$	$\frac{187}{40}$	$\frac{9}{5}$	$\frac{7}{40}$	$-\frac{1}{5}$
	13	$\frac{54}{5}$	$\frac{247}{40}$	$\frac{14}{5}$	$\frac{27}{40}$	$-\frac{1}{5}$
	14	13	$\frac{63}{8}$	4	$\frac{11}{8}$	0

Table 4.8: Specific properties of rank 2 representations in $c_{2,5} = -22/5$

	β_1	β_2	level of log. partner	level of first nullvector	level of first log. nullvector	type
$\mathcal{R}^{(2)}(11/8, 11/8)$	–	–	0	2	18	A
$\mathcal{R}^{(2)}(27/40, 27/40)$	–	–	0	4	16	A
$\mathcal{R}^{(2)}(2/5, 2/5)$	–	–	0	5	15	A
$\mathcal{R}^{(2)}(7/40, 7/40)$	–	–	0	6	14	A
$\mathcal{R}^{(2)}(-1/8, -1/8)$	–	–	0	8	12	A
$\mathcal{R}^{(2)}(0, 1)_7$	$3/5$	–	1	4	13	G
$\mathcal{R}^{(2)}(0, 1)_{13}$	$-3/2$	–	1	4	7	H
$\mathcal{R}^{(2)}(0, 4)_7$	0	$231/50$	4	1	13	I
$\mathcal{R}^{(2)}(0, 4)_{13}$	0	$231/25$	4	1	7	K
$\mathcal{R}^{(2)}(-1/5, 9/5)_9$	$-42/125$	–	2	3	11	G
$\mathcal{R}^{(2)}(-1/5, 9/5)_{11}$	$21/50$	–	2	3	9	H
$\mathcal{R}^{(2)}(-1/5, 14/5)_9$	$21/125$	$21/50$	3	2	11	I
$\mathcal{R}^{(2)}(-1/5, 14/5)_{11}$	$-126/625$	$-63/125$	3	2	9	K

as well as five border weight chains

$$\begin{aligned}
W_{(1,2)}^{\text{border, YL}} &:= \left\{ \frac{11}{8}, \frac{27}{8}, \frac{155}{8}, \dots \right\} \\
W_{(2,2)}^{\text{border, YL}} &:= \left\{ \frac{27}{40}, \frac{187}{40}, \frac{667}{40}, \dots \right\} \\
W_{(3,2)}^{\text{border, YL}} &:= \left\{ \frac{7}{40}, \frac{247}{40}, \frac{567}{40}, \dots \right\} \\
W_{(4,2)}^{\text{border, YL}} &:= \left\{ -\frac{1}{8}, \frac{63}{8}, \frac{95}{8}, \dots \right\} \\
W_{(5,1)}^{\text{border, YL}} &:= \left\{ \frac{2}{5}, \frac{27}{5}, \frac{77}{5}, \dots \right\}
\end{aligned}$$

and a chain $\{-9/40, 91/40, 391/40, \dots\}$ of weights on the corners. In table 4.8 we present all rank 2 representations which we found in our sample calculations (see appendix B.2) as well as their defining parameters. This is indeed the complete spectrum of lowest rank 2 representations to be expected according to the general considerations of section 4.6.

As in the $c_{2,3} = 0$ model case the lowest border rank 2 representations, given in the first block of table 4.8, do not need a further parameter for characterisation. Their structure is again represented by figure 4.1 **A**.

The structure of the lowest bulk rank 2 representations, given in the second block of table 4.8, is depicted in figure 4.3; their respective special type is given in the last column. The representations of type **G** and **H** exhibit their Jordan cell on the level of the first possible nullvector of the groundstate and can thus be described by just one parameter $\beta = \beta_1$

$$(L_1)^l |h + l; 1\rangle = \beta |h\rangle;$$

l denotes the level of the Jordan cell. Besides this, we have $L_p |h + l; 1\rangle = 0$ for all $p \geq 2$ and, hence, all other Virasoro monomials of length l vanish applied to $|h + l; 1\rangle$.

The representations of type **I** and **K**, however, have to accommodate a first nullvector on the groundstate already below the level of the Jordan cell. The same difficulties as in the $c_{2,3} = 0$ model apply. We again need two parameters β_1 and β_2 parameterising

$$\begin{aligned}
(L_1)^l |h + l; 1\rangle &= \beta_1 |h\rangle \\
P(L) |h + l; 1\rangle &= \beta_2 |h\rangle,
\end{aligned}$$

where we have taken $P(L) = L_4$ for $\mathcal{R}^{(2)}(0, 4)_7$ and $\mathcal{R}^{(2)}(0, 4)_{13}$ as well as $P(L) = L_2 L_1$ for $\mathcal{R}^{(2)}(-1/5, 14/5)_9$ and $\mathcal{R}^{(2)}(-1/5, 14/5)_{11}$. All other Virasoro monomials of length l vanish applied to $|h + l; 1\rangle$. This behaviour actually confirms our conjecture of section 4.4.1 that we only need two parameters for this type of representation; furthermore, the above presented parameterisation is performed exactly in the proposed way.

Again we checked for the appearance of the lowest logarithmic nullvector using the algorithm of section 4.2. This could be successfully done in all cases listed in table 4.8. For this $c_{2,5} = -22/5$ model these nullvector calculations were actually a nice and necessary check of our proposed fusion rules as this information was usually not directly accessible in the fusion spectrum due to the computational limits on L .

As a last issue in the discussion of the augmented Yang–Lee model we want to have a look at the irreducible representations with weights in the Kac-table of the corresponding non-augmented minimal model. There are two possible representations of this kind in this model, $\mathcal{V}(h = 0)$ with first nullvectors on levels 1 and 4 as well as $\mathcal{V}(h = -1/5)$ with first nullvectors on levels 2 and 3. Explicit calculations with the Nahm algorithm lead to

$$\mathcal{V}(-1/5) \otimes_f \mathcal{V}(-1/5) = \mathcal{V}(0) \oplus \mathcal{V}(-1/5) \quad (4.15)$$

$$\mathcal{V}(-1/5) \otimes_f \mathcal{V}(h) = 0 \quad \forall h \in \left\{ \frac{9}{5}, \frac{14}{5}, 4 \right\}. \quad (4.16)$$

But again using only the equations of (4.16) and the fusion rules of appendix B.2 we arrive at the contradicting results

$$\begin{aligned} & \left(\mathcal{V}(-1/5) \otimes_f \left(\mathcal{V}(14/5) \otimes_f \mathcal{V}(14/5) \right) \right) \\ &= \left(\mathcal{V}(-1/5) \otimes_f \mathcal{V}(0) \right) \oplus \left(\mathcal{V}(-1/5) \otimes_f \mathcal{V}(4) \right) \oplus \left(\mathcal{V}(-1/5) \otimes_f \mathcal{V}(-1/5) \right) \\ & \quad \oplus \left(\mathcal{V}(-1/5) \otimes_f \mathcal{V}(9/5) \right) \\ &= \left(\mathcal{V}(-1/5) \otimes_f \mathcal{V}(0) \right) \oplus \left(\mathcal{V}(-1/5) \otimes_f \mathcal{V}(-1/5) \right) \end{aligned}$$

as well as

$$\begin{aligned} \left(\left(\mathcal{V}(-1/5) \otimes_f \mathcal{V}(14/5) \right) \otimes_f \mathcal{V}(14/5) \right) &= 0 \otimes_f \mathcal{V}(14/5) \\ &= 0 \end{aligned}$$

which lead to

$$\begin{aligned} \mathcal{V}(-1/5) \otimes_f \mathcal{V}(0) &= 0 \\ \mathcal{V}(-1/5) \otimes_f \mathcal{V}(-1/5) &= 0. \end{aligned}$$

A similar calculation applies to $\mathcal{V}(0)$. Thus, we have to discard $\mathcal{V}(0)$ and $\mathcal{V}(-1/5)$ from the spectrum.

But with the same reasoning as in the augmented $c_{2,3} = 0$ model case we encounter rank 1 subrepresentations of rank 2 representations which are generated by states with weights $h = 0$ and $h = -1/5$. We therefore have to include the four rank 1 indecomposable (but not irreducible) representations $\mathcal{R}^{(1)}(0)_1$, $\mathcal{R}^{(1)}(0)_4$, $\mathcal{R}^{(1)}(-1/5)_2$ and $\mathcal{R}^{(1)}(-1/5)_3$ into the spectrum. $\mathcal{R}^{(1)}(0)_4$ actually acquires the role of the vacuum representation.

4.6 Representations and fusion product for general augmented $c_{p,q}$ models

In this section we conjecture fusion rules for general augmented $c_{p,q}$ models; we furthermore discuss their spectrum of representations which is to be consistent with the symmetry and associativity of the fusion product. This conjecture is mainly substantiated by the thorough exploration of the full fusion algebra for the lower lying representations of the augmented model $c_{2,3} = 0$ in section 4.4. In addition, we have checked the proposed rules as well as the existence of the lowest rank 2 and rank 3 indecomposable representations for a considerable number of fusion products in the augmented Yang-Lee model at $c_{2,5} = -22/5$ in section 4.5. The explicitly calculated fusion products are listed in appendix B.

4.6.1 The spectrum of representations

For weights on the border and corners of the Kac table the situation looks much the same as in the $c_{p,1}$ augmented model case [45]. States corresponding to weights on corners only generate irreducible representations. States with weights on the Kac-table border, however, also form rank 2 indecomposable representations in addition to irreducible ones. These rank 2 indecomposable representations are of the same form as described in [45, 44]. They are either generated by two groundstates whose weights are given by the lowest weight of one of the weight chains corresponding to the Kac table border, see figure 4.1 **A**, or by two successive weights in the weight chain, as in figure 4.1 **B**. For case **A** we actually do not need a further parameter to describe the representation; in case **B** one further parameter β is sufficient—it is taken to parameterise the equation

$$(L_1)^l |h + l; 1\rangle = \beta |h\rangle. \quad (4.17)$$

As we can see in figure 4.1 these representations can actually be thought to consist of several towers of states, each generated from a basic state by application of negative Virasoro modes; these towers of states are very close to the corresponding irreducible representations of the same weight as they exhibit the same number of nullvectors at the levels given by the Kac table and, hence, the same number of states. They (usually) are, however, not irreducible; but we can think of them as former irreducible representations which have been indecomposably connected to form an indecomposable representation. This indecomposable connection expresses itself by the indecomposable action of L_0 as well as the non-trivial action of a few of the positive Virasoro modes. We need three such towers to build the indecomposable representation in case **A**, four in case **B**.

The weights in the bulk of the Kac table exhibit an even richer structure as they also form rank 3 representations of the Virasoro algebra. Let us first describe the rank 2 representations. All possibilities of choosing one weight each from two adjacent sets in the weight chain will deliver the weights of the two generating states of a bulk rank

2 representation which is generically unique. Only in case that this set of two weights $h(r_1, s_1), h(r_2, s_2)$ contains the lowest weight of this weight chain, let it be $h(r_1, s_1)$, there are still two possible representations with this set of weights. The additional index is given by the level w of the weight in the second set of the weight chain which is not (!) the first possible nullvector on $h(r_2, s_2)$, i.e. which is not equal to $h(r_2, s_2) + r_2 s_2$. The nullvector structure of these bulk rank 2 representations is a generalisation of the one on the border. There are four different types of nullvector structure, depicted in figure 4.1. The types **G** and **H** are very similar to the case on the border and also need only one additional parameter β taken to parameterise equation (4.17). The novel feature of types **I** and **K** is that they exhibit a first nullvector already below the level of the first logarithmic partner. This makes it necessary to at least present two non-zero parameters to describe these representations. They have to be chosen as described for the examples in section 4.4. Conjecturally, two is also a sufficient number of parameters. Figure 4.1 also shows that all four possible types of bulk rank 2 representations can be split up into four towers of states in the above described spirit.

But the really new feature of the possible bulk representations are rank 3 representations. These need four generating states and are found in two different types. The first of these two types is generated by two states of the lowest weight of this weight chain as well as two states which are of the same weight in the second set of this weight chain. This type is realised for the two lowest rank 3 representations for a given bulk weight chain. The example $\mathcal{R}^{(3)}(0, 0, 1, 1)$ is described in section 4.4.1 and depicted in figure 4.4. As discussed there, one can actually build this representation by connecting three rank 2 bulk representations roughly according to figure 4.1 **A**. Then, there is only one additional parameter which is necessary to describe the representation.

The second type, which is supposedly the generic one, is generated by states of weights from three adjacent sets in a bulk weight chain—we have to take both weights from the middle set as well as one from each of the other two. This renders all possible rank 3 representations. They are uniquely described by this set of four generating weights. The example $\mathcal{R}^{(3)}(0, 1, 2, 5)$, its defining parameters and its composition of rank 2 representations have been discussed in section 4.4.1. This representation could be composed by indecomposably connecting four bulk rank 2 representations, roughly following figure 4.1 **B**. Unfortunately, this is the only example of this supposedly generic type of rank 3 representation which is at our grasp up to the level where the rank 3 behaviour appears for the first time. Hence, these generalisations have to be taken with the necessary caution, but nevertheless, they are motivated by similar generalisations for the rank 2 representations. However, we expect the necessity to introduce more defining parameters in cases where there appear more nullvectors on levels lower than the first rank 3 Jordan cell.

Knowing how to compose the rank 3 representations of rank 2 representations we automatically get the split-up of the whole rank 3 representation into towers of states as discussed above for the rank 2 case.

Last but not least we still have to describe the spectrum of irreducible representations corresponding to weights in the Kac table bulk. The calculations for $c_{2,3} = 0$

and $c_{2,5} = -22/5$ (see sections 4.4.3 and 4.5) show that it is not possible to include irreducible representations corresponding to weights in the bulk which appear in the Kac table of the corresponding non-augmented minimal model $c_{p,q}$, i.e. weights in the Kac table segment $1 \leq r < q$, $1 \leq s < p$. These weights exactly correspond to the lowest weight of each bulk weight chain. As shown in the examples the inclusion of these irreducible representations would simply violate the symmetry and associativity of the fusion product. On the other hand, the fusion of the border and corner irreducible representations produces rank 2 representations $\mathcal{R}^{(2)}(h(r_1, s_1), h(r_2, s_2))_w$ which contain the lowest weights of the corresponding bulk weight chain, let it be $h(r_1, s_1)$ in this case, as a generating state. This lowest weight state even generates an indecomposable subrepresentation of $\mathcal{R}^{(2)}(h(r_1, s_1), h(r_2, s_2))_w$ which does not exhibit higher rank behaviour. As they are subrepresentations of existing representations, these kinds of representations have to appear in the spectrum as well and will be denoted by $\mathcal{R}^{(1)}(h(r_1, s_1))_{h(r_2, s_2) - h(r_1, s_1)}$. In the fusion rules (r_1, s_1) appears to be that entry in the minimal model Kac table which does not have its nullvector at $h(r_2, s_2)$. Hence, (r_1, s_1) seems to be sufficient to describe this rank 1 representation and we can set

$$\mathcal{R}_{(r_1, s_1)}^{(1)}(h(r_1, s_1)) := \mathcal{R}^{(1)}(h(r_1, s_1))_{h(r_2, s_2) - h(r_1, s_1)}.$$

This is the first example of a case where a rank 1 indecomposable representation on a weight h appears in the spectrum although the corresponding irreducible representation on h cannot be included consistently. The other weights in the bulk of the Kac table induce ordinary irreducible representations which are consistent with the fusion algebra.

4.6.2 The fusion of irreducible representations

Consider first the fusion of two irreducible representations. If we describe an irreducible representation $\mathcal{V}_{(r,s)}^i(h)$ corresponding to a conformal weight h on a corner or a border in the Kac table, we choose the index (r, s) with the smallest product rs . If there are two pairs with the same product, we choose the one with larger r (although this last point is mere convention and does not effect the result). Then, the fusion product for $i, j \in \{\text{corner}, \text{border}\}$ simply amounts to the untruncated BPZ-rules

$$\left(\mathcal{V}_{(r_1, s_1)}^i(h_1) \otimes \mathcal{V}_{(r_2, s_2)}^j(h_2) \right)_f = \sum_{\substack{r_3 = |r_1 - r_2| + 1 \\ \text{step 2}}}^{r_1 + r_2 - 1} \sum_{\substack{s_3 = |s_1 - s_2| + 1 \\ \text{step 2}}}^{s_1 + s_2 - 1} \tilde{\mathcal{V}}_{(r_3, s_3)} \Big|_{\text{rules}}. \quad (4.18)$$

On the right hand side, however, we do not simply encounter a sum over irreducible representations again. Some of the resulting $\tilde{\mathcal{V}}_{(r,s)}$ are automatically combined into rank 2 or rank 3 representations. The corresponding **rules** how to do this combination (indicated as constraints in the equation) are given by:

1. For (r, s) on a corner $\tilde{\mathcal{V}}_{(r,s)}$ is simply replaced by the corresponding irreducible representation $\mathcal{V}_{(r,s)}^{\text{corner}}(h(r, s))$.

2. Concerning the set of all (r, s) on the right hand side of (4.18) which correspond to weights on the border there are two possibilities how to encounter rank 2 representations. If we find twice the same weight $h(r_1, s_1) = h(r_2, s_2)$ which is the lowest of a weight chain these two need to be replaced by the rank 2 representation $\mathcal{R}^{(2)}(h(r_1, s_1), h(r_2, s_2))$. Then, if we find two weights $h(m_1, m_1), h(m_2, m_2)$ of the same weight chain adjacent to each other in the chain, these need to be replaced by $\mathcal{R}^{(2)}(h(m_1, n_1), h(m_2, n_2))$. All other weights in this set simply form irreducible representations and are replaced by $\mathcal{V}_{(r,s)}^{\text{border}}(h(r, s))$.
3. For the set of all (r, s) on the right hand side of (4.18) which correspond to weights in the bulk we first need to identify the rank 3 representations. Rank 3 representations need four generating states of the two possible types described in the preceding subsection: either the two lowest weights and twice the same weight of the second set of a bulk weight chain; or weights from three adjacent sets of a bulk weight chain—both weights of the middle set and one from each of the other two. The last is the generic case. If we encounter a set of four weights in this manner we need to replace them by the rank 3 representation $\mathcal{R}^{(3)}(h(r_1, s_1), h(r_2, s_2), h(r_3, s_3), h(r_4, s_4))$.
4. Rank 2 representations need two generating states. For bulk representations these consist of one weight each from two adjacent sets in the weight chain. If this set of two weights $h(r_1, s_1), h(r_2, s_2)$ contains the lowest weight of this weight chain, let it be $h(r_1, s_1)$, there are still two possible representations with this set of weights. The additional index is given by the level w of the weight in the third set of the weight chain which is not (!) the first possible nullvector on $h(r_2, s_2)$, i.e. which is not equal to $h(r_2, s_2) + r_2 s_2$. Every two weights of this form have to be replaced by the rank 2 representation $\mathcal{R}^{(2)}(h(r_1, s_1), h(r_2, s_2))_w$.
5. After extraction of all rank 3 and rank 2 representations from the set of all (r, s) within the bulk we find to each lowest weight $h(r_1, s_1)$ of a bulk weight chain a corresponding weight $h(r_2, s_2)$ of the second tuple of this weight chain. These form the rank 1 indecomposable representation $\mathcal{R}^{(1)}(h(r_1, s_1))_{h(r_2, s_2) - h(r_1, s_1)}$.
6. All (r, s) corresponding to weights in the bulk which have not been used up in the three preceding points have to be replaced by $\mathcal{V}_{(r,s)}(h(r, s))$.

This set of rules requires the following remarks:

- Unfortunately, one cannot write down the fusion rules for general augmented theories in such an elegant manner as for the augmented $c_{p,1}$ models [45]. First of all, we do not have border representations just on one side such that a restriction to an infinite strip of the Kac-table nicely promotes the first border conformal weights beyond that strip to corresponding rank 2 representations. Nevertheless, the property that the second conformal weight to a border conformal weight (ordered by the level of their first nullvectors, resp. products rs) somehow represents

the rank 2 representation seems to persist. Secondly, for the bulk there are simply not enough entries in the Kac table in order to uniquely label all different irreducible, rank 2 and rank 3 representations.

- The fifth rule which describes the appearance of $\mathcal{R}^{(1)}(h(r_1, s_1))_{h(r_2, s_2) - h(r_1, s_1)}$ is not needed for the fusion of border and corner representations with itself. Actually, the examples show that starting with border and corner representations the whole fusion closes without the inclusion of any irreducible or rank 1 representation corresponding to weights in the bulk. It is only the appearance of these irreducible or rank 1 representations as subrepresentations of rank 2 and rank 3 representations that makes us include these in the theory. We advocate that it is only this setting they should be thought of to exist in. This point of view is strongly stressed by the existence of the above discussed rank 1 representations on the lowest weights of the bulk weight chains. Indeed, only their embedding in a rank 2 representation makes the absence of one of the first two nullvectors possible as it prevents this singular vector (which itself spans an irreducible subrepresentation of the rank 1 representation) to be a nullvector in the whole space of states.

If we want to write down the fusion product with representations corresponding to conformal weights in the bulk we need more information than the first nullvector. For these we choose as index the set of the two pairs $\{(r_1, s_1), (r_2, s_2)\}$ with the two lowest products $r_1 s_1, r_2 s_2$. As there are exactly as many entries in the Kac table for these bulk representations as there are nullvectors in the nullvector cascade and as all these nullvectors in the cascade are mutually distinct, this choice is unique. Using $A(r, m) := \{|r - m| + 1, |r - m| + 3, \dots, r + m - 1\}$ we define the following two sets

$$\begin{aligned} S_{\text{eb}}(r, s | m_1, n_1, m_2, n_2) \\ := \{(p, q) | p \in A(r, m_1), q \in A(s, n_1)\} \cap \{(p, q) | p \in A(r, m_2), q \in A(s, n_2)\} \end{aligned}$$

as well as

$$\begin{aligned} S_{\text{bb}}(r_1, s_1, r_2, s_2 | m_1, n_1, m_2, n_2) \\ := \left(\{(p, q) | p \in A(r_1, m_1), q \in A(s_1, n_1)\} \cap \{(p, q) | p \in A(r_2, m_2), q \in A(s_2, n_2)\} \right) \\ \cup \left(\{(p, q) | p \in A(r_2, m_1), q \in A(s_2, n_1)\} \cap \{(p, q) | p \in A(r_1, m_2), q \in A(s_1, n_2)\} \right). \end{aligned}$$

These define the parameter ranges in the following fusion rules with bulk representations, $i \in \{\text{corner}, \text{border}\}$,

$$\begin{aligned} \left(\mathcal{V}_{(r,s)}^i(h_1) \otimes \mathcal{V}_{\{(m_1, n_1), (m_2, n_2)\}}^{\text{bulk}}(h_2) \right)_{\text{f}} &= \sum_{(s,t) \in S_{\text{eb}}(r, s | m_1, n_1, m_2, n_2)} \tilde{\mathcal{V}}_{(s,t)} \Big|_{\text{rules}} \\ \left(\mathcal{V}_{\{(r_1, s_1), (r_2, s_2)\}}^{\text{bulk}}(h_1) \otimes \mathcal{V}_{\{(m_1, n_1), (m_2, n_2)\}}^{\text{bulk}}(h_2) \right)_{\text{f}} &= \sum_{(s,t) \in S_{\text{bb}}(r_1, s_1, r_2, s_2 | m_1, n_1, m_2, n_2)} \tilde{\mathcal{V}}_{(s,t)} \Big|_{\text{rules}}. \end{aligned}$$

The fusion rules for the rank 1 indecomposable representations actually look much the same as for border and corner representations, $i \in \{\text{corner}, \text{border}\}$,

$$\begin{aligned} \left(\mathcal{R}_{(r_1, s_1)}^{(1)}(h_1) \otimes \mathcal{V}_{(r_2, s_2)}^i(h_2) \right)_f &= \sum_{\substack{r_3=r_1+r_2-1 \\ \text{step 2}}} \sum_{\substack{s_3=s_1+s_2-1 \\ \text{step 2}}} \tilde{\mathcal{V}}_{(r_3, s_3)} \Big|_{\text{rules}}, \\ \left(\mathcal{R}_{(r_1, s_1)}^{(1)}(h_1) \otimes \mathcal{R}_{(r_2, s_2)}^{(1)}(h_2) \right)_f &= \sum_{\substack{r_3=r_1+r_2-1 \\ \text{step 2}}} \sum_{\substack{s_3=s_1+s_2-1 \\ \text{step 2}}} \tilde{\mathcal{V}}_{(r_3, s_3)} \Big|_{\text{rules}}, \\ \left(\mathcal{R}_{(r, s)}^{(1)}(h_1) \otimes \mathcal{V}_{\{(m_1, n_1), (m_2, n_2)\}}^{\text{bulk}}(h_2) \right)_f &= \sum_{(s, t) \in S_{\text{eb}}(r, s | m_1, n_1, m_2, n_2)} \tilde{\mathcal{V}}_{(s, t)} \Big|_{\text{rules}}. \end{aligned}$$

It is only the rule (5) we have to modify slightly in this case:

- 5'. After extraction of all rank 3 and rank 2 representations from the set of all (r, s) each lowest weight $h(r_1, s_1)$ of a bulk weight chain corresponds to the rank 1 indecomposable representation $\mathcal{R}_{(r_1, s_1)}^{(1)}(h(r_1, s_1))$.

The reason is that treating the rank 1 indecomposable representations as generated from one state we will also get only one generating state for each rank 1 indecomposable representation in the fusion process.

4.6.3 The fusion with higher rank representations

Now, we can give the fusion rules with higher rank representations based on the above calculated fusion rules. These higher rank fusion rules make use of the above elaborated fact that all higher rank representations can be constructed by indecomposably connecting a number of representations of one rank lower. Certainly, these constituents are usually no true subrepresentations. But nevertheless they exhibit in sum the same number of states as the composed higher representation and even their nullvector structure survives in a certain way as “special” vectors of the new larger representation. E.g. generically one needs four $\mathcal{V}_{(r, s)}$ representations to compose a rank 2 representation.

The following general rules for fusion with higher rank representations apply successively with rising rank:

1. First split one higher rank representation into its constituents of one rank lower.
2. Calculate the fusion rules with these constituents as known before (or iterate this process until you reach a level where the fusion rules are already known).
3. If you now find the right constituents for a higher rank representation within the result (e.g. all four $\tilde{\mathcal{V}}$ for a generic rank 2 representation) you have to combine them to this higher rank representation. All other parts of the total result remain as they are. This re-introduces the indecomposable structure which has been broken up in step one where possible.

4. The one exception to the last step applies to the indecomposable rank 1 representations $\mathcal{R}^{(1)}(h(r_1, s_1))_{h(r_2, s_2) - h(r_1, s_1)}$ on the lowest weight $h(r_1, s_1)$ of a weight chain. Whenever we find that instead of $\mathcal{R}^{(1)}(h(r_1, s_1))_{h(r_2, s_2) - h(r_1, s_1)}$ the corresponding subrepresentation $\mathcal{V}(h(r_2, s_2))$ can be used as a building block of a rank 2 representation we need to replace $\mathcal{R}^{(1)}(h(r_1, s_1))_{h(r_2, s_2) - h(r_1, s_1)}$ by $\mathcal{V}(h(r_2, s_2))$. We then proceed as described in the preceding step.

This last case is only encountered if we fuse irreducible bulk representations with higher rank bulk representations. Its artificiality stems from the fact that the irreducible bulk representations only exist as subrepresentations of the rank 2 representations—it is these rank 2 representations we actually have to look at when considering fusion rules. Let us give two examples of the $c_{2,3} = 0$ fusion to show how these rules work

$$\begin{aligned}
\mathcal{V}(5/8) \otimes_f \mathcal{R}^{(2)}(5/8, 5/8) &\xrightarrow{\text{split-up}} \mathcal{V}(5/8) \otimes_f \left(2\mathcal{V}(5/8) \oplus \mathcal{V}(21/8) \right) \\
&= 2\mathcal{R}^{(2)}(0, 2)_7 \oplus \mathcal{R}^{(2)}(1, 5) \\
&\xrightarrow{\text{re-combination}} \mathcal{R}^{(3)}(0, 0, 2, 2) \\
\mathcal{V}(5/8) \otimes_f \mathcal{R}^{(2)}(1/3, 1/3) &\xrightarrow{\text{split-up}} \mathcal{V}(5/8) \otimes_f \left(2\mathcal{V}(1/3) \oplus \mathcal{V}(10/3) \right) \\
&= 2\mathcal{V}(-1/24) \oplus \mathcal{V}(35/24) \\
&\xrightarrow{\text{re-combination}} 2\mathcal{V}(-1/24) \oplus \mathcal{V}(35/24) .
\end{aligned}$$

These fusion rules for higher rank representations, finally, complete the set of fusion rules for general augmented $c_{p,q}$ models.

Chapter 5

Conclusion

But it was a neat theory, and he was in love with it. The only consolation he drew from the present chaos was that his theory managed to explain it.

Thomas Pynchon: *V*.

In summary, this thesis contains work in two different areas which seek to extend the success story of conformal field theory: the extension of the symmetry algebra by inclusion of supersymmetry as well as the relaxation of conformal field theory to logarithmic conformal field theory.

In the first part of this thesis, we have examined the moduli space of $N = (4, 4)$ superconformal field theories with central charge $c = 6$ which corresponds to the moduli space of sigma models on compact four-dimensional manifolds obeying the Calabi-Yau conditions. In particular, we have discussed the K3 component of this moduli space. We have shown that the two subvarieties of \mathbb{Z}_2 and \mathbb{Z}_4 orbifolds intersect in one point within the K3 moduli space by giving an explicit isomorphism of the respective lattices and four-planes which describe the corresponding theories on the two subvarieties. We have also given an isomorphism of the corresponding CFT models at the intersection point. Up to now, this identification had only been known by indirect arguments using the orbifold procedure. Furthermore, we have argued that both subvarieties are indeed orthogonal to each other at the point of intersection. We have then used the geometric data of the identification in order to relate the coordinates of the two subvarieties and, finally, to determine a geometric geodesic between these two subvarieties. This is already an important step towards the exploration of generic points in K3 moduli space which can be reached via such a geodesic originating in a known model. To complete this project we need the corresponding geodesic of conformal field theory which has to be found by methods of conformal deformation theory. Although an integration of a conformal deformation along such a geodesic has not yet been achieved we have commented on advances in this most difficult point of the above exploration. The main difficulty arises from the fact that we have not yet found a suitable regularisation in

this strictly two-dimensional setting which is at the same time unique for the whole model, meaningful as well as calculable.

In the second part of the thesis we have elaborated higher rank indecomposable structures in the context of logarithmic conformal field theories. We have, in particular, inspected a special series of logarithmic CFT models, the augmented $c_{p,q}$ models, which are a generalisation of the well known augmented $c_{p,1}$ models. For both types of models we have constructed logarithmic nullvectors, i.e. nullvectors which include descendants of higher Jordan level. But most importantly, we have calculated the lower Virasoro representation content as well as the fusion algebra for two examples of these augmented $c_{p,q}$ models, the augmented $c_{2,3} = 0$ model as well as the augmented Yang-Lee model at $c_{2,5} = -22/5$. In order to perform these calculations we have implemented the Nahm algorithm for the determination of the fusion product on the computer. These models exhibit a much richer structure than the augmented $c_{p,1}$ models with several new rank 2 and, for the first time, rank 3 representations. We have elaborated these new rank 3 representations in great detail.

The results of these calculations seem to be sufficiently generic so that we have conjectured the field content and the fusion algebra for general augmented $c_{p,q}$ models. These conjectured fusion rules still inherit much of the BPZ fusion structure. The main generalisation lies in the fact that we do not interpret the BPZ fusion rules “minimally” for these models. This “minimal” refers to the BPZ fusion rules for the non-augmented minimal models where one takes a section over all ways of applying the untruncated BPZ rules. The augmented fusion rules allow for definitely more representation content. This is, however, in perfect accordance with and directly reduces to the already known rules for the special case of augmented $c_{p,1}$ models in [45].

There are two particularly astonishing features about these results. First of all, we have shown that the fusion rules are not associative in general. This lack of associativity has very good physical reasons, though. Let us denote the irreducible representations of weights in the Kac table domain of the proper minimal model by $\mathcal{V}(h_i)$ and the additional irreducible representations which we want to add in the augmented models by $\mathcal{V}'(h'_j)$. Then, it is impossible to combine these two sets of representations $\mathcal{V}(h_i)$ and $\mathcal{V}'(h'_j)$ into one consistent conformal field theory; within the augmented theory the weights in the Kac table domain of the corresponding proper minimal model only appear for generating states in reducible but indecomposable representations. This is due to mathematical arguments which we have developed for the augmented $c_{2,3} = 0$ and the augmented Yang-Lee model explicitly and which generalise to all augmented $c_{p,q}$ models. In particular, we do not have an irreducible vacuum representation, which would be located in this domain, either. However, in both examples there is a very sound vacuum representation which is a rank 1 indecomposable but not irreducible subrepresentation of a rank 2 representation.

The second astonishing feature consists in the observation that the rank 3 representations seem to be composed of rank 2 representations in exactly the same way as the rank 2 representations are composed of irreducible ones. This is a very nice structural property of these logarithmic CFT models.

Our explicit construction of the representations in the augmented $c_{2,3} = 0$ theory settles the long standing puzzle of how a consistent non-trivial $c = 0$ theory with logarithmic behaviour might look like. This has a direct impact on models with central charge $c = 0$ for several interesting physical phenomena as e.g. percolation [140, 141, 142, 61], quenched disorder models [143, 144], or the dilute case in polymer physics [36]. In particular, the construction of a consistent vacuum representation and character remained an open question within the above mentioned models up to now. As the $h = 0$ representation exhibits a singular vector on level 2, it was especially not clear how to define a sensible energy momentum tensor; all suggestions of how to solve this problem were either inconsistent or incomplete (see [61] for a more extensive discussion of this problem). In this thesis we have constructed such a consistent vacuum representation $\mathcal{R}^{(1)}(0)_2$ which also includes the energy momentum tensor in a natural way.

Finally, we have seen that three of the augmented $c_{2,3} = 0$ representations perfectly fit the numerically calculated state content of representations in a $c = 0$ model in [41] which describes an XXZ quantum spin chain. This opens a new connection of logarithmic CFT to quantum spin chains which will hopefully lead to a fruitful exchange between these two fields of research. In particular, it is a very interesting question whether the augmented Yang-Lee model as well as the other augmented $c_{p,q}$ models are also linked to quantum spin chains in a similar fashion. Besides the great interest in spin chains within the string theory community, these models are also important for a variety of other physical models as stochastic processes, especially certain growth models, or the integer quantum Hall effect (see e.g. [41, 145]).

There are certainly numerous ways to continue from the results of this thesis. Concerning the K3 moduli space the main problem of how to consistently regularise the deformation integrals such that we can integrate a deformation along a geodesic still remains open. As already mentioned, a free field construction of a Gepner model or a torus orbifold model in K3 moduli space would greatly amend this problem. Indeed, the continuation of a model given in a free field construction by continuation of its central charge should provide a regularisation scheme which is at the same time unique for the whole model, meaningful in that respect that it actually locates the singularities and calculable. The orthogonality of the two subvarieties proven in this thesis might also be of some help. At the point of intersection it allows us to describe some of the nontrivial twistfield deformations of one type of orbifold by the well known torus type deformations of the other. This might enable us to test and to understand more about these nontrivial twistfield deformations which also describe deformations towards the unknown regions of moduli space from a generic orbifold theory and which are usually much harder to compute. A further unsolved problem that might be analysed this way is the curious symmetry which we observed in the dependence of the deformation of a vertex operator in an orbifold model on the conformal dimension about the point $h = 1/8$ [103]. The deformation integrals discussed in this thesis are aimed at describing the deformation of the conformal weights of CFT models along the geodesic, i.e. the deformation of their spectra. This information would already provide crucial new insights. However, in order to completely control the new CFT models along that

geodesic one still needs to calculate the deformation of the three point functions and, hence, of the structure constants as well. The methods should stay pretty much the same, the integrals to be calculated, though, will become even more complicated.

Concerning the logarithmic CFT side of this thesis one can certainly use the explicitly constructed higher rank nullvectors to calculate corresponding correlation functions and, hence, analyse the physical dynamics of these theories. This would have to proceed along the lines indicated in [58].

However, the main open question for the augmented $c_{p,q}$ models is to find the complete symmetry algebra of the theory. As the augmented $c_{p,1}$ models are known to include an enhanced triplet \mathcal{W} -algebra $\mathcal{W}(2, 2p-1, 2p-1, 2p-1)$ the natural question arises whether the general augmented $c_{p,q}$ models exhibit a similar enhanced symmetry algebra. Indeed, one finds a set of modular functions which can be associated to a $c_{p,q}$ model and which seem to allow the incorporation of higher rank representations similarly to the $c_{p,1}$ model case (as in [49]). And even the mere fact that the Virasoro fusion rules so nicely generalise from the $c_{p,1}$ model case with the known triplet \mathcal{W} -algebra is a further good hint for a larger symmetry algebra. This may be exemplified by the existence of a representation like $\mathcal{V}(7)$ in the $c_{2,3} = 0$ model whose fusion rules behave in just the same way as the ones of the “spin representation” $\mathcal{V}_{1,p}$ in the $c_{p,1}$ models. Indeed, in the $c_{p,1}$ models this spin representation behaves roughly like a square root of the \mathcal{W} -representation.

The representation of the modular group given by the above mentioned set of modular functions is already very restrictive; e.g. in case of the $c_{2,3} = 0$ model it suffices to know the field content up to level 7 in order to precisely pinpoint the full \mathcal{W} -representation. We believe that this restrictiveness together with our new knowledge of the precise structure of the Virasoro representations should lead to a consistent set of modular functions which represent the right \mathcal{W} -characters. Following the lines of [50] the S matrix of these characters should, then, lead to an adapted version of celebrated Verlinde formula and should, thus, yield reasonable fusion rules for the \mathcal{W} -representations. This is subject to ongoing research [135].

On the other hand, it does not seem too far out of reach to construct generic \mathcal{W} -nullvectors along the lines set out in this work. The knowledge of such nullvectors would enable us to prove rationality, or at least C_2 -cofiniteness, for augmented $c_{p,q}$ models using the approach of [52]. One might also think about whether the Kazhdan-Lusztig correspondence of [146, 147] could be generalised to augmented $c_{p,q}$ models and, hence, reveals a deep relation between these models and quantum groups.

Furthermore, it could be interesting to examine tensor products of these models in order to obtain conformal field theories with higher central charge. Certainly, these are not unitary theories as in the Gepner model case. But inspired by the Gepner construction one could think about whether such tensor products, restricted in a suitable manner, describe string theory on non-trivial non-compact spaces or even multiple Schramm-Loewner evolution.

In the end, it is astonishing to see that the two seemingly quite different approaches to extend conformal field theory as presented in this work, supersymmetry and loga-

rithmic CFT, might be connected by some deeper relation. On the one hand, $N = 2$ supersymmetric models in the context of polymers and percolation seem to exhibit indecomposable behaviour [35, 36], and a WZW model on the supergroup $GL(1|1)$ also implies logarithmic CFT [148]. On the other hand, fields of particular higher rank representations can be consistently combined in a superfield formalism [59, 60]. However, it seems too early to ascertain whether the considerations in both of these directions within this work will contribute to a deeper understanding of this relation.

Acknowledgements

This work would not have been possible without the support of many people and institutions. First and foremost I would like to thank my supervisor Prof. Dr. Werner Nahm for his guidance, many ingenious ideas, and his never ending interest in this work. I am particularly grateful to my co-supervisor Dr. Michael Flohr for his collaboration on logarithmic CFT and for all his encouragement and enthusiasm, which helped me overcome difficult times during my PhD. I am also grateful to Prof. Dr. Hans-Peter Nilles for acting as second referee for this thesis.

Many other people have contributed to this thesis with scientific discussions or good ideas, in the progress of the work as well as in finding its dead ends. In this respect I am particularly indebted to Prof. Dr. Rainald Flume, Dr. Stefan Förste, Dr. Alexander Nichols, Prof. Dr. Stefan Weinzierl, Dr. Katrin Wendland, and Prof. Dr. Alexander B. Zamolodchikov. Furthermore, I would like to thank the Bonn Condensed Matter Theory Group for the kind permission to use their computer cluster.

I am thankful to all members of the theory department of the Physical Institute Bonn for a pleasant and stimulating work atmosphere throughout the whole time of my Masters and PhD theses, in particular to the members of the Nahm and Flohr groups, to David Heilmann and Dr. Martin Walter, to our always helpful “secretaries” (rather managers) Dagmar Faßbender and Patricia Zündorf, and last but definitely not least to our “Mädchen für alles” Dr. Andreas Wißkirchen.

I would like to thank the Studienstiftung des Deutschen Volkes and in particular my “Vertrauensdozent” Prof. Dr. Hans-Martin Seitz for their support throughout my studies and PhD thesis and for providing me with numerous stimuli on the scientific as well as on the non-scientific level. Moreover, I am thankful to the Dublin Institute for Advanced Studies and all the people there for their hospitality during parts of this work.

Such a huge project would never have found its good end without the right support in the non-scientific world. I am very grateful to my parents Ingrid and Gerd who also made it possible for me to study physics in the first place. And, I would not have survived this PhD thesis without the never ending, sharing love and support of my dear Katrin!

Appendix A

Explicit Jordan diagonalisation of L_0 for rank 3 representations

In this appendix we want to present a basis of states for the lowest levels of several rank 3 representations which we regard in this thesis. These bases are chosen in such a way that the L_0 matrix appears in a Jordan diagonal form. The vectors of the bases are denoted by n_i with a running index as assigned by the computer programme. (The indices are chosen anew for each representation!) Vectors which are not shown to be equal to descendants of some other vectors are understood to be generating states. On the right hand side of each table we have denoted only the Jordan block in L_0 for the respective states. Different Jordan blocks are separated by lines. All other L_0 entries are zero.

A.1 $\mathcal{R}^{(3)}(0, 0, 1, 1)$

The generating states for $\mathcal{R}^{(3)}(0, 0, 1, 1)$ are denoted by n_2 , n_3 , n_5 and n_6 at levels 0, 0, 1, 1 respectively. We give the explicit states up to level 5.

states	L_0 matrix
n_2	0 1
n_3	0 0
$n_4 = L_{-1} n_2$	1 1 0
n_5	0 1 1
n_6	0 0 1
$n_{19} = L_{-1} n_3 - n_5$	1
$n_7 = L_{-1}^2 n_2$	2 1 0
$n_8 = L_{-1} n_5$	0 2 1
$n_9 = L_{-1} n_6$	0 0 2
$n_{20} = (L_{-2} - \frac{3}{2} L_{-1}^2) n_3$	2
$n_{32} = L_{-1}^2 n_3 - L_{-1} n_5 = L_{-1} n_{19}$	2

states	L_0 matrix
$n_{10} = L_{-2}L_{-1}n_2$	3 1 0
$n_{11} = L_{-2}n_5$	0 3 1
$n_{12} = L_{-2}n_6$	0 0 3
$n_{23} = L_{-1}^3n_2$	3 1 0
$n_{24} = L_{-1}^2n_5$	0 3 1
$n_{25} = L_{-1}^2n_6$	0 0 3
$n_{33} = (L_{-3} + L_{-2}L_{-1} - \frac{3}{2}L_{-1}^3)n_3 = L_{-1}n_{20}$	3
$n_{42} = L_{-2}L_{-1}n_3 - L_{-2}n_5 = L_{-2}n_{19}$	3
$n_{49} = L_{-1}^3n_3 - L_{-1}^2n_5 = L_{-1}^2n_{19}$	3
$n_{13} = L_{-3}L_{-1}n_2$	4 1 0
$n_{14} = L_{-3}n_5$	0 4 1
$n_{15} = L_{-3}n_6$	0 0 4
$n_{26} = L_{-2}L_{-1}^2n_2$	4 1 0
$n_{27} = L_{-2}L_{-1}n_5$	0 4 1
$n_{28} = L_{-2}L_{-1}n_6$	0 0 4
$n_{36} = L_{-1}^4n_2$	4 1 0
$n_{37} = L_{-1}^3n_5$	0 4 1
$n_{38} = L_{-1}^3n_6$	0 0 4
$n_{43} = (2L_{-4} + 2L_{-3}L_{-1} + L_{-2}L_{-1}^2 - \frac{3}{2}L_{-1}^4)n_3 = L_{-1}^2n_{20}$	4
$n_{50} = L_{-3}L_{-1}n_3 - L_{-3}n_5 = L_{-3}n_{19}$	4
$n_{55} = (L_{-2}^2 - \frac{3}{2}L_{-2}L_{-1}^2)n_3 = L_{-2}n_{20}$	4
$n_{59} = L_{-2}L_{-1}^2n_3 - L_{-2}L_{-1}n_5 = L_{-2}L_{-1}n_{19}$	4
$n_{62} = L_{-1}^4n_3 - L_{-1}^3n_5 = L_{-1}^3n_{19}$	4
$n_{16} = L_{-4}L_{-1}n_2$	5 1 0
$n_{17} = L_{-4}n_5$	0 5 1
$n_{18} = L_{-4}n_6$	0 0 5
$n_{29} = L_{-3}L_{-1}^2n_2$	5 1 0
$n_{30} = L_{-3}L_{-1}n_5$	0 5 1
$n_{31} = L_{-3}L_{-1}n_6$	0 0 5
$n_{39} = L_{-2}^2L_{-1}n_2$	5 1 0
$n_{40} = L_{-2}^2n_5$	0 5 1
$n_{41} = L_{-2}^2n_6$	0 0 5
$n_{46} = L_{-2}L_{-1}^3n_2$	5 1 0
$n_{47} = L_{-2}L_{-1}^2n_5$	0 5 1
$n_{48} = L_{-2}L_{-1}^2n_6$	0 0 5
$n_{51} = (L_{-1}^4 - 4L_{-4} - \frac{20}{3}L_{-2}L_{-1}^2 + 4L_{-3}L_{-1} + 4L_{-2}^2)n_5$	5 1
$n_{52} = (L_{-1}^4 - 4L_{-4} - \frac{20}{3}L_{-2}L_{-1}^2 + 4L_{-3}L_{-1} + 4L_{-2}^2)n_6$	0 5
$n_{56} = (L_{-5} + L_{-3}L_{-2} + L_{-2}^2L_{-1} - \frac{3}{2}L_{-2}L_{-1}^3)n_3 = L_{-2}L_{-1}n_{20}$	5
$n_{60} = L_{-4}L_{-1}n_3 - L_{-4}n_5 = L_{-4}n_{19}$	5
$n_{63} = (L_{-3}L_{-2} - \frac{3}{2}L_{-3}L_{-1}^2)n_3 = L_{-3}n_{20}$	5
$n_{64} = L_{-3}L_{-1}^2n_3 - L_{-3}L_{-1}n_5 = L_{-3}L_{-1}n_{19}$	5
$n_{65} = L_{-2}^2L_{-1}n_3 - L_{-2}^2n_5 = L_{-2}^2n_{19}$	5
$n_{66} = L_{-2}L_{-1}^3n_3 - L_{-2}L_{-1}^2n_5 = L_{-2}L_{-1}^2n_{19}$	5

A.2 $\mathcal{R}^{(3)}(0, 0, 2, 2)$

For $\mathcal{R}^{(3)}(0, 0, 2, 2)$ we have the four generating states n_{15} , n_{16} , n_{18} and n_{19} at levels 0, 0, 2, 2 respectively. We give the explicit states up to level 4. The fact that rank 3 cell

descendants seem to have states with different descendant moding is an effect of normal ordering. Let us take the rank 3 cell at level 3. Then $L_{-1} n_{17} = L_{-1} L_{-2} n_{15}$ equates to $L_{-3} n_{15}$ by normal ordering and usage of the nullvector condition $L_{-1} n_{15} = 0$. Hence, this whole rank 3 cell is the usual level 1 descendant of the rank 3 cell at level 2.

states	L_0 matrix
n_{15}	0 1
n_{16}	0 0
$n_0 = L_{-1} n_{16}$	1
$n_{17} = L_{-2} n_{15}$	2 1 0
n_{18}	0 2 1
n_{19}	0 0 2
$n_{26} = L_{-2} n_{16} - n_{18}$	2
$n_{41} = L_{-1}^2 n_{16}$	2
$n_{20} = L_{-3} n_{15} = L_{-1} n_{17}$	3 1 0
$n_{21} = L_{-1} n_{18}$	0 3 1
$n_{22} = L_{-1} n_{19}$	0 0 3
$n_{27} = (L_{-3} + L_{-2} L_{-1}) n_{16} - L_{-1} n_{18} = L_{-1} n_{26}$	3
$n_{42} = L_{-2} L_{-1} n_{16}$	3
$n_{50} = L_{-1}^3 n_{16}$	3
$n_{23} = L_{-2}^2 n_{15} = L_{-2} n_{17}$	4 1 0
$n_{24} = L_{-2} n_{18}$	0 4 1
$n_{25} = L_{-2} n_{19}$	0 0 4
$n_{38} = L_{-4} n_{15} = \frac{1}{2} L_{-1}^2 n_{17}$	4 1 0
$n_{39} = \frac{1}{2} L_{-1}^2 n_{18}$	0 4 1
$n_{40} = \frac{1}{2} L_{-1}^2 n_{19}$	0 0 4
$n_{43} = (2L_{-4} + 2L_{-3}L_{-1} + L_{-2}L_{-1}^2) n_{16} - L_{-1}^2 n_{18} = L_{-1}^2 n_{26}$	4
$n_{51} = L_{-3} L_{-1} n_{16}$	4
$n_{56} = L_{-2}^2 n_{16} - L_{-2} n_{18} = L_{-2} n_{26}$	4
$n_{59} = L_{-2} L_{-1}^2 n_{16}$	4
$n_{60} = L_{-1}^4 n_{16}$	4

A.3 $\mathcal{R}^{(3)}(0, 1, 2, 5)$

The generating states for this representation are n_0 , n_5 , n_{24} and n_{18} at levels 0, 1, 2, 5 respectively. We give the explicit states up to level 5, the first appearance of the full rank 3 structure.

states	L_0 matrix
n_0	0
$n_4 = L_{-1} n_0$	1 1
n_5	0 1
$n_6 = L_{-1}^2 n_0 = L_{-1} n_4$	2 1
$n_7 = L_{-1} n_5$	0 2
$n_{23} = L_{-2} n_0$	2 1
n_{24}	0 2

states	L_0 matrix
$n_8 = L_{-2}L_{-1}n_0 = L_{-2}n_4$	3 1
$n_9 = L_{-2}n_5$	0 3
$n_{25} = L_{-1}^3n_0 = L_{-1}^2n_4$	3 1
$n_{26} = L_{-1}^2n_5$	0 3
$n_{38} = (L_{-3} + L_{-2}L_{-1})n_0 = L_{-1}n_{23}$	3 1
$n_{39} = L_{-1}n_{24}$	0 3
$n_{10} = L_{-3}L_{-1}n_0 = L_{-3}n_4$	4 1
$n_{11} = L_{-3}n_5$	0 4
$n_{27} = L_{-2}L_{-1}^2n_0 = L_{-2}L_{-1}n_4$	4 1
$n_{28} = L_{-2}L_{-1}n_5$	0 4
$n_{40} = L_{-2}^2n_0 = L_{-2}n_{23}$	4 1
$n_{41} = L_{-2}n_{24}$	0 4
$n_{48} = L_{-1}^4n_0 = L_{-1}^3n_4$	4 1
$n_{49} = L_{-1}^3n_5$	0 4
$n_{56} = (2L_{-4} + 2L_{-3}L_{-1} + L_{-2}L_{-1}^2)n_0 = L_{-1}^2n_{23}$	4 1
$n_{57} = L_{-1}^2n_{24}$	0 4
$n_{16} = \frac{4655}{31758}(L_{-4}L_{-1} - L_{-3}L_{-1}^2 + \frac{5}{3}L_{-2}L_{-1}^3 - L_{-2}^2L_{-1} - \frac{1}{4}L_{-1}^5)n_0$	5 1 0
$n_{17} = \frac{4655}{63516}\left((L_{-4} - \frac{5}{2}L_{-3}L_{-1} - L_{-2}^2 + \frac{19}{6}L_{-2}L_{-1}^2 - \frac{1}{2}L_{-1}^4)n_5 + (L_{-3} - L_{-2}L_{-1} + \frac{1}{6}L_{-1}^3)n_{24}\right)$	0 5 1
n_{18}	0 0 5
$n_{29} = L_{-3}L_{-1}^2n_0 = L_{-3}L_{-1}n_4$	5 1
$n_{30} = L_{-3}L_{-1}n_5$	0 5
$n_{42} = L_{-3}L_{-2}n_0 = L_{-3}n_{23}$	5 1
$n_{43} = L_{-3}n_{24}$	0 5
$n_{50} = L_{-2}^2L_{-1}n_0 = L_{-2}^2n_4$	5 1
$n_{51} = L_{-2}^2n_5$	0 5
$n_{58} = L_{-2}L_{-1}^3n_0 = L_{-2}L_{-1}^2n_4$	5 1
$n_{59} = L_{-2}L_{-1}^2n_5$	0 5
$n_{63} = L_{-1}^5n_0 = L_{-1}^4n_4$	5 1
$n_{64} = L_{-1}^4n_5$	0 5
$n_{68} = (6L_{-5} + 6L_{-4}L_{-1} + 3L_{-3}L_{-1}^2 + L_{-2}L_{-1}^3)n_0 = L_{-1}^3n_{23}$	5 1
$n_{69} = L_{-1}^3n_{24}$	0 5
$n_{70} = (L_{-4} + \frac{1}{2}L_{-3}L_{-1} - L_{-2}^2 + \frac{1}{6}L_{-2}L_{-1}^2)n_5 - (L_{-3} - L_{-2}L_{-1} + \frac{1}{6}L_{-1}^3)n_{24}$	5

Appendix B

Explicit fusion rules for two augmented models

In this appendix we give the explicit results of the fusion product calculation for two augmented minimal models with central charges $c_{2,3} = 0$ and $c_{2,3} = -22/5$. There are two different types of calculations which we used to obtain these fusion products and which are described in more detail in the main part of this dissertation. The first method uses the computer implementation of the Nahm algorithm and is used for the fusion of irreducible and rank 1 representations with themselves as well as with rank 2 representations. Besides the result the corresponding tables contain the level L at which we calculated the new representation as well as the maximal level \tilde{L} up to which we took the corresponding constraints into account. The second method uses the consistency conditions of symmetry and associativity of the fusion product and is used to infer the fusion of higher rank representations from the already known fusion of the lower rank and irreducible representations.

When applying the first method the computational power restricts the level L at which the fused representations are calculated. These restrictions are unfortunately quite severe for the fusion with higher representations. Hence, it was sometimes not possible to reach a high enough L to actually see the indecomposable structure of all component representations of the result. We, nevertheless, denoted the result as we would expect it according to the proposed fusion rules—to discern this guessed higher representations from the explicit results we indicated them by a question mark. But certainly our results are always in agreement with these possible higher rank representations up to the level L given in the table.

B.1 Fusion rules for $c_{2,3} = 0$

The following table contains the results of our explicit calculations of the fusion product of irreducible and rank 1 representations with each other in the augmented $c_{2,3} = 0$ model. The first column gives the representations to be fused. Then the level L at

which we calculated the new representation as well as the maximal level \tilde{L} up to which we took the corresponding constraints into account are given. The last column contains the result.

		L	\tilde{L}_{\max}	Fusion product
$\mathcal{V}(5/8)$	$\otimes_f \mathcal{V}(5/8)$	6	11	$\mathcal{R}^{(2)}(0, 2)_7$
	$\otimes_f \mathcal{V}(1/3)$	6	11	$\mathcal{V}(-1/24)$
	$\otimes_f \mathcal{V}(1/8)$	7	8	$\mathcal{R}^{(2)}(0, 1)_5$
	$\otimes_f \mathcal{V}(-1/24)$	6	9	$\mathcal{R}^{(2)}(1/3, 1/3)$
	$\otimes_f \mathcal{V}(33/8)$	6	11	$\mathcal{R}^{(2)}(2, 7)$
	$\otimes_f \mathcal{V}(10/3)$	6	7	$\mathcal{V}(35/24)$
	$\otimes_f \mathcal{V}(21/8)$	6	11	$\mathcal{R}^{(2)}(1, 5)$
	$\otimes_f \mathcal{V}(35/24)$	5	7	$\mathcal{R}^{(2)}(1/3, 10/3)$
	$\otimes_f \mathcal{V}(2)$	6	9	$\mathcal{V}(5/8)$
	$\otimes_f \mathcal{V}(1)$	6	9	$\mathcal{V}(1/8)$
	$\otimes_f \mathcal{V}(7)$	6	9	$\mathcal{V}(33/8)$
	$\otimes_f \mathcal{V}(5)$	6	9	$\mathcal{V}(21/8)$
$\mathcal{V}(1/3)$	$\otimes_f \mathcal{V}(1/3)$	6	11	$\mathcal{R}^{(2)}(0, 2)_5 \oplus \mathcal{V}(1/3)$
	$\otimes_f \mathcal{V}(1/8)$	6	9	$\mathcal{R}^{(2)}(1/8, 1/8)$
	$\otimes_f \mathcal{V}(-1/24)$	6	9	$\mathcal{R}^{(2)}(5/8, 5/8) \oplus \mathcal{V}(-1/24)$
	$\otimes_f \mathcal{V}(33/8)$	6	9	$\mathcal{V}(35/24)$
	$\otimes_f \mathcal{V}(10/3)$	6	9	$\mathcal{R}^{(2)}(1, 7) \oplus \mathcal{V}(10/3)$
	$\otimes_f \mathcal{V}(21/8)$	6	9	$\mathcal{R}^{(2)}(5/8, 21/8)$
	$\otimes_f \mathcal{V}(35/24)$	5	7	$\mathcal{R}^{(2)}(1/8, 33/8) \oplus \mathcal{V}(35/24)$
	$\otimes_f \mathcal{V}(2)$	6	9	$\mathcal{V}(1/3)$
	$\otimes_f \mathcal{V}(1)$	6	9	$\mathcal{R}^{(2)}(0, 1)_7$
	$\otimes_f \mathcal{V}(7)$	6	9	$\mathcal{V}(10/3)$
$\otimes_f \mathcal{V}(5)$	6	9	$\mathcal{R}^{(2)}(2, 5)$	
$\mathcal{V}(1/8)$	$\otimes_f \mathcal{V}(1/8)$	6	8	$\mathcal{R}^{(2)}(1/3, 1/3) \oplus \mathcal{R}^{(2)}(0, 2)_7$
	$\otimes_f \mathcal{V}(-1/24)$	6	7	$\mathcal{R}^{(3)}(0, 0, 1, 1)$
	$\otimes_f \mathcal{V}(33/8)$	6	9	$\mathcal{R}^{(2)}(1, 5)$
	$\otimes_f \mathcal{V}(10/3)$	6	8	$\mathcal{R}^{(2)}(5/8, 21/8)$
	$\otimes_f \mathcal{V}(21/8)$	5	7	$\mathcal{R}^{(2)}(1/3, 10/3) \oplus \mathcal{R}^{(2)}(2, 7)$
	$\otimes_f \mathcal{V}(35/24)$	5	7	$\mathcal{R}^{(3)}(0, 1, 2, 5)$
	$\otimes_f \mathcal{V}(2)$	6	9	$\mathcal{V}(1/8)$
	$\otimes_f \mathcal{V}(1)$	5	7	$\mathcal{V}(5/8) \oplus \mathcal{V}(-1/24)$
	$\otimes_f \mathcal{V}(7)$	6	8	$\mathcal{V}(21/8)$
	$\otimes_f \mathcal{V}(5)$	6	7	$\mathcal{V}(33/8) \oplus \mathcal{V}(35/24)$
$\mathcal{V}(-1/24)$	$\otimes_f \mathcal{V}(-1/24)$	5	7	$\mathcal{R}^{(3)}(0, 0, 2, 2) \oplus \mathcal{R}^{(2)}(1/3, 1/3)$
	$\otimes_f \mathcal{V}(21/8)$	5	7	$\mathcal{R}^{(3)}(0, 1, 2, 5)$
	$\otimes_f \mathcal{V}(35/24)$	4	6	$\mathcal{R}^{(3)}(0, 1, 2, 7)? \oplus \mathcal{R}^{(2)}(1/3, 10/3)$
	$\otimes_f \mathcal{V}(5)$	5	7	$\mathcal{R}^{(2)}(5/8, 21/8)$
	$\otimes_f \mathcal{V}(143/24)$	0	6	$\mathcal{R}^{(3)}(1, 5, 7, 15)? \oplus \mathcal{R}^{(2)}(10/3, 28/3)?$

	L	\tilde{L}_{\max}	Fusion product
$\mathcal{V}(33/8) \otimes_f \mathcal{V}(33/8)$	6	8	$\mathcal{R}^{(2)}(0, 2)_7 \oplus \mathcal{R}^{(2)}(7, 15)?$
$\otimes_f \mathcal{V}(10/3)$	5	7	$\mathcal{V}(-1/24) \oplus \mathcal{V}(143/24)$
$\otimes_f \mathcal{V}(-1/24)$	5	7	$\mathcal{R}^{(2)}(1/3, 10/3)$
$\otimes_f \mathcal{V}(21/8)$	5	7	$\mathcal{R}^{(2)}(0, 1)_5 \oplus \mathcal{R}^{(2)}(5, 12)?$
$\otimes_f \mathcal{V}(35/24)$	6	7	$\mathcal{R}^{(2)}(1/3, 1/3) \oplus \mathcal{R}^{(2)}(10/3, 28/3)$
$\otimes_f \mathcal{V}(1)$	6	9	$\mathcal{V}(21/8)$
$\otimes_f \mathcal{V}(7)$	5	7	$\mathcal{V}(5/8) \oplus \mathcal{V}(85/8)$
$\otimes_f \mathcal{V}(5)$	6	8	$\mathcal{V}(1/8) \oplus \mathcal{V}(65/8)$
$\mathcal{V}(10/3) \otimes_f \mathcal{V}(10/3)$	5	7	$\mathcal{R}^{(2)}(0, 2)_5 \oplus \mathcal{R}^{(2)}(5, 15)? \oplus \mathcal{V}(1/3) \oplus \mathcal{V}(28/3)$
$\otimes_f \mathcal{V}(-1/24)$	5	7	$\mathcal{R}^{(2)}(1/8, 33/8) \oplus \mathcal{V}(35/24)$
$\otimes_f \mathcal{V}(21/8)$	5	7	$\mathcal{R}^{(2)}(1/8, 1/8) \oplus \mathcal{R}^{(2)}(33/8, 65/8)$
$\otimes_f \mathcal{V}(35/24)$	4	6	$\mathcal{R}^{(2)}(5/8, 5/8) \oplus \mathcal{R}^{(2)}(21/8, 85/8)? \oplus \mathcal{V}(-1/24)$ $\oplus \mathcal{V}(143/24)$
$\otimes_f \mathcal{V}(5)$	3	9	$\mathcal{R}^{(2)}(0, 1)_7 \oplus \mathcal{R}^{(2)}(7, 12)?$
$\mathcal{V}(21/8) \otimes_f \mathcal{V}(21/8)$	4	6	$\mathcal{R}^{(2)}(1/3, 1/3) \oplus \mathcal{R}^{(2)}(10/3, 28/3)? \oplus \mathcal{R}^{(2)}(0, 2)_7$ $\oplus \mathcal{R}^{(2)}(7, 15)?$
$\otimes_f \mathcal{V}(35/24)$	4	6	$\mathcal{R}^{(3)}(0, 0, 1, 1) \oplus \mathcal{R}^{(3)}(2, 5, 7, 12)?$
$\mathcal{V}(35/24) \otimes_f \mathcal{V}(35/24)$	3	5	$\mathcal{R}^{(3)}(0, 0, 2, 2) \oplus \mathcal{R}^{(3)}(1, 5, 7, 15)? \oplus \mathcal{R}^{(2)}(1/3, 1/3)$ $\oplus \mathcal{R}^{(2)}(10/3, 28/3)?$
$\mathcal{V}(2) \otimes_f \mathcal{V}(-1/24)$	6	9	$\mathcal{V}(-1/24)$
$\otimes_f \mathcal{V}(33/8)$	6	8	$\mathcal{V}(33/8)$
$\otimes_f \mathcal{V}(10/3)$	6	7	$\mathcal{V}(10/3)$
$\otimes_f \mathcal{V}(21/8)$	6	9	$\mathcal{V}(21/8)$
$\otimes_f \mathcal{V}(35/24)$	5	7	$\mathcal{V}(35/24)$
$\otimes_f \mathcal{V}(2)$	6	9	$\mathcal{R}^{(1)}(0)_2$
$\otimes_f \mathcal{V}(1)$	6	9	$\mathcal{R}^{(1)}(0)_1$
$\otimes_f \mathcal{V}(7)$	6	9	$\mathcal{V}(7)$
$\otimes_f \mathcal{V}(5)$	6	9	$\mathcal{V}(5)$
$\otimes_f \mathcal{R}^{(1)}(0)_2$	6	9	$\mathcal{V}(2)$
$\otimes_f \mathcal{R}^{(1)}(0)_1$	6	9	$\mathcal{V}(1)$
$\mathcal{V}(1) \otimes_f \mathcal{V}(-1/24)$	5	7	$\mathcal{R}^{(2)}(1/8, 1/8)$
$\otimes_f \mathcal{V}(10/3)$	5	7	$\mathcal{R}^{(2)}(2, 5)$
$\otimes_f \mathcal{V}(21/8)$	5	7	$\mathcal{V}(33/8) \oplus \mathcal{V}(35/24)$
$\otimes_f \mathcal{V}(35/24)$	5	7	$\mathcal{R}^{(2)}(5/8, 21/8)$
$\otimes_f \mathcal{V}(1)$	6	8	$\mathcal{R}^{(1)}(0)_2 \oplus \mathcal{V}(1/3)$
$\otimes_f \mathcal{V}(7)$	5	7	$\mathcal{V}(5)$
$\otimes_f \mathcal{V}(5)$	5	7	$\mathcal{V}(7) \oplus \mathcal{V}(10/3)$

		L	\tilde{L}_{\max}	Fusion product
$\mathcal{V}(7)$	$\otimes_f \mathcal{V}(-1/24)$	5	7	$\mathcal{V}(35/24)$
	$\otimes_f \mathcal{V}(10/3)$	5	7	$\mathcal{V}(1/3) \oplus \mathcal{V}(28/3)$
	$\otimes_f \mathcal{V}(21/8)$	5	7	$\mathcal{V}(1/8) \oplus \mathcal{V}(65/8)$
	$\otimes_f \mathcal{V}(35/24)$	4	6	$\mathcal{V}(-1/24) \oplus \mathcal{V}(143/24)$
	$\otimes_f \mathcal{V}(7)$	5	7	$\mathcal{R}^{(1)}(0)_2 \oplus \mathcal{V}(15)$
	$\otimes_f \mathcal{V}(5)$	5	7	$\mathcal{R}^{(1)}(0)_1 \oplus \mathcal{V}(12)$
$\mathcal{V}(5)$	$\otimes_f \mathcal{V}(21/8)$	3	6	$\mathcal{V}(5/8) \oplus \mathcal{V}(-1/24) \oplus \mathcal{V}(85/8) \oplus \mathcal{V}(143/24)$
	$\otimes_f \mathcal{V}(35/24)$	4	6	$\mathcal{R}^{(2)}(1/8, 1/8) \oplus \mathcal{R}^{(2)}(33/8, 65/8)$
	$\otimes_f \mathcal{V}(5)$	5	7	$\mathcal{R}^{(1)}(0)_2 \oplus \mathcal{V}(15) \oplus \mathcal{V}(1/3) \oplus \mathcal{V}(28/3)$
$\mathcal{R}^{(1)}(0)_2$	$\otimes_f \mathcal{V}(5/8)$	6	9	$\mathcal{V}(5/8)$
	$\otimes_f \mathcal{V}(1/3)$	6	9	$\mathcal{V}(1/3)$
	$\otimes_f \mathcal{V}(1/8)$	6	9	$\mathcal{V}(1/8)$
	$\otimes_f \mathcal{V}(-1/24)$	6	9	$\mathcal{V}(-1/24)$
	$\otimes_f \mathcal{V}(33/8)$	6	9	$\mathcal{V}(33/8)$
	$\otimes_f \mathcal{V}(10/3)$	6	9	$\mathcal{V}(10/3)$
	$\otimes_f \mathcal{V}(21/8)$	6	9	$\mathcal{V}(21/8)$
	$\otimes_f \mathcal{V}(35/24)$	6	9	$\mathcal{V}(35/24)$
	$\otimes_f \mathcal{V}(2)$	6	9	$\mathcal{V}(2)$
	$\otimes_f \mathcal{V}(1)$	6	9	$\mathcal{V}(1)$
	$\otimes_f \mathcal{V}(7)$	6	9	$\mathcal{V}(7)$
	$\otimes_f \mathcal{V}(5)$	6	9	$\mathcal{V}(5)$
	$\otimes_f \mathcal{R}^{(1)}(0)_2$	6	9	$\mathcal{R}^{(1)}(0)_2$
	$\otimes_f \mathcal{R}^{(1)}(0)_1$	6	9	$\mathcal{R}^{(1)}(0)_1$
$\mathcal{R}^{(1)}(0)_1$	$\otimes_f \mathcal{V}(5/8)$	6	9	$\mathcal{V}(1/8)$
	$\otimes_f \mathcal{V}(1/3)$	6	9	$\mathcal{R}^{(2)}(0, 1)_7$
	$\otimes_f \mathcal{V}(1/8)$	6	9	$\mathcal{V}(5/8) \oplus \mathcal{V}(-1/24)$
	$\otimes_f \mathcal{V}(-1/24)$	6	9	$\mathcal{R}^{(2)}(1/8, 1/8)$
	$\otimes_f \mathcal{V}(33/8)$	6	9	$\mathcal{V}(21/8)$
	$\otimes_f \mathcal{V}(10/3)$	6	9	$\mathcal{R}^{(2)}(2, 5)$
	$\otimes_f \mathcal{V}(21/8)$	6	9	$\mathcal{V}(33/8) \oplus \mathcal{V}(35/24)$
	$\otimes_f \mathcal{V}(35/24)$	6	9	$\mathcal{R}^{(2)}(5/8, 21/8)$
	$\otimes_f \mathcal{V}(2)$	6	9	$\mathcal{V}(1)$
	$\otimes_f \mathcal{V}(1)$	6	9	$\mathcal{V}(2) \oplus \mathcal{V}(1/3)$
	$\otimes_f \mathcal{V}(7)$	6	9	$\mathcal{V}(5)$
	$\otimes_f \mathcal{V}(5)$	6	9	$\mathcal{V}(7) \oplus \mathcal{V}(10/3)$
	$\otimes_f \mathcal{R}^{(1)}(0)_2$	6	9	$\mathcal{R}^{(1)}(0)_1$
	$\otimes_f \mathcal{R}^{(1)}(0)_1$	6	9	$\mathcal{R}^{(1)}(0)_2 \oplus \mathcal{V}(1/3)$

The next table lists our results for the fusion of irreducible and rank 1 representations with rank 2 representations.

	L	\tilde{L}_{\max}	Fusion product
$\mathcal{V}(5/8) \otimes_f \mathcal{R}^{(2)}(5/8, 5/8)$	5	7	$\mathcal{R}^{(3)}(0, 0, 2, 2)$
$\otimes_f \mathcal{R}^{(2)}(1/3, 1/3)$	5	7	$2\mathcal{V}(-1/24) \oplus \mathcal{V}(35/24)$
$\otimes_f \mathcal{R}^{(2)}(1/8, 1/8)$	5	7	$\mathcal{R}^{(3)}(0, 0, 1, 1)$
$\otimes_f \mathcal{R}^{(2)}(5/8, 21/8)$	5	8	$\mathcal{R}^{(3)}(0, 1, 2, 5)$
$\otimes_f \mathcal{R}^{(2)}(1/3, 10/3)$	4	6	$\mathcal{V}(-1/24) \oplus 2\mathcal{V}(35/24) \oplus \mathcal{V}(143/24)$
$\otimes_f \mathcal{R}^{(2)}(1/8, 33/8)$	4	6	$\mathcal{R}(0, 1, 2, 7)?$
$\otimes_f \mathcal{R}^{(2)}(0, 1)_5$	4	6	$2\mathcal{V}(1/8) \oplus \mathcal{V}(21/8)$
$\otimes_f \mathcal{R}^{(2)}(0, 1)_7$	4	6	$\mathcal{R}^{(2)}(1/8, 1/8)$
$\otimes_f \mathcal{R}^{(2)}(0, 2)_5$	4	6	$\mathcal{R}^{(2)}(5/8, 5/8)$
$\otimes_f \mathcal{R}^{(2)}(0, 2)_7$	4	7	$2\mathcal{V}(5/8) \oplus \mathcal{V}(33/8)$
$\otimes_f \mathcal{R}^{(2)}(1, 5)$	4	6	$\mathcal{V}(1/8) \oplus 2\mathcal{V}(21/8) \oplus \mathcal{V}(65/8)$
$\otimes_f \mathcal{R}^{(2)}(2, 5)$	4	6	$\mathcal{R}^{(2)}(5/8, 21/8) \oplus \mathcal{V}(65/8)$
$\otimes_f \mathcal{R}^{(2)}(1, 7)$	4	8	$\mathcal{R}^{(2)}(1/8, 33/8)$
$\otimes_f \mathcal{R}^{(2)}(2, 7)$	4	7	$\mathcal{V}(5/8) \oplus 2\mathcal{V}(33/8) \oplus \mathcal{V}(85/8)$
$\mathcal{V}(1/3) \otimes_f \mathcal{R}^{(2)}(5/8, 5/8)$	5	7	$\mathcal{R}^{(2)}(5/8, 21/8) \oplus 2\mathcal{V}(-1/24)$
$\otimes_f \mathcal{R}^{(2)}(1/3, 1/3)$	5	7	$\mathcal{R}^{(3)}(0, 0, 2, 2) \oplus \mathcal{R}^{(2)}(1/3, 1/3)$
$\otimes_f \mathcal{R}^{(2)}(1/8, 1/8)$	4	7	$2\mathcal{R}^{(2)}(1/8, 1/8) \oplus \mathcal{V}(35/24)$
$\otimes_f \mathcal{R}^{(2)}(5/8, 21/8)$	3	10	$2\mathcal{R}^{(2)}(5/8, 21/8) \oplus \mathcal{V}(-1/24) \oplus \mathcal{V}(143/24)$
$\otimes_f \mathcal{R}^{(2)}(1/3, 10/3)$	3	6	$\mathcal{R}^{(3)}(0, 1, 2, 7)? \oplus \mathcal{R}^{(2)}(1/3, 10/3)$
$\otimes_f \mathcal{R}^{(2)}(1/8, 33/8)$	4	7	$\mathcal{R}^{(2)}(1/8, 1/8) \oplus \mathcal{R}^{(2)}(33/8, 65/8) \oplus 2\mathcal{V}(35/24)$
$\otimes_f \mathcal{R}^{(2)}(0, 1)_5$	4	6	$\mathcal{R}^{(3)}(0, 0, 1, 1)$
$\otimes_f \mathcal{R}^{(2)}(0, 1)_7$	4	6	$2\mathcal{R}^{(2)}(0, 1)_7 \oplus \mathcal{V}(10/3)$
$\otimes_f \mathcal{R}^{(2)}(0, 2)_5$	4	7	$\mathcal{R}^{(2)}(2, 5) \oplus 2\mathcal{V}(1/3)$
$\otimes_f \mathcal{R}^{(2)}(0, 2)_7$	4	6	$\mathcal{R}^{(2)}(1/3, 1/3)$
$\otimes_f \mathcal{R}^{(2)}(1, 5)$	5	9	$\mathcal{R}^{(3)}(0, 1, 2, 5)$
$\otimes_f \mathcal{R}^{(2)}(2, 5)$	4	6	$2\mathcal{R}^{(2)}(2, 5) \oplus \mathcal{V}(1/3) \oplus \mathcal{V}(28/3)$
$\otimes_f \mathcal{R}^{(2)}(1, 7)$	4	8	$\mathcal{R}^{(2)}(0, 1)_7 \oplus \mathcal{R}^{(2)}(7, 12)? \oplus 2\mathcal{V}(10/3)$
$\otimes_f \mathcal{R}^{(2)}(2, 7)$	4	7	$\mathcal{R}^{(2)}(1/3, 10/3)$
$\mathcal{V}(1/8) \otimes_f \mathcal{R}^{(2)}(5/8, 5/8)$	5	7	$\mathcal{R}^{(3)}(0, 0, 1, 1) \oplus \mathcal{R}^{(2)}(1/3, 10/3)$
$\otimes_f \mathcal{R}^{(2)}(1/3, 1/3)$	5	7	$2\mathcal{R}^{(2)}(1/8, 1/8) \oplus \mathcal{R}^{(2)}(5/8, 21/8)$
$\otimes_f \mathcal{R}^{(2)}(1/8, 1/8)$	5	7	$\mathcal{R}^{(3)}(0, 0, 2, 2) \oplus 2\mathcal{R}^{(2)}(1/3, 1/3)$
$\otimes_f \mathcal{R}^{(2)}(5/8, 21/8)$	3	6	$\mathcal{R}^{(3)}(0, 1, 2, 7)? \oplus 2\mathcal{R}^{(2)}(1/3, 10/3)$
$\otimes_f \mathcal{R}^{(2)}(1/3, 10/3)$	3	6	$\mathcal{R}^{(2)}(1/8, 1/8) \oplus 2\mathcal{R}^{(2)}(5/8, 21/8) \oplus \mathcal{R}^{(2)}(33/8, 65/8)?$
$\otimes_f \mathcal{R}^{(2)}(1/8, 33/8)$	3	6	$\mathcal{R}^{(3)}(0, 1, 2, 5)? \oplus \mathcal{R}^{(2)}(1/3, 1/3) \oplus \mathcal{R}^{(2)}(10/3, 28/3)?$
$\otimes_f \mathcal{R}^{(2)}(0, 1)_5$	4	6	$2\mathcal{V}(5/8) \oplus \mathcal{V}(33/8) \oplus 2\mathcal{V}(-1/24) \oplus \mathcal{V}(35/24)$
$\otimes_f \mathcal{R}^{(2)}(0, 1)_7$	4	6	$\mathcal{R}^{(2)}(5/8, 5/8) \oplus 2\mathcal{V}(-1/24)$
$\otimes_f \mathcal{R}^{(2)}(0, 2)_5$	4	6	$\mathcal{R}^{(2)}(1/8, 1/8) \oplus \mathcal{V}(35/24)$
$\otimes_f \mathcal{R}^{(2)}(0, 2)_7$	4	7	$2\mathcal{V}(1/8) \oplus \mathcal{V}(21/8)$

	L	\tilde{L}_{\max}	Fusion product
$\mathcal{V}(1/8) \otimes_f \mathcal{R}^{(2)}(1, 5)$	3	6	$\mathcal{V}(5/8) \oplus 2\mathcal{V}(33/8) \oplus \mathcal{V}(85/8) \oplus \mathcal{V}(-1/24)$ $\oplus 2\mathcal{V}(-35/24) \oplus \mathcal{V}(143/24)$
$\otimes_f \mathcal{R}^{(2)}(2, 5)$	4	6	$\mathcal{R}^{(2)}(1/8, 33/8) \oplus 2\mathcal{V}(35/24)$
$\otimes_f \mathcal{R}^{(2)}(1, 7)$	3	8	$\mathcal{R}^{(2)}(5/8, 21/8) \oplus \mathcal{V}(-1/24) \oplus \mathcal{V}(143/24)$
$\otimes_f \mathcal{R}^{(2)}(2, 7)$	4	7	$\mathcal{V}(1/8) \oplus 2\mathcal{V}(21/8) \oplus \mathcal{V}(65/8)$
$\mathcal{V}(-1/24) \otimes_f \mathcal{R}^{(2)}(5/8, 5/8)$	4	6	$\mathcal{R}^{(3)}(0, 1, 2, 5)? \oplus 2\mathcal{R}^{(2)}(1/3, 1/3)$
$\otimes_f \mathcal{R}^{(2)}(1/3, 1/3)$	4	6	$2\mathcal{R}^{(2)}(5/8, 5/8) \oplus \mathcal{R}^{(2)}(1/8, 33/8) \oplus 2\mathcal{V}(-1/24)$ $\oplus \mathcal{V}(35/24)$
$\otimes_f \mathcal{R}^{(2)}(1/8, 1/8)$	4	6	$2\mathcal{R}^{(3)}(0, 0, 1, 1) \oplus \mathcal{R}^{(2)}(1/3, 10/3)$
$\otimes_f \mathcal{R}^{(2)}(5/8, 21/8)$	2	5	$2\mathcal{R}^{(3)}(0, 1, 2, 5)? \oplus \mathcal{R}^{(2)}(1/3, 1/3) \oplus \mathcal{R}^{(2)}(10/3, 28/3)?$
$\otimes_f \mathcal{R}^{(2)}(1/3, 10/3)$	2	5	$\mathcal{R}^{(2)}(5/8, 5/8) \oplus 2\mathcal{R}^{(2)}(1/8, 33/8)? \oplus \mathcal{R}^{(2)}(21/8, 85/8)?$ $\oplus \mathcal{V}(-1/24) \oplus 2\mathcal{V}(35/24) \oplus \mathcal{V}(143/24)$
$\otimes_f \mathcal{R}^{(2)}(1/8, 33/8)$	3	6	$\mathcal{R}(0, 0, 1, 1) \oplus \mathcal{R}(2, 5, 7, 12)? \oplus 2\mathcal{R}^{(2)}(1/3, 10/3)$
$\otimes_f \mathcal{R}^{(2)}(0, 1)_5$	4	6	$2\mathcal{R}^{(2)}(1/8, 1/8) \oplus \mathcal{R}^{(2)}(5/8, 21/8)$
$\otimes_f \mathcal{R}^{(2)}(0, 1)_7$	4	6	$2\mathcal{R}^{(2)}(1/8, 1/8) \oplus \mathcal{V}(35/24)$
$\otimes_f \mathcal{R}^{(2)}(0, 2)_5$	4	7	$\mathcal{R}^{(2)}(5/8, 21/8) \oplus 2\mathcal{V}(-1/24)$
$\otimes_f \mathcal{R}^{(2)}(0, 2)_7$	4	7	$2\mathcal{V}(-1/24) \oplus \mathcal{V}(35/24)$
$\otimes_f \mathcal{R}^{(2)}(1, 5)$	2	8	$\mathcal{R}^{(2)}(1/8, 1/8) \oplus 2\mathcal{R}^{(2)}(5/8, 21/8) \oplus \mathcal{R}^{(2)}(33/8, 65/8)?$
$\otimes_f \mathcal{R}^{(2)}(2, 5)$	3	6	$2\mathcal{R}^{(2)}(5/8, 21/8) \oplus \mathcal{V}(-1/24) \oplus \mathcal{V}(143/24)$
$\otimes_f \mathcal{R}^{(2)}(1, 7)$	2	8	$\mathcal{R}^{(2)}(1/8, 1/8) \oplus \mathcal{R}^{(2)}(33/8, 65/8)? \oplus 2\mathcal{V}(35/24)$
$\otimes_f \mathcal{R}^{(2)}(2, 7)$	3	6	$\mathcal{V}(-1/24) \oplus 2\mathcal{V}(35/24) \oplus \mathcal{V}(143/24)$
$\mathcal{V}(33/8) \otimes_f \mathcal{R}^{(2)}(5/8, 5/8)$	3	9	$\mathcal{R}^{(3)}(0, 1, 2, 7)?$
$\otimes_f \mathcal{R}^{(2)}(1/3, 1/3)$	3	9	$\mathcal{V}(-1/24) \oplus 2\mathcal{V}(35/24) \oplus \mathcal{V}(143/24)$
$\otimes_f \mathcal{R}^{(2)}(1/8, 1/8)$	3	7	$\mathcal{R}^{(3)}(0, 1, 2, 5)?$
$\otimes_f \mathcal{R}^{(2)}(5/8, 21/8)$	2	8	$\mathcal{R}^{(3)}(0, 0, 1, 1) \oplus \mathcal{R}^{(3)}(2, 5, 7, 12)?$
$\otimes_f \mathcal{R}^{(2)}(1/3, 10/3)$	1	9	$2\mathcal{V}(-1/24) \oplus 2\mathcal{V}(35/24) \oplus 2\mathcal{V}(143/24)$ $\oplus \mathcal{V}(323/24)$
$\otimes_f \mathcal{R}^{(2)}(1/8, 33/8)$	2	10	$\mathcal{R}(0, 0, 2, 2) \oplus \mathcal{R}^{(3)}(1, 5, 7, 15)?$
$\otimes_f \mathcal{R}^{(2)}(0, 1)_5$	3	9	$\mathcal{V}(1/8) \oplus 2\mathcal{V}(21/8) \oplus \mathcal{V}(65/8)$
$\otimes_f \mathcal{R}^{(2)}(0, 1)_7$	3	7	$\mathcal{R}^{(2)}(5/8, 21/8)$
$\otimes_f \mathcal{R}^{(2)}(0, 2)_5$	3	9	$\mathcal{R}^{(2)}(1/8, 33/8)?$
$\otimes_f \mathcal{R}^{(2)}(0, 2)_7$	3	9	$\mathcal{V}(5/8) \oplus 2\mathcal{V}(33/8) \oplus \mathcal{V}(85/8)$
$\otimes_f \mathcal{R}^{(2)}(1, 5)$	2	9	$2\mathcal{V}(1/8) \oplus 2\mathcal{V}(21/8) \oplus 2\mathcal{V}(65/8) \oplus \mathcal{V}(133/8)$
$\otimes_f \mathcal{R}^{(2)}(2, 5)$	2	9	$\mathcal{R}^{(2)}(1/8, 1/8) \oplus \mathcal{R}^{(2)}(33/8, 65/8)?$
$\otimes_f \mathcal{R}^{(2)}(1, 7)$	2	8	$\mathcal{R}^{(2)}(5/8, 5/8) \oplus \mathcal{R}^{(2)}(21/8, 85/8)?$
$\otimes_f \mathcal{R}^{(2)}(2, 7)$	2	9	$2\mathcal{V}(5/8) \oplus 2\mathcal{V}(33/8) \oplus 2\mathcal{V}(85/8) \oplus \mathcal{V}(161/8)$
$\mathcal{V}(10/3) \otimes_f \mathcal{R}^{(2)}(5/8, 5/8)$	2	8	$\mathcal{R}^{(2)}(1/8, 1/8) \oplus \mathcal{R}^{(2)}(33/8, 65/8)? \oplus 2\mathcal{V}(35/24)$
$\otimes_f \mathcal{R}^{(2)}(1/3, 1/3)$	2	8	$\mathcal{R}^{(3)}(0, 1, 2, 7)? \oplus \mathcal{R}^{(2)}(1/3, 10/3)?$
$\otimes_f \mathcal{R}^{(2)}(1/8, 1/8)$	2	8	$2\mathcal{R}^{(2)}(5/8, 21/8) \oplus \mathcal{V}(-1/24) \oplus \mathcal{V}(143/24)$
$\otimes_f \mathcal{R}^{(2)}(0, 1)_5$	2	8	$\mathcal{R}^{(3)}(0, 1, 2, 5)?$
$\otimes_f \mathcal{R}^{(2)}(0, 1)_7$	2	8	$2\mathcal{R}^{(2)}(2, 5)? \oplus \mathcal{V}(1/3) \oplus \mathcal{V}(28/3)$
$\otimes_f \mathcal{R}^{(2)}(0, 2)_5$	2	8	$\mathcal{R}^{(2)}(0, 1)_7 \oplus \mathcal{R}^{(2)}(7, 12)? \oplus 2\mathcal{V}(10/3)$
$\otimes_f \mathcal{R}^{(2)}(0, 2)_7$	2	8	$\mathcal{R}^{(2)}(1/3, 10/3)?$

	L	\tilde{L}_{\max}	Fusion product	
$\mathcal{V}(21/8) \otimes_f \mathcal{R}^{(2)}(5/8, 5/8)$	2	8	$\mathcal{R}^{(3)}(0, 1, 2, 5)? \oplus \mathcal{R}^{(2)}(1/3, 1/3) \oplus \mathcal{R}^{(2)}(10/3, 28/3)?$	
	$\otimes_f \mathcal{R}^{(2)}(1/3, 1/3)$	2	8	$\mathcal{R}^{(2)}(1/8, 1/8) \oplus 2\mathcal{R}^{(2)}(5/8, 21/8) \oplus \mathcal{R}^{(2)}(33/8, 65/8)?$
	$\otimes_f \mathcal{R}^{(2)}(1/8, 1/8)$	2	8	$\mathcal{R}^{(3)}(0, 1, 2, 7)? \oplus 2\mathcal{R}^{(2)}(1/3, 10/3)?$
	$\otimes_f \mathcal{R}^{(2)}(0, 1)_5$	2	8	$\mathcal{V}(5/8) \oplus 2\mathcal{V}(33/8) \oplus \mathcal{V}(85/8) \oplus \mathcal{V}(-1/24)$ $\oplus 2\mathcal{V}(35/24) \oplus \mathcal{V}(143/24)$
	$\otimes_f \mathcal{R}^{(2)}(0, 1)_7$	2	8	$\mathcal{R}^{(2)}(1/8, 33/8)? \oplus 2\mathcal{V}(35/24)$
	$\otimes_f \mathcal{R}^{(2)}(0, 2)_5$	2	8	$\mathcal{R}^{(2)}(5/8, 21/8) \oplus \mathcal{V}(-1/24) \oplus \mathcal{V}(143/24)$
	$\otimes_f \mathcal{R}^{(2)}(0, 2)_7$	2	8	$\mathcal{V}(1/8) \oplus 2\mathcal{V}(21/8) \oplus \mathcal{V}(65/8)$
	$\mathcal{V}(2) \otimes_f \mathcal{R}^{(2)}(5/8, 5/8)$	5	7	$\mathcal{R}^{(2)}(5/8, 5/8)$
$\otimes_f \mathcal{R}^{(2)}(1/3, 1/3)$		5	7	$\mathcal{R}^{(2)}(1/3, 1/3)$
$\otimes_f \mathcal{R}^{(2)}(1/8, 1/8)$		5	7	$\mathcal{R}^{(2)}(1/8, 1/8)$
$\otimes_f \mathcal{R}^{(2)}(5/8, 21/8)$		4	7	$\mathcal{R}^{(2)}(5/8, 21/8)$
$\otimes_f \mathcal{R}^{(2)}(1/3, 10/3)$		4	7	$\mathcal{R}^{(2)}(1/3, 10/3)$
$\otimes_f \mathcal{R}^{(2)}(1/8, 33/8)$		4	7	$\mathcal{R}^{(2)}(1/8, 33/8)$
$\otimes_f \mathcal{R}^{(2)}(0, 1)_5$		4	6	$\mathcal{R}^{(2)}(0, 1)_5$
$\otimes_f \mathcal{R}^{(2)}(0, 1)_7$		4	6	$\mathcal{R}^{(2)}(0, 1)_7$
$\otimes_f \mathcal{R}^{(2)}(0, 2)_5$		4	6	$\mathcal{R}^{(2)}(0, 2)_5$
$\otimes_f \mathcal{R}^{(2)}(0, 2)_7$		4	6	$\mathcal{R}^{(2)}(0, 2)_7$
$\otimes_f \mathcal{R}^{(2)}(1, 5)$		4	6	$\mathcal{R}^{(2)}(1, 5)$
$\otimes_f \mathcal{R}^{(2)}(2, 5)$		4	6	$\mathcal{R}^{(2)}(2, 5)$
$\otimes_f \mathcal{R}^{(2)}(1, 7)$		6	8	$\mathcal{R}^{(2)}(1, 7)$
$\otimes_f \mathcal{R}^{(2)}(2, 7)$		6	8	$\mathcal{R}^{(2)}(2, 7)$
$\mathcal{V}(1) \otimes_f \mathcal{R}^{(2)}(5/8, 5/8)$	5	7	$\mathcal{R}^{(2)}(1/8, 1/8) \oplus \mathcal{V}(35/24)$	
	$\otimes_f \mathcal{R}^{(2)}(1/3, 1/3)$	5	7	$\mathcal{R}^{(3)}(0, 0, 1, 1)$
	$\otimes_f \mathcal{R}^{(2)}(1/8, 1/8)$	5	7	$\mathcal{R}^{(2)}(5/8, 5/8) \oplus 2\mathcal{V}(-1/24)$
	$\otimes_f \mathcal{R}^{(2)}(5/8, 21/8)$	4	7	$\mathcal{R}^{(2)}(1/8, 33/8) \oplus 2\mathcal{V}(35/24)$
	$\otimes_f \mathcal{R}^{(2)}(1/3, 10/3)$	3	6	$\mathcal{R}^{(3)}(0, 1, 2, 5)?$
	$\otimes_f \mathcal{R}^{(2)}(1/8, 33/8)$	4	5	$\mathcal{R}^{(2)}(5/8, 21/8) \oplus \mathcal{V}(-1/24) \oplus \mathcal{V}(143/24)$
	$\otimes_f \mathcal{R}^{(2)}(0, 1)_5$	4	6	$\mathcal{R}^{(2)}(0, 2)_7 \oplus \mathcal{R}^{(2)}(1/3, 1/3)$
	$\otimes_f \mathcal{R}^{(2)}(0, 1)_7$	4	6	$\mathcal{R}^{(2)}(0, 2)_5 \oplus 2\mathcal{V}(1/3)$
	$\otimes_f \mathcal{R}^{(2)}(0, 2)_5$	4	7	$\mathcal{R}^{(2)}(0, 1)_7 \oplus \mathcal{V}(10/3)$
	$\otimes_f \mathcal{R}^{(2)}(0, 2)_7$	4	7	$\mathcal{R}^{(2)}(0, 1)_5$
	$\otimes_f \mathcal{R}^{(2)}(1, 5)$	4	6	$\mathcal{R}^{(2)}(2, 7)? \oplus \mathcal{R}^{(2)}(1/3, 10/3)$
	$\otimes_f \mathcal{R}^{(2)}(2, 5)$	4	6	$\mathcal{R}^{(2)}(1, 7)? \oplus 2\mathcal{V}(10/3)$
	$\otimes_f \mathcal{R}^{(2)}(1, 7)$	4	8	$\mathcal{R}^{(2)}(2, 5) \oplus \mathcal{V}(1/3) \oplus \mathcal{V}(28/3)$
	$\otimes_f \mathcal{R}^{(2)}(2, 7)$	4	7	$\mathcal{R}^{(2)}(1, 5)$
$\mathcal{V}(7) \otimes_f \mathcal{R}^{(2)}(5/8, 5/8)$	4	8	$\mathcal{R}^{(2)}(1/8, 33/8)$	
	$\otimes_f \mathcal{R}^{(2)}(1/3, 1/3)$	4	8	$\mathcal{R}^{(2)}(1/3, 10/3)$
	$\otimes_f \mathcal{R}^{(2)}(1/8, 1/8)$	4	9	$\mathcal{R}^{(2)}(5/8, 21/8)$
	$\otimes_f \mathcal{R}^{(2)}(5/8, 21/8)$	3	7	$\mathcal{R}^{(2)}(1/8, 1/8) \oplus \mathcal{R}^{(2)}(33/8, 65/8)?$
	$\otimes_f \mathcal{R}^{(2)}(1/3, 10/3)$	3	6	$\mathcal{R}^{(2)}(1/3, 1/3) \oplus \mathcal{R}^{(2)}(10/3, 28/3)?$
	$\otimes_f \mathcal{R}^{(2)}(1/8, 33/8)$	3	7	$\mathcal{R}^{(2)}(5/8, 5/8) \oplus \mathcal{R}^{(2)}(21/8, 85/8)?$

			L	\tilde{L}_{\max}	Fusion product	
$\mathcal{V}(7)$	\otimes_f	$\mathcal{R}^{(2)}(0, 1)_5$	4	6	$\mathcal{R}^{(2)}(1, 5)$	
	\otimes_f	$\mathcal{R}^{(2)}(0, 1)_7$	4	6	$\mathcal{R}^{(2)}(2, 5)$	
	\otimes_f	$\mathcal{R}^{(2)}(0, 2)_5$	6	7	$\mathcal{R}^{(2)}(1, 7)$	
	\otimes_f	$\mathcal{R}^{(2)}(0, 2)_7$	5	7	$\mathcal{R}^{(2)}(2, 7)$	
	\otimes_f	$\mathcal{R}^{(2)}(1, 5)$	4	6	$\mathcal{R}^{(2)}(0, 1)_5 \oplus \mathcal{R}^{(2)}(5, 12)?$	
	\otimes_f	$\mathcal{R}^{(2)}(2, 5)$	4	6	$\mathcal{R}^{(2)}(0, 1)_7 \oplus \mathcal{R}^{(2)}(7, 12)?$	
	\otimes_f	$\mathcal{R}^{(2)}(1, 7)$	3	6	$\mathcal{R}^{(2)}(0, 2)_5 \oplus \mathcal{R}^{(2)}(5, 15)?$	
	\otimes_f	$\mathcal{R}^{(2)}(2, 7)$	4	7	$\mathcal{R}^{(2)}(0, 2)_7 \oplus \mathcal{R}^{(2)}(7, 15)?$	
$\mathcal{V}(5)$	\otimes_f	$\mathcal{R}^{(2)}(5/8, 5/8)$	3	7	$\mathcal{R}^{(2)}(5/8, 21/8) \oplus \mathcal{V}(-1/24) \oplus \mathcal{V}(143/24)$	
	\otimes_f	$\mathcal{R}^{(2)}(1/3, 1/3)$	3	7	$\mathcal{R}^{(3)}(0, 1, 2, 5)?$	
	\otimes_f	$\mathcal{R}^{(2)}(1/8, 1/8)$	3	7	$\mathcal{R}^{(2)}(1/8, 33/8)? \oplus 2\mathcal{V}(35/24)$	
	\otimes_f	$\mathcal{R}^{(2)}(5/8, 21/8)$	2	8	$\mathcal{R}^{(2)}(5/8, 5/8) \oplus \mathcal{R}^{(2)}(21/8, 85/8)? \oplus 2\mathcal{V}(-1/24)$ $\oplus 2\mathcal{V}(143/24)$	
	\otimes_f	$\mathcal{R}^{(2)}(1/3, 10/3)$	2	8	$\mathcal{R}^{(3)}(0, 0, 1, 1) \oplus \mathcal{R}^{(3)}(2, 5, 7, 12)?$	
	\otimes_f	$\mathcal{R}^{(2)}(1/8, 33/8)$	2	8	$\mathcal{R}^{(2)}(1/8, 1/8) \oplus \mathcal{R}^{(2)}(33/8, 65/8)? \oplus 2\mathcal{V}(35/24)$ $\oplus \mathcal{V}(323/24)$	
	\otimes_f	$\mathcal{R}^{(2)}(0, 1)_5$	3	8	$\mathcal{R}^{(2)}(2, 7)? \oplus \mathcal{R}^{(2)}(1/3, 10/3)$	
	\otimes_f	$\mathcal{R}^{(2)}(0, 1)_7$	3	9	$\mathcal{R}^{(2)}(1, 7)? \oplus 2\mathcal{V}(10/3)$	
	\otimes_f	$\mathcal{R}^{(2)}(0, 2)_5$	3	8	$\mathcal{R}^{(2)}(2, 5) \oplus \mathcal{V}(1/3) \oplus \mathcal{V}(28/3)$	
	\otimes_f	$\mathcal{R}^{(2)}(0, 2)_7$	3	8	$\mathcal{R}^{(2)}(1, 5)?$	
	\otimes_f	$\mathcal{R}^{(2)}(1, 5)$	2	8	$\mathcal{R}^{(2)}(0, 2)_7 \oplus \mathcal{R}^{(2)}(7, 15)? \oplus \mathcal{R}^{(2)}(1/3, 1/3)$ $\oplus \mathcal{R}^{(2)}(10/3, 28/3)?$	
	\otimes_f	$\mathcal{R}^{(2)}(2, 5)$	2	8	$\mathcal{R}^{(2)}(0, 2)_5 \oplus \mathcal{R}^{(2)}(5, 15)? \oplus 2\mathcal{V}(1/3) \oplus 2\mathcal{V}(28/3)$	
	\otimes_f	$\mathcal{R}^{(2)}(1, 7)$	2	8	$\mathcal{R}^{(2)}(0, 1)_7 \oplus \mathcal{R}^{(2)}(7, 12)? \oplus 2\mathcal{V}(10/3) \oplus \mathcal{V}(55/3)$	
	\otimes_f	$\mathcal{R}^{(2)}(2, 7)$	2	8	$\mathcal{R}^{(2)}(0, 1)_5 \oplus \mathcal{R}^{(2)}(5, 12)?$	
	$\mathcal{R}^{(1)}(0)_2$	\otimes_f	$\mathcal{R}^{(2)}(5/8, 5/8)$	5	7	$\mathcal{R}^{(2)}(5/8, 5/8)$
		\otimes_f	$\mathcal{R}^{(2)}(1/3, 1/3)$	5	7	$\mathcal{R}^{(2)}(1/3, 1/3)$
\otimes_f		$\mathcal{R}^{(2)}(1/8, 1/8)$	5	7	$\mathcal{R}^{(2)}(1/8, 1/8)$	
\otimes_f		$\mathcal{R}^{(2)}(5/8, 21/8)$	4	7	$\mathcal{R}^{(2)}(5/8, 21/8)$	
\otimes_f		$\mathcal{R}^{(2)}(1/3, 10/3)$	4	7	$\mathcal{R}^{(2)}(1/3, 10/3)$	
\otimes_f		$\mathcal{R}^{(2)}(1/8, 33/8)$	4	7	$\mathcal{R}^{(2)}(1/8, 33/8)$	
\otimes_f		$\mathcal{R}^{(2)}(0, 1)_5$	5	7	$\mathcal{R}^{(2)}(0, 1)_5$	
\otimes_f		$\mathcal{R}^{(2)}(0, 1)_7$	5	7	$\mathcal{R}^{(2)}(0, 1)_7$	
\otimes_f		$\mathcal{R}^{(2)}(0, 2)_5$	5	7	$\mathcal{R}^{(2)}(0, 2)_5$	
\otimes_f		$\mathcal{R}^{(2)}(0, 2)_7$	5	7	$\mathcal{R}^{(2)}(0, 2)_7$	
\otimes_f		$\mathcal{R}^{(2)}(1, 5)$	4	7	$\mathcal{R}^{(2)}(1, 5)$	
\otimes_f		$\mathcal{R}^{(2)}(2, 5)$	4	7	$\mathcal{R}^{(2)}(2, 5)$	
\otimes_f		$\mathcal{R}^{(2)}(1, 7)$	6	7	$\mathcal{R}^{(2)}(1, 7)$	
\otimes_f		$\mathcal{R}^{(2)}(2, 7)$	6	7	$\mathcal{R}^{(2)}(2, 7)$	

	L	\tilde{L}_{\max}	Fusion product
$\mathcal{R}^{(1)}(0)_1 \otimes_f \mathcal{R}^{(2)}(5/8, 5/8)$	5	7	$\mathcal{R}^{(2)}(1/8, 1/8) \oplus \mathcal{V}(35/24)$
$\otimes_f \mathcal{R}^{(2)}(1/3, 1/3)$	5	7	$\mathcal{R}^{(3)}(0, 0, 1, 1)$
$\otimes_f \mathcal{R}^{(2)}(1/8, 1/8)$	5	7	$\mathcal{R}^{(2)}(5/8, 5/8) \oplus 2\mathcal{V}(-1/24)$
$\otimes_f \mathcal{R}^{(2)}(5/8, 21/8)$	4	7	$\mathcal{R}^{(2)}(1/8, 33/8) \oplus 2\mathcal{V}(35/24)$
$\otimes_f \mathcal{R}^{(2)}(1/3, 10/3)$	4	7	$\mathcal{R}^{(3)}(0, 1, 2, 5)?$
$\otimes_f \mathcal{R}^{(2)}(1/8, 33/8)$	4	7	$\mathcal{R}^{(2)}(5/8, 21/8) \oplus \mathcal{V}(-1/24) \oplus \mathcal{V}(143/24)$
$\otimes_f \mathcal{R}^{(2)}(0, 1)_5$	5	7	$\mathcal{R}^{(2)}(0, 2)_7 \oplus \mathcal{R}^{(2)}(1/3, 1/3)$
$\otimes_f \mathcal{R}^{(2)}(0, 1)_7$	5	7	$\mathcal{R}^{(2)}(0, 2)_5 \oplus 2\mathcal{V}(1/3)$
$\otimes_f \mathcal{R}^{(2)}(0, 2)_5$	5	7	$\mathcal{R}^{(2)}(0, 1)_7 \oplus \mathcal{V}(10/3)$
$\otimes_f \mathcal{R}^{(2)}(0, 2)_7$	5	7	$\mathcal{R}^{(2)}(0, 1)_5$
$\otimes_f \mathcal{R}^{(2)}(1, 5)$	4	7	$\mathcal{R}^{(2)}(2, 7)? \oplus \mathcal{R}^{(2)}(1/3, 10/3)$
$\otimes_f \mathcal{R}^{(2)}(2, 5)$	4	7	$\mathcal{R}^{(2)}(1, 7)? \oplus 2\mathcal{V}(10/3)$
$\otimes_f \mathcal{R}^{(2)}(1, 7)$	4	7	$\mathcal{R}^{(2)}(2, 5) \oplus \mathcal{V}(1/3) \oplus \mathcal{V}(28/3)$
$\otimes_f \mathcal{R}^{(2)}(2, 7)$	4	7	$\mathcal{R}^{(2)}(1, 5)$

In order to extract the fusion of higher rank representations we used the symmetry and associativity properties of the fusion product along the lines described in section 4.4.3. For these calculations we applied our explicit results of the Nahm algorithm in the form stated in the tables above. The results are listed below.

	Fusion product
$\mathcal{R}^{(2)}(5/8, 5/8) \otimes_f \mathcal{R}^{(2)}(5/8, 5/8)$	$2\mathcal{R}^{(3)}(0, 0, 2, 2) \oplus \mathcal{R}^{(3)}(0, 1, 2, 5) \oplus \mathcal{R}^{(2)}(1/3, 1/3)$ $\oplus \mathcal{R}^{(2)}(10/3, 28/3)$
$\otimes_f \mathcal{R}^{(2)}(1/3, 1/3)$	$\mathcal{R}^{(2)}(1/8, 1/8) \oplus 2\mathcal{R}^{(2)}(5/8, 21/8) \oplus \mathcal{R}^{(2)}(33/8, 65/8)$ $\oplus 4\mathcal{V}(-1/24) \oplus 2\mathcal{V}(35/24)$
$\otimes_f \mathcal{R}^{(2)}(1/8, 1/8)$	$2\mathcal{R}^{(3)}(0, 0, 1, 1) \oplus \mathcal{R}^{(3)}(0, 1, 2, 7) \oplus 2\mathcal{R}^{(2)}(1/3, 10/3)$
$\otimes_f \mathcal{R}^{(2)}(5/8, 21/8)$	$\mathcal{R}^{(3)}(0, 0, 2, 2) \oplus 2\mathcal{R}^{(3)}(0, 1, 2, 5) \oplus \mathcal{R}^{(3)}(1, 5, 7, 15)$ $\oplus 2\mathcal{R}^{(2)}(1/3, 1/3) \oplus 2\mathcal{R}^{(2)}(10/3, 28/3)$
$\otimes_f \mathcal{R}^{(2)}(1/3, 10/3)$	$2\mathcal{R}^{(2)}(1/8, 1/8) \oplus 2\mathcal{R}^{(2)}(5/8, 21/8) \oplus 2\mathcal{R}^{(2)}(33/8, 65/8)$ $\oplus \mathcal{R}^{(2)}(85/8, 133/8) \oplus 2\mathcal{V}(-1/24) \oplus 4\mathcal{V}(35/24)$ $\oplus 2\mathcal{V}(143/24)$
$\otimes_f \mathcal{R}^{(2)}(1/8, 33/8)$	$\mathcal{R}^{(3)}(0, 0, 1, 1) \oplus 2\mathcal{R}^{(3)}(0, 1, 2, 7) \oplus \mathcal{R}^{(3)}(2, 5, 7, 12)$ $\oplus 2\mathcal{R}^{(2)}(1/3, 10/3) \oplus \mathcal{R}^{(2)}(28/3, 55/3)$
$\otimes_f \mathcal{R}^{(2)}(0, 1)_5$	$2\mathcal{R}^{(2)}(1/8, 1/8) \oplus \mathcal{R}^{(2)}(5/8, 21/8) \oplus \mathcal{V}(-1/24) \oplus 2\mathcal{V}(35/24)$ $\oplus \mathcal{V}(143/24)$
$\otimes_f \mathcal{R}^{(2)}(0, 1)_7$	$2\mathcal{R}^{(2)}(1/8, 1/8) \oplus \mathcal{R}^{(2)}(1/8, 33/8) \oplus 2\mathcal{V}(35/24)$
$\otimes_f \mathcal{R}^{(2)}(0, 2)_5$	$2\mathcal{R}^{(2)}(5/8, 5/8) \oplus \mathcal{R}^{(2)}(5/8, 21/8) \oplus \mathcal{V}(-1/24) \oplus \mathcal{V}(143/24)$
$\otimes_f \mathcal{R}^{(2)}(0, 2)_7$	$2\mathcal{R}^{(2)}(5/8, 5/8) \oplus \mathcal{R}^{(2)}(1/8, 33/8)$

	Fusion product
$\mathcal{R}^{(2)}(1/3, 1/3) \otimes_f \mathcal{R}^{(2)}(1/3, 1/3)$	$2\mathcal{R}^{(3)}(0, 0, 2, 2) \oplus \mathcal{R}^{(3)}(0, 1, 2, 7) \oplus 2\mathcal{R}^{(2)}(1/3, 1/3)$ $\oplus \mathcal{R}^{(2)}(1/3, 10/3)$
$\otimes_f \mathcal{R}^{(2)}(1/8, 1/8)$	$4\mathcal{R}^{(2)}(1/8, 1/8) \oplus 2\mathcal{R}^{(2)}(5/8, 21/8) \oplus \mathcal{V}(-1/24)$ $\oplus 2\mathcal{V}(35/24) \oplus \mathcal{V}(143/24)$
$\otimes_f \mathcal{R}^{(2)}(5/8, 21/8)$	$2\mathcal{R}^{(2)}(1/8, 1/8) \oplus 4\mathcal{R}^{(2)}(5/8, 21/8) \oplus 2\mathcal{R}^{(2)}(33/8, 65/8)$ $\oplus 2\mathcal{V}(-1/24) \oplus 2\mathcal{V}(35/24) \oplus 2\mathcal{V}(143/24) \oplus \mathcal{V}(323/24)$
$\otimes_f \mathcal{R}^{(2)}(1/3, 10/3)$	$\mathcal{R}^{(3)}(0, 0, 2, 2) \oplus 2\mathcal{R}^{(3)}(0, 1, 2, 7) \oplus \mathcal{R}^{(3)}(1, 5, 7, 12)$ $\oplus \mathcal{R}^{(2)}(1/3, 1/3) \oplus 2\mathcal{R}^{(2)}(1/3, 10/3) \oplus \mathcal{R}^{(2)}(10/3, 28/3)$
$\otimes_f \mathcal{R}^{(2)}(1/8, 33/8)$	$2\mathcal{R}^{(2)}(1/8, 1/8) \oplus 2\mathcal{R}^{(2)}(5/8, 21/8) \oplus 2\mathcal{R}^{(2)}(33/8, 65/8)$ $\oplus \mathcal{R}^{(2)}(85/8, 133/8) \oplus 2\mathcal{V}(-1/24) \oplus 4\mathcal{V}(35/24)$ $\oplus 2\mathcal{V}(143/24)$
$\otimes_f \mathcal{R}^{(2)}(0, 1)_5$	$2\mathcal{R}^{(3)}(0, 0, 1, 1) \oplus \mathcal{R}^{(3)}(0, 1, 2, 5)$
$\otimes_f \mathcal{R}^{(2)}(0, 1)_7$	$2\mathcal{R}^{(3)}(0, 0, 1, 1) \oplus \mathcal{R}^{(2)}(1/3, 10/3)$
$\otimes_f \mathcal{R}^{(2)}(0, 2)_5$	$\mathcal{R}^{(3)}(0, 1, 2, 5) \oplus 2\mathcal{R}^{(2)}(1/3, 1/3)$
$\otimes_f \mathcal{R}^{(2)}(0, 2)_7$	$2\mathcal{R}^{(2)}(1/3, 1/3) \oplus \mathcal{R}^{(2)}(1/3, 10/3)$
$\mathcal{R}^{(2)}(1/8, 1/8) \otimes_f \mathcal{R}^{(2)}(1/8, 1/8)$	$2\mathcal{R}^{(3)}(0, 0, 2, 2) \oplus \mathcal{R}^{(3)}(0, 1, 2, 5) \oplus 4\mathcal{R}^{(2)}(1/3, 1/3)$
$\otimes_f \mathcal{R}^{(2)}(5/8, 21/8)$	$\mathcal{R}^{(3)}(0, 0, 1, 1) \oplus 2\mathcal{R}^{(3)}(0, 1, 2, 7) \oplus \mathcal{R}^{(3)}(2, 5, 7, 12)$ $\oplus 4\mathcal{R}^{(2)}(1/3, 10/3)$
$\otimes_f \mathcal{R}^{(2)}(1/3, 10/3)$	$2\mathcal{R}^{(2)}(1/8, 1/8) \oplus 4\mathcal{R}^{(2)}(5/8, 21/8) \oplus 2\mathcal{R}^{(2)}(33/8, 65/8)$ $\oplus 2\mathcal{V}(-1/24) \oplus 2\mathcal{V}(35/24) \oplus 2\mathcal{V}(143/24) \oplus \mathcal{V}(323/24)$
$\otimes_f \mathcal{R}^{(2)}(1/8, 33/8)$	$\mathcal{R}^{(3)}(0, 0, 2, 2) \oplus 2\mathcal{R}^{(3)}(0, 1, 2, 5) \oplus \mathcal{R}^{(3)}(1, 5, 7, 15)$ $\oplus 2\mathcal{R}^{(2)}(1/3, 1/3) \oplus 2\mathcal{R}^{(2)}(10/3, 28/3)$
$\otimes_f \mathcal{R}^{(2)}(0, 1)_5$	$2\mathcal{R}^{(2)}(5/8, 5/8) \oplus \mathcal{R}^{(2)}(1/8, 33/8) \oplus 4\mathcal{V}(-1/24)$ $\oplus 2\mathcal{V}(35/24)$
$\otimes_f \mathcal{R}^{(2)}(0, 1)_7$	$2\mathcal{R}^{(2)}(5/8, 5/8) \oplus \mathcal{R}^{(2)}(5/8, 21/8) \oplus 4\mathcal{V}(-1/24)$
$\otimes_f \mathcal{R}^{(2)}(0, 2)_5$	$2\mathcal{R}^{(2)}(1/8, 1/8) \oplus \mathcal{R}^{(2)}(1/8, 33/8) \oplus 2\mathcal{V}(35/24)$
$\otimes_f \mathcal{R}^{(2)}(0, 2)_7$	$2\mathcal{R}^{(2)}(1/8, 1/8) \oplus \mathcal{R}^{(2)}(5/8, 21/8)$
$\mathcal{R}^{(2)}(0, 1)_5 \otimes_f \mathcal{R}^{(2)}(0, 1)_5$	$2\mathcal{R}^{(2)}(0, 2)_7 \oplus \mathcal{R}^{(2)}(2, 7) \oplus 2\mathcal{R}^{(2)}(1/3, 1/3)$ $\oplus \mathcal{R}^{(2)}(1/3, 10/3)$
$\otimes_f \mathcal{R}^{(2)}(0, 1)_7$	$\mathcal{R}^{(3)}(0, 0, 2, 2) \oplus 2\mathcal{R}^{(2)}(1/3, 1/3)$
$\otimes_f \mathcal{R}^{(2)}(0, 2)_5$	$\mathcal{R}^{(3)}(0, 0, 1, 1) \oplus \mathcal{R}^{(2)}(1/3, 10/3)$
$\otimes_f \mathcal{R}^{(2)}(0, 2)_7$	$2\mathcal{R}^{(2)}(0, 1)_5 \oplus \mathcal{R}^{(2)}(1, 5)$
$\mathcal{R}^{(2)}(0, 1)_7 \otimes_f \mathcal{R}^{(2)}(0, 1)_7$	$2\mathcal{R}^{(2)}(0, 2)_5 \oplus \mathcal{R}^{(2)}(2, 5) \oplus 4\mathcal{V}(1/3)$
$\otimes_f \mathcal{R}^{(2)}(0, 2)_5$	$2\mathcal{R}^{(2)}(0, 1)_7 \oplus \mathcal{R}^{(2)}(1, 7) \oplus 2\mathcal{V}(10/3)$
$\otimes_f \mathcal{R}^{(2)}(0, 2)_7$	$\mathcal{R}^{(3)}(0, 0, 1, 1)$
$\mathcal{R}^{(2)}(0, 2)_5 \otimes_f \mathcal{R}^{(2)}(0, 2)_5$	$2\mathcal{R}^{(2)}(0, 2)_5 \oplus \mathcal{R}^{(2)}(2, 5) \oplus \mathcal{V}(1/3) \oplus \mathcal{V}(28/3)$
$\otimes_f \mathcal{R}^{(2)}(0, 2)_7$	$\mathcal{R}^{(3)}(0, 0, 2, 2)$
$\mathcal{R}^{(2)}(0, 2)_7 \otimes_f \mathcal{R}^{(2)}(0, 2)_7$	$2\mathcal{R}^{(2)}(0, 2)_7 \oplus \mathcal{R}^{(2)}(2, 7)$

		Fusion product
$\mathcal{R}^{(3)}(0, 0, 1, 1)$	$\otimes_f \mathcal{V}(5/8)$	$2\mathcal{R}^{(2)}(1/8, 1/8) \oplus \mathcal{R}^{(2)}(5/8, 21/8)$
	$\otimes_f \mathcal{V}(1/3)$	$2\mathcal{R}^{(3)}(0, 0, 1, 1) \oplus \mathcal{R}^{(2)}(1/3, 10/3)$
	$\otimes_f \mathcal{V}(1/8)$	$2\mathcal{R}^{(2)}(5/8, 5/8) \oplus \mathcal{R}^{(2)}(1/8, 33/8) \oplus 4\mathcal{V}(-1/24) \oplus 2\mathcal{V}(35/24)$
	$\otimes_f \mathcal{V}(-1/24)$	$4\mathcal{R}^{(2)}(1/8, 1/8) \oplus 2\mathcal{R}^{(2)}(5/8, 21/8) \oplus \mathcal{V}(-1/24)$ $\oplus 2\mathcal{V}(35/24) \oplus \mathcal{V}(143/24)$
	$\otimes_f \mathcal{V}(2)$	$\mathcal{R}^{(3)}(0, 0, 1, 1)$
	$\otimes_f \mathcal{V}(1)$	$\mathcal{R}^{(3)}(0, 0, 2, 2) \oplus 2\mathcal{R}^{(2)}(1/3, 1/3)$
	$\otimes_f \mathcal{V}(7)$	$\mathcal{R}^{(3)}(0, 1, 2, 5)$
	$\otimes_f \mathcal{V}(5)$	$\mathcal{R}^{(3)}(0, 1, 2, 7) \oplus 2\mathcal{R}^{(2)}(1/3, 10/3)$
	$\otimes_f \mathcal{R}^{(1)}(0)_2$	$\mathcal{R}^{(3)}(0, 0, 1, 1)$
	$\otimes_f \mathcal{R}^{(1)}(0)_1$	$\mathcal{R}^{(3)}(0, 0, 2, 2) \oplus 2\mathcal{R}^{(2)}(1/3, 1/3)$
	$\otimes_f \mathcal{R}^{(2)}(5/8, 5/8)$	$\mathcal{R}^{(2)}(5/8, 5/8) \oplus 2\mathcal{R}^{(2)}(5/8, 21/8) \oplus \mathcal{R}^{(2)}(21/8, 85/8)$ $\oplus 4\mathcal{R}^{(2)}(1/8, 1/8) \oplus 2\mathcal{R}^{(2)}(1/8, 33/8)$ $\oplus 2\mathcal{V}(-1/24) \oplus 4\mathcal{V}(35/24) \oplus 2\mathcal{V}(143/24)$
	$\otimes_f \mathcal{R}^{(2)}(1/3, 1/3)$	$4\mathcal{R}^{(3)}(0, 0, 1, 1) \oplus 2\mathcal{R}^{(3)}(0, 1, 2, 5) \oplus \mathcal{R}^{(2)}(1/3, 1/3)$ $\oplus 2\mathcal{R}^{(2)}(1/3, 10/3) \oplus \mathcal{R}^{(2)}(10/3, 28/3)$
	$\otimes_f \mathcal{R}^{(2)}(1/8, 1/8)$	$4\mathcal{R}^{(2)}(5/8, 5/8) \oplus 2\mathcal{R}^{(2)}(5/8, 21/8) \oplus \mathcal{R}^{(2)}(1/8, 1/8)$ $\oplus 2\mathcal{R}^{(2)}(1/8, 33/8) \oplus \mathcal{R}^{(2)}(33/8, 65/8)$ $\oplus 8\mathcal{V}(-1/24) \oplus 4\mathcal{V}(35/24)$
	$\otimes_f \mathcal{R}^{(2)}(0, 1)_5$	$2\mathcal{R}^{(3)}(0, 0, 2, 2) \oplus \mathcal{R}^{(3)}(0, 1, 2, 7) \oplus 4\mathcal{R}^{(2)}(1/3, 1/3)$ $\oplus 2\mathcal{R}^{(2)}(1/3, 10/3)$
	$\otimes_f \mathcal{R}^{(2)}(0, 1)_7$	$2\mathcal{R}^{(3)}(0, 0, 2, 2) \oplus \mathcal{R}^{(3)}(0, 1, 2, 5) \oplus 4\mathcal{R}^{(2)}(1/3, 1/3)$
	$\otimes_f \mathcal{R}^{(2)}(0, 2)_5$	$2\mathcal{R}^{(3)}(0, 0, 1, 1) \oplus \mathcal{R}^{(3)}(0, 1, 2, 7) \oplus 2\mathcal{R}^{(2)}(1/3, 10/3)$
	$\otimes_f \mathcal{R}^{(2)}(0, 2)_7$	$2\mathcal{R}^{(3)}(0, 0, 1, 1) \oplus \mathcal{R}^{(3)}(0, 1, 2, 5)$
	$\otimes_f \mathcal{R}^{(3)}(0, 0, 1, 1)$	$4\mathcal{R}^{(3)}(0, 0, 2, 2) \oplus 2\mathcal{R}^{(3)}(0, 1, 2, 5) \oplus \mathcal{R}^{(3)}(0, 0, 1, 1)$ $\oplus 2\mathcal{R}^{(3)}(0, 1, 2, 7) \oplus \mathcal{R}^{(3)}(2, 5, 7, 12)$ $\oplus 8\mathcal{R}^{(2)}(1/3, 1/3) \oplus 4\mathcal{R}^{(2)}(1/3, 10/3)$
	$\otimes_f \mathcal{R}^{(3)}(0, 0, 2, 2)$	$\mathcal{R}^{(3)}(0, 0, 2, 2) \oplus 2\mathcal{R}^{(3)}(0, 1, 2, 5) \oplus \mathcal{R}^{(3)}(1, 5, 7, 15)$ $\oplus 4\mathcal{R}^{(3)}(0, 0, 1, 1) \oplus 2\mathcal{R}^{(3)}(0, 1, 2, 7) \oplus 2\mathcal{R}^{(2)}(1/3, 1/3)$ $\oplus 4\mathcal{R}^{(2)}(1/3, 10/3) \oplus 2\mathcal{R}^{(2)}(10/3, 28/3)$
	$\mathcal{R}^{(3)}(0, 0, 2, 2)$	$\otimes_f \mathcal{V}(5/8)$
$\otimes_f \mathcal{V}(1/3)$		$\mathcal{R}^{(3)}(0, 1, 2, 5) \oplus 2\mathcal{R}^{(2)}(1/3, 1/3)$
$\otimes_f \mathcal{V}(1/8)$		$2\mathcal{R}^{(2)}(1/8, 1/8) \oplus \mathcal{R}^{(2)}(5/8, 21/8) \oplus \mathcal{V}(-1/24)$ $\oplus 2\mathcal{V}(35/24) \oplus \mathcal{V}(143/24)$
$\otimes_f \mathcal{V}(-1/24)$		$\mathcal{R}^{(2)}(1/8, 1/8) \oplus 2\mathcal{R}^{(2)}(5/8, 21/8) \oplus \mathcal{R}^{(2)}(33/8, 65/8)$ $\oplus 4\mathcal{V}(-1/24) \oplus 2\mathcal{V}(35/24)$
$\otimes_f \mathcal{V}(2)$		$\mathcal{R}^{(3)}(0, 0, 2, 2)$
$\otimes_f \mathcal{V}(1)$		$\mathcal{R}^{(3)}(0, 0, 1, 1) \oplus \mathcal{R}^{(2)}(1/3, 10/3)$
$\otimes_f \mathcal{V}(7)$		$\mathcal{R}^{(3)}(0, 1, 2, 7)$
$\otimes_f \mathcal{V}(5)$		$\mathcal{R}^{(3)}(0, 1, 2, 5) \oplus \mathcal{R}^{(2)}(1/3, 1/3) \oplus \mathcal{R}^{(2)}(10/3, 28/3)$
$\otimes_f \mathcal{R}^{(1)}(0)_2$		$\mathcal{R}^{(3)}(0, 0, 2, 2)$
$\otimes_f \mathcal{R}^{(1)}(0)_1$		$\mathcal{R}^{(3)}(0, 0, 1, 1) \oplus \mathcal{R}^{(2)}(1/3, 10/3)$

	Fusion product
$\mathcal{R}^{(3)}(0, 0, 2, 2) \otimes_f \mathcal{R}^{(2)}(5/8, 5/8)$	$4 \mathcal{R}^{(2)}(5/8, 5/8) \oplus 2 \mathcal{R}^{(2)}(5/8, 21/8) \oplus \mathcal{R}^{(2)}(1/8, 1/8)$ $\oplus 2 \mathcal{R}^{(2)}(1/8, 33/8) \oplus \mathcal{R}^{(2)}(33/8, 65/8) \oplus 2 \mathcal{V}(-1/24)$ $\oplus 2 \mathcal{V}(35/24) \oplus 2 \mathcal{V}(143/24) \oplus \mathcal{V}(323/24)$
$\otimes_f \mathcal{R}^{(2)}(1/3, 1/3)$	$\mathcal{R}^{(3)}(0, 0, 1, 1) \oplus 2 \mathcal{R}^{(3)}(0, 1, 2, 5) \oplus \mathcal{R}^{(3)}(2, 5, 7, 12)$ $\oplus 4 \mathcal{R}^{(2)}(1/3, 1/3) \oplus 2 \mathcal{R}^{(2)}(1/3, 10/3)$
$\otimes_f \mathcal{R}^{(2)}(1/8, 1/8)$	$\mathcal{R}^{(2)}(5/8, 5/8) \oplus 2 \mathcal{R}^{(2)}(5/8, 21/8) \oplus \mathcal{R}^{(2)}(21/8, 85/8)$ $\oplus 4 \mathcal{R}^{(2)}(1/8, 1/8) \oplus 2 \mathcal{R}^{(2)}(1/8, 33/8)$ $\oplus 2 \mathcal{V}(-1/24) \oplus 4 \mathcal{V}(35/24) \oplus 2 \mathcal{V}(143/24)$
$\otimes_f \mathcal{R}^{(2)}(0, 1)_5$	$2 \mathcal{R}^{(3)}(0, 0, 1, 1) \oplus \mathcal{R}^{(3)}(0, 1, 2, 5) \oplus \mathcal{R}^{(2)}(1/3, 1/3)$ $\oplus 2 \mathcal{R}^{(2)}(1/3, 10/3) \oplus \mathcal{R}^{(2)}(10/3, 28/3)$
$\otimes_f \mathcal{R}^{(2)}(0, 1)_7$	$2 \mathcal{R}^{(3)}(0, 0, 1, 1) \oplus \mathcal{R}^{(3)}(0, 1, 2, 7) \oplus 2 \mathcal{R}^{(2)}(1/3, 10/3)$
$\otimes_f \mathcal{R}^{(2)}(0, 2)_5$	$2 \mathcal{R}^{(3)}(0, 0, 2, 2) \oplus \mathcal{R}^{(3)}(0, 1, 2, 5) \oplus \mathcal{R}^{(2)}(1/3, 1/3) \oplus$ $\mathcal{R}^{(2)}(10/3, 28/3)$
$\otimes_f \mathcal{R}^{(2)}(0, 2)_7$	$2 \mathcal{R}^{(3)}(0, 0, 2, 2) \oplus \mathcal{R}^{(3)}(0, 1, 2, 7)$
$\otimes_f \mathcal{R}^{(3)}(0, 0, 2, 2)$	$4 \mathcal{R}^{(3)}(0, 0, 2, 2) \oplus 2 \mathcal{R}^{(3)}(0, 1, 2, 5) \oplus \mathcal{R}^{(3)}(0, 0, 1, 1)$ $\oplus 2 \mathcal{R}^{(3)}(0, 1, 2, 7) \oplus \mathcal{R}^{(3)}(2, 5, 7, 12) \oplus 2 \mathcal{R}^{(2)}(1/3, 1/3)$ $\oplus 2 \mathcal{R}^{(2)}(1/3, 10/3) \oplus 2 \mathcal{R}^{(2)}(10/3, 28/3) \oplus \mathcal{R}^{(2)}(28/3, 55/3)$
$\mathcal{R}^{(3)}(0, 1, 2, 5) \otimes_f \mathcal{V}(5/8)$	$2 \mathcal{R}^{(2)}(5/8, 21/8) \oplus \mathcal{R}^{(2)}(1/8, 1/8) \oplus \mathcal{R}^{(2)}(33/8, 65/8)$
$\otimes_f \mathcal{V}(1/3)$	$2 \mathcal{R}^{(3)}(0, 1, 2, 5) \oplus \mathcal{R}^{(2)}(1/3, 1/3) \oplus \mathcal{R}^{(2)}(10/3, 28/3)$
$\otimes_f \mathcal{V}(1/8)$	$\mathcal{R}^{(2)}(5/8, 5/8) \oplus 2 \mathcal{R}^{(2)}(1/8, 33/8) \oplus \mathcal{R}^{(2)}(21/8, 85/8)$ $\oplus 2 \mathcal{V}(-1/24) \oplus 4 \mathcal{V}(35/24) \oplus 2 \mathcal{V}(143/24)$
$\otimes_f \mathcal{V}(-1/24)$	$2 \mathcal{R}^{(2)}(1/8, 1/8) \oplus 4 \mathcal{R}^{(2)}(5/8, 21/8) \oplus 2 \mathcal{R}^{(2)}(33/8, 65/8)$ $\oplus 2 \mathcal{V}(-1/24) \oplus 2 \mathcal{V}(35/24) \oplus 2 \mathcal{V}(143/24) \oplus \mathcal{V}(323/24)$
$\otimes_f \mathcal{V}(2)$	$\mathcal{R}^{(3)}(0, 1, 2, 5)$
$\otimes_f \mathcal{V}(1)$	$\mathcal{R}^{(3)}(0, 1, 2, 7) \oplus 2 \mathcal{R}^{(2)}(1/3, 10/3)$
$\otimes_f \mathcal{R}^{(1)}(0)_2$	$\mathcal{R}^{(3)}(0, 1, 2, 5)$
$\otimes_f \mathcal{R}^{(1)}(0)_1$	$\mathcal{R}^{(3)}(0, 1, 2, 7) \oplus 2 \mathcal{R}^{(2)}(1/3, 10/3)$
$\otimes_f \mathcal{R}^{(2)}(0, 2)_7$	$\mathcal{R}^{(3)}(0, 0, 1, 1) \oplus 2 \mathcal{R}^{(3)}(0, 1, 2, 5) \oplus \mathcal{R}^{(3)}(2, 5, 7, 12)$

B.2 Fusion rules for $c_{2,5} = -22/5$

In the following table we have collected the results of our explicit calculations of the fusion product of irreducible representations in the augmented $c_{2,5} = -22/5$ model. These results are certainly not complete, but mainly serve to compute the lowest higher rank representations as well as to check the proposed fusion rules on a variety of examples.

	L	\tilde{L}_{\max}	Fusion product
$\mathcal{V}(11/8) \otimes_f \mathcal{V}(11/8)$	5	7	$\mathcal{R}^{(2)}(0, 4)_{13}$
$\otimes_f \mathcal{V}(27/40)$	5	7	$\mathcal{R}^{(2)}(-1/5, 14/5)_{11}$
$\otimes_f \mathcal{V}(2/5)$	5	7	$\mathcal{V}(-9/40)$
$\otimes_f \mathcal{V}(7/40)$	5	7	$\mathcal{R}^{(2)}(-1/5, 9/5)_9$
$\otimes_f \mathcal{V}(-1/8)$	7	8	$\mathcal{R}^{(2)}(0, 1)_7$
$\otimes_f \mathcal{V}(-9/40)$	4	6	$\mathcal{R}^{(2)}(2/5, 2/5)$
$\mathcal{V}(27/40) \otimes_f \mathcal{V}(27/40)$	5	7	$\mathcal{R}^{(2)}(0, 4)_{13} \oplus \mathcal{R}^{(2)}(-1/5, 9/5)_9$
$\otimes_f \mathcal{V}(2/5)$	5	7	$\mathcal{R}^{(2)}(-1/8, -1/8)$
$\otimes_f \mathcal{V}(7/40)$	5	7	$\mathcal{R}^{(2)}(0, 1)_7 \oplus \mathcal{R}^{(2)}(-1/5, 14/5)_{11}$
$\otimes_f \mathcal{V}(-1/8)$	5	7	$\mathcal{R}^{(2)}(-1/5, 9/5)_9 \oplus \mathcal{R}^{(2)}(2/5, 2/5)$
$\otimes_f \mathcal{V}(-9/40)$	4	6	$\mathcal{R}^{(3)}(0, 0, 1, 1)$
$\mathcal{V}(2/5) \otimes_f \mathcal{V}(11/8)$	5	7	$\mathcal{V}(-9/40)$
$\otimes_f \mathcal{V}(27/40)$	5	7	$\mathcal{R}^{(2)}(-1/8, -1/8)$
$\otimes_f \mathcal{V}(2/5)$	5	7	$\mathcal{R}^{(2)}(0, 4)_7 \oplus \mathcal{R}^{(2)}(-1/5, 9/5)_{11} \oplus \mathcal{V}(2/5)$
$\otimes_f \mathcal{V}(7/40)$	4	6	$\mathcal{R}^{(2)}(7/40, 7/40) \oplus \mathcal{V}(-9/40)$
$\otimes_f \mathcal{V}(-1/8)$	4	6	$\mathcal{R}^{(2)}(-1/8, -1/8) \oplus \mathcal{R}^{(2)}(27/40, 27/40)$
$\otimes_f \mathcal{V}(-9/40)$	3	5	$\mathcal{R}^{(2)}(7/40, 7/40) \oplus \mathcal{R}^{(2)}(11/8, 11/8) \oplus \mathcal{V}(-9/40)$
$\otimes_f \mathcal{R}^{(1)}(0)_1$	5	7	$\mathcal{R}^{(2)}(0, 1)_{13} \oplus \mathcal{R}^{(2)}(-1/5, 14/5)_9$
$\otimes_f \mathcal{V}(1)$	3	9	$\mathcal{R}^{(2)}(0, 1)_{13} \oplus \mathcal{R}^{(2)}(-1/5, 14/5)_9$
$\mathcal{V}(7/40) \otimes_f \mathcal{V}(7/40)$	4	6	$\mathcal{R}^{(2)}(0, 4)_{13} \oplus \mathcal{R}^{(2)}(-1/5, 9/5)_9 \oplus \mathcal{R}^{(2)}(2/5, 2/5)$
$\otimes_f \mathcal{V}(-1/8)$	4	6	$\mathcal{R}^{(3)}(0, 0, 1, 1) \oplus \mathcal{R}^{(2)}(-1/5, 14/5)_{11}$
$\otimes_f \mathcal{V}(-9/40)$	4	6	$\mathcal{R}^{(3)}(-1/5, -1/5, 9/5, 9/5) \oplus \mathcal{R}^{(2)}(2/5, 2/5)$
$\mathcal{V}(-1/8) \otimes_f \mathcal{V}(-1/8)$	3	5	$\mathcal{R}^{(3)}(-1/5, -1/5, 9/5, 9/5) \oplus \mathcal{R}^{(2)}(0, 4)_{13}$ $\oplus \mathcal{R}^{(2)}(2/5, 2/5)$
$\otimes_f \mathcal{V}(-9/40)$	4	6	$\mathcal{R}^{(3)}(0, 0, 1, 1) \oplus \mathcal{R}^{(3)}(-1/5, -1/5, 14/5, 14/5)$
$\mathcal{V}(-9/40) \otimes_f \mathcal{V}(-9/40)$	4	5	$\mathcal{R}^{(3)}(0, 0, 4, 4) \oplus \mathcal{R}^{(3)}(-1/5, -1/5, 9/5, 9/5)$ $\oplus \mathcal{R}^{(2)}(2/5, 2/5)$
$\mathcal{V}(14/5) \otimes_f \mathcal{V}(14/5)$	2	8	$\mathcal{R}^{(1)}(0)_4 \oplus \mathcal{R}^{(1)}(-1/5)_2$
$\otimes_f \mathcal{R}^{(1)}(-1/5)_2$	2	8	$\mathcal{V}(1) \oplus \mathcal{V}(14/5)$
$\otimes_f \mathcal{R}^{(1)}(-1/5)_3$	2	8	$\mathcal{V}(4) \oplus \mathcal{V}(9/5)$
$\mathcal{V}(4) \otimes_f \mathcal{V}(4)$	2	9	$\mathcal{R}^{(1)}(0)_4$
$\otimes_f \mathcal{R}^{(1)}(0)_1$	2	9	$\mathcal{V}(1)$
$\otimes_f \mathcal{R}^{(1)}(0)_4$	2	9	$\mathcal{V}(4)$

Appendix C

Examples of logarithmic nullvectors for augmented minimal models

C.1 An explicit nullvector for $c_{3,1} = -7$

As a further example for a type **B** rank 2 logarithmic nullvector (see figure 4.1) we give the respective nullvector with lowest lying vector at $h = -1/4$ and Jordan cell at $h = 7/4$ in the augmented model of $c_{3,1} = -7$ which appears at level 10. For the sake of reasonable brevity we have set the overall normalisation to 1 and also eliminated any freedom due to the existence of lower nullvectors in the irreducible subrepresentation by setting any further free parameter to 0; the parameter β certainly still remains as it is a parameter of the representation as introduced in section 4.1:

$$\begin{aligned} & \left(\left(\frac{7168}{27} - 512\beta \right) L_{-3} L_{-2}^2 L_{-1}^3 + \left(-\frac{1280}{81} + \frac{256}{9}\beta \right) L_{-5} L_{-2} L_{-1}^3 + \left(-\frac{21376}{27} - \frac{128}{3}\beta \right) L_{-4} L_{-3} L_{-1}^3 \right. \\ & + \left(\frac{8552}{27} + \frac{3280}{9}\beta \right) L_{-7} L_{-1}^3 + \left(-\frac{4096}{27} + \frac{512}{3}\beta \right) L_{-2}^4 L_{-1}^2 + \left(\frac{67840}{81} + \frac{256}{9}\beta \right) L_{-4} L_{-2}^2 L_{-1}^2 \\ & + \left(-\frac{18112}{81} + \frac{8192}{9}\beta \right) L_{-3}^2 L_{-2} L_{-1}^2 + \left(\frac{30080}{81} - \frac{11008}{9}\beta \right) L_{-6} L_{-2} L_{-1}^2 + (8 + 48\beta) L_{-5} L_{-3} L_{-1}^2 \\ & + \left(-\frac{3968}{27} - \frac{736}{3}\beta \right) L_{-4}^2 L_{-1}^2 + \left(\frac{24752}{81} - \frac{2992}{9}\beta \right) L_{-8} L_{-1}^2 + \left(-\frac{7168}{81} + \frac{512}{3}\beta \right) L_{-3} L_{-2}^3 L_{-1} \\ & + \left(\frac{1280}{243} + \frac{2048}{27}\beta \right) L_{-5} L_{-2}^2 L_{-1} + \left(\frac{21376}{81} + \frac{3968}{9}\beta \right) L_{-4} L_{-3} L_{-2} L_{-1} - \frac{3008}{9}\beta L_{-3}^3 L_{-1} \\ & + \left(-\frac{8552}{81} - 496\beta \right) L_{-7} L_{-2} L_{-1} + \frac{2720}{3}\beta L_{-6} L_{-3} L_{-1} - 208\beta L_{-5} L_{-4} L_{-1} + \frac{5564}{9}\beta L_{-9} L_{-1} \\ & + \left(\frac{4096}{81} - \frac{512}{9}\beta \right) L_{-2}^5 + \left(-\frac{67840}{243} - \frac{6400}{27}\beta \right) L_{-4} L_{-2}^3 + \left(-\frac{3392}{243} + \frac{1024}{27}\beta \right) L_{-3}^2 L_{-2}^2 \\ & + \left(-\frac{30080}{243} + \frac{11776}{27}\beta \right) L_{-6} L_{-2}^2 + \left(-\frac{42376}{243} - \frac{496}{27}\beta \right) L_{-5} L_{-3} L_{-2} + \left(\frac{3968}{81} + \frac{4576}{9}\beta \right) L_{-4}^2 L_{-2} \\ & + \left(-\frac{110768}{243} + \frac{15904}{27}\beta \right) L_{-8} L_{-2} + \left(\frac{21376}{81} - \frac{832}{9}\beta \right) L_{-4} L_{-2}^2 + \left(-\frac{30056}{81} + 288\beta \right) L_{-7} L_{-3} \\ & + \frac{448}{3}\beta L_{-6} L_{-4} + \left(\frac{1280}{243} + \frac{1580}{27}\beta \right) L_{-5}^2 + \left(-\frac{28672}{27} + 2128\beta \right) L_{-10} \Big) |h-l\rangle \\ & + \left(L_{-1}^8 - 28L_{-2} L_{-1}^6 + 28L_{-3} L_{-1}^5 + \frac{658}{3} L_{-2}^2 L_{-1}^4 - 132L_{-4} L_{-1}^4 - \frac{1048}{3} L_{-3} L_{-2} L_{-1}^3 \right. \\ & \left. + \frac{976}{9} L_{-5} L_{-1}^3 - \frac{12916}{27} L_{-2}^3 L_{-1}^2 + \frac{8344}{9} L_{-4} L_{-2} L_{-1}^2 + \frac{1604}{9} L_{-3}^2 L_{-1}^2 + 240L_{-6} L_{-1}^2 \right) \end{aligned}$$

$$+668L_{-3}L_{-2}^2L_{-1} - \frac{1312}{3}L_{-5}L_{-2}L_{-1} - 576L_{-4}L_{-3}L_{-1} - 186L_{-7}L_{-1} - \frac{1708}{3}L_{-4}L_{-2}^2 \\ + \frac{1225}{9}L_{-2}^4 - \frac{728}{3}L_{-3}^2L_{-2} - 224L_{-6}L_{-2} + \frac{602}{3}L_{-5}L_{-3} + 252L_{-4}^2 - 476L_{-8} \Big| h; 1 \Big\rangle$$

C.2 Explicit nullvectors on the border of $\mathbf{c}_{2,3} = 0$

In the following we give the explicit form of the nullvector of type **A** for the triplet T_1 , which has a Jordan cell at lowest weight $h = 1/8$ and appears at level 8. We have set the overall normalisation to 1 in this expression; any further free parameters, however, appear as calculated (noted as m_i). We also note again that β is not a free parameter of the logarithmic nullvector calculation but a parameter of the representation as introduced in section 4.1:

$$\left(m_{21}L_{-1}^8 + m_{20}L_{-2}L_{-1}^6 + m_{19}L_{-3}L_{-1}^5 + m_{18}L_{-2}^2L_{-1}^4 + m_{17}L_{-4}L_{-1}^4 \right. \\ + \left(\frac{64}{9} - \frac{13}{3}m_{19} - \frac{278}{3}m_{21} - 7m_{20} \right) L_{-3}L_{-2}L_{-1}^3 + \left(\frac{616}{9} - \frac{698}{9}m_{21} - 7m_{20} \right) L_{-5}L_{-1}^3 \\ + \left(-\frac{4069}{54}m_{21} - \frac{13}{3}m_{18} - \frac{217}{12}m_{20} \right) L_{-2}^3L_{-1}^2 + \left(\frac{2870}{9} + 15m_{21} - 5m_{20} \right) L_{-6}L_{-1}^2 \\ + \left(\frac{752}{9} - \frac{1475}{9}m_{21} - \frac{5}{2}m_{20} - \frac{13}{3}m_{17} \right) L_{-4}L_{-2}L_{-1}^2 + \left(-\frac{640}{9} - \frac{35}{12}m_{21} - \frac{1}{2}m_{17} \right) L_{-2}^4 \\ + \left(-\frac{2164}{9} - \frac{8}{3}m_{19} - \frac{301}{9}m_{21} \right) L_{-3}^2L_{-1}^2 + \left(\frac{5425}{432}m_{21} + \frac{25}{36}m_{18} + \frac{325}{108}m_{20} \right) L_{-2}^4 \\ + \left(-540 + 142m_{21} + \frac{10}{3}m_{18} + \frac{461}{18}m_{20} \right) L_{-5}L_{-2}L_{-1} + \left(\frac{1888}{27} + \frac{25}{36}m_{19} + \frac{955}{18}m_{21} + \right. \\ \left. \frac{5}{3}m_{18} + 10m_{20} \right) L_{-3}L_{-2}^2L_{-1} + \left(\frac{2768}{9} + \frac{17}{6}m_{19} + 143m_{21} + \frac{5}{3}m_{17} \right) L_{-4}L_{-3}L_{-1} \\ + \left(-\frac{614}{3} + \frac{17}{6}m_{19} + \frac{14059}{36}m_{21} + 5m_{18} + \frac{281}{6}m_{20} \right) L_{-7}L_{-1} + \left(-\frac{104}{9} + \frac{1087}{36}m_{21} \right. \\ \left. - \frac{1}{2}m_{18} + \frac{11}{18}m_{20} + \frac{25}{36}m_{17} \right) L_{-4}L_{-2}^2 + \left(\frac{266}{27} + \frac{25}{18}m_{19} + \frac{250}{9}m_{21} + \frac{25}{18}m_{20} \right) L_{-3}^2L_{-2} \\ + \left(-\frac{43}{3} + \frac{131}{18}m_{21} - 2m_{18} - \frac{19}{3}m_{20} \right) L_{-6}L_{-2} + \left(\frac{2482}{27} - \frac{29}{36}m_{19} + \frac{131}{4}m_{21} \right. \\ \left. + \frac{25}{9}m_{20} \right) L_{-5}L_{-3} + \left(\frac{1220}{27} - \frac{29}{18}m_{19} - \frac{3985}{18}m_{21} - 4m_{18} - \frac{247}{9}m_{20} \right) L_{-8} \Big| h - l \Big\rangle \\ + \left(L_{-1}^8 - \frac{58}{3}L_{-2}L_{-1}^6 + \frac{70}{3}L_{-3}L_{-1}^5 + \frac{1547}{18}L_{-2}^2L_{-1}^4 - \frac{347}{3}L_{-4}L_{-1}^4 - \frac{526}{9}L_{-3}L_{-2}L_{-1}^3 \right. \\ + \frac{520}{9}L_{-5}L_{-1}^3 - \frac{589}{6}L_{-2}^3L_{-1}^2 + \frac{1157}{3}L_{-4}L_{-2}L_{-1}^2 - \frac{287}{3}L_{-3}^2L_{-1}^2 + \frac{335}{3}L_{-6}L_{-1}^2 \\ + \frac{115}{6}L_{-3}L_{-2}^2L_{-1} - \frac{200}{3}L_{-5}L_{-2}L_{-1} + \frac{49}{3}L_{-4}L_{-3}L_{-1} - \frac{229}{12}L_{-7}L_{-1} + \frac{225}{16}L_{-2}^4 \\ \left. - \frac{1259}{12}L_{-4}L_{-2}^2 + \frac{100}{3}L_{-3}^2L_{-2} - \frac{253}{6}L_{-6}L_{-2} - \frac{159}{4}L_{-5}L_{-3} + \frac{659}{12}L_{-4}^2 - \frac{433}{6}L_{-8} \right) \Big| h; 1 \Big\rangle$$

We also give the type **B** logarithmic nullvector for the triplet T_2 , which has a Jordan cell at $h = 21/8$, a lowest weight at $h = 5/8$ and appears at level 16. As this expression is very lengthy we have again set the overall normalisation to 1 and also eliminated any further freedom by setting any further free parameter to 0:

$$\left(-\frac{149120}{27} - \frac{11648}{9}\beta \right) L_{-3}L_{-2}^2L_{-1}^9 + \left(-\frac{6100784}{81} - \frac{4996016}{405}\beta \right) L_{-5}L_{-2}L_{-1}^9 + \left(-\frac{564736}{27} - \right. \\ \left. \frac{2531584}{135}\beta \right) L_{-4}L_{-3}L_{-1}^9 + \left(\frac{1492754}{27} - \frac{761422}{135}\beta \right) L_{-7}L_{-1}^9 + \left(\frac{58240}{27} + \frac{11648}{27}\beta \right) L_{-2}^4L_{-1}^8 \\ + \left(\frac{10401664}{81} + \frac{9886336}{405}\beta \right) L_{-4}L_{-2}^2L_{-1}^8 + \left(\frac{6547352}{81} + \frac{13290968}{405}\beta \right) L_{-3}^2L_{-2}L_{-1}^8 + \left(\frac{11199188}{81} \right. \\ \left. + \frac{11666036}{405}\beta \right) L_{-6}L_{-2}L_{-1}^8 + \left(\frac{11824162}{81} + \frac{16560418}{405}\beta \right) L_{-5}L_{-3}L_{-1}^8 + \left(-\frac{2163322}{27} \right. \\ \left. + \frac{18004358}{135}\beta \right) L_{-4}^2L_{-1}^8 + \left(\frac{25195051}{81} - \frac{19264057}{81}\beta \right) L_{-8}L_{-1}^8 + \left(-\frac{298240}{27} - \frac{55552}{27}\beta \right) L_{-3}L_{-2}^3L_{-1}^7$$

$$\begin{aligned}
& + \left(\frac{389529760}{243} + \frac{72031904}{243} \beta \right) L_{-5} L_{-2}^2 L_{-1}^7 + \left(-\frac{43345088}{81} - \frac{4798528}{81} \beta \right) L_{-4} L_{-3} L_{-2} L_{-1}^7 \\
& + \left(-\frac{161243044}{81} + \frac{264057116}{405} \beta \right) L_{-7} L_{-2} L_{-1}^7 + \left(-\frac{3836560}{27} - \frac{1439984}{15} \beta \right) L_{-3}^3 L_{-1}^7 + \left(-\frac{39224696}{81} \right. \\
& + \left. \frac{79328632}{405} \beta \right) L_{-6} L_{-3} L_{-1}^7 + \left(-\frac{30255232}{81} - \frac{420183616}{405} \beta \right) L_{-5} L_{-4} L_{-1}^7 \\
& + \left(-\frac{115606213}{81} + \frac{317139341}{405} \beta \right) L_{-9} L_{-1}^7 + \left(-\frac{546560}{81} - \frac{109312}{81} \beta \right) L_{-2}^5 L_{-1}^6 \\
& + \left(-\frac{504068096}{243} - \frac{414460928}{1215} \beta \right) L_{-4} L_{-2}^3 L_{-1}^6 + \left(-\frac{32395888}{243} - \frac{221287024}{1215} \beta \right) L_{-3}^2 L_{-2}^2 L_{-1}^6 \\
& + \left(-\frac{688257640}{243} - \frac{1894942504}{1215} \beta \right) L_{-6} L_{-2}^2 L_{-1}^6 + \left(-\frac{171246124}{81} - \frac{23791292}{81} \beta \right) L_{-5} L_{-3} L_{-2} L_{-1}^6 \\
& + \left(\frac{436742516}{81} - \frac{285590284}{405} \beta \right) L_{-4}^2 L_{-2} L_{-1}^6 + \left(-\frac{1311363362}{243} + \frac{618446318}{243} \beta \right) L_{-8} L_{-2} L_{-1}^6 + \\
& \left(-\frac{14349776}{81} + \frac{87406928}{81} \beta \right) L_{-4} L_{-2}^2 L_{-1}^6 + \left(\frac{675988264}{81} - \frac{1346752232}{405} \beta \right) L_{-7} L_{-3} L_{-1}^6 \\
& + \left(\frac{130901740}{27} + \frac{530789812}{135} \beta \right) L_{-6} L_{-4} L_{-1}^6 + \left(\frac{57193417}{243} + \frac{323247827}{243} \beta \right) L_{-5} L_{-1}^6 \\
& + \left(\frac{377046397}{27} - \frac{82026941}{135} \beta \right) L_{-10} L_{-1}^6 + \left(\frac{24149440}{81} + \frac{478912}{9} \beta \right) L_{-3} L_{-2} L_{-1}^5 \\
& + \left(-\frac{6472052776}{729} - \frac{1153026056}{729} \beta \right) L_{-5} L_{-3}^2 L_{-1}^5 + \left(\frac{491223904}{81} + \frac{724362016}{405} \beta \right) L_{-4} L_{-3} L_{-2}^2 L_{-1}^5 \\
& + \left(\frac{1289170697}{81} - \frac{2296000231}{405} \beta \right) L_{-7} L_{-2}^2 L_{-1}^5 + \left(-\frac{247531144}{243} - \frac{33723704}{243} \beta \right) L_{-3}^3 L_{-2} L_{-1}^5 \\
& + \left(\frac{74820020}{9} + \frac{37930060}{9} \beta \right) L_{-6} L_{-3} L_{-2} L_{-1}^5 + \left(-\frac{349441376}{243} + \frac{8040650368}{1215} \beta \right) L_{-5} L_{-4} L_{-2} L_{-1}^5 \\
& + \left(\frac{289876117}{18} - \frac{908160193}{162} \beta \right) L_{-9} L_{-2} L_{-1}^5 + \left(-\frac{899217364}{243} - \frac{1223108068}{1215} \beta \right) L_{-5} L_{-3}^2 L_{-1}^5 \\
& + \left(\frac{54747340}{9} - \frac{21043364}{9} \beta \right) L_{-4}^2 L_{-3} L_{-1}^5 + \left(-\frac{3343815314}{243} + \frac{1020421910}{243} \beta \right) L_{-8} L_{-3} L_{-1}^5 \\
& + \left(-\frac{4106356768}{81} + \frac{423802096}{81} \beta \right) L_{-7} L_{-4} L_{-1}^5 + \left(\frac{6087567380}{243} - \frac{1708569956}{243} \beta \right) L_{-6} L_{-5} L_{-1}^5 \\
& + \left(\frac{1975182488}{243} - \frac{5191641784}{1215} \beta \right) L_{-4} L_{-2}^2 L_{-1}^5 + \left(-\frac{10951360}{243} - \frac{2190272}{243} \beta \right) L_{-2}^6 L_{-1}^4 \\
& + \left(\frac{6439826624}{729} + \frac{4398126656}{3645} \beta \right) L_{-4} L_{-2}^4 L_{-1}^4 + \left(-\frac{805947068}{729} + \frac{946244068}{3645} \beta \right) L_{-3}^2 L_{-2}^3 L_{-1}^4 \\
& + \left(\frac{9716768158}{729} + \frac{39829789006}{3645} \beta \right) L_{-6} L_{-2}^3 L_{-1}^4 + \left(\frac{1492444673}{243} - \frac{3094966463}{1215} \beta \right) L_{-5} L_{-3} L_{-2}^2 L_{-1}^4 \\
& + \left(-\frac{10110621079}{243} - \frac{300543275}{243} \beta \right) L_{-4}^2 L_{-2}^2 L_{-1}^4 + \left(\frac{12461262967}{486} - \frac{7049560643}{810} \beta \right) L_{-8} L_{-2}^2 L_{-1}^4 \\
& + \left(-\frac{23944200971}{486} - \frac{1603601245}{486} \beta \right) L_{-11} L_{-1}^5 + \left(-\frac{11528458402}{243} + \frac{25042759046}{1215} \beta \right) L_{-7} L_{-3} L_{-2} L_{-1}^4 \\
& + \left(-\frac{19090179110}{243} - \frac{62902001258}{1215} \beta \right) L_{-6} L_{-4} L_{-2} L_{-1}^4 + \left(\frac{9182523901}{1458} - \frac{9713083541}{7290} \beta \right) L_{-5}^2 L_{-2} L_{-1}^4 \\
& + \left(-\frac{65932612501}{486} - \frac{3429904271}{486} \beta \right) L_{-10} L_{-2} L_{-1}^4 + \left(\frac{383243984}{243} + \frac{323521072}{243} \beta \right) L_{-3}^4 L_{-1}^4 \\
& + \left(\frac{55495736}{27} - \frac{829672184}{81} \beta \right) L_{-6} L_{-2}^2 L_{-1}^4 + \left(\frac{1588949072}{243} + \frac{24002270192}{1215} \beta \right) L_{-5} L_{-4} L_{-3} L_{-1}^4 \\
& + \left(\frac{957145103}{243} - \frac{23998651177}{1215} \beta \right) L_{-9} L_{-3} L_{-1}^4 + \left(-\frac{44315552}{27} - \frac{171541792}{27} \beta \right) L_{-4}^3 L_{-1}^4 \\
& + \left(\frac{4968093016}{243} + \frac{5395525736}{243} \beta \right) L_{-8} L_{-4} L_{-1}^4 + \left(\frac{2882901476}{243} - \frac{33207042922}{1215} \beta \right) L_{-7} L_{-5} L_{-1}^4 \\
& + \left(-\frac{6761458844}{243} + \frac{3531609476}{243} \beta \right) L_{-6} L_{-1}^4 + \left(-\frac{5936082307}{243} - \frac{19072395649}{1215} \beta \right) L_{-12} L_{-1}^4 \\
& + \left(-\frac{260692160}{729} + \frac{1981504}{81} \beta \right) L_{-3} L_{-2}^5 L_{-1}^3 + \left(\frac{25860528968}{2187} + \frac{13853999912}{10935} \beta \right) L_{-5} L_{-2}^4 L_{-1}^3 \\
& + \left(-\frac{115094416}{9} - \frac{397874864}{81} \beta \right) L_{-4} L_{-3} L_{-2}^3 L_{-1}^3 + \left(-\frac{9183968675}{243} + \frac{60366559}{5} \beta \right) L_{-7} L_{-2}^3 L_{-1}^3 \\
& + \left(\frac{22446028}{9} + \frac{381549548}{243} \beta \right) L_{-3}^3 L_{-2}^2 L_{-1}^3 + \left(-\frac{1857923638}{243} - \frac{26692922234}{1215} \beta \right) L_{-6} L_{-3} L_{-2}^2 L_{-1}^3 \\
& + \left(\frac{18483518080}{729} - \frac{1635799888}{729} \beta \right) L_{-5} L_{-4} L_{-2}^2 L_{-1}^3 + \left(-\frac{106944789343}{2916} + \frac{123521710391}{14580} \beta \right) L_{-9} L_{-2}^2 L_{-1}^3 \\
& + \left(\frac{10262941796}{729} + \frac{4345875956}{3645} \beta \right) L_{-5} L_{-3} L_{-2} L_{-1}^3 + \left(-\frac{2914640996}{81} + \frac{5112097436}{405} \beta \right) L_{-4}^2 L_{-3} L_{-2} L_{-1}^3 \\
& + \left(\frac{41031702454}{729} - \frac{71201971634}{3645} \beta \right) L_{-8} L_{-3} L_{-2} L_{-1}^3 + \left(\frac{81698877104}{243} - \frac{40731621952}{1215} \beta \right) L_{-7} L_{-4} L_{-2} L_{-1}^3 \\
& + \left(-\frac{114847983652}{729} + \frac{184898225636}{3645} \beta \right) L_{-6} L_{-5} L_{-2} L_{-1}^3 + \left(\frac{464402212315}{1458} + \frac{154322577601}{7290} \beta \right) L_{-11} L_{-2} L_{-1}^3 \\
& + \left(\frac{15314752}{3} - \frac{1668550912}{405} \beta \right) L_{-4} L_{-3}^3 L_{-1}^3 + \left(-\frac{5194154518}{81} + \frac{2708172854}{135} \beta \right) L_{-7} L_{-2}^2 L_{-1}^3 \\
& + \left(\frac{2137814356}{81} + \frac{221522588}{81} \beta \right) L_{-6} L_{-4} L_{-3} L_{-1}^3 + \left(\frac{1006401133}{729} - \frac{51304031429}{3645} \beta \right) L_{-5}^2 L_{-3} L_{-1}^3 \\
& + \left(-\frac{418142455}{9} + \frac{10153248079}{405} \beta \right) L_{-10} L_{-3} L_{-1}^3 + \left(-\frac{913003520}{81} + \frac{3109906496}{405} \beta \right) L_{-5} L_{-2}^4 L_{-1}^3 \\
& + \left(\frac{3782161967}{81} + \frac{14793947}{135} \beta \right) L_{-9} L_{-4} L_{-1}^3 + \left(-\frac{10430827276}{243} + \frac{697278628}{405} \beta \right) L_{-8} L_{-5} L_{-1}^3 \\
& + \left(\frac{4093892420}{81} - \frac{5063706352}{405} \beta \right) L_{-7} L_{-6} L_{-1}^3 + \left(\frac{2816698331}{108} + \frac{14750597275}{324} \beta \right) L_{-13} L_{-1}^3 \\
& + \left(-\frac{3876174992}{243} - \frac{71245077136}{1215} \beta \right) L_{-5} L_{-4} L_{-3} L_{-2} L_{-1}^2 + \left(-\frac{15573821056}{2187} - \frac{5099410048}{10935} \beta \right) L_{-4} L_{-2}^5 L_{-1}^2 \\
& + \left(-\frac{240207548}{2187} - \frac{8494313084}{10935} \beta \right) L_{-3}^2 L_{-2}^4 L_{-1}^2 + \left(-\frac{47436984506}{2187} - \frac{39860881954}{2187} \beta \right) L_{-6} L_{-2}^4 L_{-1}^2
\end{aligned}$$

$$\begin{aligned}
& + \left(\frac{47109428591}{2187} + \frac{184063255247}{10935} \beta \right) L_{-5} L_{-3} L_{-2}^3 L_{-1}^2 + \left(\frac{34161020861}{729} - \frac{4963416739}{3645} \beta \right) L_{-4}^2 L_{-2}^3 L_{-1}^2 \\
& + \left(-\frac{5763567647}{1458} + \frac{2691154249}{162} \beta \right) L_{-8} L_{-2}^3 L_{-1}^2 + \left(-\frac{13695268444}{729} + \frac{7011515372}{3645} \beta \right) L_{-4} L_{-2}^3 L_{-2}^2 L_{-1}^2 \\
& + \left(\frac{21517454756}{729} - \frac{116959711288}{3645} \beta \right) L_{-7} L_{-3} L_{-2}^2 L_{-1}^2 + \left(\frac{196664238547}{729} + \frac{542209846357}{3645} \beta \right) L_{-6} L_{-4} L_{-2}^2 L_{-1}^2 \\
& + \left(-\frac{238400926535}{2916} - \frac{104126564893}{2916} \beta \right) L_{-5}^2 L_{-2}^2 L_{-1}^2 + \left(\frac{855093533125}{2916} + \frac{606232113211}{14580} \beta \right) L_{-10} L_{-2}^2 L_{-1}^2 \\
& + \left(\frac{1639307648}{729} - \frac{5639533168}{3645} \beta \right) L_{-3}^4 L_{-2} L_{-1}^2 + \left(-\frac{16056755168}{243} + \frac{3324232744}{243} \beta \right) L_{-6} L_{-3} L_{-2} L_{-1}^2 \\
& + \left(\frac{9611840}{729} + \frac{1922368}{729} \beta \right) L_{-2}^7 L_{-1}^2 + \left(-\frac{10283821591}{1458} + \frac{377475370451}{7290} \beta \right) L_{-9} L_{-3} L_{-2} L_{-1}^2 \\
& + \left(\frac{520593056}{81} + \frac{54200032}{3} \beta \right) L_{-4}^3 L_{-2} L_{-1}^2 + \left(-\frac{119998885100}{729} - \frac{62785077796}{729} \beta \right) L_{-8} L_{-4} L_{-2} L_{-1}^2 \\
& + \left(\frac{8363078144}{729} + \frac{380846363054}{3645} \beta \right) L_{-7} L_{-5} L_{-2} L_{-1}^2 + \left(\frac{82219813000}{729} - \frac{29138179912}{729} \beta \right) L_{-6}^2 L_{-2} L_{-1}^2 \\
& + \left(\frac{31541761250}{729} + \frac{97639549658}{3645} \beta \right) L_{-12} L_{-2} L_{-1}^2 + \left(\frac{3724220342}{729} + \frac{16033283606}{3645} \beta \right) L_{-5} L_{-3}^3 L_{-1}^2 \\
& + \left(-\frac{676716122}{81} - \frac{135149054}{135} \beta \right) L_{-4}^2 L_{-3} L_{-1}^2 + \left(\frac{39555209293}{729} + \frac{95016781}{3645} \beta \right) L_{-8} L_{-3}^2 L_{-1}^2 \\
& + \left(\frac{11257024304}{243} + \frac{15187070696}{1215} \beta \right) L_{-7} L_{-4} L_{-3} L_{-1}^2 + \left(-\frac{13835770486}{729} - \frac{20728972126}{3645} \beta \right) L_{-6} L_{-5} L_{-3} L_{-1}^2 \\
& + \left(\frac{161403296071}{1458} + \frac{185298212569}{7290} \beta \right) L_{-11} L_{-3} L_{-1}^2 + \left(-\frac{1353700318}{9} - \frac{5011610942}{81} \beta \right) L_{-6} L_{-4}^2 L_{-1}^2 \\
& + \left(\frac{39014405471}{729} + \frac{81704195681}{3645} \beta \right) L_{-5}^2 L_{-4} L_{-1}^2 + \left(-\frac{1251898711}{27} - \frac{3014837587}{405} \beta \right) L_{-10} L_{-4} L_{-1}^2 \\
& + \left(-\frac{54758596976}{729} - \frac{189462959732}{3645} \beta \right) L_{-9} L_{-5} L_{-1}^2 + \left(\frac{26091481631}{243} + \frac{81857918359}{1215} \beta \right) L_{-8} L_{-6} L_{-1}^2 \\
& + \left(\frac{41764853429}{243} - \frac{59364317437}{1215} \beta \right) L_{-6} L_{-5} L_{-2}^2 L_{-1} + \left(\frac{519772644341}{729} + \frac{536982902849}{3645} \beta \right) L_{-14} L_{-1}^2 \\
& + \left(\frac{16951960}{243} - \frac{9326296}{81} \beta \right) L_{-3} L_{-2}^6 L_{-1} + \left(-\frac{1718220067}{729} + \frac{565209697}{729} \beta \right) L_{-5} L_{-2}^5 L_{-1} \\
& + \left(\frac{611230072}{243} + \frac{3131873176}{1215} \beta \right) L_{-4} L_{-3} L_{-2}^4 L_{-1} + \left(\frac{16790069291}{648} - \frac{311417113}{72} \beta \right) L_{-7} L_{-4}^2 L_{-1} \\
& + \left(\frac{508133378}{243} - \frac{522868522}{1215} \beta \right) L_{-3}^3 L_{-2}^3 L_{-1} + \left(-\frac{3350726791}{243} + \frac{16970704619}{1215} \beta \right) L_{-6} L_{-3} L_{-2}^3 L_{-1} \\
& + \left(-\frac{6183346072}{243} - \frac{12019334032}{1215} \beta \right) L_{-5} L_{-4} L_{-2}^3 L_{-1} + \left(\frac{537159191}{648} - \frac{254533679}{3240} \beta \right) L_{-9} L_{-2}^3 L_{-1} \\
& + \left(-\frac{7490314333}{243} - \frac{5707344769}{1215} \beta \right) L_{-5} L_{-3}^2 L_{-2} L_{-1} + \left(\frac{4251155539}{81} - \frac{2417418029}{405} \beta \right) L_{-4} L_{-3} L_{-2}^2 L_{-1} \\
& + \left(-\frac{13774642501}{486} + \frac{47574031139}{2430} \beta \right) L_{-8} L_{-3} L_{-2}^2 L_{-1} + \left(-\frac{30597896944}{81} + \frac{7602405812}{405} \beta \right) L_{-7} L_{-4} L_{-2}^2 L_{-1} \\
& + \left(-\frac{1818452026}{81} + \frac{2487870947}{405} \beta \right) L_{-7}^2 L_{-1}^2 + \left(-\frac{598093659731}{1944} - \frac{118832263337}{9720} \beta \right) L_{-11} L_{-2}^2 L_{-1} \\
& + \left(-\frac{1127428304}{81} + \frac{2005731856}{405} \beta \right) L_{-4} L_{-3}^3 L_{-2} L_{-1} + \left(\frac{8937898306}{81} - \frac{9374211074}{405} \beta \right) L_{-7} L_{-3}^2 L_{-2} L_{-1} \\
& + \left(-\frac{2175490966}{81} - \frac{7301230378}{405} \beta \right) L_{-6} L_{-4} L_{-3} L_{-2} L_{-1} + \left(\frac{5686048555}{486} + \frac{71774155933}{2430} \beta \right) L_{-5}^2 L_{-3} L_{-2} L_{-1} \\
& + \left(\frac{5640483061}{162} - \frac{25935548597}{810} \beta \right) L_{-10} L_{-3} L_{-2} L_{-1} + \left(\frac{2068510520}{81} - \frac{175247464}{405} \beta \right) L_{-5} L_{-4} L_{-2} L_{-1} \\
& + \left(\frac{30251263}{18} - \frac{780131773}{270} \beta \right) L_{-9} L_{-4} L_{-2} L_{-1} + \left(\frac{1652402846}{81} - \frac{13911205078}{405} \beta \right) L_{-8} L_{-5} L_{-2} L_{-1} \\
& + \left(-\frac{2116132367}{27} + \frac{3248810563}{135} \beta \right) L_{-7} L_{-6} L_{-2} L_{-1} + \left(-\frac{8015375435}{648} - \frac{40699798345}{648} \beta \right) L_{-13} L_{-2} L_{-1} \\
& + \left(-\frac{124276184}{81} - \frac{369101384}{405} \beta \right) L_{-3}^5 L_{-1} + \left(\frac{474109532}{27} + \frac{439356476}{45} \beta \right) L_{-6} L_{-3}^3 L_{-1} \\
& + \left(\frac{813558668}{81} - \frac{5307013348}{405} \beta \right) L_{-5} L_{-4} L_{-3} L_{-1} + \left(-\frac{1380887179}{54} + \frac{6613469743}{270} \beta \right) L_{-9} L_{-3}^2 L_{-1} \\
& + \left(-\frac{185916220}{9} + \frac{20241916}{3} \beta \right) L_{-4}^3 L_{-3} L_{-1} + \left(\frac{242801510}{9} - \frac{4142537918}{135} \beta \right) L_{-8} L_{-4} L_{-3} L_{-1} \\
& + \left(-\frac{2519102860}{81} + \frac{1743712978}{81} \beta \right) L_{-7} L_{-5} L_{-3} L_{-1} + \left(-\frac{48696580}{81} - \frac{10819957036}{405} \beta \right) L_{-6}^2 L_{-3} L_{-1} \\
& + \left(\frac{3430860452}{81} + \frac{18602113922}{405} \beta \right) L_{-12} L_{-3} L_{-1} + \left(\frac{7433166527}{54} - \frac{2647655137}{270} \beta \right) L_{-7} L_{-4} L_{-1} \\
& + \left(-\frac{4287087352}{81} + \frac{2955645208}{81} \beta \right) L_{-6} L_{-5} L_{-4} L_{-1} + \left(-\frac{887650963}{54} - \frac{8540950477}{270} \beta \right) L_{-11} L_{-4} L_{-1} \\
& + \left(\frac{187772049}{243} - \frac{1317572437}{243} \beta \right) L_{-5}^3 L_{-1} + \left(\frac{10351048265}{81} + \frac{14282331911}{405} \beta \right) L_{-10} L_{-5} L_{-1} \\
& + \left(\frac{382719419}{9} - \frac{178157449}{3} \beta \right) L_{-9} L_{-6} L_{-1} + \left(-\frac{45624853453}{324} + \frac{38349308507}{1620} \beta \right) L_{-8} L_{-7} L_{-1} \\
& + \left(-\frac{45585350849}{162} - \frac{100134503837}{3240} \beta \right) L_{-15} L_{-1} + \left(\frac{22715000}{243} + \frac{4543000}{243} \beta \right) L_{-2}^8 \\
& + \left(-\frac{2052937000}{729} - \frac{548807000}{729} \beta \right) L_{-4} L_{-2}^6 + \left(\frac{1729008875}{1458} + \frac{700883575}{1458} \beta \right) L_{-3}^2 L_{-2}^5 \\
& + \left(\frac{31484615917}{2916} + \frac{13690595345}{2916} \beta \right) L_{-6} L_{-2}^5 + \left(-\frac{141033886615}{5832} - \frac{54089482475}{5832} \beta \right) L_{-5} L_{-3} L_{-2}^4 \\
& + \left(\frac{16209468985}{648} + \frac{4917725989}{648} \beta \right) L_{-4}^2 L_{-2}^4 + \left(-\frac{69278656301}{1296} - \frac{5818122955}{432} \beta \right) L_{-8} L_{-2}^4 \\
& + \left(\frac{327789298}{243} - \frac{182443906}{243} \beta \right) L_{-4} L_{-2}^3 L_{-2}^3 + \left(\frac{579707603}{54} + \frac{1499507321}{162} \beta \right) L_{-7} L_{-3} L_{-2}^3 \\
& + \left(-\frac{71894257961}{486} - \frac{27674494435}{486} \beta \right) L_{-6} L_{-4} L_{-2}^3 + \left(\frac{529286724439}{5832} + \frac{171551292269}{5832} \beta \right) L_{-5}^2 L_{-2}^3
\end{aligned}$$

$$\begin{aligned}
& + \left(-\frac{219343338799}{1944} - \frac{48802331837}{1944} \beta \right) L_{-10} L_{-2}^3 + \left(-\frac{752201776}{243} - \frac{99365984}{243} \beta \right) L_{-3}^4 L_{-2}^2 \\
& + \left(\frac{3167581984}{81} + \frac{164797772}{81} \beta \right) L_{-6} L_{-3}^2 L_{-2}^2 + \left(\frac{7333242724}{243} + \frac{5959030124}{243} \beta \right) L_{-5} L_{-4} L_{-3} L_{-2}^2 \\
& + \left(-\frac{3744239456}{81} - \frac{4563477511}{162} \beta \right) L_{-9} L_{-3} L_{-2}^2 + \left(-\frac{4568992472}{81} - \frac{1329441208}{81} \beta \right) L_{-4}^3 L_{-2}^2 \\
& + \left(\frac{98011788952}{243} + \frac{23350859840}{243} \beta \right) L_{-8} L_{-4} L_{-2}^2 + \left(-\frac{20981999923}{243} - \frac{24546873745}{486} \beta \right) L_{-7} L_{-5} L_{-2}^2 \\
& + \left(-\frac{12537042125}{243} + \frac{2293822643}{243} \beta \right) L_{-6}^2 L_{-2}^2 + \left(\frac{148867854119}{972} + \frac{25735300993}{972} \beta \right) L_{-12} L_{-2}^2 \\
& + \left(\frac{3397474222}{243} + \frac{592140590}{243} \beta \right) L_{-5} L_{-3}^3 L_{-2} + \left(-\frac{153629552}{81} - \frac{157430272}{81} \beta \right) L_{-4}^2 L_{-3}^2 L_{-2} \\
& + \left(-\frac{18698585200}{243} - \frac{3030629912}{243} \beta \right) L_{-8} L_{-3}^2 L_{-2} + \left(\frac{332973250}{81} + \frac{334271030}{81} \beta \right) L_{-7} L_{-4} L_{-3} L_{-2} \\
& + \left(\frac{4006295476}{243} + \frac{1534401548}{243} \beta \right) L_{-6} L_{-5} L_{-3} L_{-2} + \left(-\frac{39235245287}{243} - \frac{11785966714}{243} \beta \right) L_{-11} L_{-3} L_{-2} \\
& + \left(\frac{3943923671}{27} + 51922221 \beta \right) L_{-6} L_{-4}^2 L_{-2} + \left(-\frac{56023386371}{486} - \frac{17628497017}{486} \beta \right) L_{-5}^2 L_{-4} L_{-2} \\
& + \left(\frac{18665820475}{162} + \frac{4831631945}{162} \beta \right) L_{-10} L_{-4} L_{-2} + \left(\frac{132951996853}{486} + \frac{49107342479}{486} \beta \right) L_{-9} L_{-5} L_{-2} \\
& + \left(-\frac{2535966295}{18} - \frac{424001521}{6} \beta \right) L_{-8} L_{-6} L_{-2} + \left(-\frac{3527974355}{324} - \frac{2781374389}{324} \beta \right) L_{-7}^2 L_{-2} \\
& + \left(-\frac{256267624133}{486} - \frac{53727010357}{486} \beta \right) L_{-14} L_{-2} + \left(\frac{62662600}{81} + \frac{33837512}{81} \beta \right) L_{-4} L_{-3}^4 \\
& + \left(\frac{12081754}{81} - \frac{386061646}{81} \beta \right) L_{-7} L_{-3}^3 + \left(-\frac{1235827894}{81} + \frac{324696958}{81} \beta \right) L_{-6} L_{-4} L_{-3}^2 \\
& + \left(-\frac{734163464}{81} - \frac{27208715}{81} \beta \right) L_{-5}^2 L_{-3}^2 + \left(\frac{1700122117}{54} - \frac{141939863}{18} \beta \right) L_{-10} L_{-3}^2 \\
& + \left(-\frac{644584063}{162} - \frac{1563558899}{162} \beta \right) L_{-5} L_{-4}^2 L_{-3} + \left(-\frac{2365946831}{81} + \frac{391994255}{81} \beta \right) L_{-9} L_{-4} L_{-3} \\
& + \left(\frac{41998314095}{324} + \frac{14424238267}{324} \beta \right) L_{-8} L_{-5} L_{-3} + \left(-\frac{5696336410}{81} - \frac{1244830214}{81} \beta \right) L_{-7} L_{-6} L_{-3} \\
& + \left(-\frac{50875270591}{648} - \frac{5501974607}{162} \beta \right) L_{-13} L_{-3} + \left(\frac{141665042}{9} + \frac{45794666}{9} \beta \right) L_{-4}^4 \\
& + \left(-\frac{16720323782}{81} - \frac{4469878486}{81} \beta \right) L_{-8} L_{-4}^2 + \left(\frac{4719078932}{81} + \frac{1981388674}{81} \beta \right) L_{-7} L_{-5} L_{-4} \\
& + \left(\frac{3329574508}{27} + \frac{774237704}{27} \beta \right) L_{-6}^2 L_{-4} + \left(-\frac{24444294973}{81} - \frac{7245075107}{81} \beta \right) L_{-12} L_{-4} \\
& + \left(-\frac{17795208008}{243} - \frac{5697658762}{243} \beta \right) L_{-6} L_{-5}^2 + \left(\frac{172133662723}{648} + \frac{2558624480}{27} \beta \right) L_{-11} L_{-5} \\
& + \left(-\frac{2482312006}{81} - \frac{359398637}{81} \beta \right) L_{-10} L_{-6} + \left(-\frac{11445305005}{324} - \frac{11100560395}{648} \beta \right) L_{-9} L_{-7} \\
& + \left(\frac{88700463031}{486} + \frac{21332312435}{486} \beta \right) L_{-8}^2 + \left(-\frac{273742696867}{324} - \frac{76299006809}{324} \beta \right) L_{-16} \Big) |h-l\rangle \\
& + \left(L_{-1}^{14} - \frac{511}{6} L_{-2} L_{-1}^{12} + 273 L_{-3} L_{-1}^{11} + \frac{31031}{12} L_{-2}^2 L_{-1}^{10} - 3575 L_{-4} L_{-1}^{10} - \frac{71357}{6} L_{-3} L_{-2} L_{-1}^9 \right. \\
& + \frac{156871}{9} L_{-5} L_{-1}^9 - \frac{7702123}{216} L_{-3}^2 L_{-1}^8 + \frac{2429141}{18} L_{-4} L_{-2} L_{-1}^8 - \frac{29315}{18} L_{-3}^2 L_{-1}^8 \\
& - \frac{330200}{9} L_{-6} L_{-1}^8 + \frac{3232229}{18} L_{-3} L_{-2}^2 L_{-1}^7 - \frac{14411306}{27} L_{-5} L_{-2} L_{-1}^7 - \frac{190736}{3} L_{-4} L_{-3} L_{-1}^7 \\
& + \frac{1113553}{12} L_{-7} L_{-1}^7 + \frac{299830531}{1296} L_{-2}^4 L_{-1}^6 - \frac{87916465}{54} L_{-4} L_{-2}^2 L_{-1}^6 - \frac{1101737}{54} L_{-3}^2 L_{-2} L_{-1}^6 \\
& + \frac{25678282}{27} L_{-6} L_{-2} L_{-1}^6 + \frac{11453869}{108} L_{-5} L_{-3} L_{-1}^6 + \frac{1494307}{3} L_{-4} L_{-1}^6 - \frac{18846499}{18} L_{-8} L_{-1}^6 \\
& - \frac{120020173}{108} L_{-3} L_{-2}^3 L_{-1}^5 + \frac{9826873}{2} L_{-5} L_{-2}^2 L_{-1}^5 + \frac{12821156}{9} L_{-4} L_{-3} L_{-2} L_{-1}^5 \\
& - \frac{52971385}{24} L_{-7} L_{-2} L_{-1}^5 + \frac{858578}{9} L_{-3}^3 L_{-1}^5 + \frac{340520}{9} L_{-6} L_{-3} L_{-1}^5 - \frac{16430486}{9} L_{-5} L_{-4} L_{-1}^5 \\
& + \frac{53355355}{18} L_{-9} L_{-1}^5 - \frac{563493749}{864} L_{-2}^5 L_{-1}^4 + \frac{779378095}{108} L_{-4} L_{-2}^3 L_{-1}^4 + \frac{1494401}{3} L_{-3}^2 L_{-2}^2 L_{-1}^4 \\
& - \frac{20491817}{3} L_{-6} L_{-2}^2 L_{-1}^4 - \frac{165034463}{72} L_{-5} L_{-3} L_{-2} L_{-1}^4 - \frac{118077817}{18} L_{-4}^2 L_{-2} L_{-1}^4 \\
& + \frac{558714659}{36} L_{-8} L_{-2} L_{-1}^4 - \frac{5919766}{9} L_{-4} L_{-2}^2 L_{-1}^4 + \frac{173851973}{72} L_{-7} L_{-3} L_{-1}^4 \\
& - \frac{3001604}{3} L_{-6} L_{-4} L_{-1}^4 + \frac{209551}{3} L_{-5}^2 L_{-1}^4 + \frac{19970203}{9} L_{-10} L_{-1}^4 + \frac{370750733}{144} L_{-3} L_{-2}^4 L_{-1}^3 \\
& - \frac{88749761}{6} L_{-5} L_{-3}^2 L_{-1}^3 - \frac{69331496}{9} L_{-4} L_{-3} L_{-2}^2 L_{-1}^3 + \frac{588707659}{48} L_{-7} L_{-2}^2 L_{-1}^3 \\
& - \frac{47120023}{54} L_{-3}^3 L_{-2} L_{-1}^3 + \frac{4427710}{3} L_{-6} L_{-3} L_{-2} L_{-1}^3 + \frac{149796614}{9} L_{-5} L_{-4} L_{-2} L_{-1}^3 \\
& - \frac{1533491879}{54} L_{-9} L_{-2} L_{-1}^3 + \frac{52642805}{36} L_{-5} L_{-3}^2 L_{-1}^3 + 2193925 L_{-4}^2 L_{-3} L_{-1}^3 \\
& - \frac{244608971}{18} L_{-8} L_{-3} L_{-1}^3 - \frac{68361415}{12} L_{-7} L_{-4} L_{-1}^3 + \frac{104958070}{9} L_{-6} L_{-5} L_{-1}^3 \\
& - \frac{3755911505}{144} L_{-11} L_{-1}^3 + \frac{359158375}{576} L_{-2}^6 L_{-1}^2 - \frac{1422954571}{144} L_{-4} L_{-2}^4 L_{-1}^2 - \frac{110349109}{72} L_{-3}^2 L_{-2}^2 L_{-1}^2 \\
& + \frac{242776861}{18} L_{-6} L_{-2}^2 L_{-1}^2 + \frac{417557591}{48} L_{-5} L_{-3} L_{-2}^2 L_{-1}^2 + \frac{215671777}{12} L_{-4}^2 L_{-2}^2 L_{-1}^2 \\
& - \frac{1133758667}{24} L_{-8} L_{-2}^2 L_{-1}^2 + \frac{9402171}{2} L_{-4} L_{-2}^2 L_{-3} L_{-2} L_{-1}^2 - \frac{46173362}{3} L_{-7} L_{-3} L_{-2} L_{-1}^2 \Big)
\end{aligned}$$

$$\begin{aligned}
& + \frac{8619874}{3} L_{-6} L_{-4} L_{-2} L_{-1}^2 - 346185 L_{-5}^2 L_{-2} L_{-1}^2 - 12764834 L_{-10} L_{-2} L_{-1}^2 + \frac{781726}{9} L_{-3}^4 L_{-1}^2 \\
& - \frac{6265157}{3} L_{-6} L_{-3}^2 L_{-1}^2 - \frac{17503249}{4} L_{-5} L_{-4} L_{-3} L_{-1}^2 + \frac{851252395}{72} L_{-9} L_{-3} L_{-1}^2 \\
& - \frac{10377505}{3} L_{-4}^3 L_{-1}^2 + \frac{88750081}{2} L_{-8} L_{-4} L_{-1}^2 - \frac{107002967}{48} L_{-7} L_{-5} L_{-1}^2 - 15108105 L_{-6}^2 L_{-1}^2 \\
& + \frac{421427881}{12} L_{-12} L_{-1}^2 - \frac{429866875}{288} L_{-3} L_{-2}^5 L_{-1} + \frac{1485768463}{144} L_{-5} L_{-2}^4 L_{-1} \\
& + \frac{75890573}{9} L_{-4} L_{-3} L_{-2}^3 L_{-1} - \frac{3917780737}{288} L_{-7} L_{-2}^3 L_{-1} + \frac{47264245}{36} L_{-3}^3 L_{-2}^2 L_{-1} \\
& - \frac{14009867}{3} L_{-6} L_{-3} L_{-2}^2 L_{-1} - \frac{47369767}{2} L_{-5} L_{-4} L_{-2}^2 L_{-1} + \frac{3093452827}{72} L_{-9} L_{-2}^2 L_{-1} \\
& - \frac{114347681}{24} L_{-5} L_{-3}^2 L_{-2} L_{-1} - \frac{46986829}{6} L_{-4} L_{-3} L_{-2} L_{-1} + \frac{171211201}{4} L_{-8} L_{-3} L_{-2} L_{-1} \\
& + \frac{452772625}{24} L_{-7} L_{-4} L_{-2} L_{-1} - \frac{96873449}{3} L_{-6} L_{-5} L_{-2} L_{-1} + \frac{2348340155}{32} L_{-11} L_{-2} L_{-1} \\
& - \frac{8346652}{9} L_{-4} L_{-3}^3 L_{-1} + \frac{36927503}{12} L_{-7} L_{-3}^2 L_{-1} + 1760132 L_{-6} L_{-4} L_{-3} L_{-1} - \frac{41087977}{12} L_{-6} L_{-2}^4 \\
& + \frac{2278813}{12} L_{-5}^2 L_{-3} L_{-1} + 12560898 L_{-10} L_{-3} L_{-1} + 5520381 L_{-5} L_{-4}^2 L_{-1} + \frac{16051875}{32} L_{-3}^2 L_{-2}^4 \\
& - 504079789 L_{-9} L_{-4} L_{-1} - \frac{114043262}{3} L_{-8} L_{-5} L_{-1} + 17921683 L_{-7} L_{-6} L_{-1} + \frac{178458875}{96} L_{-4} L_{-2}^5 \\
& + \frac{3300324455}{144} L_{-13} L_{-1} - \frac{11116875}{128} L_{-7}^2 - \frac{111748133}{32} L_{-5} L_{-3} L_{-2}^3 - \frac{136597993}{24} L_{-4}^2 L_{-2}^3 \\
& + \frac{262660881}{16} L_{-8} L_{-2}^3 - \frac{11084647}{4} L_{-4} L_{-3}^2 L_{-2} + \frac{273622811}{32} L_{-7} L_{-3} L_{-2}^2 - 22330 L_{-6} L_{-4} L_{-2}^2 \\
& + \frac{690417}{4} L_{-5}^2 L_{-2}^2 + \frac{69379331}{12} L_{-10} L_{-2}^2 - \frac{1549555}{12} L_{-3}^4 L_{-2} + \frac{4463795}{2} L_{-6} L_{-3}^2 L_{-2} \\
& + \frac{43957095}{8} L_{-5} L_{-4} L_{-3} L_{-2} - \frac{249418197}{16} L_{-9} L_{-3} L_{-2} + \frac{60703909}{18} L_{-4}^3 L_{-2} - \frac{17478125}{4} L_{-8} L_{-2}^3 \\
& - \frac{531624373}{12} L_{-8} L_{-4} L_{-2} + \frac{245476273}{96} L_{-7} L_{-5} L_{-2} + \frac{90955697}{6} L_{-6}^2 L_{-2} - \frac{844913671}{24} L_{-12} L_{-2} \\
& + \frac{8812909}{24} L_{-3} L_{-2}^3 + \frac{6587483}{6} L_{-4}^2 L_{-2}^3 - \frac{103274297}{24} L_{-7} L_{-4} L_{-3} + 2522646 L_{-6} L_{-5} L_{-3} \\
& - \frac{210841967}{24} L_{-11} L_{-3} + \frac{3034556}{3} L_{-6} L_{-4}^2 - 525399 L_{-5}^2 L_{-4} - 17243744 L_{-10} L_{-4} \\
& + \frac{64762145}{6} L_{-9} L_{-5} + 6664196 L_{-8} L_{-6} - \frac{400057469}{96} L_{-7}^2 - \frac{254131871}{12} L_{-14} \Big) |h; 1\rangle.
\end{aligned}$$

C.3 Explicit nullvectors in the bulk of $\mathfrak{c}_{2,3} = 0$

In the following we give the explicit form of the nullvector of type **E** which has a Jordan cell at $h = 1$, lowest weight $h = 0$ and appears at level 12. Again, for the sake of brevity, we have set the overall normalisation to 1 and also eliminated any further freedom by setting any further free parameter to 0; again, the parameter β remains as it is a parameter of the representation as introduced in section 4.2.3:

$$\begin{aligned}
& \left(-\frac{44800}{27} L_{-3} L_{-2}^4 L_{-1} + \left(\frac{358528}{27} - \frac{4000}{9} \beta\right) L_{-5} L_{-2}^3 L_{-1} + \left(\frac{117920}{27} + \frac{49600}{9} \beta\right) L_{-4} L_{-3} L_{-2}^2 L_{-1} \right. \\
& + \left(-\frac{1543136}{81} - \frac{814208}{81} \beta\right) L_{-7} L_{-2}^2 L_{-1} + \left(-\frac{572912}{81} - \frac{100000}{27} \beta\right) L_{-3}^3 L_{-2} L_{-1} \\
& + \left(\frac{620576}{9} - \frac{217408}{9} \beta\right) L_{-6} L_{-3} L_{-2} L_{-1} + \left(-\frac{1214624}{27} + \frac{243424}{9} \beta\right) L_{-5} L_{-4} L_{-2} L_{-1} \\
& + \left(\frac{3934496}{81} - \frac{341888}{27} \beta\right) L_{-9} L_{-2} L_{-1} + \left(\frac{551312}{27} + \frac{396352}{9} \beta\right) L_{-5} L_{-3}^2 L_{-1} \\
& + \left(-\frac{91424}{9} - \frac{116416}{3} \beta\right) L_{-4} L_{-3} L_{-1} + \left(-\frac{619904}{27} - 1408 \beta\right) L_{-8} L_{-3} L_{-1} \\
& + \left(\frac{548672}{9} + \frac{769984}{9} \beta\right) L_{-7} L_{-4} L_{-1} + \left(-\frac{4270240}{81} - \frac{532160}{9} \beta\right) L_{-6} L_{-5} L_{-1} \\
& + \left(\frac{3200}{9} - \frac{44800}{27} \beta\right) L_{-4} L_{-2}^4 + \left(\frac{10400}{3} + \frac{11200}{9} \beta\right) L_{-3}^2 L_{-2}^3 + \left(-\frac{2984320}{243} + \frac{585856}{27} \beta\right) L_{-6} L_{-2}^3 \\
& + \left(-\frac{1611424}{81} - \frac{1122080}{27} \beta\right) L_{-5} L_{-3} L_{-2}^2 + \left(-\frac{63488}{27} + 36864 \beta\right) L_{-4} L_{-2}^3 L_{-2} \\
& + \left(\frac{309376}{9} + \frac{72832}{3} \beta\right) L_{-11} L_{-1} + \left(\frac{571936}{81} + \frac{304064}{9} \beta\right) L_{-8} L_{-2}^2 + \left(\frac{195488}{27} - \frac{9920}{3} \beta\right) L_{-4}^2 L_{-2}^2 \\
& + \left(\frac{229504}{81} - \frac{515328}{81} \beta\right) L_{-7} L_{-3} L_{-2} + \left(-\frac{1020352}{81} - \frac{1000192}{9} \beta\right) L_{-6} L_{-4} L_{-2} \\
& + \left(\frac{451616}{27} + \frac{709312}{9} \beta\right) L_{-5}^2 L_{-2} + \left(-\frac{200192}{9} - \frac{279040}{3} \beta\right) L_{-10} L_{-2} + \left(\frac{40096}{81} - \frac{318016}{27} \beta\right) L_{-3}^4 \\
& + \left(-\frac{693152}{81} + \frac{1014976}{9} \beta\right) L_{-6} L_{-2}^3 + \left(-\frac{1646560}{81} + \frac{3016960}{27} \beta\right) L_{-9} L_{-3} + \left(\frac{1521088}{81} - \frac{762496}{9} \beta\right) L_{-2}^6 \\
& \left. + \left(-\frac{35168}{9} + \frac{95168}{3} \beta\right) L_{-4}^3 + \left(\frac{128672}{27} - \frac{892096}{9} \beta\right) L_{-8} L_{-4} + \left(-\frac{758240}{81} + \frac{6217312}{81} \beta\right) L_{-7} L_{-5} \right)
\end{aligned}$$

$$\begin{aligned}
& + \left(\frac{306176}{27} - \frac{234080}{3} \beta \right) L_{-5} L_{-4} L_{-3} + \left(-\frac{947200}{27} + \frac{758080}{9} \beta \right) L_{-12} \Big) |h-l\rangle \\
& + \left(L_{-1}^{11} - 44L_{-2}L_{-1}^9 + 88L_{-3}L_{-1}^8 + \frac{1804}{3}L_{-2}^2L_{-1}^7 - 836L_{-4}L_{-1}^7 - 1320L_{-3}L_{-2}L_{-1}^6 \right. \\
& + \frac{16456}{9}L_{-5}L_{-1}^6 - \frac{85184}{27}L_{-2}^3L_{-1}^5 + \frac{107536}{9}L_{-4}L_{-2}L_{-1}^5 - \frac{12232}{9}L_{-3}^2L_{-1}^5 + \frac{4640}{9}L_{-6}L_{-1}^5 \\
& + \frac{52448}{9}L_{-3}L_{-2}^2L_{-1}^4 - \frac{168112}{9}L_{-5}L_{-2}L_{-1}^4 + 720L_{-4}L_{-3}L_{-1}^4 - 1360L_{-7}L_{-1}^4 + \frac{53504}{9}L_{-2}^4L_{-1}^3 \\
& - \frac{373888}{9}L_{-4}L_{-2}^2L_{-1}^3 + \frac{59072}{9}L_{-3}^2L_{-2}L_{-1}^3 - \frac{13760}{9}L_{-6}L_{-2}L_{-1}^3 - \frac{56896}{9}L_{-5}L_{-3}L_{-1}^3 \\
& + 15520L_{-4}^2L_{-1}^3 - \frac{214816}{9}L_{-8}L_{-1}^3 - \frac{22784}{3}L_{-3}L_{-2}^3L_{-1}^2 + \frac{120320}{3}L_{-5}L_{-2}^2L_{-1}^2 \\
& - \frac{7040}{3}L_{-4}L_{-3}L_{-2}L_{-1}^2 + \frac{3904}{3}L_{-7}L_{-2}L_{-1}^2 + \frac{22016}{9}L_{-3}^3L_{-1}^2 + 3008L_{-6}L_{-3}L_{-1}^2 \\
& - \frac{46016}{3}L_{-5}L_{-4}L_{-1}^2 + \frac{161152}{9}L_{-9}L_{-1}^2 - \frac{8192}{3}L_{-5}^2L_{-1} + 29696L_{-4}L_{-2}^3L_{-1} \\
& - 4672L_{-3}^2L_{-2}L_{-1} - \frac{2048}{3}L_{-6}L_{-2}^2L_{-1} + \frac{27392}{3}L_{-5}L_{-3}L_{-2}L_{-1} - \frac{94208}{3}L_{-4}^2L_{-2}L_{-1} \\
& + 53120L_{-8}L_{-2}L_{-1} + \frac{1984}{3}L_{-4}L_{-3}^2L_{-1} + \frac{24832}{3}L_{-7}L_{-3}L_{-1} - \frac{45952}{3}L_{-6}L_{-4}L_{-1} \\
& - \frac{3776}{3}L_{-5}^2L_{-1} + 22784L_{-10}L_{-1} + \frac{4096}{3}L_{-3}L_{-2}^4 - 9984L_{-5}L_{-2}^3 + 128L_{-4}L_{-3}L_{-2}^2 \\
& + \frac{3328}{3}L_{-7}L_{-2}^2 - \frac{3968}{3}L_{-3}^3L_{-2} - \frac{5632}{3}L_{-6}L_{-3}L_{-2} + \frac{33536}{3}L_{-5}L_{-4}L_{-2} \\
& - \frac{39808}{3}L_{-9}L_{-2} + \frac{4480}{3}L_{-5}L_{-3}^2 - \frac{3200}{3}L_{-4}^2L_{-3} - 4480L_{-8}L_{-3} \\
& \left. - \frac{6656}{3}L_{-7}L_{-4} + 8064L_{-6}L_{-5} - \frac{48256}{3}L_{-11} \right) |h; 1\rangle.
\end{aligned}$$

The explicit form of the nullvector of type \mathbf{F} which has a Jordan cell at $h = 2$, lowest weight $h = 0$ and also appears at level 12 is given below. As we need the full beauty of this result in the argument of section 4.2.3 any free parameter appears as calculated (noted as m_i); only the overall normalisation we have set to 1:

$$\begin{aligned}
& \left(m_{76}L_{-1}^{12} + m_{75}L_{-2}L_{-1}^{10} + m_{74}L_{-3}L_{-1}^9 + m_{73}L_{-2}^2L_{-1}^8 + m_{72}L_{-4}L_{-1}^8 \right. \\
& + m_{71}L_{-3}L_{-2}L_{-1}^7 + m_{70}L_{-5}L_{-1}^7 + m_{69}L_{-2}^3L_{-1}^6 + m_{68}L_{-4}L_{-2}L_{-1}^6 + m_{67}L_{-3}^2L_{-1}^6 \\
& + m_{66}L_{-6}L_{-1}^6 + m_{65}L_{-3}L_{-2}^2L_{-1}^5 + m_{64}L_{-5}L_{-2}L_{-1}^5 + m_{63}L_{-4}L_{-3}L_{-1}^5 \\
& + m_{62}L_{-7}L_{-1}^5 + m_{61}L_{-2}^4L_{-1}^4 + m_{60}L_{-4}L_{-2}^2L_{-1}^4 + m_{59}L_{-3}^2L_{-2}L_{-1}^4 \\
& + m_{58}L_{-6}L_{-2}L_{-1}^4 + m_{57}L_{-5}L_{-3}L_{-1}^4 + m_{56}L_{-2}^4L_{-1}^4 + m_{55}L_{-8}L_{-1}^4 \\
& + m_{54}L_{-3}L_{-2}^3L_{-1}^3 + m_{53}L_{-5}L_{-2}^2L_{-1}^3 + m_{52}L_{-4}L_{-3}L_{-2}L_{-1}^3 + m_{51}L_{-7}L_{-2}L_{-1}^3 \\
& + m_{50}L_{-3}^3L_{-1}^3 + m_{49}L_{-6}L_{-3}L_{-1}^3 + m_{48}L_{-5}L_{-4}L_{-1}^3 + m_{47}L_{-9}L_{-1}^3 + m_{46}L_{-5}^2L_{-1}^3 \\
& + m_{45}L_{-4}L_{-2}^3L_{-1}^2 + m_{44}L_{-3}^2L_{-2}^2L_{-1}^2 + m_{43}L_{-6}L_{-2}^2L_{-1}^2 + m_{42}L_{-5}L_{-3}L_{-2}L_{-1}^2 \\
& + m_{41}L_{-4}^2L_{-2}L_{-1}^2 + m_{40}L_{-8}L_{-2}L_{-1}^2 + m_{39}L_{-4}L_{-3}^2L_{-1}^2 + m_{38}L_{-7}L_{-3}L_{-1}^2 \\
& + m_{37}L_{-6}L_{-4}L_{-1}^2 + m_{36}L_{-5}^2L_{-1}^2 + m_{35}L_{-10}L_{-1}^2 + m_{34}L_{-3}L_{-2}^4L_{-1} \\
& + m_{33}L_{-5}L_{-3}^2L_{-1} + m_{32}L_{-4}L_{-3}L_{-2}^2L_{-1} + m_{31}L_{-7}L_{-2}^2L_{-1} + m_{30}L_{-3}^3L_{-2}L_{-1} \\
& + m_{29}L_{-6}L_{-3}L_{-2}L_{-1} + m_{28}L_{-5}L_{-4}L_{-2}L_{-1} + m_{27}L_{-9}L_{-2}L_{-1} + m_{26}L_{-5}L_{-3}^2L_{-1} \\
& + m_{25}L_{-4}^2L_{-3}L_{-1} + m_{24}L_{-8}L_{-3}L_{-1} + m_{23}L_{-7}L_{-4}L_{-1} + m_{22}L_{-6}L_{-5}L_{-1} + \\
& m_{21}L_{-11}L_{-1} - 4096L_{-4}L_{-2}^4 + 3072L_{-3}^2L_{-2}^3 + (12800 - 8192\beta)L_{-6}L_{-2}^3 \\
& + (-32960 + 14336\beta)L_{-5}L_{-3}L_{-2}^2 + (30976 + 6144\beta)L_{-4}^2L_{-2}^2 + (-25088 - 17920\beta)L_{-8}L_{-2}^2 \\
& + (-4736 - 18432\beta)L_{-4}L_{-3}^2L_{-2} + (18560 + 32640\beta)L_{-7}L_{-3}L_{-2} \\
& + (-73216 + 50176\beta)L_{-6}L_{-4}L_{-2} + (54464 - 36608\beta)L_{-5}^2L_{-2} + (-496 + 5760\beta)L_{-4}^4 \\
& + (-18432 + 48128\beta)L_{-10}L_{-2} + (12096 - 54784\beta)L_{-6}L_{-3}^2 + (2432 + 40448\beta)L_{-5}L_{-4}L_{-3} \\
& + (-11648 - 59008\beta)L_{-9}L_{-3} + \left(-\frac{22144}{3} - 17408\beta \right) L_{-4}^3 + (27264 + 55040\beta)L_{-8}L_{-4} \\
& \left. + (-5120 - 39040\beta)L_{-7}L_{-5} + (-4288 + 41472\beta)L_{-6}^2 + (31552 - 35328\beta)L_{-12} \right) |h-l\rangle
\end{aligned}$$

$$\begin{aligned}
& + \left(L_{-1}^{10} - \frac{130}{3} L_{-2} L_{-1}^8 + \frac{284}{3} L_{-3} L_{-1}^7 + \frac{5152}{9} L_{-2}^2 L_{-1}^6 - 776 L_{-4} L_{-1}^6 - 1488 L_{-3} L_{-2} L_{-1}^5 \right. \\
& + \frac{6232}{3} L_{-5} L_{-1}^5 - \frac{8320}{3} L_{-2}^3 L_{-1}^4 + \frac{29440}{3} L_{-4} L_{-2} L_{-1}^4 - \frac{2752}{3} L_{-3}^2 L_{-1}^4 + 640 L_{-6} L_{-1}^4 \\
& + \frac{21376}{3} L_{-3} L_{-2}^2 L_{-1}^3 - \frac{67264}{3} L_{-5} L_{-2} L_{-1}^3 + \frac{800}{3} L_{-4} L_{-3} L_{-1}^3 - 800 L_{-7} L_{-1}^3 + 4096 L_{-2}^4 L_{-1}^2 \\
& - 23552 L_{-4} L_{-2}^2 L_{-1}^2 + 992 L_{-3}^2 L_{-2} L_{-1}^2 - 3840 L_{-6} L_{-2} L_{-1}^2 + 8896 L_{-5} L_{-3} L_{-1}^2 \\
& - 9024 L_{-8} L_{-1}^2 - 10240 L_{-3} L_{-2}^3 L_{-1} + 48768 L_{-5} L_{-2}^2 L_{-1} + 4160 L_{-4} L_{-3} L_{-2} L_{-1} \\
& - 4992 L_{-7} L_{-2} L_{-1} + 18048 L_{-6} L_{-3} L_{-1} - 23552 L_{-5} L_{-4} L_{-1} + 30528 L_{-9} L_{-1} \\
& - 8192 L_{-4} L_{-2}^3 + 10240 L_{-3}^2 L_{-2}^2 + 1024 L_{-6} L_{-2}^2 - 60800 L_{-5} L_{-3} L_{-2} \\
& + 47104 L_{-4}^2 L_{-2} - 30720 L_{-8} L_{-2} - 6144 L_{-4} L_{-2}^3 + 15232 L_{-7} L_{-3} \\
& \left. - 39424 L_{-6} L_{-4} + 36992 L_{-5}^2 - 24576 L_{-10} \right) |h; 1\rangle.
\end{aligned}$$

Bibliography

- [1] I. Gelfand and D. Fuks, *Cohomologies of the Lie algebra of the vector fields on the circle*, *Funct. Anal. Appl.* **2** (1968) 342.
- [2] V. Kac, *Contravariant form for infinite dimensional Lie algebras and superalgebras*, vol. 94 of *Lecture Notes in Physics*. Springer Verlag, Berlin, 1979.
- [3] B. L. Feigin and D. B. Fuks, *Verma modules over the Virasoro algebra*, *Funct. Anal. Appl.* **17** (1983) 241–242.
- [4] A. A. Belavin, A. M. Polyakov, and A. B. Zamolodchikov, *Infinite conformal symmetry in two-dimensional quantum field theory*, *Nucl. Phys.* **B241** (1984) 333–380.
- [5] W. E. Thirring, *A soluble relativistic field theory*, *Annals Phys.* **3** (1958) 91–112.
- [6] W. Nahm, *Conformal field theory: A bridge over troubled waters*, in *Quantum field theory, A 20th century profile* (A. Mitra, ed.), pp. 571–604. Hindustan Book Agency (India) and Indian Nat. Science Academy, 2000.
- [7] D. Friedan, Z.-a. Qiu, and S. H. Shenker, *Conformal invariance, unitarity and two-dimensional critical exponents*, *Phys. Rev. Lett.* **52** (1984) 1575–1578.
- [8] J. L. Cardy, *Conformal invariance and statistical mechanics*, in *Fields, strings and critical phenomena, Les Houches, Session XLIX*, pp. 169–243, Elsevier Science Publishers B.V., 1989.
- [9] P. D. Francesco, P. Mathieu, and D. Senechal, *Conformal field theory*. Springer, New York, 1997.
- [10] M. B. Green, J. H. Schwarz, and E. Witten, *Superstring Theory. Vol. 1 & 2*. Cambridge University Press, Cambridge, 1987.
- [11] J. Polchinski, *String Theory*. Cambridge University Press, Cambridge, 1998.
- [12] J. L. Cardy and D. C. Lewellen, *Bulk and boundary operators in conformal field theory*, *Phys. Lett.* **B259** (1991) 274–278.

- [13] M. Oshikawa and I. Affleck, *Boundary conformal field theory approach to the critical two-dimensional Ising model with a defect line*, *Nucl. Phys.* **B495** (1997) 533–582, [[cond-mat/9612187](#)].
- [14] A. Recknagel and V. Schomerus, *Boundary deformation theory and moduli spaces of D-branes*, *Nucl. Phys.* **B545** (1999) 233–282, [[hep-th/9811237](#)].
- [15] R. E. Behrend, P. A. Pearce, V. B. Petkova, and J.-B. Zuber, *Boundary conditions in rational conformal field theories*, *Nucl. Phys.* **B570** (2000) 525–589, [[hep-th/9908036](#)].
- [16] M. R. Gaberdiel and H. Klemm, *$N = 2$ superconformal boundary states for free bosons and fermions*, *Nucl. Phys.* **B693** (2004) 281–301, [[hep-th/0404062](#)].
- [17] M. A. I. Flohr, *Logarithmic conformal field theory or how to compute a torus amplitude on the sphere*, in *From fields to strings* (M. Shifman, ed.), vol. 2, pp. 1201–1256, 2004. [hep-th/0407003](#).
- [18] J. Fröhlich and T. Kerler, *Universality in quantum Hall systems*, *Nucl. Phys.* **B354** (1991) 369–417.
- [19] M. Flohr and R. Varnhagen, *Infinite symmetry in the fractional quantum Hall effect*, *J. Phys.* **A27** (1994) 3999–4010, [[hep-th/9309083](#)].
- [20] V. Gurarie, M. Flohr, and C. Nayak, *The Haldane-Rezayi quantum Hall state and conformal field theory*, *Nucl. Phys.* **B498** (1997) 513–538, [[cond-mat/9701212](#)].
- [21] R. E. Borcherds, *Vertex algebras, Kac-Moody algebras, and the monster*, *Proc. Nat. Acad. Sci.* **83** (1986) 3068–3071.
- [22] I. Frenkel, Y.-Z. Huang, and J. Lepowsky, *On axiomatic approaches to vertex operator algebras and modules*, *Memoirs Amer. Math. Soc.* **104** (1989).
- [23] J. Lepowsky and H. Li, *Introduction to Vertex Operator Algebras and their Representations*. Progress in Mathematics. Birkhäuser, 2004.
- [24] P. Candelas, X. C. De La Ossa, P. S. Green, and L. Parkes, *A pair of Calabi-Yau manifolds as an exactly soluble superconformal theory*, *Nucl. Phys.* **B359** (1991) 21–74.
- [25] M. Kontsevich and Y. Soibelman, *Homological mirror symmetry and torus fibrations*, [math.sg/0011041](#).
- [26] W. Nahm and K. Wendland, *Mirror symmetry on Kummer type $K3$ surfaces*, *Commun. Math. Phys.* **243** (2003) 557–582, [[hep-th/0106104](#)].

- [27] W. Barth, K. Hulek, C. Peters, and A. Van de Ven, *Compact Complex Surfaces*. Springer, Berlin, 2004.
- [28] N. Seiberg, *Observations on the moduli space of superconformal field theories*, *Nucl. Phys.* **B303** (1988) 286.
- [29] P. S. Aspinwall and D. R. Morrison, *String theory on K3 surfaces*, in *Mirror symmetry* (B. Greene and S. Yau, eds.), vol. II, pp. 703–716. 1994. [hep-th/9404151](#).
- [30] P. S. Aspinwall, *K3 surfaces and string duality*, in *Differential geometry inspired by string theory* (S. Yau, ed.), 1996. [hep-th/9611137](#).
- [31] W. Nahm and K. Wendland, *A hiker's guide to K3: Aspects of $N = (4, 4)$ superconformal field theory with central charge $c = 6$* , *Commun. Math. Phys.* **216** (2001) 85–138, [[hep-th/9912067](#)].
- [32] K. Wendland, *Moduli Spaces of Unitary Conformal Field Theories*. PhD thesis, University of Bonn, Bonn, 2000.
- [33] K. Wendland, *Consistency of orbifold conformal field theories on K3*, *Adv. Theor. Math. Phys.* **5** (2002) 429–456, [[hep-th/0010281](#)].
- [34] L. P. Kadanoff, *Multicritical behavior at the Kosterlitz-Thouless critical point*, *Ann. Physics* **120** (1978) 39–71.
- [35] H. Saleur, *Geometrical lattice models for $N = 2$ supersymmetric theories in two dimensions*, *Nucl. Phys.* **B382** (1992) 532–560, [[hep-th/9111008](#)].
- [36] H. Saleur, *Polymers and percolation in two dimensions and twisted $N = 2$ supersymmetry*, *Nucl. Phys.* **B382** (1992) 486–531, [[hep-th/9111007](#)].
- [37] P. Ruelle, *A $c = -2$ boundary changing operator for the Abelian sandpile model*, *Phys. Lett.* **B539** (2002) 172–177, [[hep-th/0203105](#)].
- [38] E. Gravanis and N. E. Mavromatos, *Impulse action on D -particles in Robertson-Walker space times, higher-order logarithmic conformal algebras and cosmological horizons*, [hep-th/0106146](#).
- [39] I. Bakas and K. Sfetsos, *PP-waves and logarithmic conformal field theories*, *Nucl. Phys.* **B639** (2002) 223–240, [[hep-th/0205006](#)].
- [40] N. Lambert, H. Liu, and J. Maldacena, *Closed strings from decaying D -branes*, [hep-th/0303139](#).
- [41] P. A. Pearce, V. Rittenberg, and J. de Gier, *Critical $Q = 1$ Potts model and Temperley-Lieb stochastic processes*, [cond-mat/0108051](#).

- [42] J. A. Minahan and K. Zarembo, *The Bethe-ansatz for $N = 4$ super Yang-Mills*, *JHEP* **03** (2003) 013, [[hep-th/0212208](#)].
- [43] N. Beisert, V. Dippel, and M. Staudacher, *A novel long range spin chain and planar $N = 4$ super Yang-Mills*, *JHEP* **07** (2004) 075, [[hep-th/0405001](#)].
- [44] F. Rohsiepe, *On reducible but indecomposable representations of the Virasoro algebra*, [hep-th/9611160](#).
- [45] M. R. Gaberdiel and H. G. Kausch, *Indecomposable fusion products*, *Nucl. Phys.* **B477** (1996) 293–318, [[hep-th/9604026](#)].
- [46] M. R. Gaberdiel and H. G. Kausch, *A rational logarithmic conformal field theory*, *Phys. Lett.* **B386** (1996) 131–137, [[hep-th/9606050](#)].
- [47] M. R. Gaberdiel and H. G. Kausch, *A local logarithmic conformal field theory*, *Nucl. Phys.* **B538** (1999) 631–658, [[hep-th/9807091](#)].
- [48] H. G. Kausch, *Extended conformal algebras generated by a multiplet of primary fields*, *Phys. Lett.* **B259** (1991) 448–455.
- [49] M. A. I. Flohr, *On modular invariant partition functions of conformal field theories with logarithmic operators*, *Int. J. Mod. Phys.* **A11** (1996) 4147–4172, [[hep-th/9509166](#)].
- [50] M. A. I. Flohr, *On fusion rules in logarithmic conformal field theories*, *Int. J. Mod. Phys.* **A12** (1997) 1943–1958, [[hep-th/9605151](#)].
- [51] M. Flohr and M. R. Gaberdiel, *Logarithmic torus amplitudes*, *J. Phys.* **A39** (2006) 1955–1968, [[hep-th/0509075](#)].
- [52] N. Carqueville and M. Flohr, *Nonmeromorphic operator product expansion and C_2 -cofiniteness for a family of \mathcal{W} -algebras*, *J. Phys.* **A39** (2006) 951–966, [[math-ph/0508015](#)].
- [53] H. G. Kausch, *Symplectic fermions*, *Nucl. Phys.* **B583** (2000) 513–541, [[hep-th/0003029](#)].
- [54] M. Krohn and M. Flohr, *Ghost systems revisited: Modified Virasoro generators and logarithmic conformal field theories*, *JHEP* **01** (2003) 020, [[hep-th/0212016](#)].
- [55] M. Flohr, *Operator product expansion in logarithmic conformal field theory*, *Nucl. Phys.* **B634** (2002) 511–545, [[hep-th/0107242](#)].
- [56] M. Flohr and M. Krohn, *Four-point functions in logarithmic conformal field theories*, [hep-th/0504211](#).

- [57] M. A. I. Flohr, *Singular vectors in logarithmic conformal field theories*, *Nucl. Phys.* **B514** (1998) 523–552, [[hep-th/9707090](#)].
- [58] M. Flohr, *Null vectors in logarithmic conformal field theory*, [hep-th/0009137](#).
- [59] S. Moghimi-Araghi, S. Rouhani, and M. Saadat, *Logarithmic conformal field theory through nilpotent conformal dimensions*, *Nucl. Phys.* **B599** (2001) 531–546, [[hep-th/0008165](#)].
- [60] S. Moghimi-Araghi, S. Rouhani, and M. Saadat, *Use of nilpotent weights in logarithmic conformal field theories*, *Int. J. Mod. Phys.* **A18** (2003) 4747–4770, [[hep-th/0201099](#)].
- [61] M. Flohr and A. Müller-Lohmann, *Notes on non-trivial and logarithmic CFTs with $c = 0$* , *J. Stat. Mech.* **0604** (2006) P002, [[hep-th/0510096](#)].
- [62] G. Felder, J. Fröhlich, and G. Keller, *Braid matrices and structure constants for minimal conformal models*, *Commun. Math. Phys.* **124** (1989) 647–664.
- [63] G. Felder, J. Fröhlich, and G. Keller, *On the structure of unitary conformal field theory. 2. Representation theoretic approach*, *Commun. Math. Phys.* **130** (1990) 1.
- [64] M. Gaberdiel, *Fusion in conformal field theory as the tensor product of the symmetry algebra*, *Int. J. Mod. Phys.* **A9** (1994) 4619–4636, [[hep-th/9307183](#)].
- [65] J. Lepowsky, *From the representation theory of vertex operator algebras to modular tensor categories in conformal field theory*, *Proc. Nat. Acad. Sci.* **102** (2005) 5304–5305, [[math.qa/0504311](#)].
- [66] C. Schweigert, J. Fuchs, and I. Runkel, *Categorification and correlation functions in conformal field theory*, [math.ct/0602079](#).
- [67] W. Nahm, *Quasirational fusion products*, *Int. J. Mod. Phys.* **B8** (1994) 3693–3702, [[hep-th/9402039](#)].
- [68] J. S. Caux, I. I. Kogan, and A. M. Tsvetlik, *Logarithmic operators and hidden continuous symmetry in critical disordered models*, *Nucl. Phys.* **B466** (1996) 444–462, [[hep-th/9511134](#)].
- [69] Z. Maassarani and D. Serban, *Non-unitary conformal field theory and logarithmic operators for disordered systems*, *Nucl. Phys.* **B489** (1997) 603–625, [[hep-th/9605062](#)].
- [70] A. M. Ghezelbash and V. Karimipour, *Global conformal invariance in D dimensions and logarithmic correlation functions*, *Phys. Lett.* **B402** (1997) 282–289, [[hep-th/9704082](#)].

- [71] J. Rasmussen, *Jordan cells in logarithmic limits of conformal field theory*, hep-th/0406110.
- [72] J. Rasmussen, *On conformal Jordan cells of finite and infinite rank*, *Lett. Math. Phys.* **73** (2005) 83–90, [hep-th/0408029].
- [73] P. Ginsparg, *Applied conformal field theory*, in *Lectures given at Les Houches Summer School in Theoretical Physics*, Les Houches, 1988.
- [74] A. N. Schellekens, *Introduction to conformal field theory*, *Fortsch. Phys.* **44** (1996) 605–705.
- [75] M. R. Gaberdiel and P. Goddard, *Axiomatic conformal field theory*, *Commun. Math. Phys.* **209** (2000) 549, [hep-th/9810019].
- [76] M. R. Gaberdiel, *An introduction to conformal field theory*, *Rept. Prog. Phys.* **63** (2000) 607, [hep-th/9910156].
- [77] B. R. Greene, *String theory on Calabi-Yau manifolds*, in *Lectures given at Theoretical Advanced Study Institute in Elementary Particle Physics (TASI 96): Fields, Strings, and Duality*, TASI 96, Boulder CO, 1996. hep-th/9702155.
- [78] T. Eguchi and A. Taormina, *Character formulas for the $N = 4$ superconformal algebra*, *Phys. Lett.* **B200** (1988) 315.
- [79] T. Eguchi and A. Taormina, *Unitary representations of $N = 4$ superconformal algebra*, *Phys. Lett.* **B196** (1987) 75.
- [80] T. Eguchi and A. Taormina, *On the unitary representations of $N = 2$ and $N = 4$ superconformal algebras*, *Phys. Lett.* **B210** (1988) 125.
- [81] A. Taormina, *The $N=2$ and $N=4$ superconformal algebras and string compactifications*, in *Islamabad 1989, Proceedings, Mathematical physics*, pp. 349–370, 1989.
- [82] M. Flohr, *Bits and pieces in logarithmic conformal field theory*, *Int. J. Mod. Phys.* **A18** (2003) 4497–4592, [hep-th/0111228].
- [83] M. R. Gaberdiel, *An algebraic approach to logarithmic conformal field theory*, *Int. J. Mod. Phys.* **A18** (2003) 4593–4638, [hep-th/0111260].
- [84] S. Kawai, *Logarithmic conformal field theory with boundary*, *Int. J. Mod. Phys.* **A18** (2003) 4655–4684, [hep-th/0204169].
- [85] A. Nichols, *$SU(2)_k$ logarithmic conformal field theories*. PhD thesis, University of Oxford, 2002. hep-th/0210070.

- [86] A. Rocha-Caridi, *Vacuum vector representations of the Virasoro algebra*, in *Vertex Operators in Mathematics and Physics* (J. Lepowsky, ed.), p. 451, Springer, 1985.
- [87] P. Goddard and D. I. Olive, *Kac-Moody and Virasoro algebras in relation to quantum physics*, *Int. J. Mod. Phys. A***1** (1986) 303.
- [88] D. Jungnickel, *Correlation functions of two-dimensional twisted conformal field theories*. PhD thesis, Max-Planck-Institut für Physik, München, 1992.
- [89] K. S. Narain, *New heterotic string theories in uncompactified dimensions < 10* , *Phys. Lett. B***169** (1986) 41.
- [90] K. S. Narain, M. H. Sarmadi, and E. Witten, *A note on toroidal compactification of heterotic string theory*, *Nucl. Phys. B***279** (1987) 369.
- [91] W. Fulton and J. Harris, *Representation theory*. Springer, New-York, 1991.
- [92] L. Dixon, J. A. Harvey, C. Vafa, and E. Witten, *Strings on orbifolds*, *Nucl. Phys. B***261** (1985) 678–686.
- [93] L. Dixon, J. A. Harvey, C. Vafa, and E. Witten, *Strings on orbifolds. 2*, *Nucl. Phys. B***274** (1986) 285–314.
- [94] L. Dixon, D. Friedan, E. Martinec, and S. Shenker, *The conformal field theory of orbifolds*, *Nucl. Phys. B***282** (1987) 13–73.
- [95] L. J. Dixon, *Some world sheet properties of superstring compactifications, on orbifolds and otherwise*, in *Lectures given at the 1987 ICTP Summer Workshop in High Energy Physics and Cosmology*, ICTP Trieste, 1987.
- [96] K. Wendland, *Superconformal orbifolds involving the fermion number operator*, *Int. J. Mod. Phys. A***19** (2004) 3637–3667.
- [97] Lepowsky, *Calculus of twisted vertex operators*, *Proc. Nat. Acad. Sci. U.S.A.* **82** (1985) 8295–8299.
- [98] S. Hamidi and C. Vafa, *Interactions on orbifolds*, *Nucl. Phys. B***279** (1987) 465.
- [99] M. Bershadsky and A. Radul, *Conformal field theories with additional $Z(N)$ symmetry*, *Int. J. Mod. Phys. A***2** (1987) 165–178.
- [100] M. Bershadsky and A. Radul, *G loop amplitudes in bosonic string theory in terms of branch points*, *Phys. Lett. B***193** (1987) 213–218.
- [101] J. J. Atick, L. J. Dixon, P. A. Griffin, and D. Nemeschansky, *Multiloop twist field correlation functions for $Z(N)$ orbifolds*, *Nucl. Phys. B***298** (1988) 1–35.

- [102] J. Erler, D. Jungnickel, J. Lauer, and J. Mas, *String emission from twisted sectors: cocycle operators and modular background symmetries*, *Ann. Phys.* **217** (1992) 318–363.
- [103] H. Eberle, *Twistfield perturbations of vertex operators in the \mathbb{Z}_2 -orbifold model*, *JHEP* **06** (2002) 022, [[hep-th/0103059](#)].
- [104] J. Distler and B. R. Greene, *Some exact results on the superpotential from Calabi-Yau compactifications*, *Nucl. Phys.* **B309** (1988) 295.
- [105] M. Terhoeven, *Gepner Modelle und \mathcal{W} -Algebren*, Master’s thesis, University of Bonn, 1992.
- [106] P. Di Vecchia, J. L. Petersen, M. Yu, and H. B. Zheng, *Explicit construction of unitary representations of the $N = 2$ superconformal algebra*, *Phys. Lett.* **B174** (1986) 280.
- [107] W. Boucher, D. Friedan, and A. Kent, *Determinant formulae and unitarity for the $N = 2$ superconformal algebras in two-dimensions or exact results on string compactification*, *Phys. Lett.* **B172** (1986) 316.
- [108] Z.-a. Qiu, *Modular invariant partition functions for $N = 2$ superconformal field theories*, *Phys. Lett.* **B198** (1987) 497.
- [109] J. Fuchs, A. Klemm, and M. G. Schmidt, *Orbifolds by cyclic permutations in Gepner type superstrings and in the corresponding Calabi-Yau manifolds*, *Ann. Phys.* **214** (1992) 221–257.
- [110] D. Gepner, *Exactly solvable string compactifications on manifolds of $SU(N)$ holonomy*, *Phys. Lett.* **B199** (1987) 380–388.
- [111] D. Gepner, *Space-time supersymmetry in compactified string theory and superconformal models*, *Nucl. Phys.* **B296** (1988) 757.
- [112] T. Eguchi, H. Ooguri, A. Taormina, and S.-K. Yang, *Superconformal algebras and string compactification on manifolds with $SU(n)$ holonomy*, *Nucl. Phys.* **B315** (1989) 193.
- [113] K. Wendland, *Orbifold constructions of $K3$: A link between conformal field theory and geometry*, [hep-th/0112006](#).
- [114] H. Eberle, *On explicit results at the intersection of the \mathbb{Z}_2 and \mathbb{Z}_4 orbifold subvarieties in $K3$ moduli space*, *JHEP* **08** (2004) 015, [[hep-th/0407170](#)].
- [115] K. Wendland, *A family of SCFTs hosting all ‘very attractive’ relatives of the $(2)^4$ Gepner model*, *JHEP* **03** (2006) 102, [[hep-th/0512223](#)].

- [116] P. Griffiths and J. Harris, *Principles of algebraic geometry*. Wiley & Sons, Inc., New York, 1994.
- [117] S. Helgason, *Differential Geometry and Symmetric Spaces*. Academic Press, New York and London, 1962.
- [118] A. Cuyt and L. Wuytack, *Nonlinear Methods in Numerical Analysis*. North-Holland Mathematics Studies 136. Elsevier Science Publishers, Amsterdam, 1987.
- [119] R. Dijkgraaf, E. Verlinde, and H. Verlinde, *On moduli spaces of conformal field theories $c \geq 1$* , in *Copenhagen 1987, Proceedings, Perspectives in String Theory*, pp. 117–137, 1987.
- [120] P. Ginsparg, *Curiosities at $c = 1$* , *Nucl. Phys.* **B295** (1988) 153–170.
- [121] J. L. Cardy, *Continuously varying exponents and the value of the central charge*, *J. Phys. A* **A20** (1987) L891.
- [122] F. Constantinescu and R. Flume, *Perturbation theory around two-dimensional critical systems through holomorphic decomposition*, *J. Phys.* **A23** (1990) 2971–2986.
- [123] P. Chason, F. Constantinescu, and R. Flume, *Deformations along critical lines of field theories in two dimensions*, *Phys. Lett.* **B257** (1991) 63–68.
- [124] S. D. Mathur, *Quantum Kac-Moody symmetry in integrable field theories*, *Nucl. Phys.* **B369** (1992) 433–460.
- [125] K. Cho and K. Matsumoto, *Intersection theory for twisted cohomologies and twisted Riemann's period relations I*, *Nagoya Math. J.* **139** (1995) 67–86.
- [126] A. A. Belavin, V. A. Belavin, A. V. Litvinov, Y. P. Pugai, and A. B. Zamolodchikov, *On correlation functions in the perturbed minimal models $M(2, 2n + 1)$* , *Nucl. Phys.* **B676** (2004) 587–614, [[hep-th/0309137](#)].
- [127] K. Mimachi and M. Yoshida, *Intersection numbers of twisted cycles and the correlation functions of the conformal field theory*, *Commun. Math. Phys.* **234** (2003) 339–358, [[math.ag/0208097](#)].
- [128] K. Mimachi and M. Yoshida, *Intersection numbers of twisted cycles associated with the Selberg integral and an application to the conformal field theory*, *Commun. Math. Phys.* **250** (2004) 23–45.
- [129] E. R. Speer, *Analytic renormalization*, *J. Math. Phys.* **9** (1968) 1404.
- [130] E. R. Speer, *Dimensional and analytic renormalization*, in *Renormalization Theory* (G. Velo and A. Wightman, eds.), pp. 25–93, D. Reidel Publishing Company, 1975.

- [131] S. Moch, P. Uwer, and S. Weinzierl, *Nested sums, expansion of transcendental functions and multi-scale multi-loop integrals*, *J. Math. Phys.* **43** (2002) 3363–3386, [[hep-ph/0110083](#)].
- [132] S. Weinzierl, *Symbolic expansion of transcendental functions*, *Comput. Phys. Commun.* **145** (2002) 357–370, [[math-ph/0201011](#)].
- [133] S. Weinzierl, *Expansion around half-integer values, binomial sums and inverse binomial sums*, [hep-ph/0402131](#).
- [134] C. Bauer, A. Frink, and R. Kreckel, *Introduction to the GiNaC framework for symbolic computation within the C++ programming language*, *J. Symbolic Computation* **33** (2002) 1, [[cs.sc/0004015](#)]. The GiNaC library is available at <http://www.ginac.de>.
- [135] H. Eberle, M. Flohr, and A. Nichols. In preparation.
- [136] H. Eberle and M. Flohr, *Notes on generalised nullvectors in logarithmic CFT*, *Nucl. Phys.* **B741** (2006) 441–466, [[hep-th/0512254](#)].
- [137] I. I. Kogan and A. Lewis, *Origin of logarithmic operators in conformal field theories*, *Nucl. Phys.* **B509** (1998) 687–704, [[hep-th/9705240](#)].
- [138] H. Eberle and M. Flohr, *Virasoro representations and fusion for general augmented minimal models*, [hep-th/0604097](#).
- [139] M. Gaberdiel, *Fusion rules of chiral algebras*, *Nucl. Phys.* **B417** (1994) 130–150, [[hep-th/9309105](#)].
- [140] G. M. T. Watts, *A crossing probability for critical percolation in two dimensions*, *J. Phys.* **A29** (1996) L363, [[cond-mat/9603167](#)].
- [141] J. Cardy, *Lectures on conformal invariance and percolation*, [math-ph/0103018](#).
- [142] M. A. I. Flohr and A. Müller-Lohmann, *Conformal field theory properties of two-dimensional percolation*, *J. Stat. Mech.* **0512** (2005) P004, [[hep-th/0507211](#)].
- [143] V. Gurarie and A. W. W. Ludwig, *Conformal algebras of 2D disordered systems*, *J. Phys.* **A35** (2002) L377–L384, [[cond-mat/9911392](#)].
- [144] V. Gurarie and A. W. W. Ludwig, *Conformal field theory at central charge $c = 0$ and two dimensional critical systems with quenched disorder*, [hep-th/0409105](#).
- [145] N. Read and H. Saleur, *Exact spectra of conformal supersymmetric nonlinear sigma models in two dimensions*, *Nucl. Phys.* **B613** (2001) 409, [[hep-th/0106124](#)].

- [146] B. L. Feigin, A. M. Gainutdinov, A. M. Semikhatov, and I. Y. Tipunin, *Modular group representations and fusion in logarithmic conformal field theories and in the quantum group center*, [hep-th/0504093](#).
- [147] B. L. Feigin, A. M. Gainutdinov, A. M. Semikhatov, and I. Y. Tipunin, *Kazhdan–Lusztig correspondence for the representation category of the triplet \mathcal{W} -algebra in logarithmic conformal field theory*, [math.qa/0512621](#).
- [148] V. Schomerus and H. Saleur, *The $GL(1|1)$ WZW model: From supergeometry to logarithmic CFT*, *Nucl. Phys.* **B734** (2006) 221–245, [[hep-th/0510032](#)].